



HAL
open science

Impact of mechanical stress on nucleus morphology and transcription on skeletal muscle

Saline Jabre

► **To cite this version:**

Saline Jabre. Impact of mechanical stress on nucleus morphology and transcription on skeletal muscle. Cellular Biology. Sorbonne Université; Université Saint-Esprit (Kaslik, Liban), 2022. English. NNT : 2022SORUS561 . tel-04317459

HAL Id: tel-04317459

<https://theses.hal.science/tel-04317459>

Submitted on 1 Dec 2023

HAL is a multi-disciplinary open access archive for the deposit and dissemination of scientific research documents, whether they are published or not. The documents may come from teaching and research institutions in France or abroad, or from public or private research centers.

L'archive ouverte pluridisciplinaire **HAL**, est destinée au dépôt et à la diffusion de documents scientifiques de niveau recherche, publiés ou non, émanant des établissements d'enseignement et de recherche français ou étrangers, des laboratoires publics ou privés.

Sorbonne Université
Université Saint-Esprit de Kaslik

ED515 : Complexité du vivant

*UMRS974 / Équipe 2 : Organisation de la cellule musculaire et thérapie de la myopathie
centronucléaire autosomique dominante*
équipe de recherche

**Impact of mechanical stress on nucleus morphology and
transcription on skeletal muscle**

Par Saline Jabre

Thèse de doctorat de Biologie

Dirigée par Catherine Coirault et Walid Hleihel

Présentée et soutenue publiquement le 21 octobre 2022

Devant un jury composé de :

Dr. Batonnet-Pichon Sabrina, Maître de conférences, Rapporteur

Pr. Fares Nassim, Enseignant-Chercheur, Rapporteur

Pr. Agbulut Onnik, Professeur, Examineur

Dr. Hoyek Fadi, Professeur associé, Examineur

Dr. Etienne-Manneville Sandrine, Directrice de recherche, Invité

Dr. Coirault Catherine, Directrice de recherche, directrice de thèse

Pr. Hleihel Walid, Professeur, Directeur de thèse

La science est d'une grande beauté.

Un scientifique dans son laboratoire

est un enfant placé devant des phénomènes naturels

qui l'impressionnent comme des contes de fées.

~Marie Curie~

Remerciements

Avec une grande reconnaissance, je remercie chaleureusement Catherine Coirault, ma directrice de thèse pour son intelligence et ses éclairages, pour son humanité et son amitié, pour sa patience et ses multiples secours, pour son écoute et ses précieux conseils.

Malgré 8 mois de blocage administratif et le covid qui a compliqué davantage la situation, tu as toujours cru en moi et ensemble, nous avons pu réaliser ce travail.

Je tiens à exprimer ma gratitude et mon estime profond à Walid Hleihel, mon co-directeur pour ses brillants conseils et ses connaissances, pour ses encouragements et son soutien, pour sa confiance et son écoute, pour ses aides et son dévouement. Sans vous je ne serais pas là. Cette thèse c'est la mienne mais aussi la votre.

J'adresse mes remerciements aux membres du jury : Monsieur le président, Pr. Onnik Agbulut, je vous remercie de l'honneur que vous m'avez fait en acceptant de présider notre jury.

Merci aux rapporteurs Dr Sabrina Batonnet-Pichon et monsieur Nassim Farès, toute ma reconnaissance pour votre patience et vos remarques pertinentes qui ont rendu ce travail encore plus intéressant.

Je vous remercie Dr Sandrine Etienne-Manneville et Pr Fadi Hoyek, pour vos enseignements et vous suis très reconnaissante d'avoir porté de l'intérêt à ce travail.

D'immenses remerciements pour notre chef ultime Marc Bitoun pour sa sagesse, son charisme et ses conseils. Merci d'avoir rigolé et apprécié mes blagues nulles et surtout de m'avoir appris que nous sommes les créateurs de la connaissance.

Mes chaleureux et affectifs remerciements à toute l'équipe deux, merci pour vos idées, inspirations et propositions qui ont rendu mon travail plus facile et plus riche.

Merci à Bruno Cadot pour le Spinning Disk de la plateforme MyoImage où j'ai passé beaucoup plus d'heures qu'autorisé.

Merci pour toutes celles et ceux qui ont partagé mon quotidien au labo: «les jeunes »vous étiez ma motivation. Merci pour les afterworks, votre sympathie, votre fraternité, pour les moments de folie que nous avons vécus ensemble. Merci pour le sentiment d'être en famille, une famille qui t'aime malgré tout.

Xavière, un grand merci du fond du cœur, merci d'être patiente avec moi, d'être prête à m'aider à surmonter tous mes problèmes. Merci d'avoir cru en moi et de m'avoir reboostée quand j'avais perdu la motivation. Je te dois beaucoup.

Lylia, merci pour les gâteaux, pour ta confiance et ton humour.

Kevin, merci pour les cookies que tu voulais m'offrir mais que tu as mangé sur le chemin.

Pour Eline, Charles, Alexandra et Ludovic il n'y a pas de mot assez fort pour exprimer ma gratitude pour tout le bien que vous m'avez fait tout au long de ses années. C'est super de vous avoir comme force et amour auprès de moi.

Alexis un merci ne suffit pas pour ta patience, ta sagesse et ton amour inconditionnel pour tes amis, merci pour ton humilité.

À ma chère maman, source inépuisable d'amour, de patience et de sacrifice, quoique je puisse t'écrire, je ne pourrai t'exprimer ma grande et profonde reconnaissance. Je t'aime très fort.

Merci Papa, merci de m'avoir appris que rien n'est impossible avec la persévérance et la foi, ma joie est immense lorsque les gens parlent de toi et me disent: « ton papa doit être très fier de toi » c'est ma meilleure motivation pour continuer.

Pour mon frère un chaleureux merci de m'avoir épaulée dans les moments délicats.

Merci à mes oncles et mes tantes, envers qui j'ai une affection sans mesure.

Pour Stephanie et Mary, celles qui sont prêtes à m'aider même si elles ne savent pas comment.

Pour soeur Marie Reine qui a veillé sur moi et qui s'est souciée de tout, avec une affection chaleureuse un grand et sincère merci pour tout ce que tu as fait. Tu m'as aidé inlassablement et écouté attentivement. Merci pour Marie-jeanne, Marie Viannette et Félix.

Mes remerciements pour Elie, Jérémie et Luciana qui ont dû me supporter.

À Nancy, ma sœur de vie, merci pour ton amour et encouragements que j'ai senti des États-Unis et malgré la distance, ma fan numéro 1 pendant toutes ces années. Tu as toujours fait preuve d'un soutien sans faille.

Pour mes amis au Liban et mes amis de l'artisanat Monastique, les mots me manquent pour vous exprimer mon attachement et ma gratitude pour tout votre amour.

Merci à ma famille corse : Aline, Olivier, Nanou et Lesia. Je vous aime.

Père Elie, il n'y a pas de mots assez forts pour te remercier, je ne sais même pas par où commencer. Merci d'être à l'écoute dans les moments difficiles, merci pour tes conseils à tous

les niveaux. Merci de m'avoir soutenue quand j'étais au plus mal. Merci d'être le meilleur exemple à suivre pour moi : quelqu'un qui donne sans limite et sans rien attendre en retour.

Une chose est certaine : je n'aurais pas pu y arriver sans toi !

Alors du fond du cœur : merci

Summary

REMERCIEMENTS	2
SUMMARY.....	6
INTRODUCTION	8
I. SKELETAL MUSCLE	8
<i>i. Generalities</i>	<i>8</i>
<i>ii. The myofibrils.....</i>	<i>10</i>
II. EMBRYOGENESIS AND MUSCLE DIFFERENTIATION	12
III. SATELLITE CELLS	14
IV. MECHANOTRANSDUCTION	15
<i>i. Definition.....</i>	<i>15</i>
<i>ii. Extracellular matrix</i>	<i>17</i>
<i>iii. The different types of forces</i>	<i>18</i>
V. STRUCTURES INVOLVED IN FORCE TRANSMISSION AND MECHANOSENSIBILITY	20
<i>i. Integrin-mediated mechanotransduction</i>	<i>20</i>
<i>ii. Actin filaments.....</i>	<i>22</i>
<i>iii. The microtubules (MTs)</i>	<i>25</i>
<i>iv. Cytoplasmic intermediate filaments (IFs).....</i>	<i>26</i>
<i>v. Nuclear envelope and LINC complex.....</i>	<i>29</i>
<i>vi. Lamins</i>	<i>32</i>
<i>vii. Chromatin.....</i>	<i>42</i>
<i>viii. Histone PTMs.....</i>	<i>44</i>
VI. NUCLEAR MECHANOTRANSDUCTION	48
VII. YAP SIGNALING PATHWAYS	50
VIII. LAMINOPATHIES	52
OBJECTIVES OF THE THESIS	55
MATERIALS AND METHODS.....	56
I. HUMAN MYOBLAST CULTURE	56
II. CELL CULTURE.....	56
III. CHEMICALS, CHROMATIN MODIFIATORS.....	57
IV. SiRNA.....	57
V. MECHANICAL STRETCH.....	58
VI. COATINGS	59
VII. IMMUNOFLUORESCENCE	59
VIII. MICROSCOPY AND IMAGE ANALYSIS.....	60
IX. SDS-PAGE AND PROTEIN ANALYSIS	60
X. CHROMATIN EXTRACTION.....	63
XI. RNA SEQ AND QUANTIFICATION OF GENE EXPRESSION.	63

XII.	ATACSEQ.....	66
XIII.	STATISTICAL ANALYSIS.....	68
RESULTS.....		69
I.	NUCLEAR CHANGES ASSOCIATED WITH MUSCLE DIFFERENTIATION.....	69
II.	EFFECTS OF A-TYPE LAMIN ON MYONUCLEI	71
	i. <i>siLMNA induced important deformations of the myonucleus shape in static conditions</i>	71
	ii. <i>Effects of siLMNA on chromatin markers in static conditions</i>	72
III.	EFFECTS OF CYCLIC STRETCH ON NUCLEUS SHAPE AND HISTONE MARKS	77
IV.	EFFECTS OF siSUN1 AND SUN2.....	86
	i. <i>Effects of SUN1 or SUN2 silencing on nuclear characteristics</i>	86
	ii. <i>Effects of SUN1 or SUN2 silencing on histone marks</i>	89
V.	CYTO-NUCLEOPLASMIC EXCHANGES	91
	i. <i>The YAP response</i>	91
	ii. <i>HDAC modification and acetylation marker intensity: effects of LMNA deficiency and stretch</i>	93
VI.	CHROMATIN STATE MODIFIES TRANSCRIPTOMIC RESPONSE OF CELLS TO MECHANICAL STRESS.....	101
	i. <i>Quality controls</i>	101
	ii. <i>Data Analysis</i>	104
DISCUSSION.....		111
LIST OF TABLES.....		114
LIST OF FIGURES.....		114
LIST OF RESULTS FIGURES.....		115
REFERENCES		116
ABBREVIATIONS		146
RÉSUMÉ EN FRANÇAIS.....		148
ABSTRACT IN ENGLISH.....		149
PUBLICATIONS.....		152

Introduction

Skeletal muscle is a highly organized tissue designed to produce force and movement. It is composed of differentiated, multinucleated and aligned myofibers responsible for contraction, and also contains a population of mononucleated muscle cell precursors, that are maintained in a quiescent state under homeostatic conditions. Myofibers form by fusion of tens of thousands of differentiated muscle cell precursors (also called myocytes) to produce multinucleated myotubes, which mature into myofibers, composed of a regular array of contractile elements, the sarcomere (Abmayr, S.M.; Pavlath, G.K et 2012). Skeletal muscle is remarkable in its ability to adapt in response to the demands imposed on it, a property referred as muscle plasticity. Low physical activity and some disease conditions lead to the reduction of myofiber size, called atrophy, whereas hypertrophy refers to the increase in myofiber size induced by high physical activity or intrinsic factors such as anabolic hormones/drugs. Over the last decades, the molecular mechanisms that regulate changes in skeletal muscle mass in response to mechanical load have been detailed (Kirby et al 2019; Ato S et al 2020; Jabre et al 2020). An emerging body of literature supports the notion that muscle plasticity is critically dependent upon nuclear mechanotransduction, which is the transduction of exterior physical forces into the nucleus to generate a biological response. Mechanical loading induces nuclear deformation, changes in the nuclear lamina polymerization, chromatin condensation state and cell signaling, which ultimately impacts myogenic cell fate decisions. Advances in deciphering the molecular mechanisms contributing to nuclear mechanotransduction strongly support the idea that defects in nuclear mechanotransduction contribute to human muscle disorders. However, the contributive role of stress and strain-induced nuclear response in normal and diseased striated muscles still remain to be determined.

I. Skeletal muscle

i. Generalities

The skeletal muscles of the human body (Figure 1) are responsible for many essential functions such as voluntary movements, and non-voluntary movements such as breathing, heat production or posture maintenance. Representing 40% of the body mass and containing 50 to 75% of the proteins of the human body, skeletal muscles are characterized by the following

properties: excitability, contractility, extensibility, and elasticity. The term striated skeletal muscle comes from the regular striation around the two main filaments actin and myosin.

A skeletal muscle consists of several bundles of muscle fibers. The epimysium is the name given to the sheath that surrounds the entire muscle. The perimysium encircles each fiber bundle. The endomysium surrounds the muscle fibers. Skeletal muscles are attached to the bones of the skeleton by tendons, which are extensions of fibers and connective tissue.

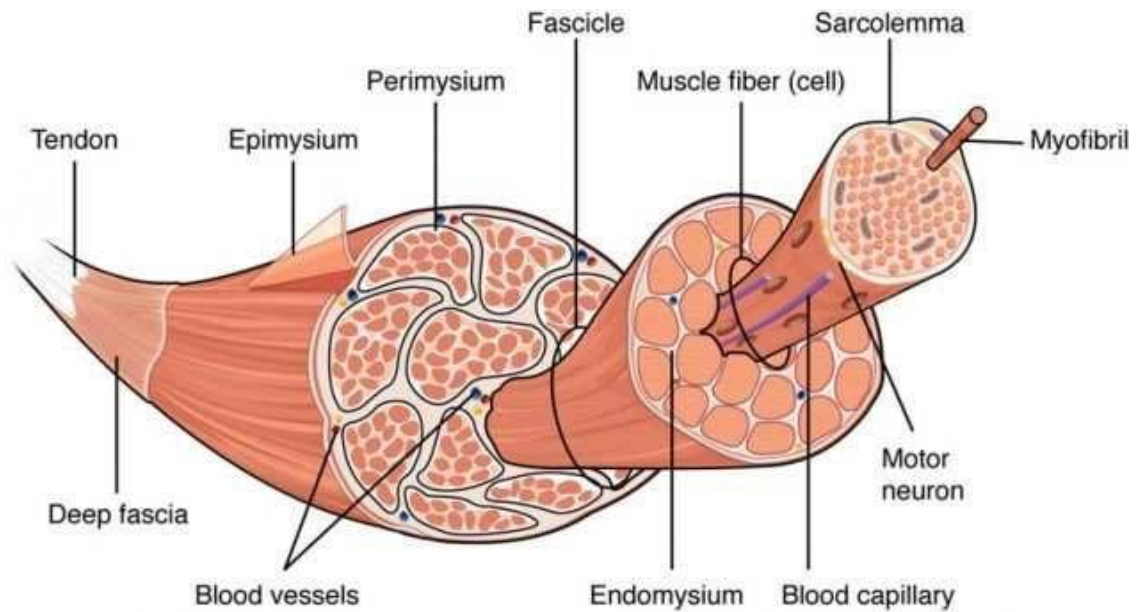


Figure 1: The human skeletal muscle layers of connective tissue.

The Three Connective Tissue Layers: Bundles of muscle fibers, called fascicles, are covered by the perimysium. Muscle fibers are covered by the endomysium.(Biga et al., s. d.)

Skeletal muscle also includes blood vessels that directly bring energy resources, energy-producing mitochondria and innervation for motor skills.

The muscle fiber is the cellular unit of contraction since each fiber can contract independently of each other. The diameter of a muscle fiber varies between 1 and 2 μm . Its length corresponds to the length of the muscle. Several muscle fibers group together in bundles of between 20 and 150 μm in diameter. A muscle fiber is plurinucleate because it results from the fusion of several myocytes. The volume of the muscle fiber is composed mostly of contractile proteins, the main ones are myosin and actin. Because of the specificities inherent to the identity of the muscle fiber, the plasma membrane, the cytoplasm, and the smooth endoplasmic reticulum are called sarcolemma, sarcoplasm and sarcoplasmic reticulum respectively.

The sarcoplasmic reticulum, which acts as a calcium reservoir, encircles the myofibrils (which constitute the contractile proteins) and forms a vast tubular network. At specific and regular points, the sarcolemma invaginates to form the transverse tubules or T-tubules. Around each T-

tubule, a part of the sarcoplasmic reticulum called the terminal cisterna gathers. Two terminal cisternae, from two adjacent striae, flank the T-tubule to form the muscular triad. The triad is the site of calcium release in response to an action potential (Figure 2).

In addition to the sarcoplasmic reticulum, the presence of numerous mitochondria is observed around the myofibrils (Pearson education 2015 et Marieb 2015)

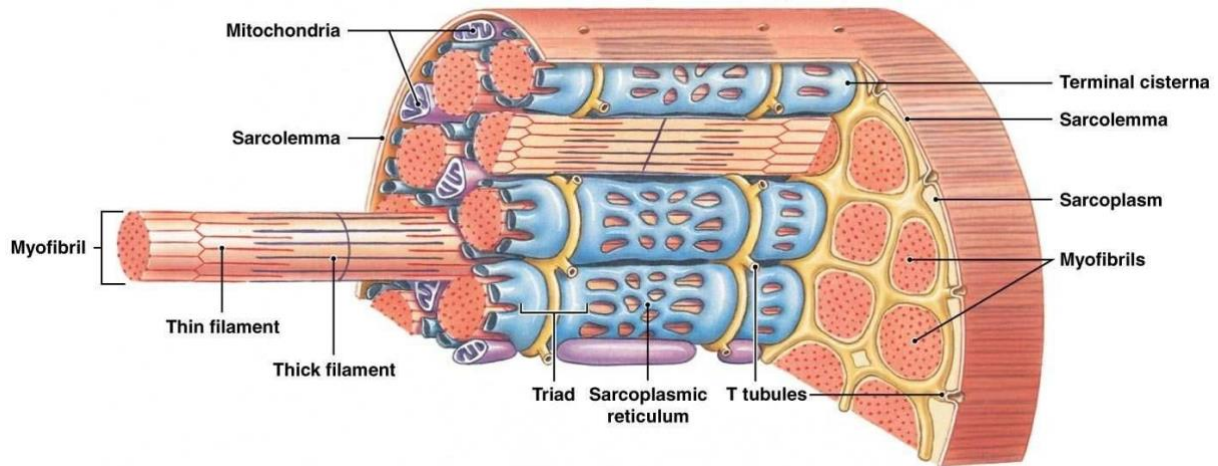


Figure 2: Structural organization of a skeletal muscle fiber.

A skeletal muscle fiber is surrounded by a plasma membrane called the sarcolemma, which contains sarcoplasm, the cytoplasm of muscle cells. A muscle fiber is composed of many myofibrils, which contain sarcomeres with light and dark regions that give the cell its striated appearance.(Pearson education 2015 et Marieb 2015)

ii. The myofibrils

The sarcomere is the area between 2 Z lines. Between two uncontracted thin filaments is the H-zone, which contains only thin filament. The M zone corresponds to the center of the H zone. The Z-line is the anchor point of the thin filaments. Electron microscopy observation reveals β

zones of distinct intensities; the dark anisotropic zone (A) and the isotropic zone (I) which appears in clear (Figure 3).

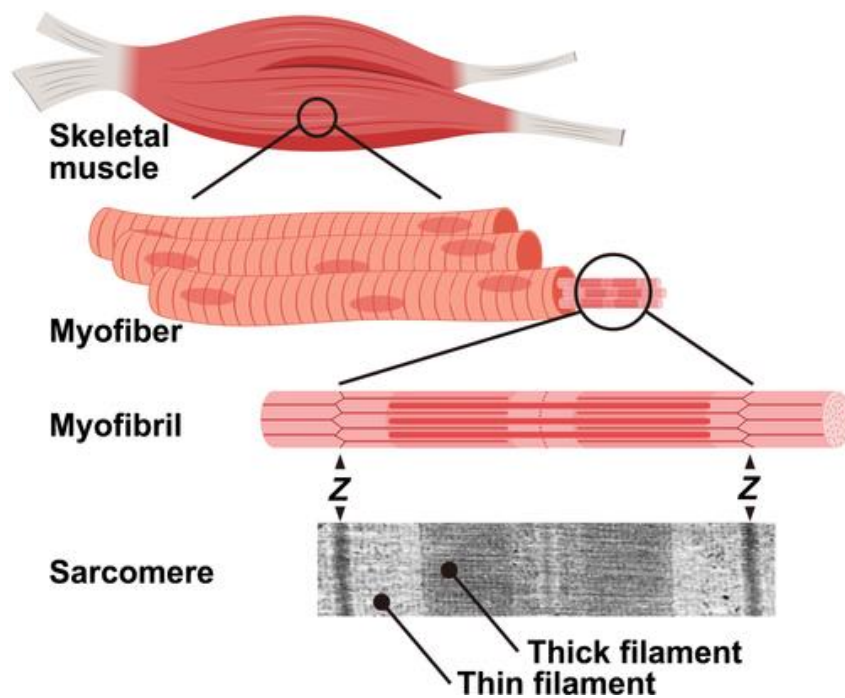


Figure 3: Structure and components of the myofibril in skeletal muscles.

Skeletal muscle tissue consists of bundles of myofibers. Myofibers contain millions of myofibrils each. Myofibrils are comprised of longitudinally aligned sarcomeres. The sarcomere consists of Z-bands, thin filaments, thick filaments and connectin/titin. Z-bands are indicated by "Z". A transmission electron micrograph of the sarcomere structure is shown at the bottom of panel. Connectin/titin is omitted in a model of "Myofibril". (Ojima 2019).

II. Embryogenesis and muscle differentiation

Skeletal muscle is the result of mesoderm's segmentation into somites. Each somite divides to give ventrally the sclerotome and dorsally the dermamyotome (Buckingham et al. 2003). The sclerotome forms the cartilage and skeleton, the dermamyotome gives the dermatome and myotome. The dermamyotome differentiates into skeletal muscle. In culture, the muscle precursor cells are also called myoblasts. Under the action of transcription factors such as MyoD, Myf5 and Pax3, myoblasts become activated and proliferate before differentiating and fusing into myotubes (Buckingham et al. 2003)(Buckingham et al. 2003). Myotubes differentiate into mature muscle fibers with peripheral nuclei and a central contractile apparatus (Figure 4). In human muscle, neuromuscular junctions provide innervation of muscle fibers by motor neurons. They form during the ninth week of embryonic development and allow transmission of the nerve message and muscle contraction (Robelin 1990).

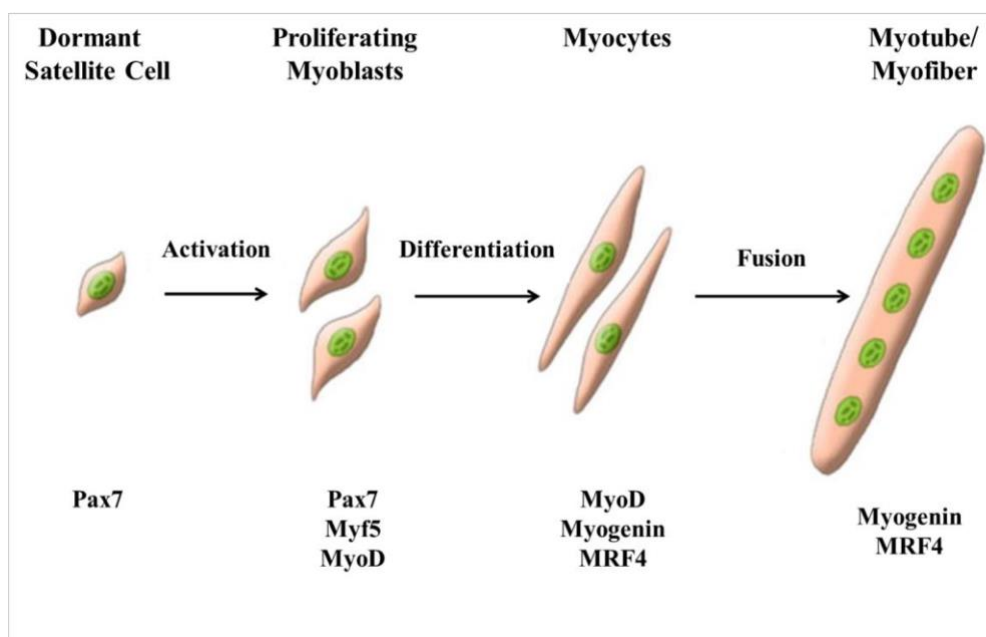


Figure 4: Schematic of adult myogenesis.

The process of adult myogenesis and the temporal expression of critical transcription factors are illustrated. Adapted from Le Grand & Rudnicki, 2007(Le Grand et Rudnicki 2007).

Myofibril formation within muscle fibers occurs in three stages. Pre-myofibrils are mini sarcomeres composed of thin filaments of actin, non-muscle type II myosin, and dense clusters of α -actinin that form so-called Z-bodies. During maturation, the nascent myofibrils recruit

titin and type II muscle myosin to form the thick filaments of sarcomeres. Eventually the myofibrils mature when the α -actinin clusters fuse to form the Z-band, the non-muscle myosin gives way entirely to muscle myosin II, the thin and thick filaments are aligned and the myofibrils are organized in the center of the muscle fiber. Myosin belongs to a superfamily of motor proteins; its activity depends on ATP (adenosine triphosphate) and allows for actin-bound mobility. It is composed of two myosin heavy chains (MHC) and two pairs of myosin light chains (MLC). MHC is expressed in four isoforms; a slow one called $\beta\beta$ -MHC and three fast ones called IIa, IIx and IIb-MHC. The distribution of MHC defines four types of fibers (slow or fast) expressing a single isoform and several hybrid fibers expressing both fast and slow MHC.

The heavy chains wrap around each other in a helical way. At least 300 myosin molecules are associated in an antiparallel way to form a 1.5 μ m long thick filament of 15nm in diameter. Myosin contains 2 globular domains, also called S1 or myosin heads that contain an actin-binding site and an Adenosine TriPhosphate (ATP) binding site (Figure 5).

MLCs associate with to the neck region of MHCs include essential light chains (ELC) and regulatory light chains (RLC). Three regulatory MLC isoforms are known in human: one slow called MLC1 and two fast called MLC1f and MLC3f (Schiaffino et Reggiani 1994).

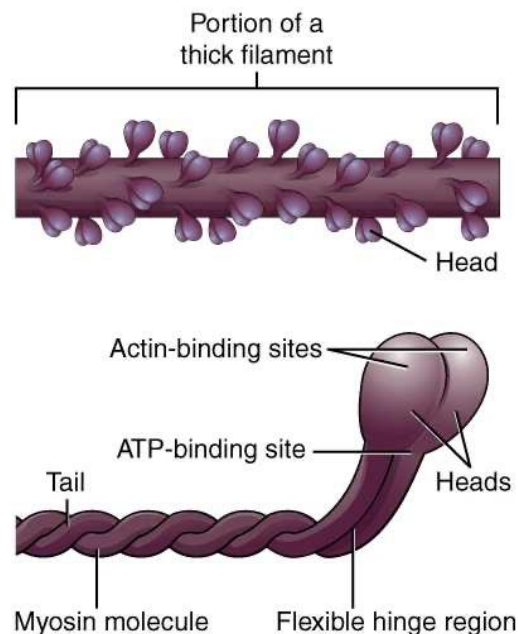


Figure 5 : Thick myofilaments composition.

Thick myofilaments composed of two heavy chains and four light chain molecules. The heavy chains consist of a tail region, flexible hinge region, and globular head which contains an Actin-binding site and a binding site for the high energy molecule ATP. (Adapted from (Biga et al., s. d.))

III. Satellite cells

Skeletal muscle has a high regenerative potential in case of injury or muscle pathology due to its ability to recapitulate the embryonic developmental program (Relaix et al. 2005). This phenomenon is possible due to muscle stem cells that were first observed in frog muscle by electron microscopy by Mauro in 1961. These cells also called satellite cells are located under the basal lamina in direct contact with the muscle fiber (Mauro 1961). They are multipotent and express the transcription factor Pax7 which is necessary for their specialization during development and their maintenance in the postnatal period.

It takes 3 to 4 weeks to a complete regeneration in human after muscle fiber injury (Mackey et Kjaer 2017). When the muscle is injured, satellite cells become activated, proliferate, and differentiate to form a new muscle fiber.

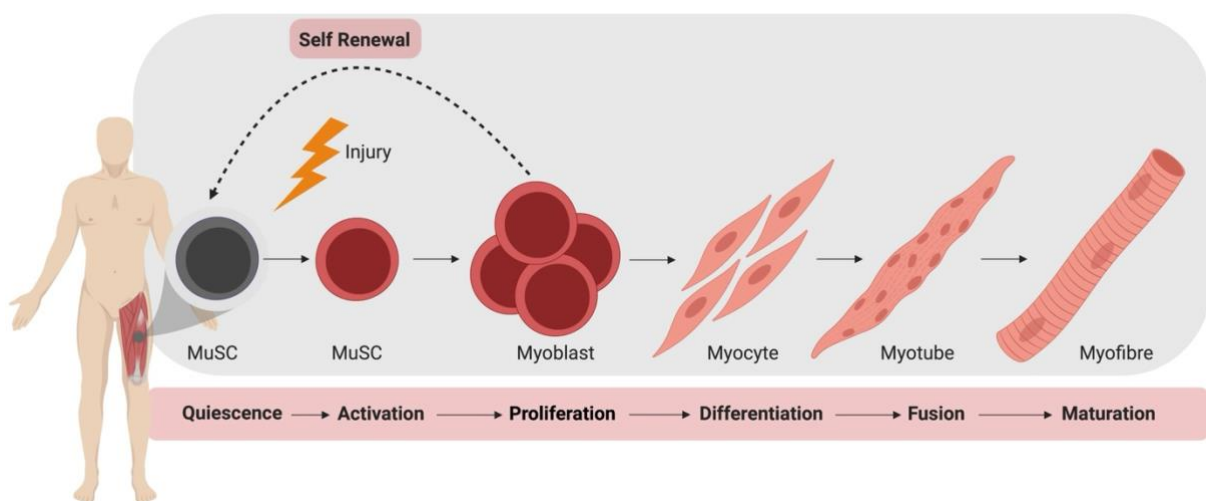


Figure 6: Muscle regeneration following injury.

Following injury, quiescent MuSCs are activated and start to proliferate rapidly (myoblasts), myoblasts fuse and start differentiation to form myotubes, which fuse and mature to generate new muscle fibers. (Nguyen et al. 2019).

A group of these cells return to quiescence to maintain the homeostasis of the stem cell pool and preserve the integrity of the muscle in case of further injury. Self-renewal of satellite cells is controlled by intracellular transcription factors as well as extracellular factors from the niche and the microenvironment. However, the capacity for self-renewal is limited, which explains the degeneration of the muscle under pathological conditions.

Muscle cell activation and differentiation is characterized by intermittent expression of specific myogenic factors. In particular, the expression of Myogenic factor 5 (Myf5) and Myogenic

Differentiation 1 (MyoD) is upregulated in the first few hours after injury. The ratio of Pax7/MyoD expression seems to determine the fate of the activated satellite cell (Olguin et al. 2007). The high ratio maintains the quiescent state, the intermediate one allows proliferation, the low one leads to differentiation. At the terminal stage of differentiation, Myogenin (MyoG), Myocyte enhancer factor-2 (Mef2) and Myf6 are expressed (Cornelison et al. 2000). In parallel, the removal of damaged muscle material by M1 macrophages takes place. Due to the fusion of satellite cells, regenerated fibers are characterized by a central localization of nuclei. The migration of nuclei occurs progressively in humans. In mice, the muscle regeneration process takes 3 weeks. In humans, the process requires at least 30 days muscle regeneration is an essential process for muscle repair after mechanical stress-induced injury.

IV. Mechanotransduction

i. Definition

Cells and tissues constantly need to sense and dynamically integrate multiple chemical and mechanical signals within the cellular microenvironment (Hansen, Moroishi, et Guan 2015)(Collinet et Lecuit 2021)(Vining et Mooney 2017). Mechanical forces are critical mediators of context-dependent cellular processes such as cell morphology, metabolic adaptation and growth, cell division, and cellular migration (Jansen et al. 2015) that in turn drive important biological processes such as stem cell differentiation, cancer progression and fibrosis (McBeath et al. 2004) (Engler et al. 2006)(Baker et al. 2015);(Przybyla, Lakins, et Weaver 2016). Mechanotransduction characterizes the process by which the cell integrates intracellular or extracellular mechanical signals and convert them into biochemical signals that trigger downstream cellular responses. Understanding how cells sense these biophysical stimuli and ultimately translate them into specific outcomes that affect the cellular function is essential for advancing the field and developing new therapeutic drugs.

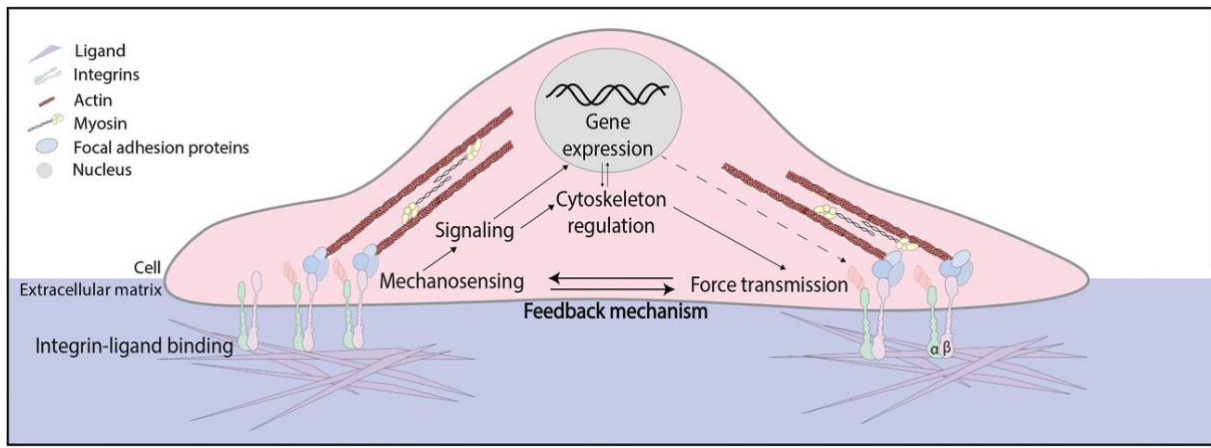


Figure 7: Mechanotransduction.

The extracellular matrix (ECM). Its structure makes it a key element in the initiation of mechanical stimuli on the cell. (Seetharaman et Etienne-Manneville 2018)

Materials can be categorized by how they change shape in response to mechanical loading, typically in a stress strain test. Mechanical stress is defined as the force per unit area, with units of Pascals (Newton/m², N/ m²) and can be in shear or normal. Strain is a normalized measure of deformation. Biological tissues and extracellular matrix (ECM) are not purely elastic materials, like a rubber ball or a spring. Rather, in response to a mechanical perturbation, they exhibit a time-dependent mechanical response and dissipate a fraction of the energy it took to deform them, a property called viscoelasticity.

Biomechanical parameters of the ECM differ according to the tissue type and can be altered by physiological and pathological conditions. Different types of externally applied stresses (i.e., compressive or shear forces) can convey to cells from their ECMs. In addition, cells interact with the ECM through dynamic processes that span a range of forces, from piconN up to hundreds of nanoN for individual cells and a range of timescales, from milliseconds to hours, leading to a complex time-dependent mechanical response of the substrates.

The elastic modulus, also called Young's modulus is defined as the ratio of the applied stress to the resulting strain in simple tensile geometry. It reflects the resistance to a deformation and is most often expressed in Pascal (Pa) or N/ μ m². It therefore reflects the macromolecular composition of this matrix and the nature of the cell-matrix interactions. Stiffness measurement can be done by indentation approaches (Rho et al. 1999).

With the biochemical microenvironment, all these physical parameters modulate the interactions of cells with ECM, resulting in cell mechanotransduction and impacting cell behaviors and the maintenance and fate of the organism's structures.

ii. Extracellular matrix

The ECM is composed of different proteins that can be grouped into 4 classes (R. O. Hynes et Naba 2012). I) Polysaccharides, which assure water retention by grouping together glycosaminoglycans; ii) glycoproteins, that contains adhesion molecules such as fibronectin and laminin; iii) fibrous proteins, which include collagen and elastin, and iv) the associated proteins such as growth factors and enzymes.

The ECM is continuously renewed through the synthesis of its constituents by specialized cells such as fibroblasts, abundantly present in connective tissue, or epithelial cells of the basal lamina (Bonnans, Chou, et Werb 2014) and through degradation provided by proteolytic enzymes, such as matrix metalloproteinases (MMPs).

In addition, during their assembly, ECM proteins can undergo post-translational modifications (PTMs) such as transglutamination, glycosylation, or cross-linking (R. O. Hynes et Naba 2012). The balance between ECM degradation and synthesis is dynamically regulated, and plays a primary role during development (Bonnans, Chou, et Werb 2014) , in angiogenesis (Marchand et al. 2019) or during tissue repair. ECM protein classes' proportion can vary greatly from tissue to tissue and the fibrous protein class is primarily responsible for the structure and the ECM elasticity due to its composition of collagen and elastic fibers.

In addition, the cross-linking levels of ECM proteins also influence its elasticity (R. O. Hynes et Naba 2012). As a result, stiffness will dynamically differ depending on the nature of the microenvironment.

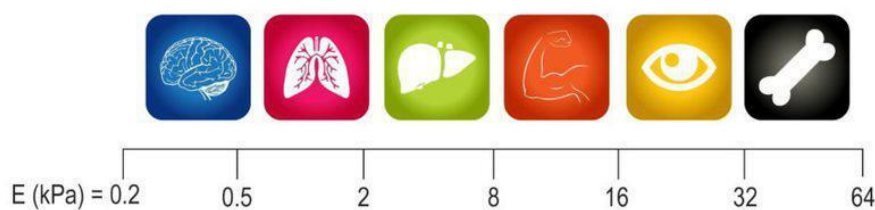


Figure 8: Matrix stiffness is a critical determinant of stem cell lineage specification.

Matrix stiffness for different types of cells. Brain tissue is very soft (~0.2 kPa), cartilage and bone tissue are very firm (>64 kPa) (Bagley 2020).

Tissues that are subject to significant mechanical stress, such as bones and muscles, have a highly organized fibrillar structure composed mainly of collagen, although possessing elastic properties. These tissues are thus highly resistant to stretching. The compliance of such ECM is thus generally very low, and the application of a high strain results in small deformation

(Boschetti et al. 2004). On the contrary, in tissues subjected to low mechanical stress, such as the brain, the ECM is rich in hydrophilic elements such as glycosaminoglycans with few fibrous elements (Mouw, Ou, et Weaver 2014). ECM from brain exhibits high compliance, and the application of the same stress results in large deformation (Hall et al. 2000). Importantly, the matrix stiffness is a critical determinant of stem cell lineage specification (Figure 8). Differentiation of muscle stem cells into myotubes is optimal at 12kPa, which corresponds to the normal muscle rigidity (Engler et al. 2006)

Figure 9 illustrates the different rigidities found in the human body.

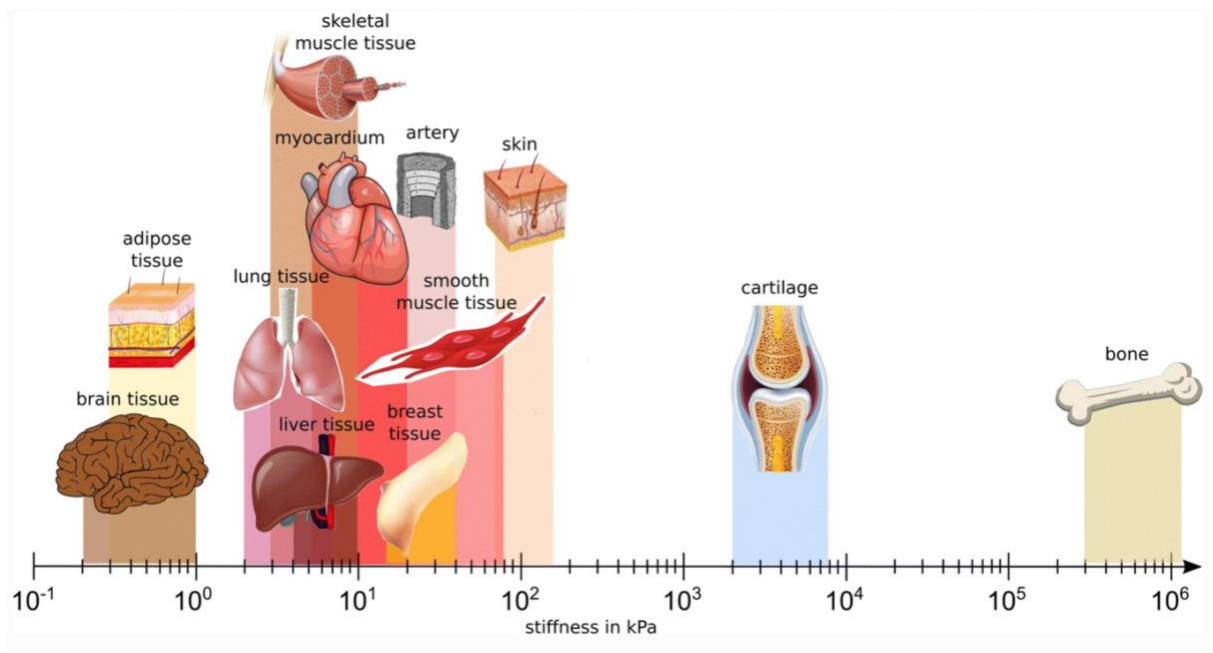


Figure 9: Mechanical properties of different human tissues.

Diagram representing the stiffness of different types of human tissues in KPa (Budday et al. 2020)

iii. The different types of forces

In addition to the physical properties of the ECM, the behavior of the cell can also be influenced by the external forces that are applied to it and by the forces it generates. Thus, depending on the tissue context, the cell can be subjected to different types of mechanical stress.

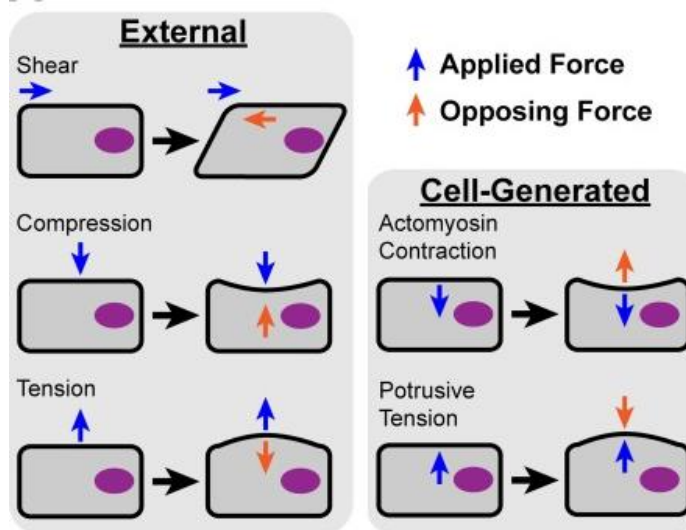


Figure 10: Schematic representation of forces exerted on cells.

Diagrams of external and internal mechanical forces applied to cells. Blue arrows represent the mechanical force applied on the cell. Orange arrows represent the balancing opposing force that coincide with the morphological response of the cell body. (Adapted from (Marjoram, Lessey, et Burridge 2014))

In the vascular system, for example, endothelial cells are subjected to parallel forces, called frictional forces, generated by the passage of blood (Dewey et al. 1981). Compression, whether anisotropic or hydrostatic is found within cells during division, during morphogenesis (Lancaster et al. 2013) or in tumor environments (figure 10). The shape of the arterial blood pressure waveform generate cyclic tension forces (the Windkessel effect), resulting in cell stretching (Belz 1995). Skeletal muscles can be subjected to different types of forces including cell stretching (Maganaris 2001), gravitational loading and forces generated by intrinsic muscle contraction. Indeed, muscles are the major force producing tissue in the human body. The molecular basis for muscle force production results from the cyclic interaction between the molecular motor, myosin II and actin filament. As already stated, at the microscopic level, contractile unit of all muscles is the sarcomere, which shortens using a sliding mechanism: bipolar myosin thick filaments pull themselves into cross-linked actin thin filaments and thus shorten the sarcomere (Huxley and Niedergerke, 1954; Huxley and Hanson, 1954). Coordinated contraction of all sarcomeres along a myofibril shortens the entire muscle and generate a mechanical force. It is important to remind that most relaxed muscles are under passive tension, even if they do not produce active contractile forces. This passive tension ensures that each myofibril spans the muscle fiber linearly, with a sarcomere length that is optimal for the next

active contraction. Titan (also called connectin), a gigantic elastic molecule that extends across half a sarcomere from the Z-disc to the M-line play a major contribution to this passive tension. In addition, cells can also generate tensile forces, through the contractility of their cytoskeleton. The forces generated by the cytoskeleton on the ECM was first demonstrated in the 1980's on fibroblasts grown on thin silicone elastomer films (Harris, Wild, et Stopak 1980). It was observed that endogenous cell tensile forces are strong enough to deform this film. These tensile forces are the result of the interaction between non-muscular myosin II and actin filaments. Different techniques aiming at dissociating better understanding the response of cells to these physical parameters have been developed. Micro-fluidic systems for instance allow to impose well-characterized friction forces on cells, by modifying the speed or viscosity of the fluid (Galbraith, Skalak, et Chien 1998). Stretching devices that can control both the percentage of cell stretch and the frequency allow to analyzed the effects tensile forces on cells or tissues (Kaunas et al. 2005). Finally, to study the effect of compression on cells, isotropic stress models such as multicellular spheroids (Sutherland 1988), or the use of AFM or rheometer for anisotropic models, have been developed (Stewart et al. 2013).

The following chapters deal more specifically with how this environment is perceived, transmitted, and transformed into a biochemical event, and how this environment will ultimately influence the behavior of the cell by modulating gene expression.

V. Structures involved in force transmission and mechanosensitivity

i. Integrin-mediated mechanotransduction

Many structures allow the transmission of mechanical forces to mechanosensitive proteins (Hoffman, Grashoff, et Schwartz 2011). These include macromolecules at the interface with the microenvironment such as extracellular receptors like integrins (Campbell et Humphries 2011), cadherins (Buckley et al. 2014) and other receptors such as proteoglycans found on endothelial cells, protocadherins, but also the plasma membrane. By linking the ECM to the intracellular cytoskeleton at adhesion sites, integrin-mediated adhesions are intrinsically mechanosensitive and present everywhere in the body.

Integrins are heterodimeric transmembrane receptors composed of an α and a β subunit. There exists at least 18 α subtypes and 8 β subtypes that can generate 24 different binding pairs,

allowing specialization of cell adhesions (Richard O. Hynes 2002) . Mechanical-induced conformational changes produce a shift between low- to high-affinity binding for ligands. Upon ligand binding, integrins are able to recruit various proteins that differ depending on the subcellular location of the adhesion structures and the tissue. Via integrins, mechanical stretch on integrins can activate cell proliferation, migration, and direct remodeling of the cytoskeleton. Major cellular and biophysical studies have focused on $\alpha5\beta1$ integrins. The change in conformation subsequent to mechanical stimulation promotes talin binding, bridging the actin cytoskeleton to focal adhesion sites (Martel et al. 2001).

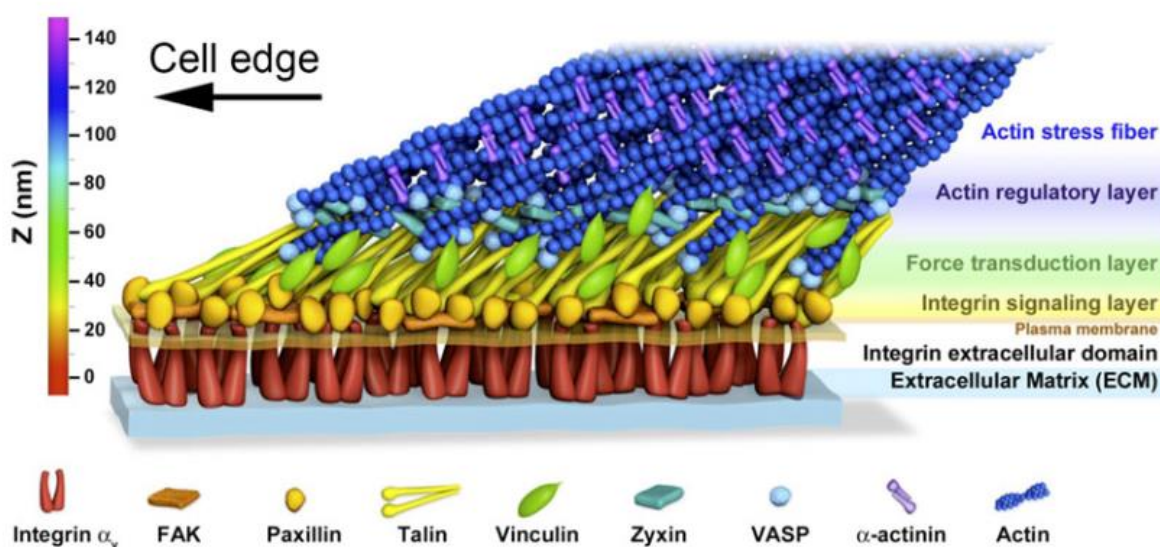


Figure 11: A model of focal adhesion molecular architecture.

A schematic model of focal adhesion molecular architecture based on iPALM analysis. Figure reproduced from Ref.(Burridge 2017)

The formation of focal adhesion is under the control of small GTPase Rho (Ridley et Hall 1992). The stabilized actin-integrin-talin complex then allows binding of signaling proteins to integrin tails, such as kinase family members Focal Adhesion Kinase (FAK) (Hildebrand, Schaller, et Parsons 1993), paxillin (Mofrad 2004), Src-family kinases (SFK), and zyxin (Beckerle 1997); (Yi et al. 2002) (Figure 11).

This network of proteins, called adhesome, acts as a scaffolding platform that strengthens the adhesion complex to support the transmission of mechanical stimuli from the ECM and plays a role in the perception of these stimuli through the recruitment of mechanosensitive proteins. Importantly, activation of these mechanosensitive proteins' controls, activates and modulates the formation of branched actin networks, Rho-Rock-dependent contractile actomyosin bundles

(Sun, Guo, et Fässler 2016) and vinculin-based protrusion and force generation (Hirata et al. 2014). In turn, remodeling of the actin cytoskeleton can have dramatic effects on cell regulation and transcriptional activity.

ii. Actin filaments

Actin is the most abundant protein in cells. Actin filaments (F-actin) can take two forms, mainly bundles, or networks, depending on regulatory proteins associated with microfilaments. Structurally, F-actin is formed by addition of globular actin (G-actin). Nucleation corresponds to the clustering of the first three G-actin monomers. The elongation of F-actin by polymerization occurs at the "barbed" or (+) end and dissociation into G-actin monomers take place at the "pointed" or (-) end (Campellone et Welch 2010)

The rate of actin polymerization and depolymerization depends on the activity of nucleators, myosin II and cap proteins that bind the ends of F-actin filaments. All these processes are finely regulated by signaling pathways and are mechanosensitive (Lessey, Guilluy, et Burridge 2012). Actin filament ranges from 5-9 nm in diameter and has 13 actin subunits between each cross-over point (produced by the 'crossing over' of the two long-pitch actin helices) (Hirokawa et al. 1982). Actin filaments can create a number of linear bundles of tens, hundreds, or even thousands of microfilaments, two-dimensional networks and three-dimensional gels that perform different functions.

Actin stress fibers enable cell adhesion while the presence of myosin enables contractility. Force generation by stress fibers is achieved in two potential manners: i) the polymerization of actin against the cell membrane : this allows the generation of force for the formation of membrane protrusions during, for example, migration ; and ii) the interaction of actin filament with non-muscle myosin II (Tojkander, Gateva, et Lappalainen 2012). A loosely organized subcortical network of actin forms the cortical actin. Bundles of actin can also form a number of protrusions like podosomes, lamellipodia, filopodia and membrane ruffles (Khurana et George 2011). The actors that crosslink actin filaments into bundles – or actin-bundling proteins – usually are small rigid proteins that force the filaments to align closely with one another. Projections of the plasma membrane like filopodia need tight, parallel bundles, organized by an actin-bundling protein like fimbrin. Contractile actin bundles are loosely arranged, allowing myosin proteins to take part in the bundle (Letort et al. 2015). Such an organization can be allowed by cross-linking protein α -actinin, a protein that belongs to the spectrin family and form an antiparallel homodimer with an actin binding head at the amino-terminus of actin

(Cooper et Schafer 2000). Alpha-actinin 1 is necessary for the attachment of actin myofilaments to the Z-lines in skeletal muscle fibers, and to the dense bodies in smooth muscle cells.

Migration fronts of motile cells are filled with a dense and complex network of branched actin. This network formed of actin filaments at 70-degree angles are organized by ARP2/3 proteins, an assembly of seven subunits, including two actin-related proteins ARP2 and ARP3 (Mullins, Heuser, et Pollard 1998)(Svitkina et Borisy 1999). ARP2/3 ATP-dependent activity is regulated by nucleating promoting factors when and where it is needed for endocytosis.

Four interdependent actin filaments with different compositions and signaling properties are typically described in motile cells (Figure 12):

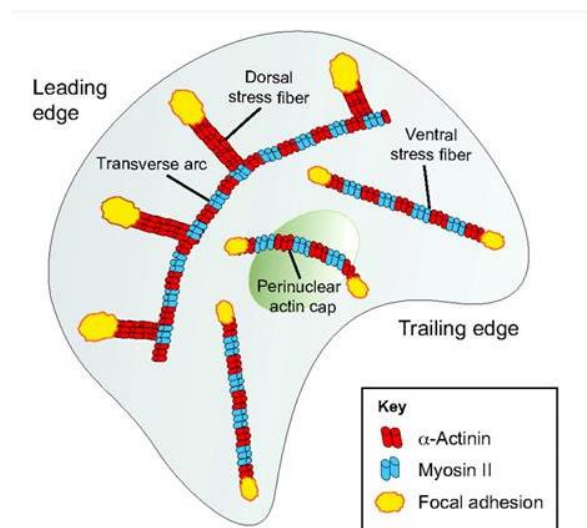


Figure 12: Schematic illustration of the stress fiber network in motile cells.

Schematic presentation motile mesenchymal cells including four stress fibers network. 1-Dorsal stress fibers, 2-transverse arcs, which are curved actomyosin bundles connected to focal adhesions through interactions with dorsal stress fibers; 3- ventral stress fibers, which are actomyosin bundles anchored to focal adhesions at both ends, and 4- perinuclear actin cap bundles, which resemble ventral stress fibers, but their central parts are located above the nucleus. Figure reproduced from Ref.(Tojkander, Gateva, et Lappalainen 2012).

- The dorsal fibers, particularly abundant in migrating cells and during cell spreading. These fibers are enriched in α -actinin but poor in non-muscular myosin II. They originate at the level of focal adhesions and polymerize towards the center of the cell (Hotulainen et Lappalainen 2006)(Upton et al. 2012).
- The transverse fibers, characterized by the presence of non-muscular myosin II. They arise at the lamellipodium/lammelar junction and extend centripetally from the cell periphery (Heath 1983)(Tojkander, Gateva, et Lappalainen 2012).

- The ventral fibers, predominantly present in slow and little moving cells. They are enriched in α -actinin and in non-muscular myosin II. They are connected to focal adhesions and arise from the fusion of dorsal and transverse fibers. They originate at the lamellipodium and move centripetally from the cell periphery (Heath 1983)(Tojkander, Gateva, et Lappalainen 2012).
- The perinuclear filaments, which are a sub-type of ventral fibers, are present specifically around the nucleus. Two sub-types of perinuclear filaments have been described: the actin cap and the actin lines associated with the nucleus (transmembrane actin-associated nuclear TAN lines). The actin cap is composed of thick parallel and highly contractile acto-myosin filaments, tightly connected to the nucleus, and attached to basal focal adhesion sites on both extremities (Khatau et al. 2009);(D.-H. Kim, Chambliss, et Wirtz 2013); (Chambliss et al. 2013). The perinuclear actin cap accumulates upon mechanical stimulation (D.-H. Kim, Chambliss, et Wirtz 2013);(Chambliss et al. 2013) and has important roles in nuclear mechanotransduction (Chambliss et al. 2013) ;(Shiu et al. 2018). The TAN lines which are perpendicular to the migration axis of mesenchymal cells (Luxton et al. 2011).

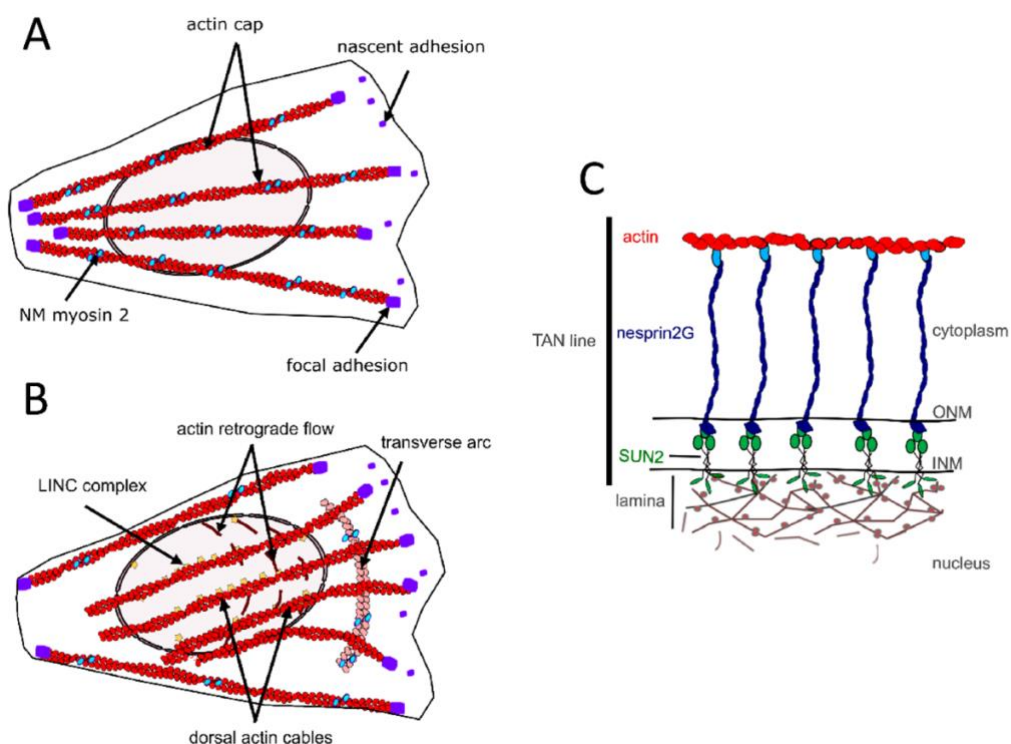


Figure 13: Components of the perinuclear actin network in muscle cell precursors (MCPs).

(A) Actin cap formed by dorsal stress fibers. (B) transmembrane actin-associated nuclear (TAN) lines. (C) Illustration of the molecular composition of a stress fiber. Illustration of the molecular composition of a TAN line. (Jabre, Hleihel, et Coirault 2021)

The actin cap is developmentally regulated, being present in myoblasts but absent in differentiated embryonic stem cells (Khatau et al. 2012) and terminally differentiated muscle cells (Roman et al. 2017). The structural and functional organization of actin cytoskeleton in the perinuclear region of myotubes remains to be precisely evaluated.

Myogenesis is characterized by extensive cytoskeletal reorganization associated with shifts in expression of actin components from non-muscle to muscle isoforms (Lloyd et al. 2004) (Sanger et al. 2016) (Hotulainen et Lappalainen 2006). Whereas actins γ and β that are present around the nucleus in myoblasts (Otey, C.A et al 1988) are downregulated, the muscle-specific isoform α -actin becomes predominant in terminally differentiated myofibers and localizes to the sarcomeric thin filaments (Bains et al. 1984) (J. J. Lin et Lin 1986). In myofibers, γ - and β -actins reside in the cortical cytoskeleton and at costameres (Pardo, Siliciano, et Craig 1983) (Rybakova, Patel, et Ervasti 2000); (Ervasti 2003). The costameric F-actin network is thought to contribute with other proteins to the radial transmission of contractile force outward from the sarcomere to the extracellular matrix, adjacent muscle fibers, and beyond (Ervasti 2003). This suggests that actin filament could predominantly transmit external forces toward the nucleus in muscle cell precursors whereas force direction could be predominantly internal and sarcomeric to external, toward extracellular matrix, in myofibers (Jabre, Hleihel, et Coirault 2021) (Figure13).

iii. The microtubules (MTs)

Microtubules are assembled from heterodimers of α and β tubulin into long hollow polymers that are ~ 25 nm wide and range in length from <1 μm to >100 μm (Pollard 2016). Microtubules have been proposed to contribute to mechanosensing due to their anisotropy (mechanical stress could be one of the main determinants behind the orientation of MTs) and their relative stiffness (Gittes et al. 1993). Indeed, MTs are three orders of magnitude stiffer than actin, IFs being the softness among the three major types of cytoskeleton filaments (Pegoraro, Janmey, et Weitz 2017). In addition, the bending stiffness of MTs allows them to maintain a given direction over large distance within the cell. Thus, the mechanical properties of MT make them well-suited to perceive cell-scale mechanical signals.

In muscle cell precursors, MTs exhibit a radial, centrosome-dominated distribution (Musa et al. 2003); (Becker, Leone, et Engel 2020) which may favor the transmission of external mechanical forces to the nucleus and influence nuclear shape (W. Wang et al. 2015) and function (Webster,

Witkin, et Cohen-Fix 2009). Muscle differentiation is associated with a large reorganization of centrosome proteins which are critical for MT nucleation and/or anchoring: during differentiation, pericentriolar proteins relocalization to the nuclear envelope (Becker, Leone, et Engel 2020) induces the redistribution of MT orientation into a more ordered paraxial array (Musa et al. 2003) (Becker, Leone, et Engel 2020)(Pizon et al. 2005). In mature myofibers, the perinuclear network of MTs, comprises cage-like structure of a high-density meshwork that may be responsible for nuclear shaping and mechanical protection. In addition, there is a circular and radial-anisotropic MTs, which are either polarized in the direction of contraction or in the lateral direction (W. Wang et al. 2015).

MTs could be modified by a high number of PTMs, affecting their function and organization. PTM can affect both the MT or the tubulin subunit (Barra et al. 1974);(Song et Brady 2015). MT post-translational modifications such as increased detyrosinated (Baldini et al. 2015); (Kreitzer, Liao, et Gundersen 1999) and binding of MTs to MT-associated proteins (MAPs), including EB1 and spectraplakine, confers stability to the MTs and are essential for maintaining myonuclear morphology (W. Wang et al. 2015). Moreover, defects in the spectrin domains of nesprin, which is associated with the nuclear networks of MTs induce myonuclear damage during contraction (W. Wang et al. 2015)(Gimpel et al. 2017)(Roman et al. 2017). This suggests that the spectrin domains of nesprin confers elastic features of the MT–spectraplakine–EB1 perinuclear network during muscle contraction (W. Wang et al. 2015).

iv. Cytoplasmic intermediate filaments (IFs)

Unlike actin filaments and MT, IFs proteins are not polarized. IFs share a uniform, global structure based on a common α -helical rod domain of approximately 310 amino acids. This common domain is flanked by head and tail domains of diverse size and structures characteristics of each IF proteins (Dutour-Provenzano et Etienne-Manneville 2021). Cytoplasmic IFs are derived from a common ancestor with the nuclear lamins from the loss of an NLS and a CAAX box motif that respectively target the lamin to the nucleus and the inner nuclear membrane. Cytoplasmic IFs assemble into a dimer through an interaction between their rod domains. Dimers assemble in an antiparallel manner to form soluble tetramers, which in turn assemble into unit length filaments (ULFs) that, via end-to-end binding, elongate into filaments with a standard diameter of approximately 10 nm (Dutour-Provenzano et Etienne-Manneville 2021).

IFs have emerged as a perfect candidate for maintaining proper nuclear mechano-response because they are able to resist high mechanical stresses, i.e., bending and stretching, to a considerable degree (Pegoraro, Janmey, et Weitz 2017);(Etienne-Manneville 2018). Indeed, IFs are surprisingly flexible (Block et al. 2015) (Fudge et al. 2003);(Mücke et al. 2005) ;(Wagner et al. 2007) and can undergo large strain-stiffening (Block et al. 2017), (Smoler et al. 2020). IFs can withstand deformations of up to 300% of their initial length without rupturing (Kreplak, Herrmann, et Aebi 2008). This property is attributed to the short persistence length of IF (1–3 μm) (Pegoraro, Janmey, et Weitz 2017). Cytoplasmic IFs can form mechanically networks, being able to crosslink to each other, to other cytoskeletal filaments, to membrane complexes, and to different organelles including the nucleus (S. Kim et Coulombe 2007) (Figure14).

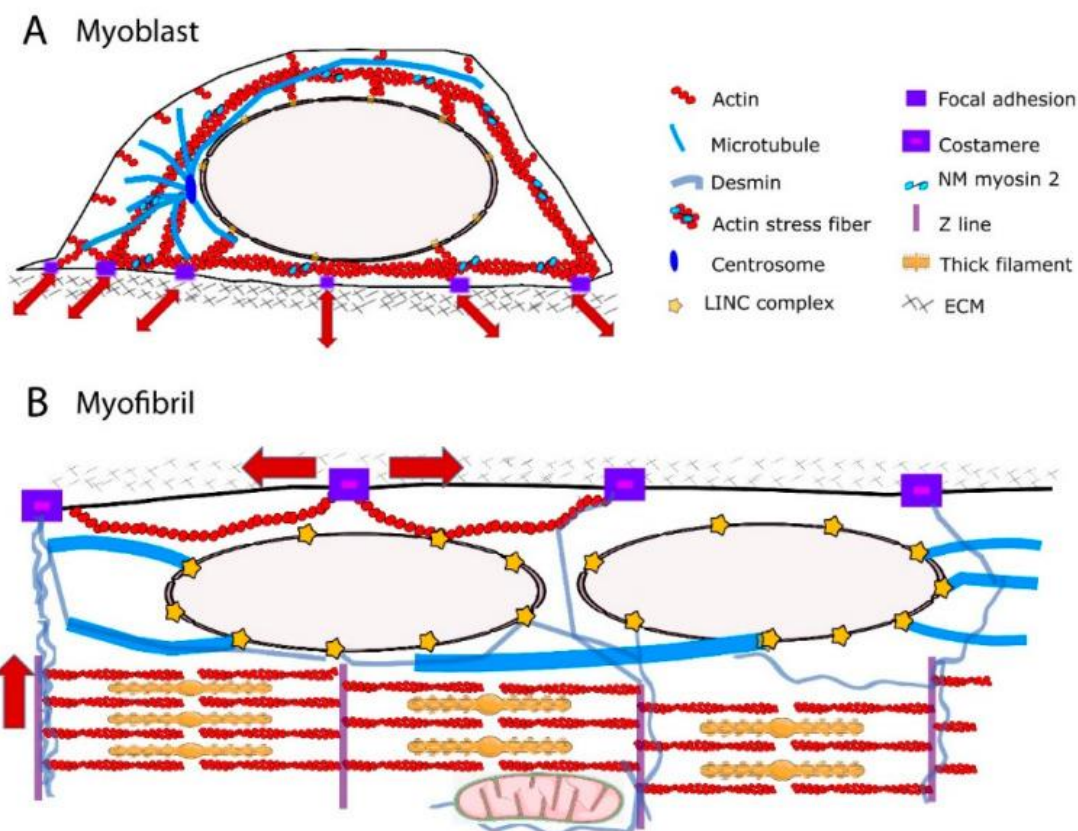


Figure 14: Schematic representation of cytoskeleton and force transmission in the myoblast and myofibril.

(A) Radial distribution of the actin, microtubule and intermediate filament (IF) networks in myoblast favors the transmission of extra- and intra-cellular forces (red arrows) to the nucleus. Direct connections between focal adhesions and the actin cytoskeleton transmit the force along actin fibers towards the nucleus. Reciprocally, intracellular forces can be transmitted from the cell interior to the extracellular matrix (ECM). Perinuclear cytoskeleton is tethered to the nucleus via Linker of Nucleoskeleton and Cytoskeleton (LINC) complex. (B) Paraxial arrays of F-actin, microtubules and IFs in myofibrils. Main directions of force transmission from the contractile apparatus to the ECM are indicated (red arrows). In skeletal muscle, contractile force can be transmitted laterally between the z-disks of neighboring myofibrils to the ECM through specific cell–matrix adhesions called costameres.(Jabre, Hleihel, et Coirault 2021)

As a consequence, a crucial role of IFs is to function as mechanical stress absorbers that protect organelles against large deformations (Y. Li et al. 2015);(Patteson et al. 2019),(Hu et al. 2019). Several IFs are expressed and developmentally regulated in human skeletal muscle cells (D Paulin et Li 2004);(Yassemi Capetanaki et al. 2007). Muscle cell precursors expressed vimentin and nestin, 2 cytoplasmic IFs that are downregulated during later differentiation (Sejersen et Lendahl 1993). Desmin, the muscle-specific IF protein is expressed at low levels in muscle cell precursors but progressively replaces vimentin and is commonly as a differentiation marker during skeletal muscle differentiation (Sejersen et Lendahl 1993)(E Lazarides 1976). Desmin binds to synemin, another non-muscle specific IF, around the α -actinin-rich Z-lines (Denise Paulin et al. 2020).

In muscle cell precursors, vimentin and desmin are stably linked to the outer nuclear membrane (Mermelstein et al. 2006) via the cytoskeletal linker protein plectin (Wilhelmsen et al. 2005), thus contributing to the perinuclear cage-like structure. In mature myofibers, desmin is organized into a three-dimensional network around the contractile apparatus, the extracellular matrix, and other cell organelles such as mitochondria, T-tubules, and nuclei (E Lazarides 1976; Elias Lazarides 1980)(Y Capetanaki 2002),(Reipert 1999).

As for all IF proteins, cytoplasmic IFs could be modified by PTMs, including phosphorylation, sumoylation, acetylation and ubiquitination that affect the dynamics, mechanics and biochemical properties of the resulting filaments. Phosphorylation and ADP-ribosylation of desmin occurs during muscle differentiation(Winter et al. 2014) which in turn regulate IF assembly and disassembly as well as interactions between IFs and other cell components and structures (Snider et Omary 2014).

In mature muscle fibers, the primary role of desmin is to link adjacent myofibrils to each other and to the ECM, via costameres (Gao et al. 2015)(Boudriau et al. 1993). Consequently, a functional reduction in desmin is associated with structural instability of the sarcomeres (Z. Li et al. 1996). Accumulating evidence indicates that desmin is also crucial as a stress-transmitting and stress-signaling network (Elias Lazarides 1980)(Price 1984)(Galou et al. 1997)(Tolstonog, Sabasch, et Traub 2002)(Boriek et al. 2001). Finally, desmin interactions with the nucleus are required to maintain nuclear architecture in cardiomyocytes (Heffler et al. 2020) and to prevent nuclear and muscle damage in response to mechanical challenges, (Langer et al. 2020);(Charrier et al. 2018). Future studies are required to precisely determine the contribution of desmin scaffolds in myonucleus architecture and function.

v. Nuclear envelope and LINC complex

The nuclear envelope (NE) is made up of the two nuclear membranes, the inner nuclear membrane (INM) and the outer nuclear membrane (ONM) that fuse at the nuclear pore complexes (NPCs). The NE is a specialized compartment that physically separates the nucleus from the cytoplasm. In addition to its role as a physical barrier, the NE regulates many cellular functions: it provides an interface between the nuclear interior, the various cytoskeletal elements, and the extracellular environment. It also regulates the nucleo-cytoplasmic transfer of proteins and is involved in several other cellular functions such as chromatin organization, DNA repair, and nuclear assembly/disassembly (Burke et Stewart 2013).

The INM and the ONM fuse around nuclear pores to form large transmembrane protein complexes, nuclear pore complex. NPC is made of proteins called nucleoporins (Nups). NPC includes a cytoplasmic ring, an inner ring, and a nucleoplasmic ring these 3 dense rings ensure the bidirectional circulation of molecules by active and passive diffusion. It has a diameter of about 100 nm and a height of 70 nm (Eibauer et al. 2015).

NPC allow ions and metabolites diffusion and even macromolecules diffusion. However, some small proteins such as histones, benefit from a facilitated transport (Lyman et al. 2002).

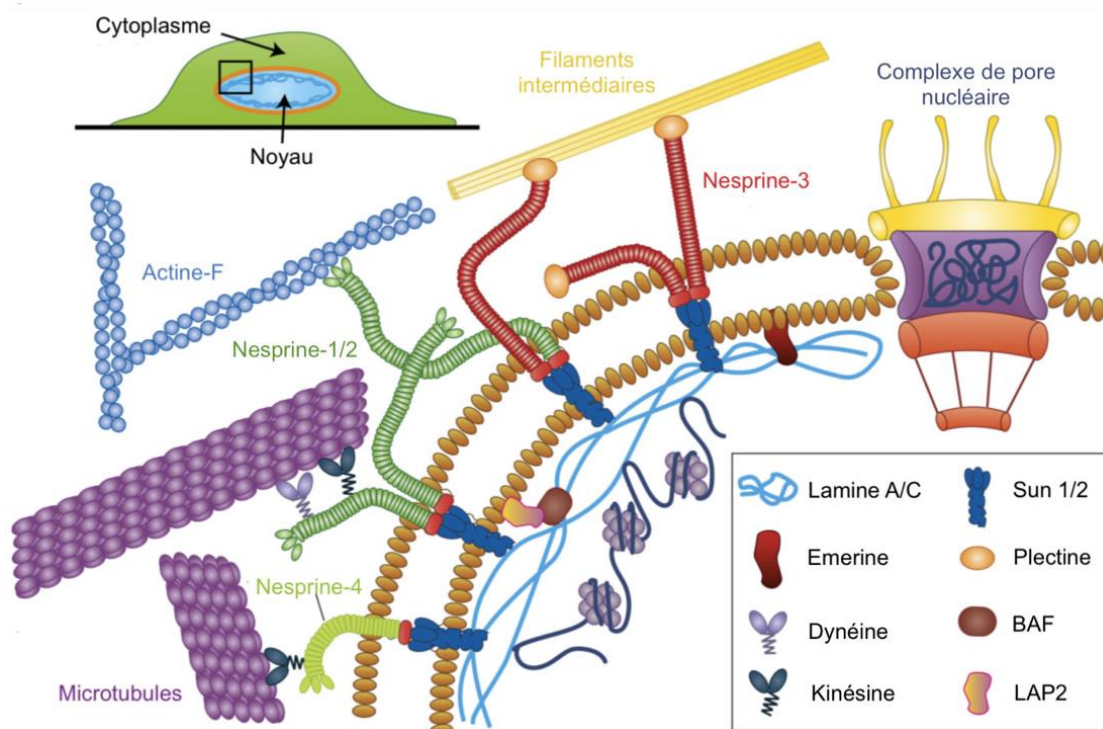


Figure 15: Schematic overview of nuclear envelope proteins involved in force transmission to the nucleus

Force transmission to the nucleus involves interaction of cytoskeletal elements (actin filaments, intermediate filaments, microtubules) with nesprin proteins on the ONM that transmit force through SUN domain proteins on the INM to the nuclear lamina and interior. Figure reproduced from ref (Kirby et Lammerding 2018)

The LINC complex is a group of proteins that provides direct physical coupling between the cytoskeleton and the NE. The LINC complex comprises outer nuclear transmembrane proteins, called nesprins (NE Spectrin-Repeat Proteins) defined by the Klarsicht-ANC1-Syne homology (KASH) domain proteins. This domain directly interacts with luminal domain of the INM proteins Sad1 and Unc-84 (SUN) proteins 1 (SUN1) and 2 (SUN2) within the perinuclear space of the nuclear envelope. KASH-domain proteins bind in the perinuclear space to SUN proteins and interact with the cytoskeletal filaments. The SUN proteins, anchored in the INM, interact with lamins and nucleoplasmic components.

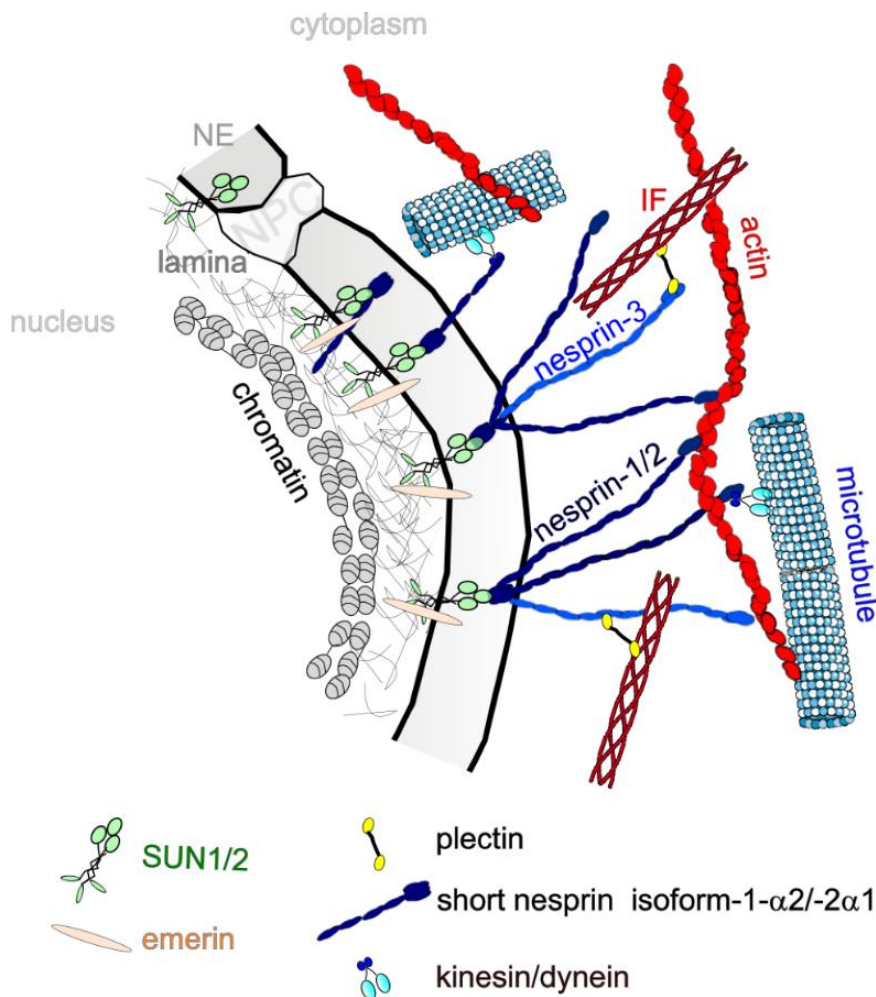


Figure 16: LINC complexes in skeletal muscle.

LINC complexes in skeletal muscle. LINC is a complex of proteins including SUN1/2 and nesprins that connect the cytoskeleton to the nucleoskeleton. Different nesprin isoforms are expressed during myogenesis: in MCPs, nesprin-1G and -2G can interact with actin and microtubules in the cytoplasm and with SUN1/2 proteins, emerin and lamins, on the inner nuclear membrane. Shorter nesprin-1 α 2 and nesprin-2 α 1 are expressed during myotube differentiation and can bind with microtubules in the cytoplasm via kinesin and other proteins such as A-kinase anchoring protein. Short nesprin-1 α 2 can also interact with intranuclear proteins such as lamins and emerin. INN: inner nuclear membrane; ONM: outer nuclear membrane (Jabre, Hleihel, et Coirault 2021).

SUN proteins are type II transmembrane proteins. They anchor to the INM by their transmembrane domain. In humans, 5 isoforms of SUN proteins exist (SUN1 to SUN5). SUN1 and SUN2 are ubiquitous while SUN3, SUN4 and SUN5 have more restricted expressions and are found almost exclusively in the male germline (Yeh et al. 2015). SUN proteins anchor the membrane with their C-terminus and their N-terminus extends into the nucleoplasm where they bind with lamins (Haque et al. 2006) and chromatin (Turgay et al. 2014).

SUN proteins have superhelix domains (CC1 and CC2) that give them a trimeric structure. These superhelical domains act as molecular spacers between the INM and ONM, allowing the nuclear envelope lumen to maintain its width (40-50 nm).

SUN proteins interact with KASH-domain proteins. SUN1 and SUN2 proteins are covalently linked with nesprins via a disulfide bridge between the N-terminal cysteine residue of the KASH peptide and a cysteine in the SUN domain. This interaction is important for stabilizing the SUN2 complex with nesprin-2 in response to tension forces (Jahed, Shams, et Mofrad 2015).

To date, six genes encoding for different nesprins-1, -2, -3, -4 lymphoid-restricted membrane protein (LRMP) and KASH5 have been identified in mammals. Nesprins-1 and -2 are ubiquitously expressed with highest representation in striated muscle (Randles et al. 2010) (Holt et al. 2019). The *SYNE-1* and *SYNE-2* genes encode the giant proteins nesprin-1 (1008 kD) and nesprin-2 (792 kD) respectively, with calponin domains at their N-terminals that bind the actin cytoskeleton (Q. Zhang et al. 2001). Nesprins-1 and -2 also bind to the molecular motors dynein and kinesin via their the cytoplasmic stretch (Starr et Fridolfsson 2010)(M. H. Wilson et Holzbaur 2015)(Chapman et al. 2014). *SYNE-1* and *SYNE-2* have multiple internal promoters giving rise to shorter nesprin isoforms which lack the actin-binding domain (Bone et Starr 2016).

Together the LINC complex and A-type lamins plays crucial roles in mechanotransduction, nuclear positioning and chromatin organization. As we will see later, the LINC complex is essential in the transmission of mechanical forces from the outside to the inside of the nucleus (Arsenovic et al. 2016) and in the anchoring and positioning of the nucleus in the cell during migration (Arbach et al. 2018);(Kutscheidt et al. 2014). Finally, among these known functions, the LINC complex, and more specifically the SUN1 and SUN2 proteins, are involved in DNA damage response. It has been shown that these proteins interacted with DNA repair players, such as DNA- dependent protein kinase (Lei et al. 2012) and play a role, in cooperation with microtubules, in bridging double-stranded DNA breaks (Aymard et al. 2017);(Lottersberger et al. 2015).

vi. Lamins

The nuclear lamina is a filamentous 10-30 nm thick network of proteins located just beneath the NE. It is mainly composed of A- and B-type type V IFs, with associated proteins such as LINC complex and an amazing number of NE transmembrane proteins (NETs) and other lamin-binding proteins.

The nucleoskeletal network anchors to the INM, NPCs, and peripheral heterochromatin (Figure 17) (T. Dechat, Gesson, et Foisner 2010);(Kittisopikul et al. 2021),(Tatli et Medalia 2018)) to influence mechanical cues and signaling pathways crucial for cellular proliferation and differentiation (review in Osmanagic-Myers S 2015(Osmanagic-Myers, Dechat, et Foisner 2015). Lamins primarily localize to the NE but a small fraction mainly of the more soluble A-type lamins are found in the nucleoplasm (Thomas Dechat et al. 2008). In addition, lamins are involved in the epigenetic regulation of chromatin with drastic consequences for gene regulation (see below).

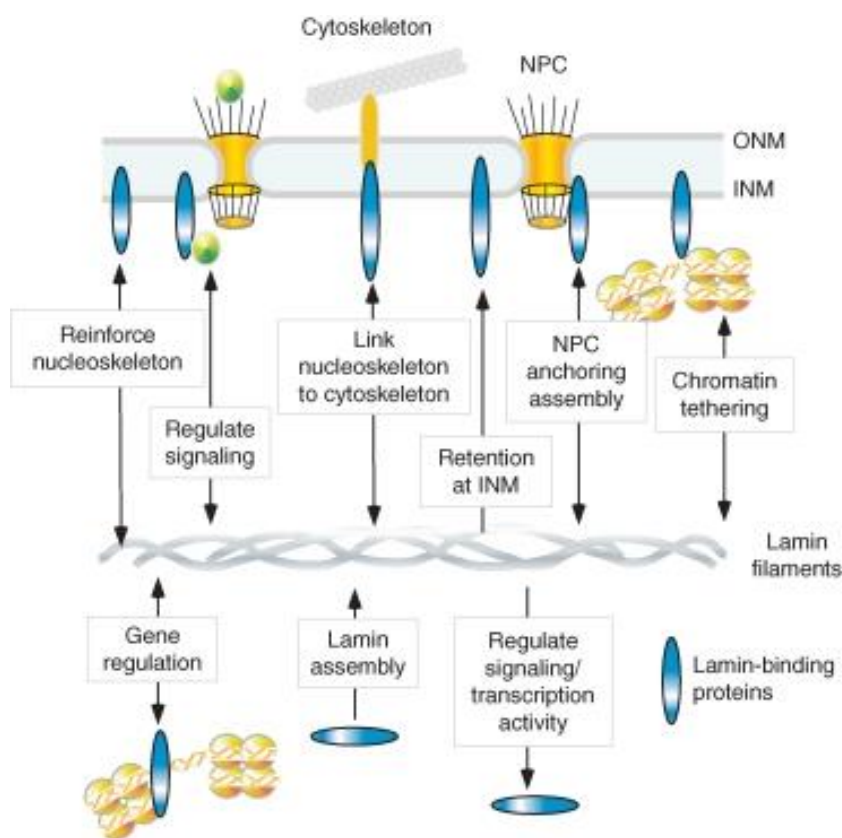


Figure 17: Role of lamins and lamin-associated proteins (LAPs) in nuclear function.

The INM, on chromatin, and in the nucleoplasm are thought to have mechanical and structural roles, such as reinforcing the nucleoskeleton, interlinking the nucleoskeleton and cytoskeleton, anchoring NPCs, and tethering chromatin to the nuclear envelope. Others regulate signaling or transcription.(K. L. Wilson et Foisner 2010)

Many lamin-binding proteins are thought to have mechanical and structural roles, such as reinforcing the nucleoskeleton, interlinking the nucleoskeleton and cytoskeleton, anchoring NPCs, and tethering chromatin to the nuclear envelope. Others regulate signaling or transcription(K. L. Wilson et Foisner 2010).

A- and B-type lamins are classified based on their structural and biochemical criteria (Gerace et Blobel 1980). A type lamins include the A, C, AΔ10 and C2 isoforms encoded by the *LMNA* gene (F. Lin et Worman 1993) (Wydner et al. 1996). B-type lamins are ubiquitous expressed and include lamin B1 and the B2 isoforms which are encoded by the *LMNB1* and *LMNB2* genes, respectively (Feng Lin et Worman 1995). B-type lamins have an important role in nuclear shape (Lammerding et al. 2006) (Coffinier et al. 2011) and structure (Turgay et al. 2017) (Dahl et al. 2004) (Shimi et al. 2015) and may provide nuclear elastic resistance (Dahl et al. 2004), particularly in cells with low A-type lamins (Lammerding et al. 2006) (Coffinier et al. 2011) (Swift et al. 2013a). This could explain its essential role in development. B-type lamin expression differs minimally across solid tissues or in response to matrix stiffness (Buxboim et al. 2017). B-type lamins do not appear to play a major role in nuclear stiffness (Lammerding et al. 2006).

Lamins A and C, the predominant isoforms of A-type lamins, are alternatively spliced products of the *LMNA* gene and are expressed in most differentiated cell types (Stephens et al. 2017; Shimi et al. 2008; Thomas Dechat et al. 2008; Moir et al. 2000). They play important roles in chromatin organization and gene expression through binding to both hetero- and euchromatic genomic regions and promoters subdomains (Naetar, Ferraioli, et Foisner 2017) (Pascual-Reguant et al. 2018). A-type lamins are completely soluble during mitosis, whereas lamins B1 and B2 remain associated with nuclear membranes (Meier et Georgatos 1994).

As already stated, lamins share similar protein domains with other IF proteins (Gruenbaum et Aebi 2014). As keratins (types I and II), desmin and vimentin (type III), and neurofilaments (type IV), lamin monomers are composed of an N-terminal head domain, a coiled-coil central rod domain, and a C-terminal globular tail domain. The central coiled coil (rod) domain composed of four α -helical subdomains (coils 1A, 1B, 2A, 2B) that are separated by flexible linker regions (Figure 18).

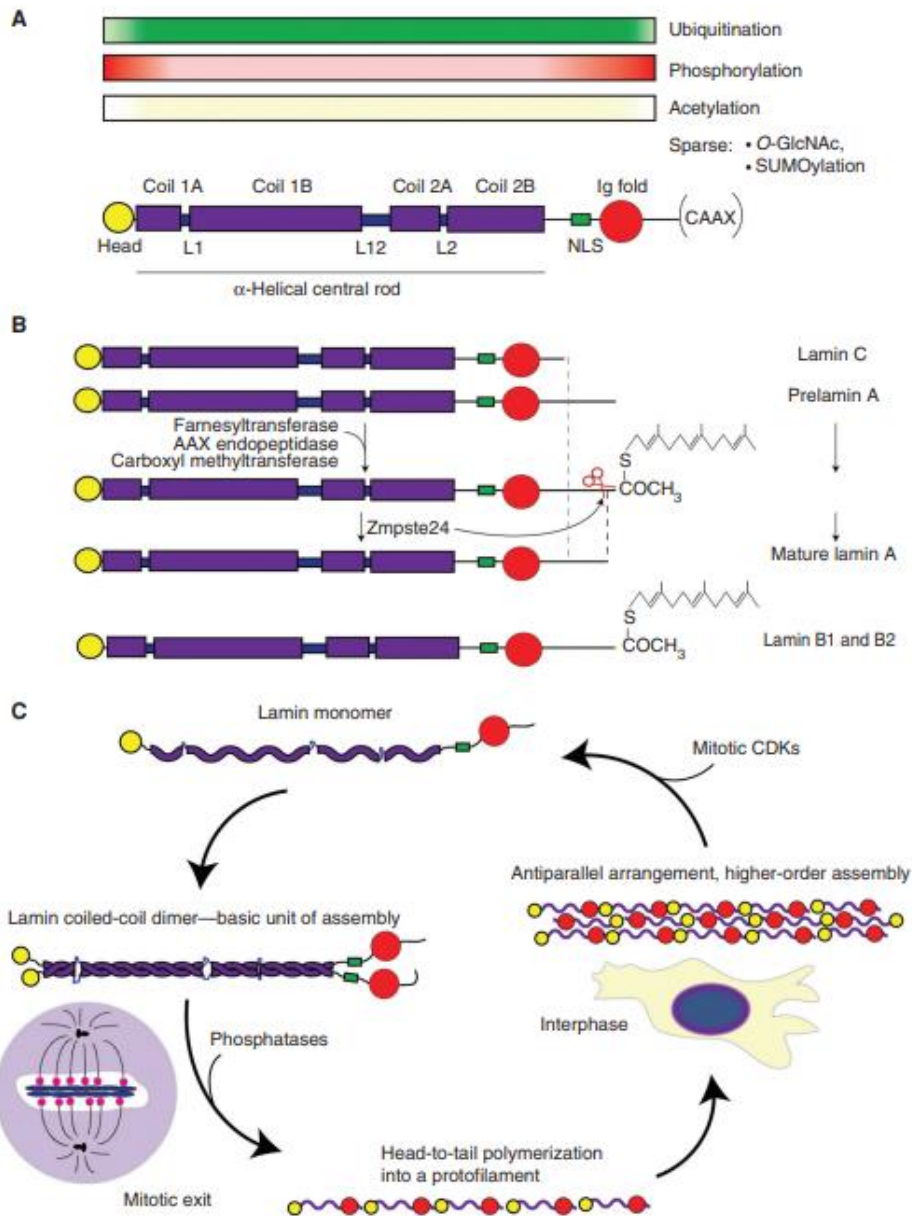


Figure 18: Assembly, processing, and regulation of lamins.

(A) The general structure of a lamin protein, consisting of a short unstructured head domain (yellow), a central α -helical rod domain comprised of four helical subregions (coils 1A, 1B, 2A, and 2B in purple) interspersed by unstructured linkers (L1, L12, and L2), a tail region that includes a nuclear localization signal (NLS) (green), an immunoglobulin-fold domain (Ig-fold) (red), and a fairly unstructured carboxy-terminal end that in most cases terminates with a carboxy-terminal CAAX motif. Also shown are potential posttranslational modifications (PTMs) ubiquitination, phosphorylation and acetylation. The color intensity is proportional to the probability of finding the PTMs. (B) Farnesylation of LMNA and LMNB1/2 at the cysteine residue of the –CAAX motif and the removal of the last three amino acids by means of an AAX endopeptidase and finally carboxymethylation via carboxyl methyltransferase. Removal of the farnesyl group of LMNA and the 15 most carboxy-terminal residues by the protease Zmpste24, rendering a fully functional and mature, lamin A protein. (C) Depicts principles of lamin assembly and their regulation through the cell cycle. Lamin coiled-coil dimer formation. Phosphorylation of lamin filaments localized at the nuclear lamina by cyclin-dependent kinase 1 (CDK1) during cells mitosis. Image derived from (Wong, Melendez-Perez, et Reddy 2022)

Lamins have six additional heptad repeats in their central rod domain (Worman 2012). The rod is flanked by an N-terminal (head) domain and a C-terminal (tail) domain containing lamin-specific motifs. The unique features of lamins are a nuclear localization signal (NLS), an immunoglobulin (Ig)-fold domain with a diameter of 3.5 nm (Turgay et al. 2017) and a CaaX motif (C, cysteine; a, aliphatic residue; X, any amino residue) that is present in lamins A, B1, and B2 but not lamin C (Figure 19).

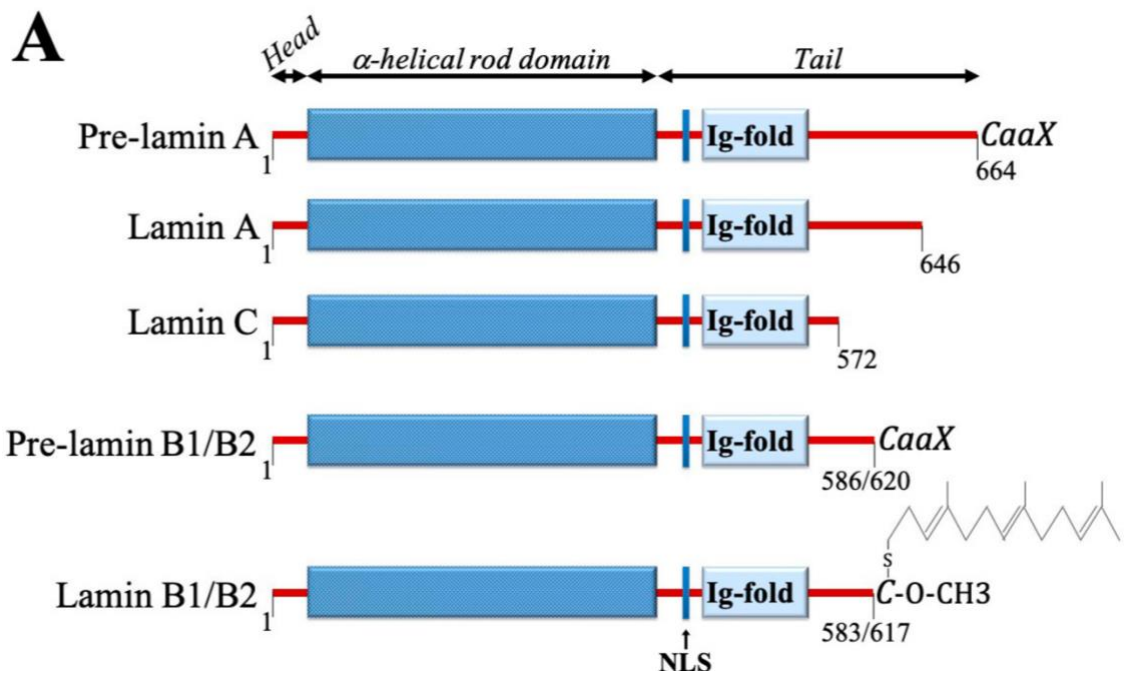


Figure 19: Nuclear lamins composition.

Schematic diagram of domain composition and the presence of CaaX motif in nuclear lamins. NLS, nuclear localization signal. The images derived from (Blank 2020).

The fundamental soluble unit of lamins is a dimer assemble in a head to tail way (Figure 20). The lamin assembly is based on based on specific associations of the elementary dimers in two directions: the lateral (side-by-side) and longitudinal (head-to-tail). Interestingly, lamin assembly is known to proceed quite differently compared to cytoplasmic IFs.

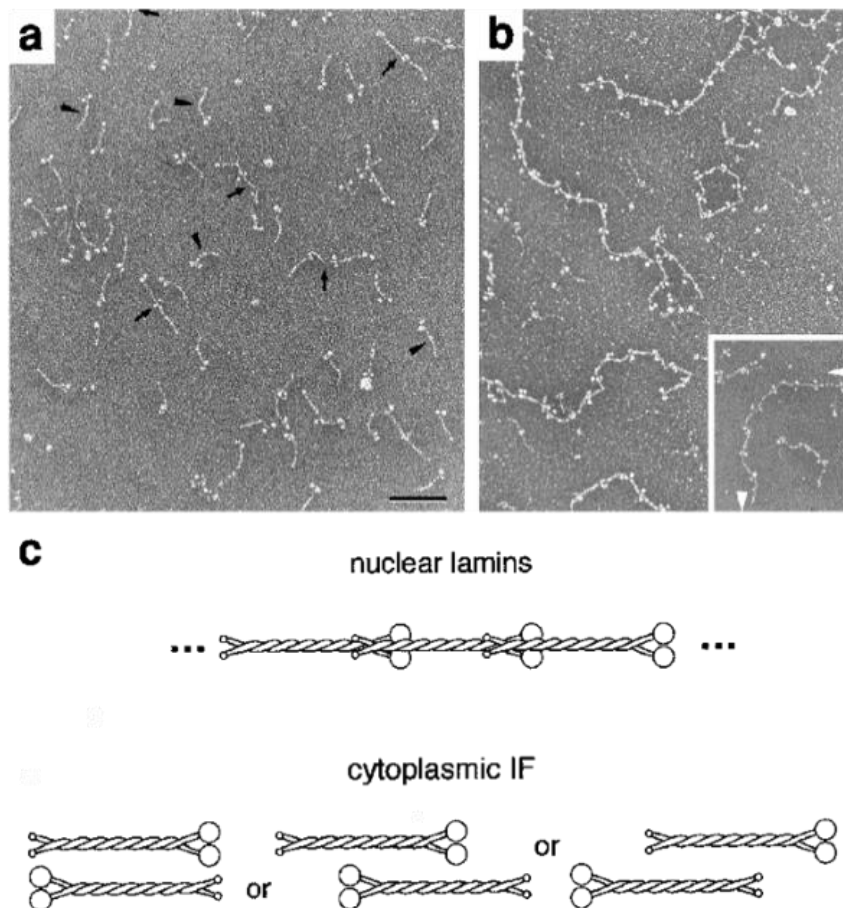


Figure 20: Assembly of lamion dimers.

(a) into linear head-to-tail polymers (b). For transmission electron microscopy, Bar, 100 nm (c) Schematic models of nuclear lamin and cytoplasmic IF protein dimers to associate into higher order. Ref (Stuurman, Heins, et Aebi 1998)

Different lamin assembly models have been proposed based on low resolution and fragmented structures (Ahn et al. 2019). Initially, assembly model with 2–4 nm overlap between the dimers emphasizes the head-to-tail interaction between the dimeric units of lamin (Kapinos et al. 2010). Recently, a cryo-electron tomography (cryo-ET) study revealed that lamins form 3.5-nm-thick filaments (Turgay et al. 2017) that are remarkably different from other canonical 10-nm thick IF proteins and the proposed assembly model of lamins (Kapinos et al. 2010). Recent data propose an anti-parallel arrangement of the two coiled-coil dimers, which is important for the assembly process and compatible with recent structural data of lamins (Ahn et al. 2019) (Figure 21).

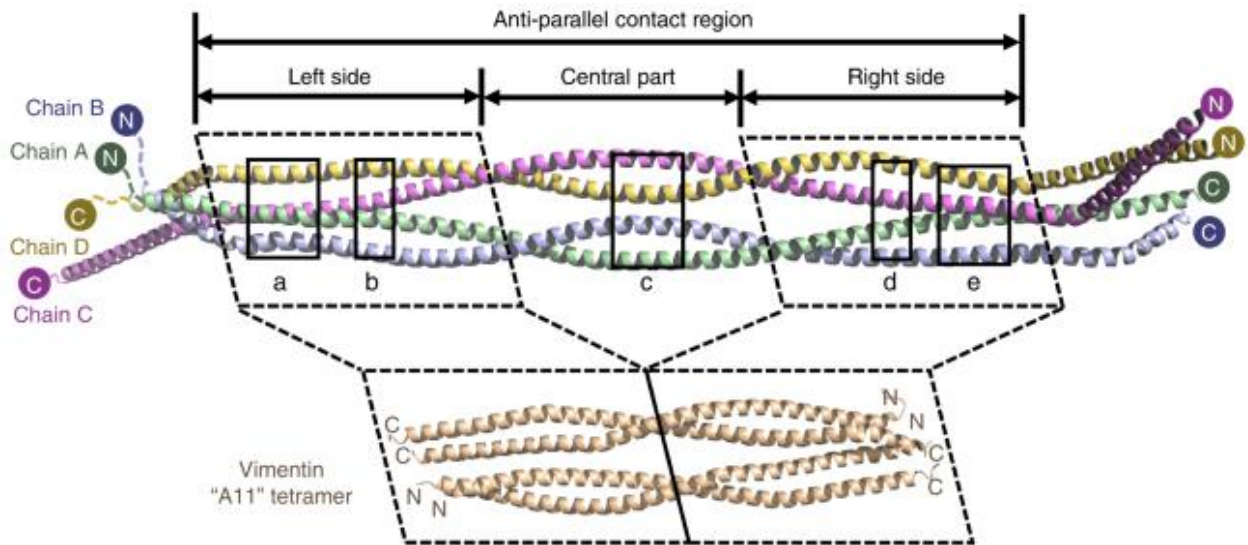


Figure 21: Structural comparison of the tetrameric structures of the lamin and vimentin.

Double-headed arrows indicate the anti-parallel contact region and its three compartments (left side, central part, and right side) of the lamin 300. Four chains (chains A–D) are in green, blue, violet, and yellow, respectively. Left and right-side parts of the lamin 300 fragment and vimentin are marked as dotted boxes. The N and C terminus of each chain is indicated by N and C, respectively (Ahn et al. 2019).

Lamins can undergo important PTMs, including addition of a farnesyl group, phosphorylation, SUMOylation and glycosylation (Snider et Omary 2014, Buxboim et al. 2014, Machowska, Piekarowicz, et Rzepecki 2015, Y.-Q. Zhang et Sarge 2008). The mammalian lamins B1, B2, and A are produced as pre-lamins with a CaaX motif at their C-termini. This motif undergoes sequential processing, which begins with farnesylation by farnesyltransferase to the cysteine residue and continues with cleavage of the last three amino acids by the zinc metalloendoprotease Zmpste24 (or FACE1). A methyl group is then added to the exposed cysteine by isoprenylcysteine carboxyl methyltransferase. Lamin A undergoes an additional cleavage of 15 amino acids upstream of the farnesylated and methylated cysteine by Zmpste24, that results in a lamin A. Mutations in either the *LMNA* or *ZMPSTE24* genes that fail to remove the farnesylated and methylated cysteine result in severe diseases such as Hutchinson–Gilford progeria syndrome.

Phosphorylations of A-type lamins on serines 22 and 395 by several protein kinases including Cdk1 are required during mitosis for mitotic disassembly of lamin filaments and nucleoplasmic localization. It has been shown that reduced nuclear stress, as occurred for instance by plating cells on soft substrates, increases Ser22 phosphorylation level (Buxboim et al. 2014). In addition, lamin A can also be phosphorylated on Ser390, Ser404, Thr424, and Ser652 residues

(Machowska, Piekarowicz, et Rzepecki 2015) Phosphorylation at Ser390 is modulated by the substrate stiffness.

Lamin A can also be modified by small ubiquitin-like modifier (SUMO) proteins in a covalent and reversible manner. Sumoylation of lamin A regulates filament formation and modulate solubility (Y.-Q. Zhang et Sarge 2008; Snider et Omary 2014). Mutations induced defects sumoylation have been implicated in the pathophysiology of Hutchinson-Gilford Progeria Syndrome (Sylvius et al. 2008) as well as in some lamin-related cardiomyopathies (Y.-Q. Zhang et Sarge 2008).

O-linked glycosylation is the enzymatic addition of β -N-acetylglucosamine (GlcNAc) by a single enzyme, O-GlcNAc transferase (OGT), to protein Ser/Thr residues (Hart et al. 2011). The functional role of lamin glycosylation is still unclear.

The level of A-type lamin is developmental and tissue specific. Importantly, the expression of A-type lamins correlates with tissue stiffness (Swift et al. 2013a), stiff tissues such as muscle having higher A-type lamin expression and stiffer nuclei than soft tissues such as brain (Figure 22) Moreover, the expression and stability of A-type lamins increase during myogenic differentiation (Lammerding et al. 2006), leading to nuclear stiffening (Pajerowski et al. 2007).

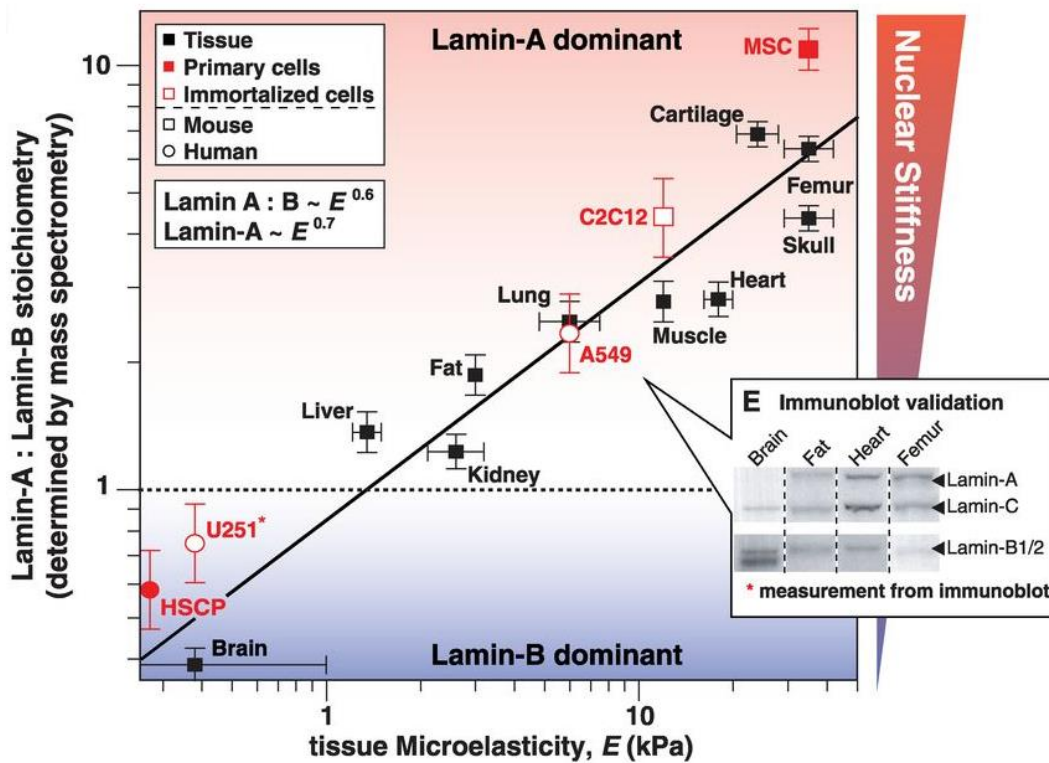


Figure 22: Lamin-A scales with tissue stiffness.

Quantitative proteomics of multiple human and mouse tissues and cells revealed scaling with E of the absolute ratio or stoichiometry of lamin-A to lamin-B through MS quantification of a pan-lamin peptide. Differences in ratios are significant with brain \ll liver $<$ fat $<$ heart, lung, and muscle \ll skull \ll femur and cartilage, where $<$ indicates $P \leq 0.05$ and \ll indicates $P \leq 0.01$. Nuclei with abundant lamin-A are stiff. Cultured cells showed the same trend as their primary source tissue. HSCP, human hematopoietic stem cell progenitors from marrow; U251, human glioblastoma cells from brain; A549, human adenocarcinoma epithelial cells from lung; C2C12, mouse myoblast cells from muscle; MSC, osteo-prone human mesenchymal stem cells from marrow. Figure reproduced from ref (Swift et al. 2013a)

NETs are tissue-specific NE proteins that interact or not with lamins (Wong, Melendez-Perez, et Reddy 2022). In addition to LINC proteins, well-studied lamin-interacting proteins (LAPs) include the LAPS/NETs containing a LEM (Lap2-emerin-Man1) domain that bind to BAF (barrier to autointegration factor), a chromatin protein. LAP2 (Lamin-associated polypeptide 2), emerlin, and MAN1 play fundamental roles in the nucleus, by interacting with INM-associated (T. Dechat 1998). LAP2a has several isoforms, one of these is nucleoplasmic and interacts with nucleoplasmic lamin A to modulate gene activation (Gesson et al. 2016). Interactions of LEM domain proteins with lamins are crucial for their correct localization at the INM (Holmer et Worman 2001; K. L. Wilson et Foisner 2010). LBR is an eight-pass transmembrane protein localized at the INM that contains a nucleoplasmic domain that codes

for a sterol reductase. LBR can bind to HP1 (heterochromatin protein 1) and PRR14 (proline-rich protein 14) and can interact with histones (Polioudaki et al. 2001; Hirano et al. 2012; Dunlevy et al. 2020).

Lamins have long been implicated in regulating the three-dimensional (3D) organization of chromatin, particularly via these heterochromatin domains found at the nuclear lamina (Figure 23, see also below). Indeed, heterochromatin is often located near the lamina at the nuclear periphery, around the nucleolus, and as patches throughout the nucleoplasm (Prasanth et al. 2005).

Lamin Associated domain (LADs) regions are large, AT-rich regions and are typically associated with gene silencing (Brown et al. 1997; Croft et al. 1999) (see below). LADs are enriched in developmental and lineage-specific genes, supporting the hypothesis that LADs are crucial for the organization and developmental control of gene expression. Interestingly, it has been proposed that active constraints on the NE are crucial for the geographic organization of LADs at the nuclear lamina (Falk et Hausmann 2020). In absence of nuclear lamina, heterochromatin tends to collapse into the nucleoplasm and forms an « inverted » type of chromatin organization (Falk et Hausmann 2020). Precise regulations between chromatin state, LAD organization and gene expression programs remain to be determined. However, the importance of LAD organization to maintain the lineage-specific epigenetic state is well established (Wong, Melendez-Perez, et Reddy 2022).

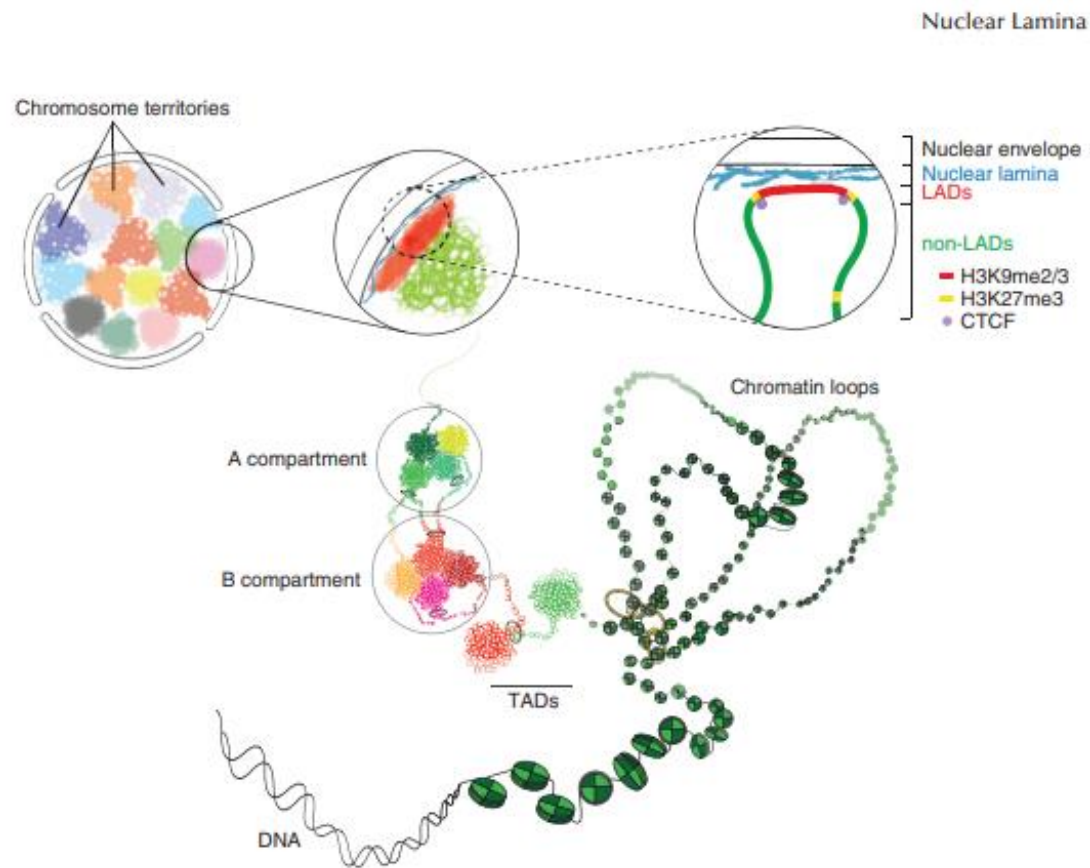


Figure 23: Schematic of the levels of chromatin folding within the higher-order 3D genome organization.

The DNA interacts with histone octamers and aggregates forming nucleosome arrays that are more or less compacted, depending on the histone variants present and the posttranslational modifications (PTMs) to their amino-terminal tails. The next level of organization is the formation of topologically associated domains (TADs) which in active chromatin domains are formed by loop extrusion via cohesin and stabilized by CCCTC-binding factor (CTCF). TADs segregate based on their transcriptional status into active A and inactive B compartments, with A compartments mostly occupying the nuclear interior and B compartments associated with transcriptionally repressive nuclear domains enriched in histone H3 lysine 9 di- and trimethylation (H3K9me2/3) and histone H3 lysine 27 trimethylation (H3K7me3) at the NE and the periphery of the nucleoli. The geographic organization of the B compartment to the nuclear envelope aids in the establishment and/or maintenance of interphase chromosome topology and hence overall genome organization. (Wong, Melendez-Perez, et Reddy 2022).

vii. Chromatin

In eukaryote cells, DNA is wrapped around histone proteins to form chromatin. Nucleosome, the basic structural unit of DNA packaging consists of a segment of DNA wound around an octamer of 4 histone proteins (H2A, H2B, H3 and H4) and resembles thread wrapped around a spool (Figure 24).

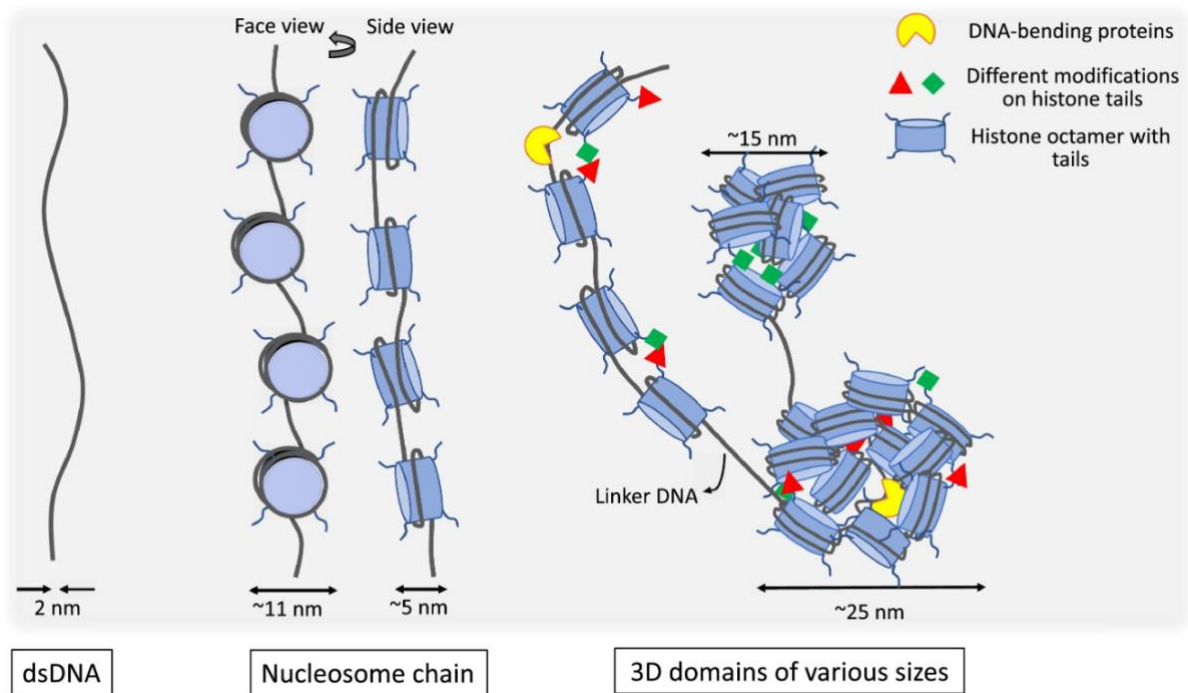


Figure 24: Chromatin organization.

Double-stranded DNA (dsDNA, black curve) is folded and wrapped around histone octamers (blue cylindrical disks with tails) to form a polymer made of nucleosomes having a width of 11 nm. This chain is further folded and arranged into many clusters (domains) of nucleosomes having variable cluster-sizes. Figure ref: (Parmar et Padinhateeri 2020)

The nucleosomes undergo reversible structural rearrangements through DNA unwrapping and rewrapping and histone core rearrangements, and they are subject to epigenetic modifications. Chromatin can be classified into heterochromatin and euchromatin, based on the condensation level during interphase. Chromatin condensation is crucial to regulate DNA accessibility: many DNA-templated processes including transcription involves packaging DNA in structures inaccessible to DNA-binding proteins (Grewal et Moazed 2003). Heterochromatinization then becomes one of the primary mechanisms used to silence chromosomal regions.

Histone modifications and DNA methylation are key epigenetic mechanisms that modulate chromatin structure and thus regulate gene expression programs controlling cell fate decisions and cell identity during development (Jaenisch et Bird 2003; Kouzarides 2007; Allis et al. 2007; Allis et Jenuwein 2016).

viii. Histone PTMs

Histones are subject to a vast array of PTMs including acetylation and methylation, (Kouzarides 2007; Allis et al. 2007). PTMs can alter direct interactions between histones and DNA and serve as docking sites for protein effectors, or readers, of these PTMs. Generally, reader proteins bind specifically to methylated histones and recruit or stabilize various components of the nuclear signaling machinery at specific genomic sites, mediating fine-tuning chromatin structure and function (Musselman et al. 2012).

Histone methylation occurs on numerous lysine and arginine residues in histones. Histone lysine methylation (me) can occur in the mono- (me1), di- (me2), or tri-methyl (me3) state, while arginine methylation is found in various symmetric and asymmetric mono- and dimethylated states. Depending on the residue modified, histone methylation is associated with either activation or repression. Trimethylation of histone H3 on lysine 4 (H3K4me3) and lysine 27 (H3K27me3) are two extensively studied histone modifications associated with transcriptionally active and repressed chromatin, respectively (Barski et al. 2007).

Heterochromatin is classically divided into constitutive heterochromatin, which mapped to pericentromeric and telomeric DNA regions and facultative heterochromatin. Constitutive heterochromatin is established early in development and anchors to the nuclear lamina. It is enriched for H3K9me2/3 (H3 lysine 9 di- and trimethylation) and HP1 proteins (Britten et Kohne 1968). Facultative heterochromatin is developmentally regulated. It is enriched for H3K27m3 and Polycomb (SET domain of PRC2, EED and SUZ12). It is found mostly outside of LADs, but is enriched at LAD borders (Harr et al. 2015).

Histone methylation is reversible thanks to histone demethylase such as the histone demethylase KDM1A/LSD1, which actively removes methylation from histone H3 on lysine 4 (H3K4) via the activity of its amine oxidase domain, using FAD as a cofactor [Shi Y et al, Cell 2004]. In addition, KDM2A/JHDM1A/FBXL11 was shown to demethylate H3K36 via its JmjC domain, which coordinates iron to mediate a 2-OG-dependent demethylation reaction (Tsukada et al. 2006). Further there is an extended family of related demethylase enzymes whose substrate specificities have been characterized in detail (reviewed in (Kooistra et Helin 2012; Black, Van Rechem, et Whetstone 2012)).

Histone acetylation generally leads to a more open chromatin structure and is associated with a transcriptionally active state. Lysine acetylation has been described on H3, H4, H2A and H2B (Musselman et al. 2012). Histone acetylation level is controlled by the activity of both lysine

acetyltransferases (HATs) which catalyse the transfer of an acetyl moiety to a Lys residue; and lysine deacetylases which catalyse acetyl group removal, some of which have been identified to acetylate or deacetylate nonhistone proteins (Shvedunova et Akhtar 2022). Importantly, lysine deacetylases fall into two subgroups: Zn²⁺-dependent histone deacetylases (HDACs) and NAD⁺-dependent sirtuins acetyl co-enzyme A (acetyl-CoA).

Euchromatin is less condensed, highly transcriptionally active and present in gene-rich genomic loci. Euchromatin is mainly located towards the nucleus interior (Hsu 1962; G. Li et Reinberg 2011). A third specialized chromatin is centromeric chromatin, present at centromeres and characterized by the presence of nucleosomes in which the canonical histone H3 is replaced by its variant CENP-A.

The organization of chromatin condensation generally depends on the state of cell differentiation, stem cells often exhibiting correlates more decondensed chromatin organisation compared to differentiated cells which present localized condensed regions of chromatin (Francastel et al. 2000). This characteristic is through to confer cell plasticity. As differentiation progress, cells gain to heterochromatin promotes gene repression and prevents inappropriate gene expression. As already stated, anchoring chromatin to the nuclear mechanism is an important mechanism for achieving gene inactivation (Pindyurin et al. 2018). Alternatively, the heterochromatin/euchromatin borders may be defined (Kharchenko et al. 2011), for example, by changing the profile of chromatin as differentiation progresses, i.e., as stem cells differentiate into the mature cell type (Marshall et Brand 2017).

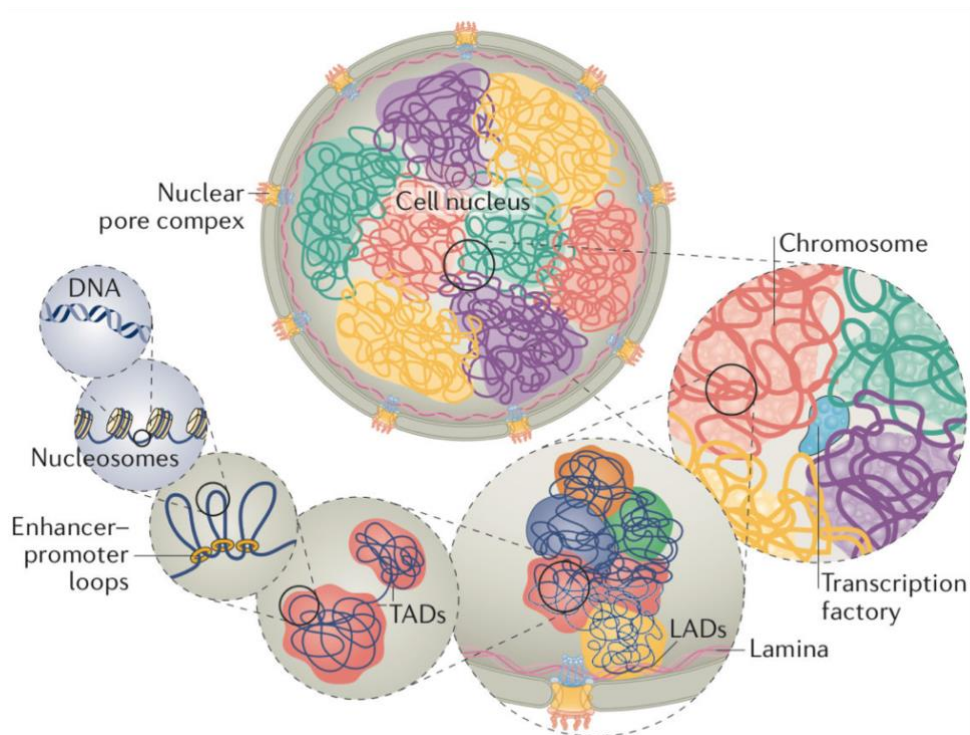


Figure 25: The functional organization of the genome.

DNA associates with several histone and non-histone proteins, and the resulting chromatin fibre is organized into loops. This fibre is further condensed into topologically associated domains (TADs). In turn, TADs are organized into transcriptionally active (euchromatin) and inactive (heterochromatin) compartments. Some of the heterochromatin regions are linked to the inner nuclear membrane at lamin-associated domains (LADs). Figure ref (Uhler et Shivashankar 2017).

The bivalent gene consisting of H3K27me3 and H3K4me3 (Bernstein et al. 2006) is associated with heterochromatin because the H3K27me3 repressive mark in developmental genes is dominant. It plays crucial role in the transition between pluripotency and committed cells. During differentiation, the H3K27me3 repressive mark is lost, and H3K4me3 activity dominates the promoter region lineage-specific genes to activate gene transcription (Collinson et al. 2016). The H3K27me3 repressive mark of the bivalent gene maintains low expression levels of developmental genes in iPCS and ESC while allowing for their transcription upon differentiation. In addition, H3K4me3 may be essential to ensure that permanent gene silencing of developmental genes does not occur (Fouse et al. 2008; Vastenhouw et Schier 2012).

It has been shown that the large number of genes containing the Polycomb group (PcG)-mediated-H3K27me3 in quiescent satellite cells were non myogenic genes. H3K27me3 regulates differentiation by silencing muscle specific genes (Asp et al. 2011; Dilworth et Blais 2011). In contrast, most of the myogenic genes lacked H3K27me3 (Liu et al. 2013). Depletion

of the polycomb repressor complex 2 (PRC2)-Ezh2, responsible for the deposition of H3K27me3, in muscle cell progenitors activates the non-myogenic gene lineages (Juan et al. 2011). Thus, H3K27me3 appears crucial to suppress the activation of alternative lineage regulators, thus regulating cell fate.

Differentiation of muscle stem cells requires: 1) the loss of repressive marks on the chromatin ; 2) the activation of the permissive marks to promote gene expression ; and 3) promotion of RNA PolIII on the promoter of the chromatin.

Satellite cell activation and proliferation is associated with silencing of muscle-specific genes by H3K27me3., under the control of the Polycomb group proteins (PcG). Phosphorylation of Ezh2, a subunit of the polycomb repressor complex 2 (PRC2) catalyses H3K27me3, resulting in gene inactivation (Palacios et al. 2010). Additional factor such as histone demethylase Jarid2 also contributes to recruit Ezh2 to the promoter of target genes (Peng et al. 2009; Pasini et al. 2010).

Differentiation into myotubes then requires the loss of H3K27me3 from promoter regions of gene of differentiation. This loss of H3K27me3 involves the KDM6 family member, UTX which demethylate H3K27me3, Msk1 kinase which modulates the binding between Ezh2 and Ezh1 (Margueron et al. 2008).

Then activation of the differentiation program requires the incorporation of H3.3 into specific genes (Harada et al. 2015). Activation of TrxG complex (Ash2L) via Mef2d and Six1 allowed the trimethylation of H3K4 (Rampalli et al. 2007).

H3K9me2 and H3K9me3 are catalyzed by the Suv39H1 methyltransferase, through interaction with MyoD (A. Mal et Harter 2003). Deposition of H3K9me3 by Suv39H1 represses the early muscle genes (A. K. Mal 2006) and is involved in the regulation of muscle specific genes during terminal differentiation (Ait-Si-Ali et al. 2004). G9a, a member of the SET domain-containing Suv39 family is thought to have extensive function in the muscle differentiation process. Interaction of G9a with MyoD results in the deposition of H3K9me2 repressive mark and inhibition of differentiation (J. Wang et Abate-Shen 2012).

MEF2 recruits the histone demethylase LSD1 that removes the H3K9me2 and H3K9me3 repressive marks from promoter regions leading to muscle differentiation (Choi et al. 2010). JMJD2A (Kdm4a) is also required to remove the Suv39h1 mediated H3K9 methylation, and it is via JMJD2A mechanisms that LSD1 appears to be facilitated (Verrier, Vandromme, et Trouche 2011).

It is important to remind that an additional level of chromatin stability is related to DNA methylation. DNA methylation is a heritable epigenetic mark which reinforces a previously silenced state by subjecting genes to irreversible transcriptional silencing even in the presence of all of the factors required for their expression (Deaton et Bird 2011; Jones 2012; Bestor, Edwards, et Boulard 2015; Schübeler 2015).

VI. Nuclear mechanotransduction

The nucleus is a mechanosensitive entity where the NE plays a role in the perception of mechanical stresses through the conformation change of lamins, the regulation of the activity and recruitment of associated proteins as well as the tensioning of the membrane (Figure 26).

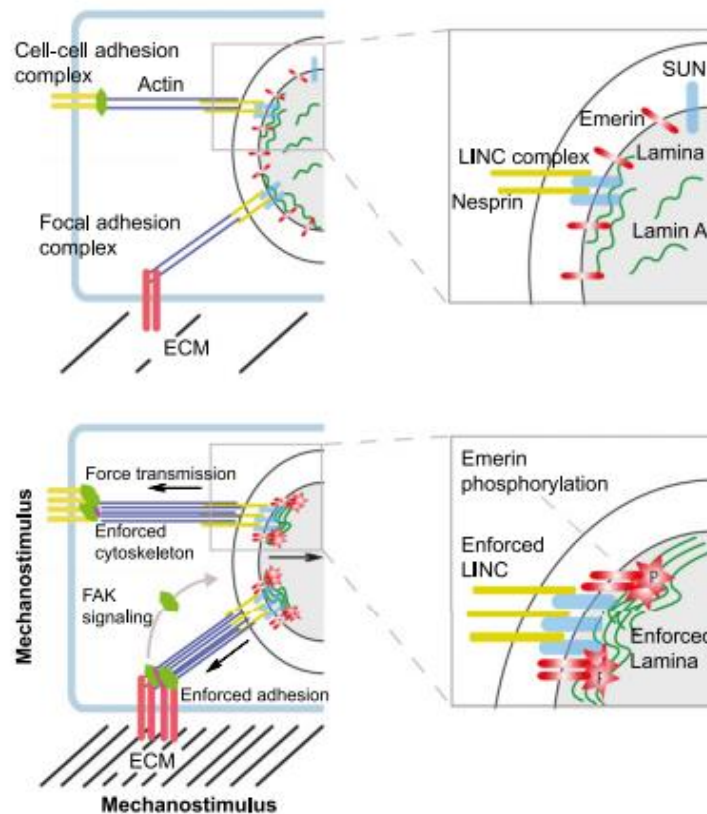


Figure 26: The mechanosensitivity pathway and the tension-induced reinforcement response.

(Top panels) Tension forces from the ECM are transmitted into the nucleus via the LINC complex and affect mechanoresponsive gene expression. (Bottom panels) Response to mechanostimulus, such as increase in ECM stiffness, adhesion complexes, the actin cytoskeleton, LINC complexes, and the lamina are reinforced by the assembly of actin filaments, increased recruitment of adhesion complex and LINC complex proteins, and stabilization and assembly of A-type lamins at the lamina, thereby counteracting forces exerted from outside. Emerin phosphorylation contributing to LINC complex reinforcement. Activation of signaling cascades on adhesion complexes, such as FAK signaling. Panels at the right depict higher-magnification views of the boxed areas in the nucleus shown in the left panels. Figure ref: (Osmanagic-Myers, Dechat, et Foisner 2015).

Lamin A/C expression, conformation, and post-translational modifications are strongly altered upon nucleus deformation. Upon nuclear mechanostimulation, nucleoplasmic domain of the inner nuclear membrane protein emerin becomes phosphorylated by the protein proto-oncogene tyrosine protein kinase Sarcoma (Src) (Bera et al. 2014; Guilluy et al. 2014). The Ig fold domain of lamin A is able to partially unfold, leading to stretching of the protein (Bera et al. 2014). A-type lamins undergoes dephosphorylation of the S22 residue, associated with relocation of the nucleoplasmic fraction to the nuclear lamina (Swift et al. 2013a; Guilluy et al. 2014; Buxboim et al. 2014). This in turn reinforces the nuclear lamina by stabilization and assembly of A-type lamins and increases nuclear stiffness (Osmanagic-Myers, Dechat, et Foisner 2015; Swift et al. 2013b) (Figure 26).

Conversely, in reduced mechanical constraints, the mobility and turnover of A-type lamins increases (Swift et al. 2013a; Buxboim et al. 2014; Makarov et al. 2019). Finally, under compression, the coiled coils in the rod domains of A-type lamin polymers are able to slide over each other to contract the length of the rod, behaving as a compression spring able to absorb pressure (Makarov et al. 2019). These structural changes require the LINC complex (D.-H. Kim et Wirtz 2015).

In addition to resist to stretching by decreasing the surface tension of the nuclear membrane (Enyedi et Niethammer 2017), lamin A/C integrity directly influences gene expression, DNA damage response, and inflammatory response in circulating cells. It also assures nuclear stiffening in response to mechanical stretch and by this it protects the DNA damage.

Since chromatin is closely linked to the nuclear lamina, changes in nuclear lamina conformations and their polarization, observed during changes in nuclear shape, could thus control chromatin architecture by specifically controlling certain territories as during cell differentiation. Therefore, gene expression may be controlled by nuclear deformation in response to mechanical forces. Consistently, application of mechanical stress to the plasma membrane via a magnetic bead to the nucleus induces chromatin stretching and increased transcription of a transgene and this response is abrogated in the absence of lamin A/C or LINC complexes (Tajik et al. 2016).

Further, application of mechanical stress to the nucleus of oligodendrocyte progenitor cells generates heterochromatin formation, reflected by tri-methylation of lysine 9 on histone 3 (H3K9me3). This response is abolished when cells are depleted for nesprin 1 (Hernandez et al. 2016).

VII. YAP signaling pathways

Yes-associated Protein (YAP), a transcriptional coactivator downstream of the Hippo pathway, has emerged as a key player in mechanotransduction (Dupont et al., 2011; Wackerhage et al., 2014). The Hippo/Yap pathways exhibit several crosstalks with Akt/mTOR or TGF β /SMAD further supporting the role of YAP in regulating muscle mass through mechanical cues (Jang et al., 2007; Alarc3n et al., 2009; Tumaneng et al., 2012; Grannas et al., 2015).

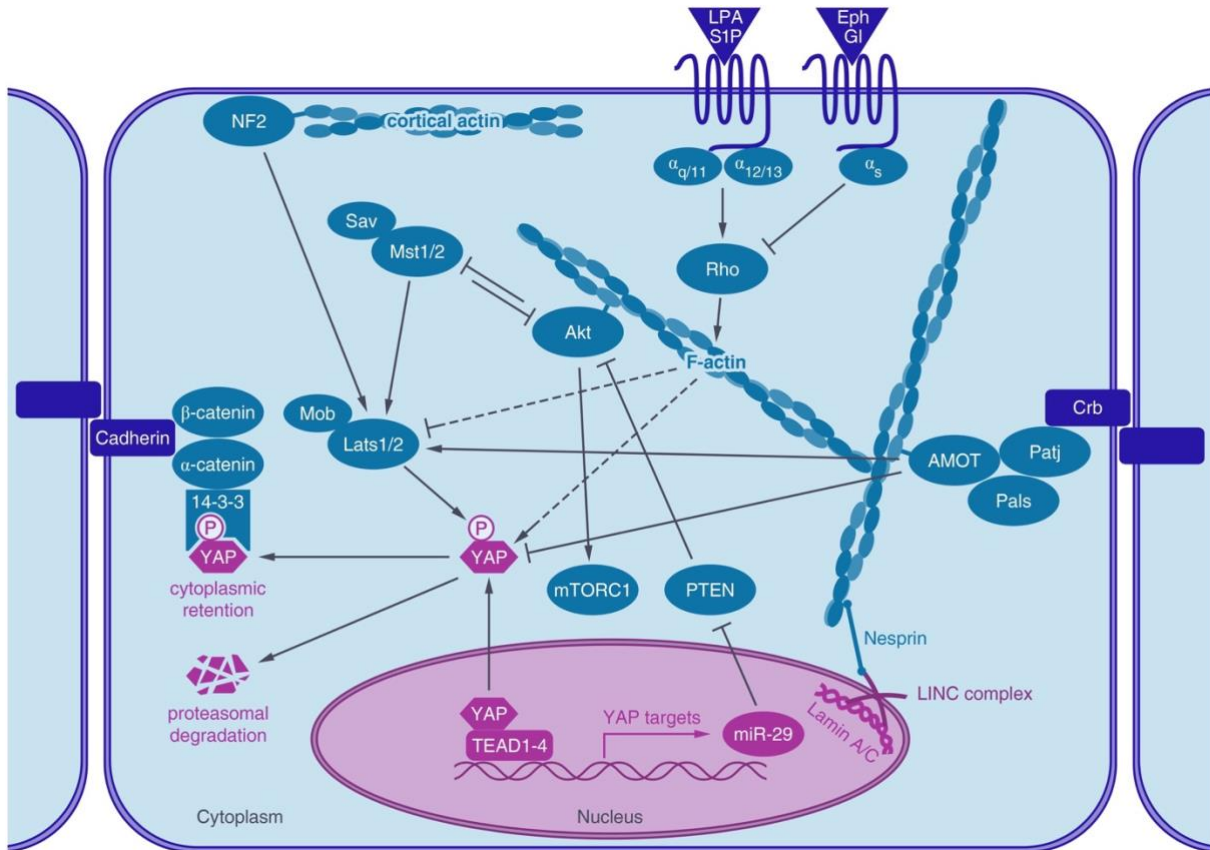


Figure 27: YAP regulation.

The actin cytoskeleton regulates YAP activity via the LINC complex and the lamins. YAP is active in the nucleus and phosphorylated and inactive in the cytoplasm. Once in the nucleus YAP activate TEAD gene expression. Phosphorylation of YAP is done by LATS1/2 kinase and leads to its degradation. Dashed lines represent the YAP and actin dynamics activity by Rho GTPases. AMOT (angiomin) and NF2 (neurofibromin 2) regulate YAP activity, either through LATS or by direct interaction. Akt binds to actin stress fibers, interacts with MST1/2 and induces the expression of a microRNA (miR-29) by YAP, which inhibits the inhibition of Akt by targeting PTEN. (Fischer et al. 2016).

YAP controls a wide range of cellular functions, including cell cycle control, cell contact inhibition and organ size, cell fate, and cell migration. Nuclear YAP activity typically enhances transcription of genes involved in cell cycle control, driving proliferation and survival, and inhibiting apoptosis (Dong et al., 2007). Prominent target genes of YAP include CTGF, Cyclin D1, AREG, Birc5 and myogenic transcription factor Myf5 (Dong et al., 2007; Zhao et al., 2008; Zhang et al., 2009; Watt et al., 2010).

YAP is modulated by diverse biomechanical signals and transduces them into cell-specific transcriptional responses, regulating cell proliferation and survival, organ growth, stem-cell renewal, and cell differentiation (Panciera et al. 2017). A major mechanism of YAP regulation occurs at the level of its subcellular localization, as YAP nuclear accumulation promotes target gene transcription and cell proliferation (reviewed in (Panciera et al. 2017; Fischer et al. 2016). After phosphorylation by LATS1/2 kinase, YAP binds to 14-3-3 proteins, leading to its cytoplasmic retention and degradation and favoring skeletal muscle differentiation (Fischer et al. 2016).

A-type lamins influence the localization and transcriptional activity of YAP (Bertrand et al. 2014; Owens et al. 2020). Lamin-A overexpression decreases both total YAP levels and nuclear localization in mesenchymal stem cells (Swift et al. 2013a). In contrast, increased YAP nuclear localization and activity in combination with reduced lamin levels is observed in cancers of many organ types (reviewed in (Irianto et al. 2016)), as well as in *LMNA* mutant MuSCs cultured on soft matrices (Bertrand et al. 2014). How mutant lamins cause defects in the YAP signaling pathway remains to be precisely determined. However, cancer (Chow, Factor, et Ullman 2012), and laminopathies (8/19/2022 1:48:00 PM), are associated with abnormal nuclear shape. This in turn has been shown to increase the rate of YAP import (Elosegui-Artola, Trepate, et Roca-Cusachs 2018; Aureille et al. 2019), by opening up nuclear pores (Elosegui-Artola, Trepate, et Roca-Cusachs 2018). Consistently, we recently shown that A-type lamin mutations responsible for congenital muscle disorders increases the nuclear import of YAP through the nuclear pore complexes (Owens et al. 2020).

VIII. *Laminopathies*

Laminopathies are heritable human diseases caused by mutations in lamins, other nuclear envelope transmembrane (NET) or lamin-associated proteins that heavily interact with lamins. Nearly 90% of laminopathies relate to *LMNA* genes, B-type lamin mutations being linked to only 2 diseases. Laminopathies form a group of heterogeneous diseases that can affect different tissues including adipose tissue, nervous system and skeletal and/or cardiac muscles. They can also cause systemic disease, the premature aging syndromes, mandibuloacral dysplasia and Werner syndrome (for a recent review see (Wong, Melendez-Perez, et Reddy 2022)). Although 75% of known mutations cause myopathies, i.e., affect mostly skeletal muscle and cardiac muscle (Figure 28). They include Emery-Dreifuss muscular dystrophy (EDMD), Limb-Girdle dystrophy type 1B (LGMD1B), autosomal dominant spinal muscular dystrophy (AD-SMA), lamin-related congenital muscular dystrophy (L-CMD) and dilated cardiomyopathy (CMDA) (Donnaloja F et al, 2020).

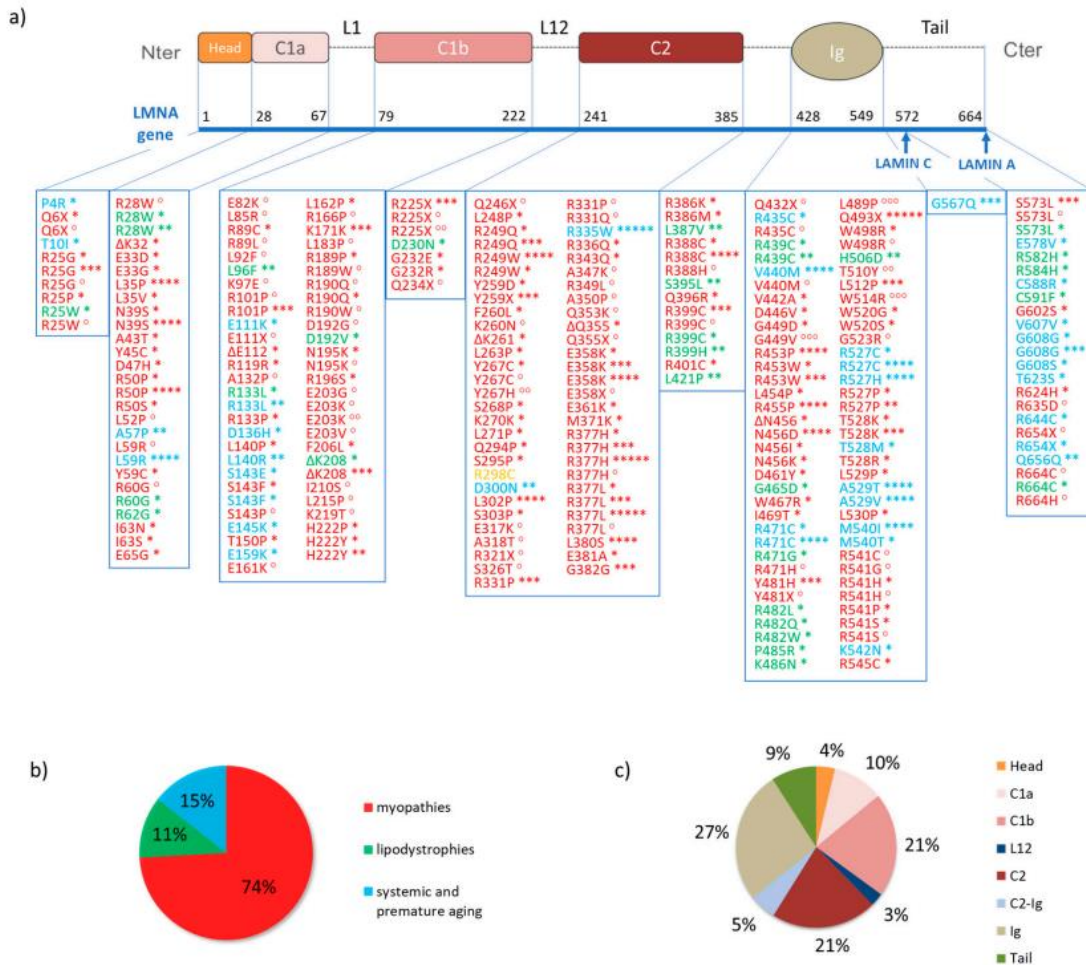


Figure 28: Single-point mutations of the LMNA gene.

(a) List of LMNA gene mutations graphically associated with distinct lamin domains. Red indicates the gene mutations related to the following myopathies: EDMD2 (*), EDMD3 (**), LGMD1B (***), CMD (****), AS-SMA (*****), CDM1A (°) and DCM-CD (°°); In green, mutations associated with lipodystrophies: FPLD2 (*) and MS (**). In yellow, the mutations causing the CMT2B1 neuropathy. Finally, blue indicates the gene mutations relative to systemic and premature aging disease: HGPS (*), WRN (**), RD (***), MADA (****), HHS (*****). (b) The percentages for each group of laminopathies. (c) The percentages for each lamin domain. Figure reproduced from ref (Donnaloja et al. 2020).

Most of the laminopathies are autosomal-dominant diseases caused by single point mutations. Bonne et al was first to associate the *LMNA* mutation with muscle disorder (Bonne et al. 1999). To date, more than 498 different LMNA mutations and 300 protein variants responsible have been identified (<http://www.umd.be/LMNA/>).

Because *LMNA* mutations mainly affected mechanically stressed muscles, it has been proposed that A-type lamin defects alter the nuclear resistance to external mechanical stimuli, resulting

in nuclear damage and increased stress sensitivity. Alternatively, the « gene expression model » proposed that lamin mutations impair lamin-chromatin interactions, chromatin organization and/or specific gene localization, thus causing gene deregulation in cells. Altered gene expression may occur directly, through defects in heterochromatin, or indirectly by the disruption of lamin-protein interactions (Review in Donnalaja F et al, 2020(Donnalaja et al. 2020)). Importantly, both the mechanical and genetic models are not mutually exclusive.

Objectives of the thesis

My PhD project had 3 main objectives.

The first aim was to determine how muscle differentiation impacted nuclear characteristics in muscle cell precursors. It is known that muscle differentiation is associated with increased expression of A-type lamins, chromatin reorganization and transcriptional changes, and cytoskeletal reorganization. We first studied how differentiation affected the morphology of the nucleus and histone post-transcriptional changes.

The 2nd aim was to understand the impact of mechanical forces on myonuclei, i.e., nuclei from post-mitotic, differentiated muscle cells. The two main components that modulate the response of the nucleus, namely A-type and chromatin compaction were taken into account, using siRNA against lamin and drugs modifying chromatin compaction. The effects of trichostatin-A (TSA), a histone deacetylase inhibitor, that favors histone acetylation and chromatin decompaction will be presented here. We analyzed nuclear characteristics and histone PTMs. In lamin deficient cells, myonuclear transcription was also analyzed using RNAseq and ATACseq.

Then, we investigated the respective roles of SUN1 and SUN2 nuclear envelope proteins on the mechanical load-mediated nuclear response in myonuclei. Nuclear morphology and histone reorganization were studied before and after stretch.

My third aim was to analyze how A-type lamin deficiency affected the stretch-induced modulations of the cyto-nucleoplasmic exchange. We analyzed YAP (Yes-Associated Protein), an essential transcription co-factor in the mechanoreponse of cells and HDACs (histone deacetylase) intracellular localization in static and stretched conditions.

HDACs are known to promote transcriptional repression and gene silencing, by removing histone acetylation. We focused on HDAC2 given that it plays important role in muscle differentiation and is known to interact with A-type lamins and contribute to the mechano-response.

Materials and methods

I. Human myoblast culture

Experiments were performed on human immortalized human muscle-precursor cells, also called myoblasts, from patients without muscular disorders. Myoblasts were immortalized on the platform of immortalization of the Research Center, using the co-transduction with both telomerase- expressing and cyclin dependent kinase 4-expressing vectors (hTERT and CDK4) (Mamchaoui et al. 2011). Two control cell lines were used (Table 1).

II. Cell culture

Human immortalized myoblasts were cultured in proliferation medium consisting of 1 vol of 199 Medium (80ml) to 4 vol DMEM (Life technologies, Paisley, UK) with 20% fetal Bovine Serum (Biosera, FB-1001) (100ml), 5 µg/ml insulin (Life technologies, Paisley, UK) (250µl), 50mg/ml Gentamycin (Gibco™, Life technologies, Carlsbad, CA, USA) (0.5ml), 50µg/ml Fetuin (Life technologies, Paisley, UK) (125µl), 5ng/ml hEGF et bFGF (Life technologies, Paisley, UK) (25µl) and 0,1mg/ml Dexamethasone (Sigma-Aldrich, St. Louis, Missouri, USA) (1ml).

Human immortalized myoblasts were seeded at 15 000 cells per cm² and allowed to proliferate. Above 80% cell density, the proliferation medium was shifted to a differentiation medium consisting of 1 vol of DMEM (50ml) to 0.001 vol of Gentamycin (50µL) and 0.001 vol of Insulin (50µL). This allow myoblasts to fuse and form plurinucleated myotubes, this phase is called differentiation.

Gentamycin was removed when siRNA treatment is applied.

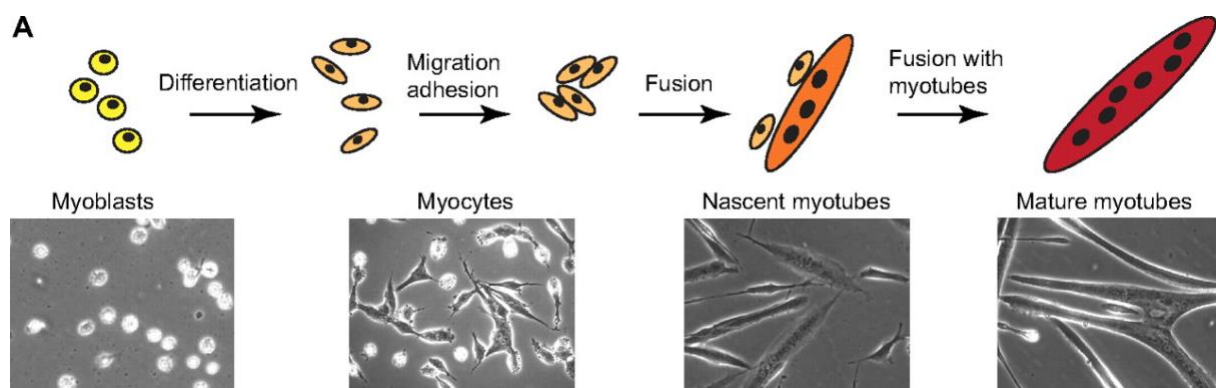


Figure 29: Myoblast differentiation in cultured muscle cells (Abmayr et Pavlath 2012).

Table 1:Immortalized cell lines

Lineages	Mutation	Patients	Muscle
WT8220	Control	Woman,12 Years old	Paraspinal
AB1167	Control	Man, 20 Years old	Facia Lata

III. Chemicals, chromatin modifiers

To modulate the chromatin state of compaction, myotubes and myoblasts were treated with chromatin modifiers. All chemicals were purchased from Sigma Aldrich unless stated otherwise. Trichostatin A (TSA) is an HDAC inhibitor that causes chromatin decompaction by increasing histone acetylation. TSA (Sigma-Aldrich, St. Louis, Missouri, USA) was diluted in Methanol. TSA efficacy, concentration (0.05 μ M, 0.1 μ M and 0.15 μ M) and time were optimized by QPCR, immunofluorescence and Western blot. 3-Dezaneplanocin A (DZNep) is a histone methyltransferase inhibitor that causes chromatin decompaction by inhibiting H3K27me3. DZNep (Sigma-Aldrich, St. Louis, Missouri, USA) was diluted with PBS. Drugs' efficacy was validated by immunofluorescence and WB on myoblasts and myotubes. TSA and DZNep were diluted to final concentrations of 0.1 μ M; 0.5 μ M; and in the culture medium. Cells were incubated with each drug for 48h. Controls were performed with the according concentration of vehicles.

IV. SiRNA

Myotubes were transfected with Lipofectamine RNAiMAX (Invitrogen, Life Technologies, Carlsbad, CA, 13778-150) according to the manufacturer's instructions. All siRNA (small-interfering ribonucleic acid) were purchased from Eurogentec, Belgium. The list of used sequences can be found in Table 2. Lipofectamine RNAiMAX is diluted in Opti-MEM™ I serum-reduced culture medium (Gibco, Life Technologies 31985-047) QSP50 μ l/well. The siRNAs are diluted in the Opti-MEM™ I as well. Mixes were prepared separately.

Table 2 : siRNA sequences list

siRNA-LAMIN A /C	5'-GCCGUGCUUCCUCUCACUCA-3' 5'-UGAGUGAGAGGAAGCACGGC-3'
siRNA-SUN2	5'-GCCUAUUCAGACGUUUCACU-3' 5'-AGUGAAACGUCUGAAUAGGC-3'
siRNA-SUN1	5'-CAGAUACACUGCAUCAUCUU -3' 5'-AAGAUGAUGCAGUGUAUCUG-3'
siRNA Negatif Control	SR-CL000-005

After 15 minutes at room temperature to allow formation of transfection complexes, siRNA mixes were added to myotubes with differentiation medium for 48h of incubation in an atmosphere of 37°C, 5% CO₂ before mechanical stretch. Efficient depletion was obtained after two successive siRNA treatments at 24hours interval.

V. Mechanical stretch

Cells were plated onto 6-well plates flexible-bottom plates (BioFlex plates; Flexcell International Corporation) coated with Matrigel Growth Factor Reduced Basement Membrane Matrix and incubated at 37°C in a CO₂ incubator.

According to the routine protocol in the lab, the cells were subjected to 10% equibiaxial cyclic stretch for 4h hours using a computer-controlled vacuum stretch apparatus (FX-4000T Tension Plus System; Flexcell International Corporation) with vacuum pressure that generate 10% mechanical stretch. Equibiaxial Loading Stations™ are designed to provide uniform radial and circumferential strains to cells. Loading Stations™ are comprised of a 3.3" x 5" Lexan® plate, and all styles except the 25mm Loading Station™ consist of two Delrin® (nylon) support and centering posts, and six removable Delrin® planar faced cylinders (or loading posts; Figure 30). The 25mm strain posts and support and centering posts are made from VisiJet® (a diacrylate compound). The two centering posts are intended to support the BioFlex® plate under high vacuum and also center the BioFlex® plate over the six loading posts. The six loading posts provide the strain surface. The posts are positioned on the Lexan® plate such that each is

centered beneath the 35 mm well bottom of a BioFlex® culture plate. Replicate control samples were maintained under static conditions with no applied cyclic stretch.

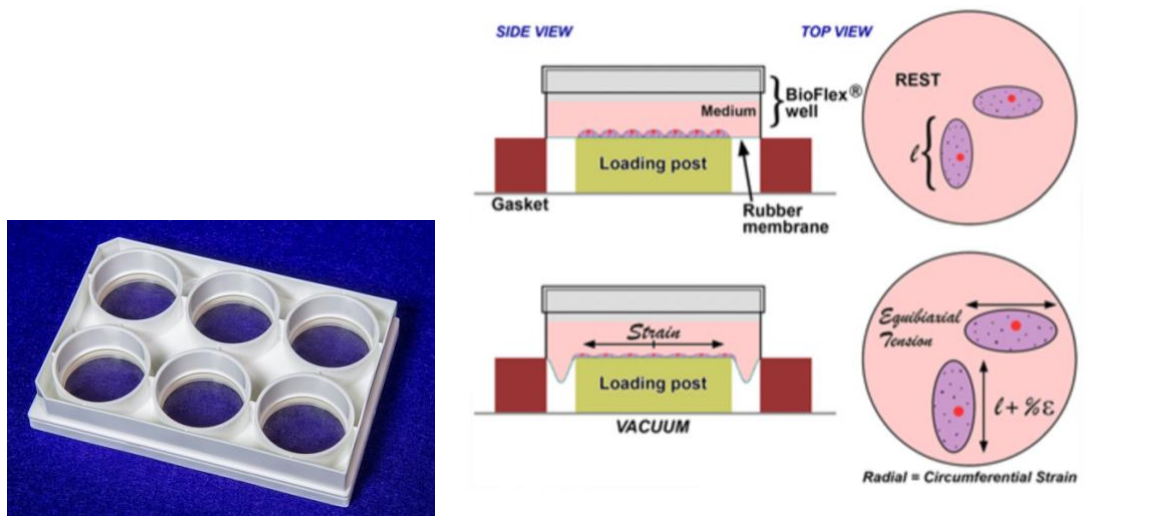


Figure 30: Application of quibiaxial strain with Flexcell® Tension Systems using Bioflex® culture plates.

VI. Coatings

Bioflex plates were coated with Matrigel® Matrix Basement Membrane Growth Factor (#CLS354234, Corning, France) diluted with cold DMEM to 1:10 and incubated at 37°C for 1 hour in a CO2 incubator. Classic plastic and glass plates were coated with fibronectin (Sigma Aldrich, St. Louis, Missouri, USA) in PBS to a final concentration of 10 µg/ml and incubated for 1h at 37°C. Then, coating solutions were removed, and one PBS wash was done, and the cell culture plastic was dried for several hours in the sterile bank.

VII. Immunofluorescence

Myoblasts were fixed for 10 minutes with 4% formaldehyde, permeabilized for 15 min with 0.1% Triton and blocked with 5% BSA diluted in PBS.

Myotubes were fixed for 20 minutes with 4% formaldehyde in PBS at room temperature (RT), permeabilized for 10 minutes with 0,5% Triton (X-100 in PBS at RT), and blocked with the saturation buffer for 30 minutes (PBS with 0.1% Triton X-100, 5% bovine serum albumin (BSA)) at room temperature with shaking. Samples are incubated with primary antibody diluted in saturation buffer overnight at 4°C with gentle shaking. The next day, the samples are washed 3 times with PBS supplemented with 0.1 Triton X-100 before incubation with the secondary

antibodies for 60 minutes at RT. As secondary antibodies, the Alexa-conjugated secondary antibody system (Invitrogen, Carlsbad, CA, USA) was utilized. Samples were washed again for 3 times 10 minutes each with 0.1% Triton X-100 PBS, and then incubated with 300nM DAPI (Sigma Aldrich, St. Louis, Missouri, USA) solution for five minutes with gentle shaking. They are finally washed one last time in 0.1% Triton X-100 PBS, 2 times for 5minutes each, and mounted with Vectashield anti-staining solution (#H-1200; Vector Laboratories, USA). For double or triple labeling, the primary antibodies (of different species) were added simultaneously at the appropriate step. The fluorescent molecules used, such as phalloidin, which allows the labeling of actin filaments (ThermoFischer Scientific, France), are incubated at the same time as the primary antibodies. For 3D images (nuclear characteristics experiments) Spacers were used to avoid smashing the nuclei and so we can get the right form, volume, area and thickness of the nucleus.

VIII. Microscopy and image analysis

Immunostainings were observed using a Nikon Ti2 spinning disk confocal microscope, driven by Metamorph software (Molecular Devices) and equipped with a motorized stage and a Yokogawa CSU-W1 spinning disk head coupled to a Prime 95 sCMOS camera (Photometrics). Super-resolution images are obtained with the LiveSR module (Gatca Systems).

Standard image analyses and quantitative immunofluorescent analyses were performed using FiJi ImageJ software (version 1.41). All relative intensities were measured via quantification of mean fluorescence intensity. Nucleocytoplasmic ratio was performed by measuring the nuclear intensity and divided by the cytoplasm intensity. Nuclear area and the A/R ratio were measured using the ROI manager feature.

IMARIS software (Oxford Instruments) was used for 3D images. The Imaris software is an interactive visualization and analysis software that allow to calculate surfaces on 3D microscopic images. Imaris software automatically detects the nucleus compartment. When the software was not able to separate myonuclei, a manual segmentation was done for every stack.

IX. SDS-PAGE and protein analysis

For total protein extraction, cells were washed once with 37°C heated PBS and then washed again on ice with cold PBS. 5 minutes on ice incubation was applied next, with 1X RIPA with anti-protease inhibitor and anti-phosphatase inhibitor. After 5 min incubation on ice, cells were

scrapped and sonicated, then centrifuge at 14 000 rpm, 4°C for 10 min. The supernatant was collected and store at -20°C until use. Protein quantification was performed using Thermo Scientific™ Pierce™ BCA Protein Assay Kit (23225).

For Western-Blot, samples were mixed with loading blue (Laemli 2x, Bio-Rad) and a reducing agent (2-Mercaptoethanol, Sigma-Aldrich). Samples denaturation was done at 95°C for 5 minutes. Samples were placed gently in the wells of a 4-20% Mini-Protean TGX Stain-Free Gels (Bio-Rad, USA). 5µl of the protein molecular weight marker (PageRuler Prestained, Thermo Scientific) was used to evaluate the molecular weight of proteins. The migration was carried out in a Tris Glycine-SDS migration buffer, for approximately 1 hour and a half at 100 volts on a BioRad® system. The proteins were transferred to nitrocellulose membranes, using transfer buffer made of 1:1:1 Bio Rad transfer buffer, ethanol and water, with a semi-dry transfer system, the Trans-Blot Turbo Transfer System from BioRad in 7 minutes (depending on protein of interest molecular weight). Membranes were saturated with a PBS-Tween 0.1% + Milk or BSA 5% with a pH = 7.4 blocking solution for 1 hour at room temperature, then incubated with the primary antibody overnight at 4°C. List, references and dilution of primary and secondary antibodies are given in Table 3 and 4 respectively. The membranes were then washed 3 times for 5 minutes each time with 0.1% PBS-Tween and then incubated with the HRP secondary antibody for 1 hour at room temperature. Membranes were washed 3 times for 5 minutes with PBS-Tween 0.1%. The presence of proteins was detected using Immobilon Western Chemiluminescent HRP Substrate (Millipore). Acquisition was performed on a ChemiDoc Imaging system (BioRad).

Table 3: Primary antibodies

Target Protein	Company	Dilution
GAPDH (ab9485)	Abcam	WB 1:1000
Histone H3 (cs9715)	Cell Signaling Technology	WB 1:1000
H3K9Ac (06-942)	Millipore	IF 1:200
H3K27me3 (cs 9733)	Cell Signaling Technology	IF 1:1600
H3K27me3 (07-449)	Millipore	WB 1:20 000
H3K9me3 (cs 5327)	Cell Signaling Technology	IF 1:100
H3K9me3 (07-523)	Millipore	WB 1:10 000
H3K4me3 (ab8580)	Abcam	IF 1:500
H3K4Ac (07-539)	SIGMA	WB 1:10 000 IF 1:500
HDAC2 (H2663)	SIGMA	IF 1:100
Lamin A+C (ab8984)	Abcam	WB 1:500 IF 1:500
LaminA (phosphor S22) (ab138450)	Abcam	WB 1:750
SUN1 (ab47405)	Abcam	WB 1:1000 IF 1:200
SUN2 (ab124916)	Abcam	WB 1:5000 IF 1:400
YAP (sc-101199)	Santa Cruz	WB 1:500 IF 1:400
Phospho-YAP (Ser127) (cs13008)	Cell Signaling Technology	WB 1:1000

Table 4: Secondary Antibodies

Secondary antibody	Reference	Dilution (Immunofluorescence)	Dilution WB
Goat anti-Mouse A488	A32723	1:500	-
Goat anti-Rabbit A488	A11034	1:500	-
Goat anti-Mouse 568	A11004	1:500	-
Goat anti-Rabbit 568	A11036	1:500	-
Donkey anti-Rabbit 647	A31573	1:500	-
Donkey anti-Mouse 647	A31571	1:500	-
Goat anti-Rabbit HRP	111-035-144	-	WB 1:10 000
Goat anti-Mouse HRP	515-035-062	-	WB 1:10 000

X. Chromatin extraction

Chromatin extraction was performed with a specific Histone Extraction Kit (abcam, ab113476). Myotubes were collected after 2min incubation with trypsin at 37°C, and then centrifugation at 1000 rpm for 5 minutes. Cell were suspended in the 1X Pre-Lysis Buffer at 10⁷ cells/ml on ice for 10 minutes with gentle stirring. Supernatant was removed after 5 minutes on ice centrifugations at 3000 rpm. The pellet was re-suspended in 3 volumes of Lysis Buffer and incubated on ice for 30 minutes. Centrifugation at 12,000 rpm for 5 minutes was followed, and supernatant fraction was transferred into new vial with 0.3 volumes of the balance-DTT Buffer. All centrifugations were done at 4°C. Protein quantification was performed using Thermo Scientific™ Pierce™ BCA Protein Assay Kit (23225).

XI. RNA seq and quantification of gene expression.

mRNA was isolated from cell lysates using the RNeasy mini kit (Qiagen) The complementary DNA (cDNA) was transcribed by SuperscriptIII (Life Technologies, Carlsbad, CA, USAEuro) or qScript™cDNA SuperMix (Quanta Biosciences, Gaithersburg, MD, USA). PerfeCTa®SYBR®Green SuperMix (Quanta, Biosciences) was used to quantify Gene expression with LightCycler 480 II (Roche Diagnostics). The primers were synthesized by Eurogentec (Liège, Belgium). Expression of all target genes was normalized to the expression of house-keeping gene RPLP0. Primer sequences are listed in Table 5.

RNA-sequencing was performed at the Genotyping/Sequencing Platform (iGENSeq ICM), Paris. RNA-sequencing was performed using NovaSeq 6000 with read depth of 2*44 million reads, and a length of 100 bases each.

Bioinformatic analyses were done at the Data Analysis Core (DAC, ex iCONICS). Quality of raw data was evaluated with FastQC (Leggett et al. 2013). Poor quality sequences and adapters were trimmed or removed with fastp tool, with default parameters, to retain only good quality paired reads. Illumina DRAGEN bio-IT Platform (v3.8.4) was used for mapping on hg38 reference genome and quantification with gencode v37 annotation gtf file. Library orientation, library composition and coverage along transcripts were checked with Picard tools. Following analysis was conducted with R software. Data were normalized with DESeq2 (v1.26.0) (Love,

Huber, et Anders 2014)bioconductor packages, prior to differential analysis with glm framework likelihood ratio test from DESeq2 workflow. Genes were considered differentially expressed if the absolute value of log2 fold-change was above one, and the false-discovery rate below 0.05. Multiple hypothesis adjusted p-values were calculated with the Benjamini-Hochberg procedure to control FDR. Finally, enrichment analysis was conducted with clusterProfiler R package (v3.14.3)(Yu et al. 2012) with Gene Set Enrichment Analysis, on GO: biological process database.

Table 5: Primers sequences

SETDB1_F :	GGAACTGGAGAAGATGGATTGTG
SETDB1_R :	GTCCCGGTATTGTAGTCCCA
RTF1_F :	GGTTCAGAAAAGCTCCACCC
RTF1_R :	GATATGTTCTTGGTCCGCTGG
EZH1_F :	AGATGAGACGGTTTTGTGCA
EZH1_R :	GTGTCATTGTGCCCTTCCTC
EHMT1-F :	ACAGAGGACGGTGATTGAGA
EHMT1-R :	GAAGTCCTGCTGTCCTCTGT
EZH2-F :	TGTGCACATCCTGACTTCTTG
EZH2-R :	ACATTATGGGTAAGCAACT
GATA3-F :	GCC-CCT-CAT-TAA-GCC-CAA-G
GATA3-R :	TTG-TGG-TGG-TCT-GAC-AGT-TCG
KAT2B-F :	AGG-AAA-ACC-TGT-GGT-TGA-AGG
KAT2B-R :	CAG-TCT-TCG-TTG-AGA-TGG-TGC
KAT2B-F2 :	GAA-AAA-CCC-TAA-CCC-CTC-ACC
KAT2B-R2 :	CCT-TGT-GGA-CAC-AGG-TAA-AGA-GA
PIH1D1-F2 :	ACC-AGA-CCA-GAA-TCG-ACA-CAA
PIH1D1-R2 :	CCT-CCT-CTA-GCA-TCT-GAA-GCA
PIH1D1-F3 :	CAG-GGA-TGT-ACC-GCC-TAC-GA
PIH1D1-R3:	CCG-CAA-GAA-ATC-GCT-GTT-CTG
LMNA_F:	AGCAAAGTGCGTGAGGAGTT
LMNA_R:	TCAGGTCACCCTCCTTCTTG
PAXBP1_F:	GAATGTTCTTCGTCCAGGAGA
PAXBP1_R:	TATCCGGCGTTTCTCATCGT
YAP_F :	GCTACAGTGTCCCTCGAACC
YAP_R :	CGGTGCATGTGTCTCCTTA
FOXO_F :	TGTTGGTTTGAACGTGGGGA
FOXO_R :	GTTTGAGGGTCTGCTTTGCC
Rplp0_F :	CTCCAAGCAGATGCAGCAGA
Rplp0_R :	ATAGCCTTGCGCATCATGGT

XII. ATACseq

The ATACseq experience was made using the ATACseq kit of Active Motif. The first step is cell sample preparation. It consists of counting the cells and aliquoting 100,000 cells into a fresh 1.5ml centrifuge tube for each sample. Then, cells were centrifuged at 1000g for 5 minutes at 4°C. Supernatant was removed. 100µl of ice-cold PBS was added on the pellet without disturbing neither resuspending. Samples were spined one more time for 500g, 5 minutes at 4°C. Supernatant were removed gently and pellet were resuspended thoroughly in 100 µl ice-cold ATAC Lysis Buffer. This step was followed immediately by a spin down at 500g for 10 minutes at 4°C. After the spin, the supernatant was very carefully removed. During this time, the Tagmentation Master Mix and the Tagmentation Reaction and purification were prepared. The Tagmentation Master Mix is made as follow (per sample): 2X Tagmentation Buffer (25 µl), 10X PBS (2 µl), 0.5% Digitonin (0,5 µl), 10% Tween 20 (0,5 µl), H2O (12 µL) and Assembled Transposomes (10 µl). 50 µl of the Tagmentation Master Mix were added to each sample and resuspended. Incubation for 30 minutes at 37°C in a thermomixer set at 800 rpm is followed. 250 µl of DNA Purification Binding Buffer with 5 µl 3M sodium acetate was added to each sample. At this step, the sample color was checked, if it was anything other bright yellow, additional 3 M sodium acetate was added.

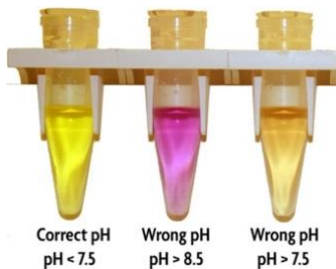


Figure 31: Solution color as a function of pH.

The DNA Purification Binding Buffer has a pH indicator dye, so that the pH of the solution can easily be determined. Each sample was transferred into its corresponding column and centrifuged at 17,000 g for 1 minute. The flow-through was discarded, and a wash was done using 750 µl of wash buffer (initially diluted with Ethanol) and centrifugation at 17,000 x g for 1 minute. To remove the residual wash buffer a centrifugation was done at 17,000 x g for 2 minutes with the column cap open. To finish the second step 35 µl of DNA Purification Elution Buffer was added to the center of the column matrix of each sample for one minute at room temperature. Centrifugation at 17,000 x g for one minute was followed. The third and final step is the PCR Amplification of Tagmented DNA, it consists of setting up the PCR reaction by adding the components in the order shown bellow. The libraries were to be multiplexed for

sequencing on the same cell flow, so a unique i5 and i7 index combination were used for each sample. Index Primers are shown on table 6.

Table 6: Index primers

Per reaction:

i7 Indexed Primer used

i7 indexed Primer 1 = i7 N701

i7 indexed Primer 2 = i7 N702

i7 indexed Primer 3 = i7 N703

i7 indexed Primer 4 = i7 N704

i5 Indexed Primer used

i5 indexed Primer 1 = i7 N501

i5 indexed Primer 2 = i7 N502

i5 indexed Primer 3 = i7 N503

i5 indexed Primer 4 = i7 N504

Table 7: Mix preparation.

Reagent	Volume
Tagmented DNA	33.5 μ l
i7 Indexed Primer (25 μ M)	2.5 μ l
i5 Indexed Primer (25 μ M)	2.5 μ l
dNTPs (10mM)	1 μ l
5X Q5 Reaction Buffer	10 μ l
Q5 Polymerase (2U/ μ l)	0.5 μ l

PCR with a heated lid was performed using the following program on a thermal cycler, 72°C for 5 minutes, 98°C for 30 seconds and 10 cycles of 98°C for 10 seconds, 63°C for 30 seconds, 72°C for 1 minute, samples were hold at 10°C.

To perform cleaning and DNA purification, 60 μ l of well mixed, prepaed as shown in table 7, room temperature SPRI Beads were added to each sample, and incubated for 5 minutes. Magnet was applied next to collect beads, once the solution is clear, the supernatant was removed and then 180 μ l of 80% ethanol to each sample was added, without mixing. After 30 seconds, supernatant was removed, and ethanol wash was repeated. After 5 minutes, the residual ethanol evaporates and the beads transits from shiny to matte; tubes were separated from the magnet and 20 μ l of DNA Purification Elution Buffer was added and vortexed to mix. Samples were than incubated for 5 minutes at room temperature. Magnet was applied to collect beads, and

supernatant was collected to a fresh tube. Samples were transferred to the ICM for library quantification.

Bioinformatic analyses were done at the Data Analysis Core (DAC, ex iCONICS).

Quality of raw data was evaluated with FastQC (Andrews et al., 2010). Poor quality sequences (minimum length: 50bp) and adapters were trimmed or removed with trimmomatic tool (Bolger, Lohse, et Usadel 2014), with default parameters, to retain only good quality paired reads. Paired-end reads were mapped to the human reference genome (build hg38) with Bowtie2 (Langmead et Salzberg 2012)(Langmead et al. 2009). Reads mapping with mitochondrial DNA were excluded from the analysis. Duplicates and reads in Encode blacklist regions were discarded with the Picard tools. Peaks were called using the MACS2 (Y. Zhang et al. 2008) program with the option callpeak. Individual peaks separated by less than 100 bp were merged with BEDOPS and features annotations were obtained from the HOMER (Heinz et al. 2010) hg38 database. Differential binding analysis was performed with DiffBind bioconductor package (V.3.4.11).

XIII. Statistical analysis

Normality test was used to determine whether sample data has been drawn from a normally distributed population. If the data falls into a normal distribution, Student's t-test was used to compare the means of two samples, and one-way ANOVA was used for more than two samples. If data did not have a normally distributed population, Kruskal-Wallis non-parametric test was used. Bonferroni post-hoc test was used to do multiple comparison pairs of columns.

Results are expressed as mean \pm standard deviation and are accompanied by the number of replicates per group and the sample size (n) used. For all measurements, a minimum of 50 nuclei were analysed in at least three independent experiments.

A p-value below 5% is considered significant (*: $p \leq 0.05$) (**: $p \leq 0.01$) (***: $p \leq 0.001$) (****: $p \leq 0.0001$). Statistical tests and graphs were performed using GraphPad Prism software.

Results

I. Nuclear changes associated with muscle differentiation

When confluent myoblasts were shifted to differentiation medium, they terminally differentiate to form multinucleated myotubes. We first sought to determine how myoblast differentiation impacts nuclear characteristics. Data were given from 2 muscle cell lines obtained from patients without muscle disorders.

As shown in Figure R1, muscle cell differentiation into myotubes was associated with a significant decrease in nuclear volume and area (each $p < 0.05$) (Figure R1 A, B and C).

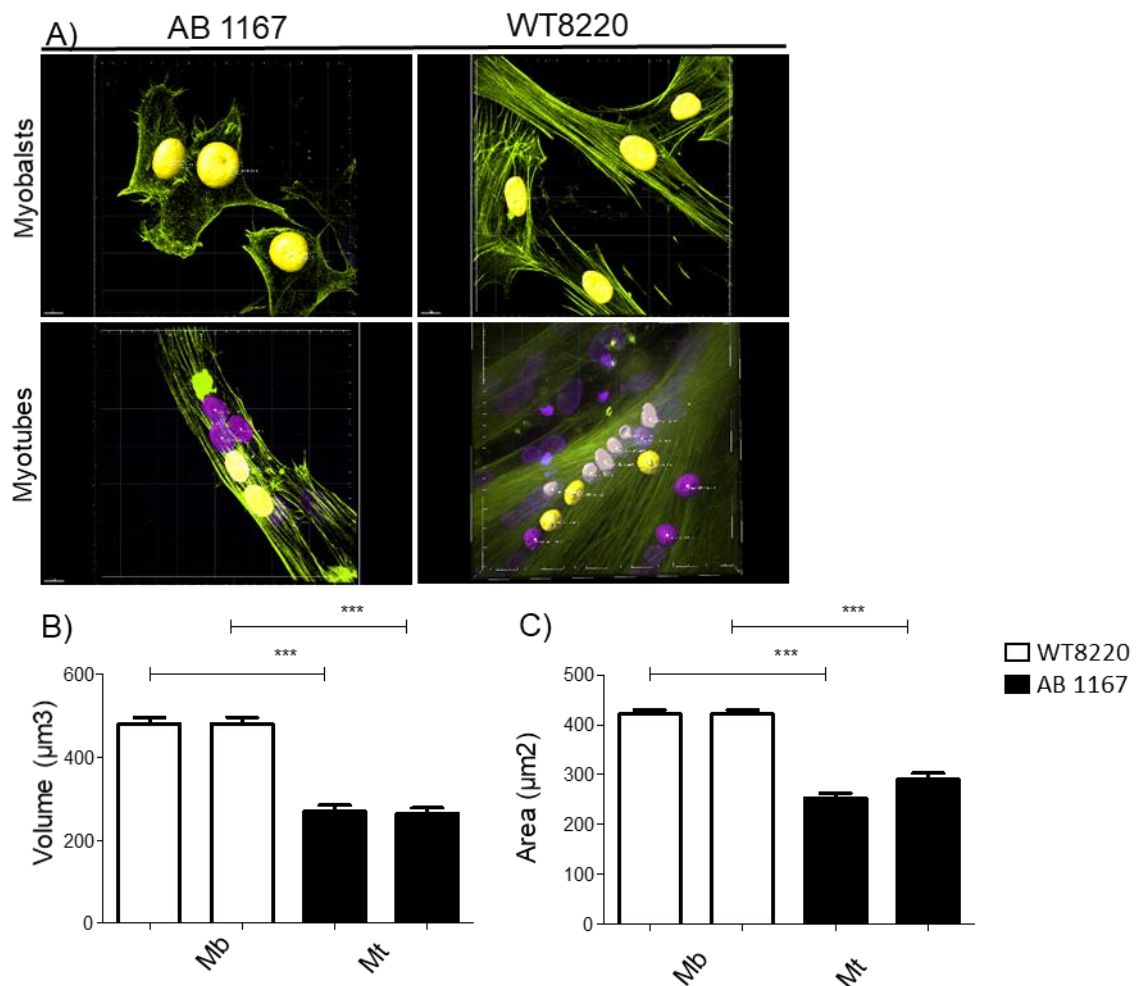


Figure R1: Nuclear segmentation and analysis of nuclear shape and volume in 2 human muscle cell lines (AB1167 and WT8220).

(A) Phalloidin and DAPI were used to label the actin cytoskeleton (in green) and nuclei. Nuclear volume and area were quantified using Imaris. Panel A shows automatically detected nucleus (in Yellow) and manually detected nucleus (purple) in 3D. (B) Quantification of the nuclear volume (C) and nuclear area. Mb=myoblast; Mt=myotube. Values are means \pm SD $n = 50$ to 150 nuclei from 3 independent experiments.

All experiments presented thereafter were obtained from the WT8220 cell line (control).

We first analyzed associated histone post-translational modifications including chromatin repression markers (H3K27me3 and H3K9me3) and chromatin active marker (H3K4me3) (Figure R2). Compared with myoblast nuclei, myonuclei had a significant lower level of the facultative heterochromatin marker H3K27me3, and higher levels in both constitutive heterochromatin marker H3K9me3 and in euchromatin marker H3K4me3.

These results are consistent with what is known about differentiation (Miyamoto, Furusawa, et Kaneko 2015) and may reflect the repression of genes related to proliferation (increase H3K9me3) associated with the activation of genes involved in differentiation (increase in H3K4me3).

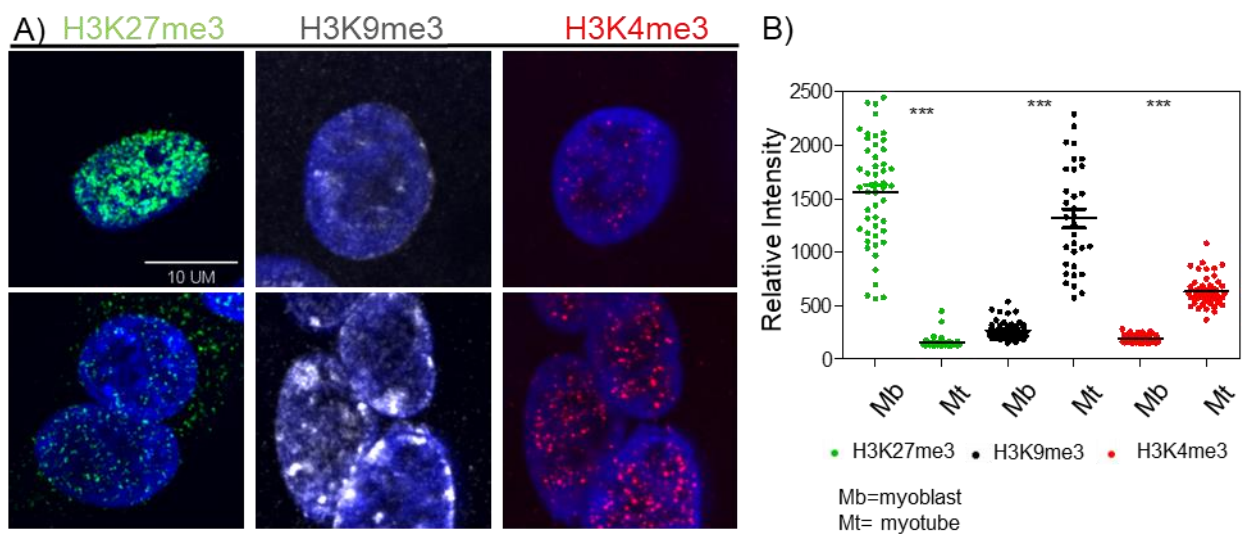


Figure R2: Immunofluorescence and quantification of histone methylation markers in myoblasts and myotubes.

H3K27me3 is a marker of the compaction of the facultative chromatin. H3K9me3 is a marker of constitutive heterochromatin. H3K4me3 is a marker of euchromatin. (A) Confocal images of myoblasts and myotubes. DNA was stained with DAPI (in blue), H3K27me3 (in green), H3K9me3 (in white) and H3K4me3 (red). (B) Quantification of the relative intensity of histone methylation markers. Mb=myoblast; Mt= myotube. n=53 nuclei from 3 independent experiments.

II. Effects of A-type lamin on myonuclei

i. *siLMNA* induced important deformations of the myonucleus shape in static conditions

The efficacy of LMNA depletion was assessed using PCR and western-blotting (Figure R3). Figure R4 shows the nuclear morphology of myotubes treated for 48 hours with *siLMNA* knockdown. A-type lamin deficient myotubes exhibited nucleus deformations, as attested by higher A/R ratio ($p < 0.05$) and significantly lower nuclear volume, despite higher nucleus area (figure R4A-D).

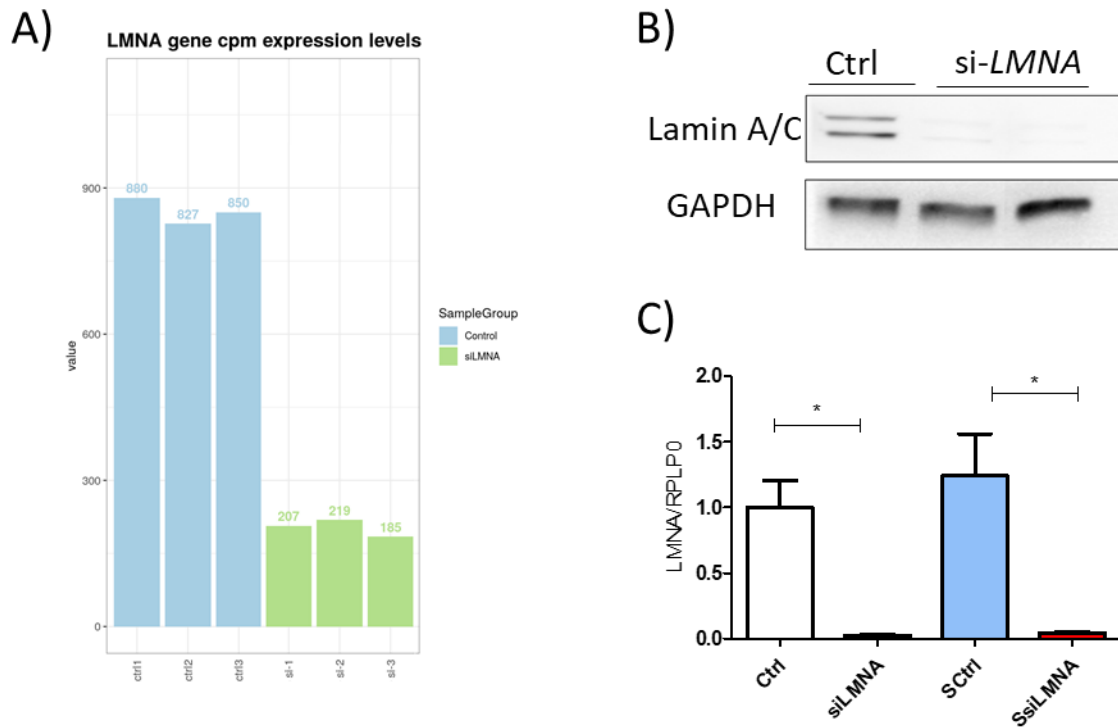


Figure R3: Validation of siRNA

(A) LMNA gene cpm expression level. (B) Representative Western blot membrane of control myotubes and *siLMNA* treated myotubes. (C) Histogram depicting relative quantification of LMNA mRNA expression in static and stretched control and *siLMNA*-treated samples.

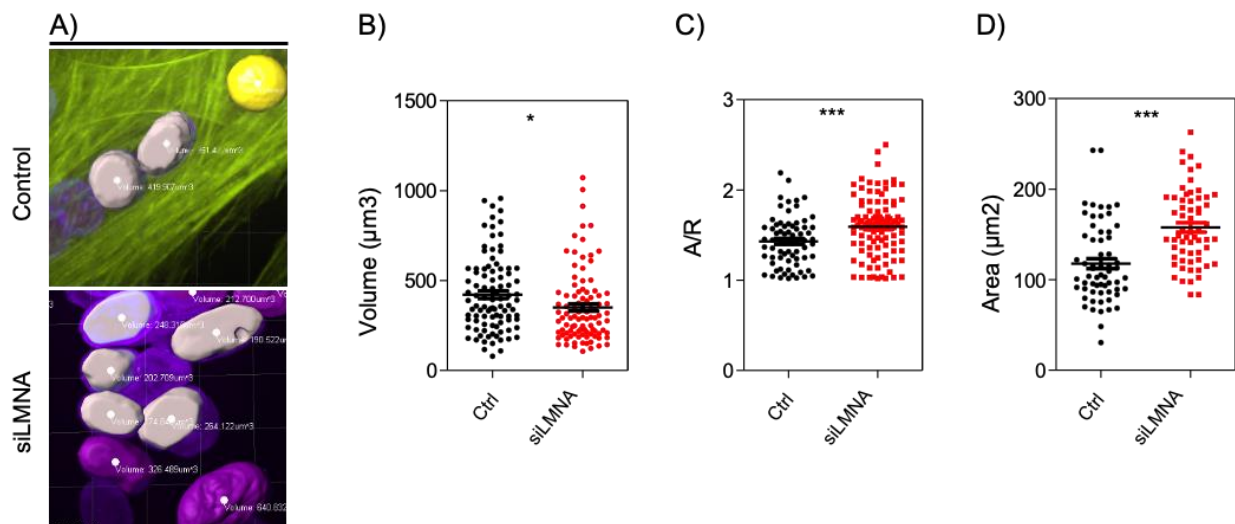


Figure R 4: Nuclear segmentation and analysis of nuclear shape and volume after LMNA knockout.

(A) Phalloidin and DAPI were used to label the actin cytoskeleton (in green) and the nuclei. Automatically detected nucleus (in Yellow) and manually detected nucleus (purple) were analyzed using Imaris. (B) Quantification of the nuclear volume (C), ratio A/R (Fiji imageJ) and (D) nuclear area. Mb=myoblast; Mt=myotube. n=175 from 3 independent experiments.

ii. Effects of siLMNA on chromatin markers in static conditions

LMNA knockout in myotubes induced important histone modification state as attested by immunofluorescence (Figure R5) and Western blots (Figure R6). Lamin deficiency was associated with a significant decrease in the facultative heterochromatin marker H3K27me3 and an increase in the constitutive heterochromatin marker H3K9me3. In addition, the euchromatin marker H3K4ac was significantly higher in LMNA deficient myotubes compared with controls (Figures R5 A-D and 6).

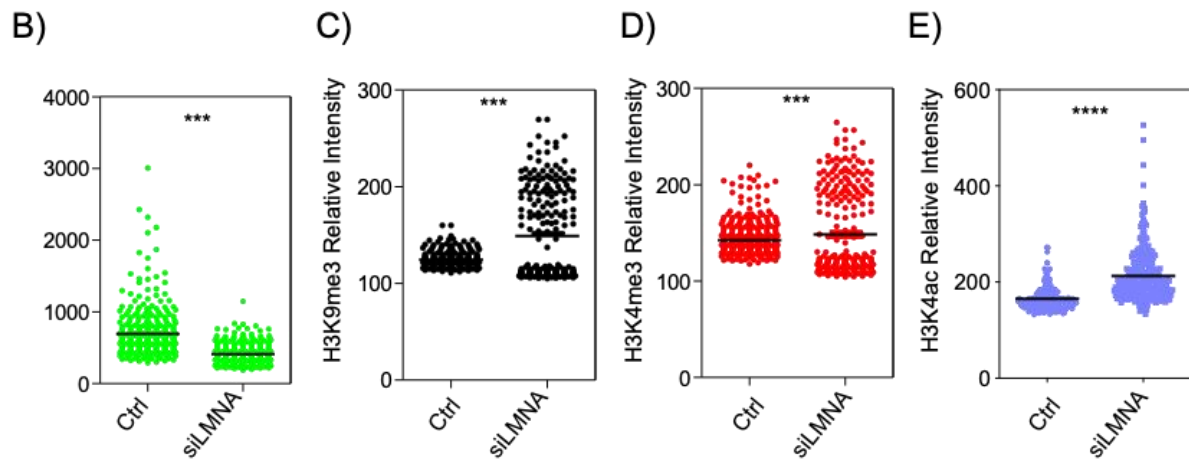
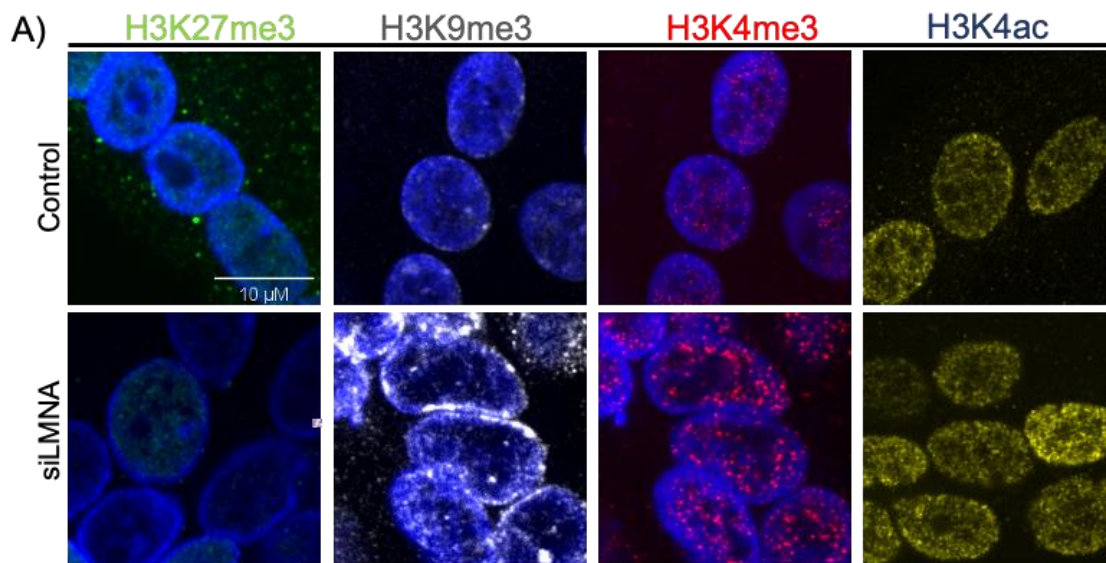


Figure R5: Immunofluorescence and quantification of histone methylation markers in control and *siLMNA* treated myotubes.

Confocal images of control myotubes and *siLMNA* treated myotubes. DNA is stained with Dapi (blue), H3K27me3 (in green), H3K9me3 (in white), H3K4me3 (red) and H3K4ac (yellow). (B) Quantification of the relative intensity of H3K27me3. (C) Quantification of the relative intensity of H3K9me3 (D) Quantification of the relative intensity of H3K4me3. (E) Quantification of the relative intensity of H3K4ac. Ctrl=Control; si-L= LMNA knockout myotubes n=at least 316 from 3 independent experiments.

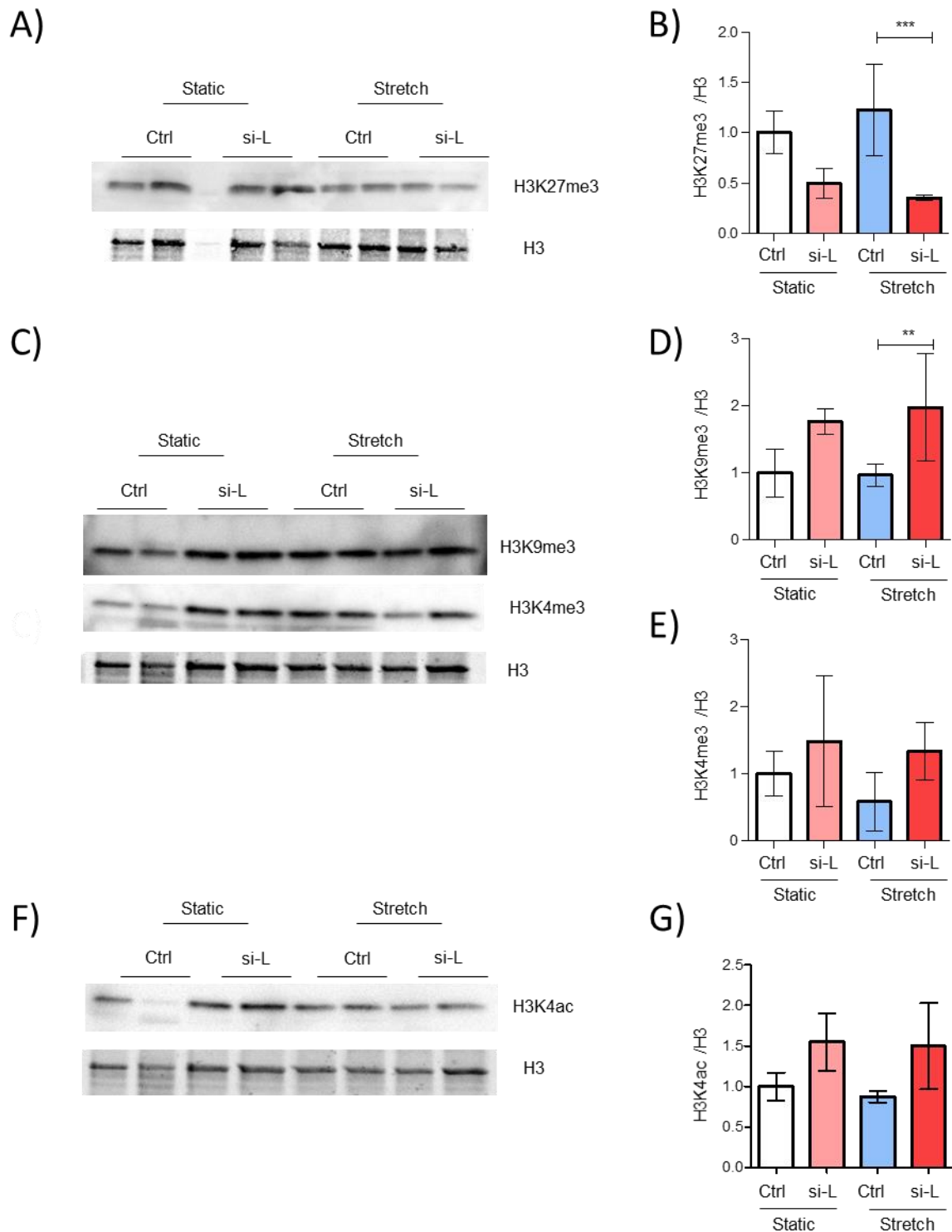


Figure R6: Western blot and quantification of histone methylation markers in siLMNA treated myotubes before and after cyclic stretch.

(A) Representative Western blot membrane of control myotubes and siLMNA treated myotubes before and after stretch for H3K27me3, H3K9me3 and H3K4me3. (B) Quantification of the protein expression of H3K27me3, H3K9me3 and (E) H3K4me3. Ctrl=Control; si-L= LMNA knockout myotubes. N=4 from 3 independent experiments. Values are means \pm SED.

RNAseq analysis in control and *LMNA* deficient myotubes was performed to analyze global changes in histone mark regulation. In static conditions, around 469 the genes were found to be upregulated and 488 to be downregulated in *LMNA* deficient myotubes.

The principal component analysis, and conventional differential expression analysis supported significant increase, in gene set in *LMNA* deficient myotubes compared to controls. Gene ontology (GO) term enrichment analysis, of differentially expressed ($p < 0.05$) genes, with the parent GO term histone modification indicated the related GO terms “H3K4 methylation” and “transcription initiation as significantly enriched in lamin deficient compared with control myotubes (Fig R7).

The expression of genes that regulate the methylation of H3K4, was upregulated in si*LMNA*-treated samples (Figure R7 C). Thus validating the immunofluorescence shown in Fig R5. A validation RT-qPCR was done for a selected gene *PIH1D*. *PIH1D* gene enables RNA polymerase I core promoter sequence-specific DNA binding activity. It is also involved in positive regulation of signal transduction.

Our results also uncover that *LMNA* knockdown leads to the upregulation of genes implicated in DNA templated transcription initiation (Figure R7 E). This result shows that the *LMNA* knockdown activates the transcription, and this result in in accordance with the observed increase in H3K4me3.

Most of the affected GO terms are related to the nucleus mechanotransduction, such as GO actin cytoskeleton, GO nuclear membrane, GO polymeric cytoskeletal fiber and GO membrane region. Interestingly, GO euchromatin and nuclear euchromatin terms were affected by si*LMNA*-treatment (Figure R7 F).

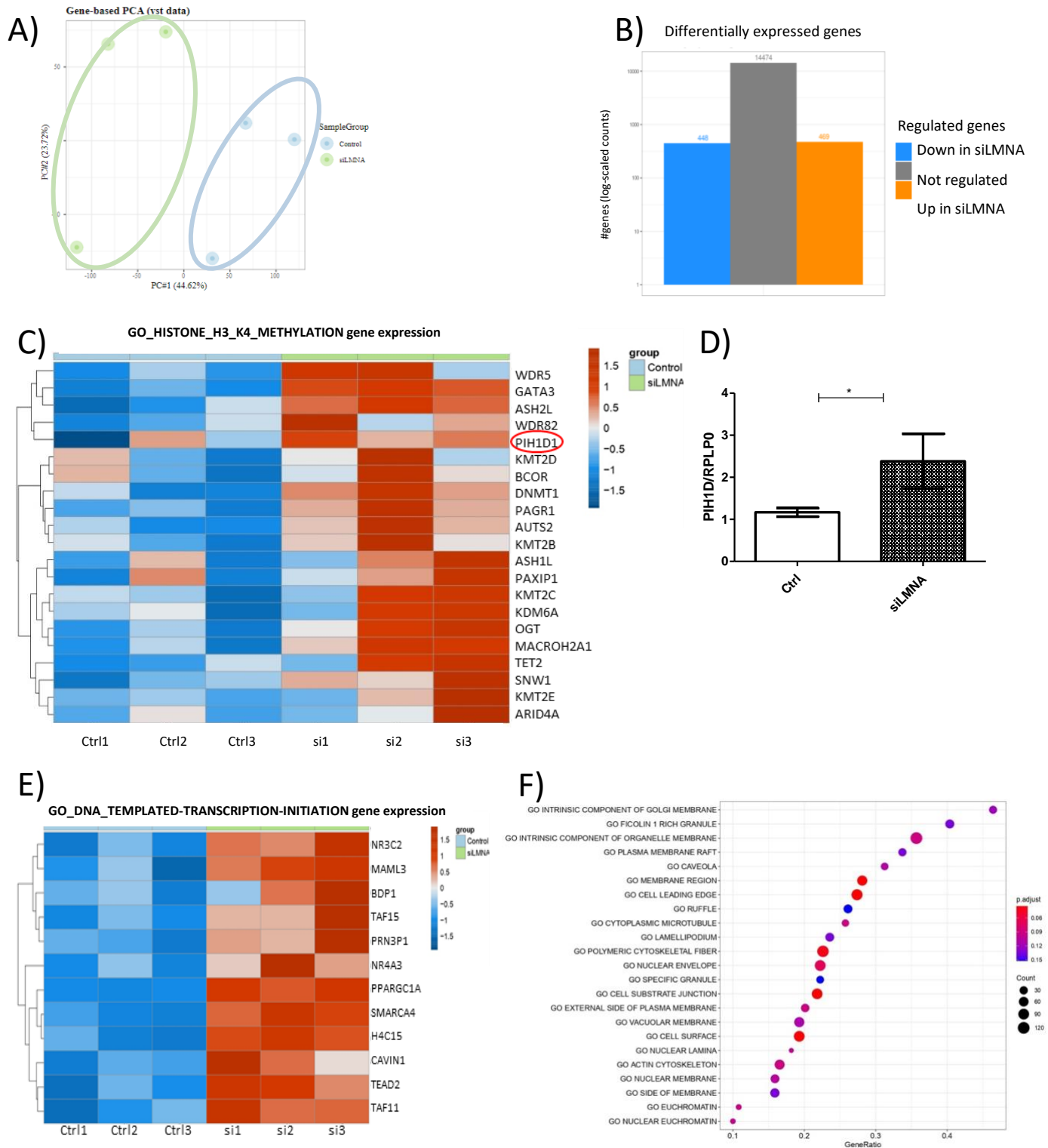


Figure R 7: PCA analysis, rt-qPCR, GO terms enriched and dot plot of Go term enriched in control and siLMNA treated myotubes.

(A) Principal component analysis of RNA-seq data. The first and second axes are represented. (B) Histogram illustrating the differentially expressed genes between control and siLMNA samples. An mRNA log₂ fold-change above an absolute value of 1 and with a p value below 0,5 was used as a threshold. (C) Heatmap of GO term “Histone H3K4methylation gene expression” for control and siMNA-treated samples. (D) Histogram depicting relative quantification of *PIH1D* mRNA expression in control and si-LMNA treated samples. (E) Heatmap of GO term “DNA templated transcription initiation gene expression”.(F) Dotplot of Go terms enriched in control compared to siLMNA myotubes. Log₂ fold-change Threshold= 1; P value=0.05. The Dotplot depicts the gene ratios (number of core genes over the total number of genes in the set). The dots are colored by the adjusted p-value and their size is proportional with the size of the gene-set.

III. Effects of cyclic stretch on nucleus shape and histone marks

How nuclear morphology and chromatin are affected by mechanical load in normal and pathological skeletal muscle remains unknown.

Myotubes were submitted to 10% cyclic stretch for 4 hours. In control myotubes, mechanical stretch significantly increased nuclear volume and the apparent nuclear area but did not modify the A/R ratio (Fig R8). In *LMNA* deficient cells, mechanical challenges majored nuclear deformations, as attested by significant increase in the A/R ratio. In addition, *LMNA* deficient stretch abolished the stretch-induced regulation in nuclear volume (Fig R8B).

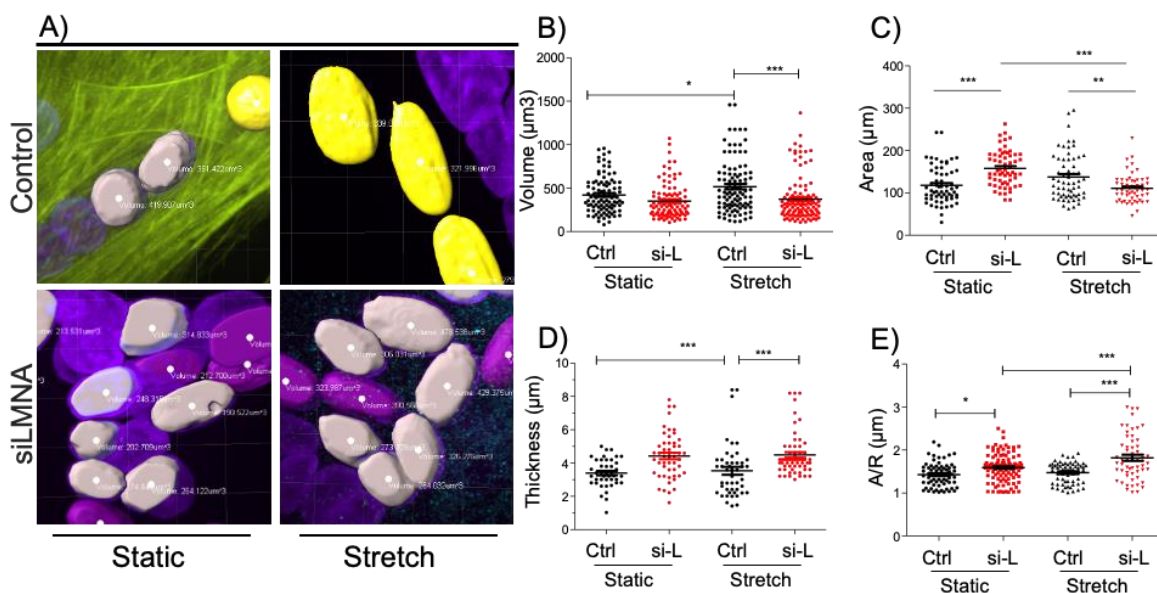


Figure R8: Nuclear segmentation and analysis of nuclear shape after *LMNA* knockout and cyclic stretch.

Phalloidin and DAPI were used to label the actin cytoskeleton (in green) and the nuclei. Automatically detected nucleus (in Yellow) and manually detected nucleus (purple) were quantified using Imaris. Comparison between myotubes in static and load state. (B) Quantification of the nuclear volume, (C) nuclear area, (D) nuclear thickness (E) and A/R ratio. Ctrl=Control; si-L= siRNA *LMNA*; n=at least 50 from 3 independent experiments.

Changes in chromatin methylation after load are shown in Figure 9R. Cyclic stretch significantly increased the facultative heterochromatin marker H3K27me3 both in control and *LMNA* deficient myotubes. Strikingly, the euchromatin marker H3K4me3 significantly increased after stretch in *LMNA* deficient myotubes whereas no significant changes were observed in controls. Further, the H3K4ac histone markers decreased after stretch in both control and *LMNA* deficient myotubes, but the H3K4ac levels remained significantly higher in lamin deficient myotubes compared with controls (figure R10). In control myotubes, no significant changes in the constitutive heterochromatin marker H3K9me3 were observed after cyclic stretch (figure R9) whereas H3K9me3 significantly increased in stretched *LMNA* KO myotubes.

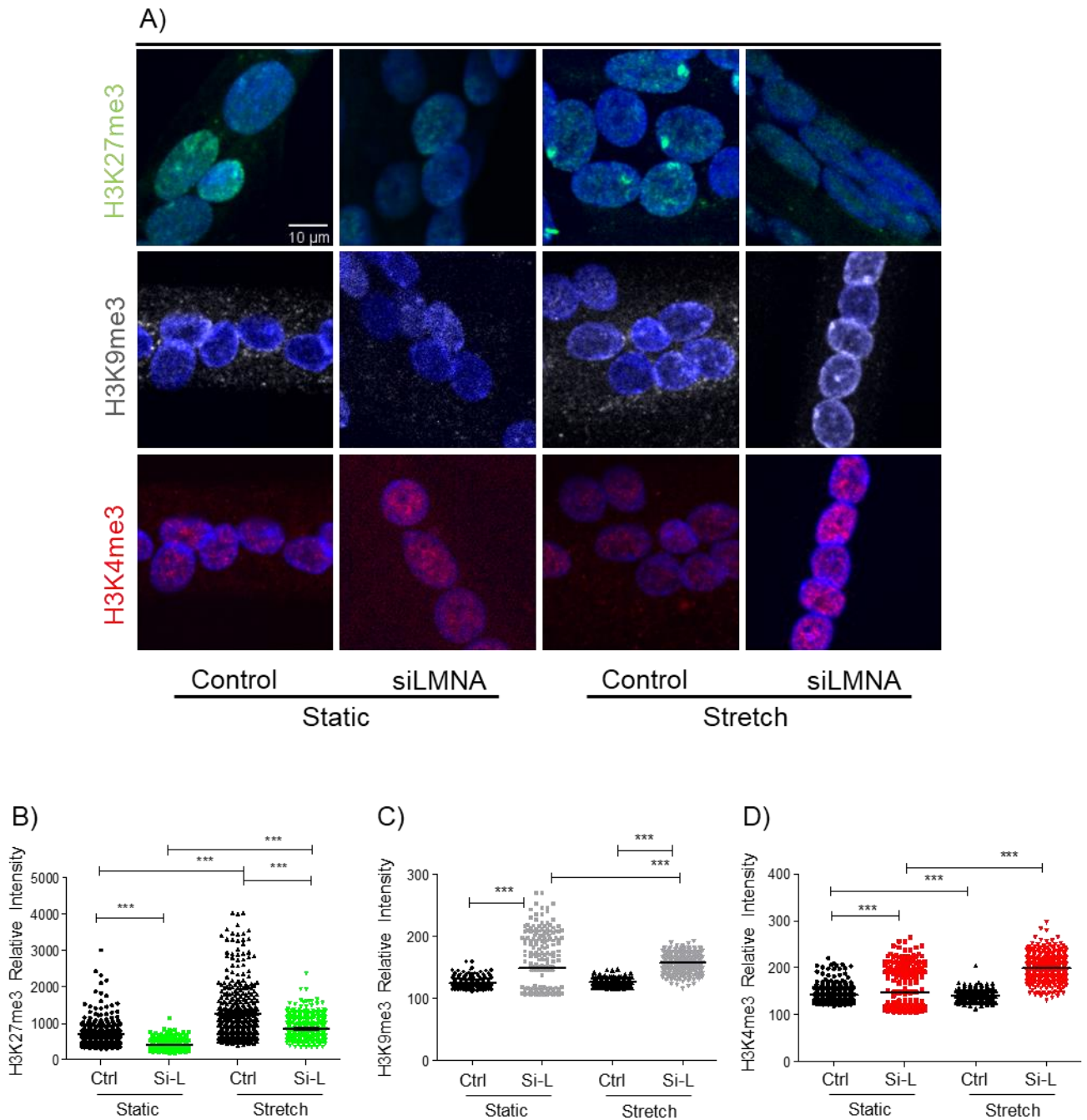


Figure R9: Immunofluorescence and quantification of histone methylation markers in siLMNA treated myotubes before and after cyclic stretch.

Confocal images of control myotubes and siLMNA treated myotubes before and after stretch. DNA is stained with Dapi (blue), H3K27me3 (in green), H3K9me3 (in white) and H3K4me3 (red). (B) Quantification of the relative intensity of H3K27me3. (C) Quantification of the relative intensity of H3K9me3 (D) Quantification of the relative intensity of H3K4me3. Ctrl=Control; si-L= LMNA knockout myotubes n=at least 316 from 3 independent experiments.

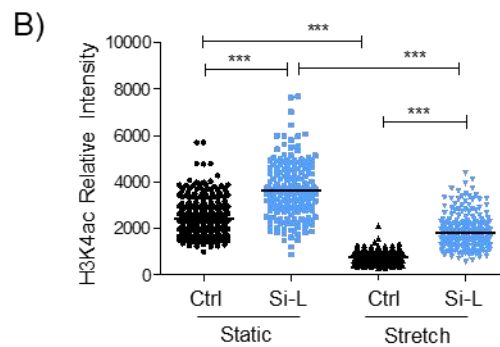
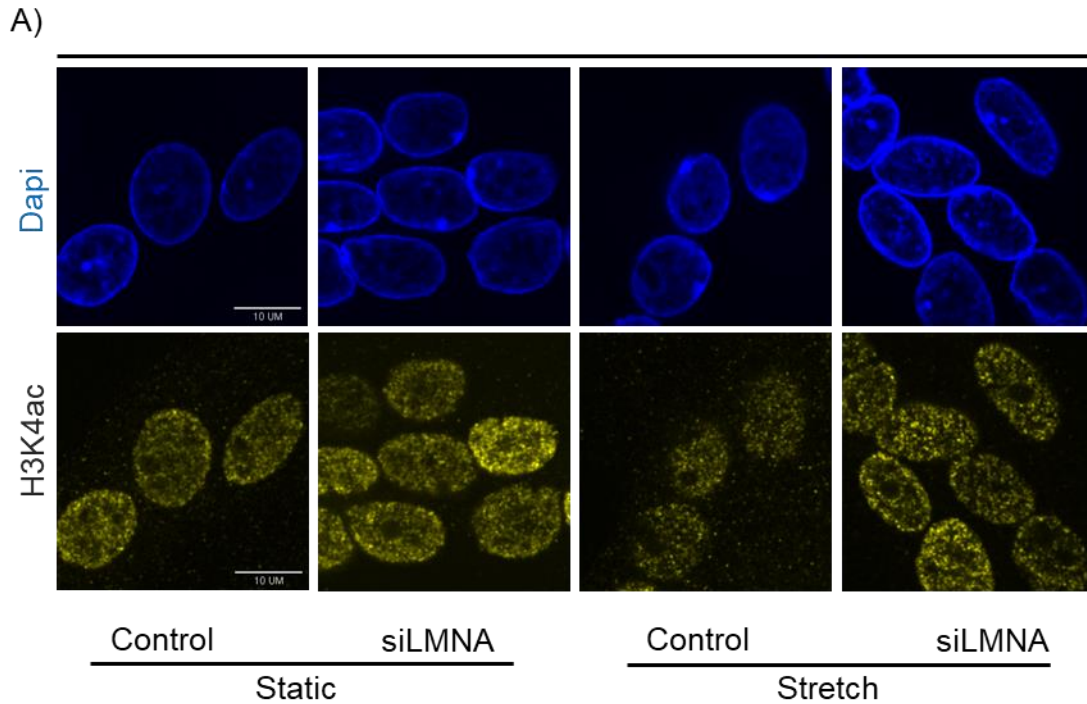


Figure R 10: Immunofluorescence and quantification of histone lysine 4 acetylation markers in siLMNA treated myotubes before and after cyclic stretch.

Confocal images of control myotubes and siLMNA treated myotubes before and after stretch. DNA is stained with Dapi (blue),H3K4ac (in yellow). (B) Quantification of the relative intensity of H3K4ac. Ctrl=Control; si-L= LMNA knockout myotubes n=at least 200 from 3 independent experiments.

PCA shows that stretch did not strikingly affect gene expression in control myotubes, with only 3 upregulated and 4 downregulated genes (Figure R 11B). In contrast, samples cluster according to the presence of A-type lamins (Figure R 11C). In addition,the siLMNA samples cluster according to the stretch condition and explain most of the variance between the sample's groups (Figure R 11D).

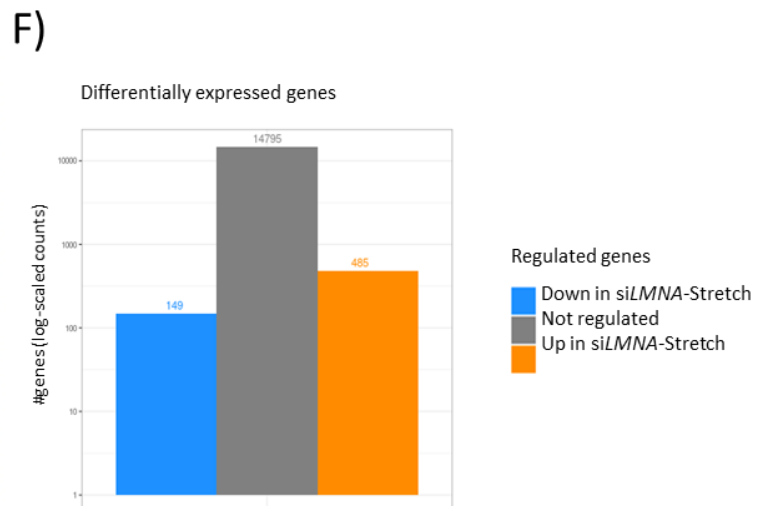
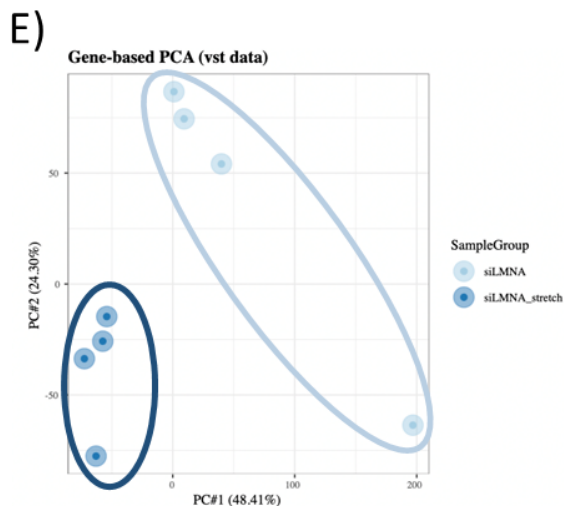
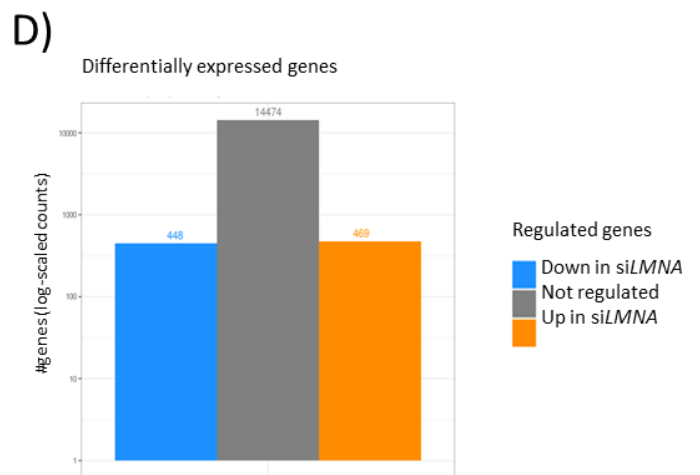
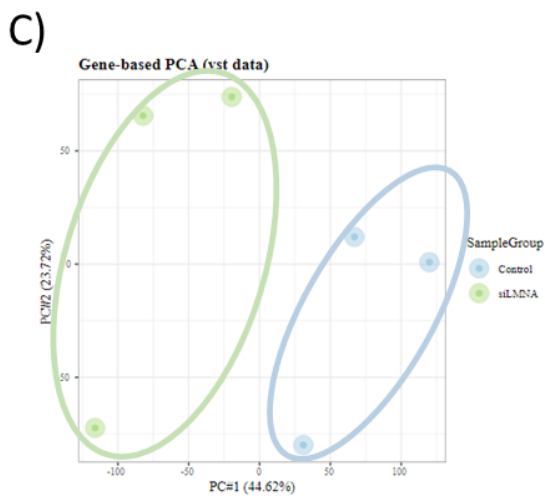
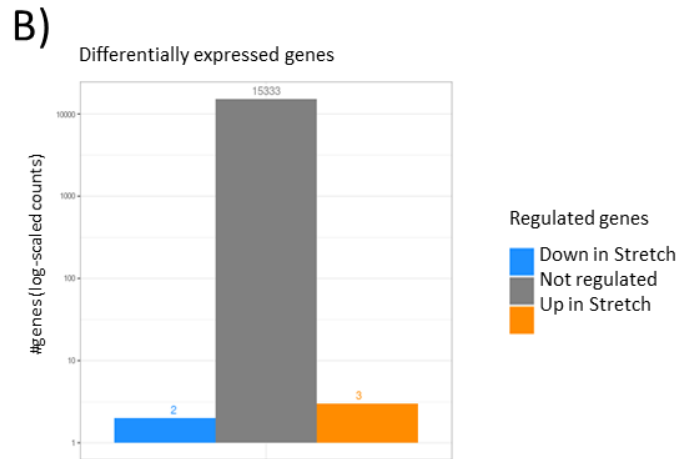
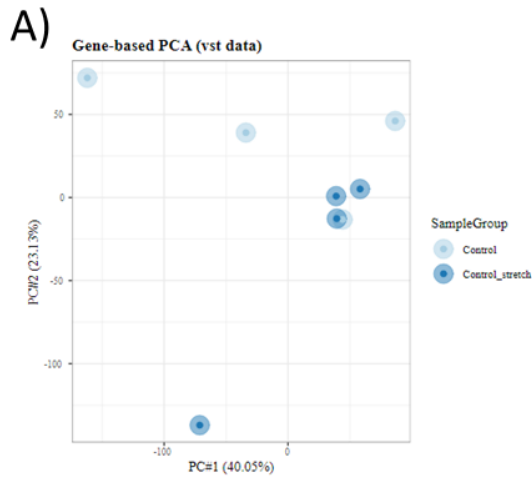


Figure R 11: RNAseq samples description and differential gene expression in static siLMNA and siLMNA stretched myotubes.

(A) Principal component analysis of RNA-seq data. The first and second axes are represented. (B) Histogram illustrating the differentially expressed genes between siLMNA and stretched siLMNA samples. An mRNA log₂ fold-change above an absolute value of 1 and with a p value below 0,5 was used as a threshold.

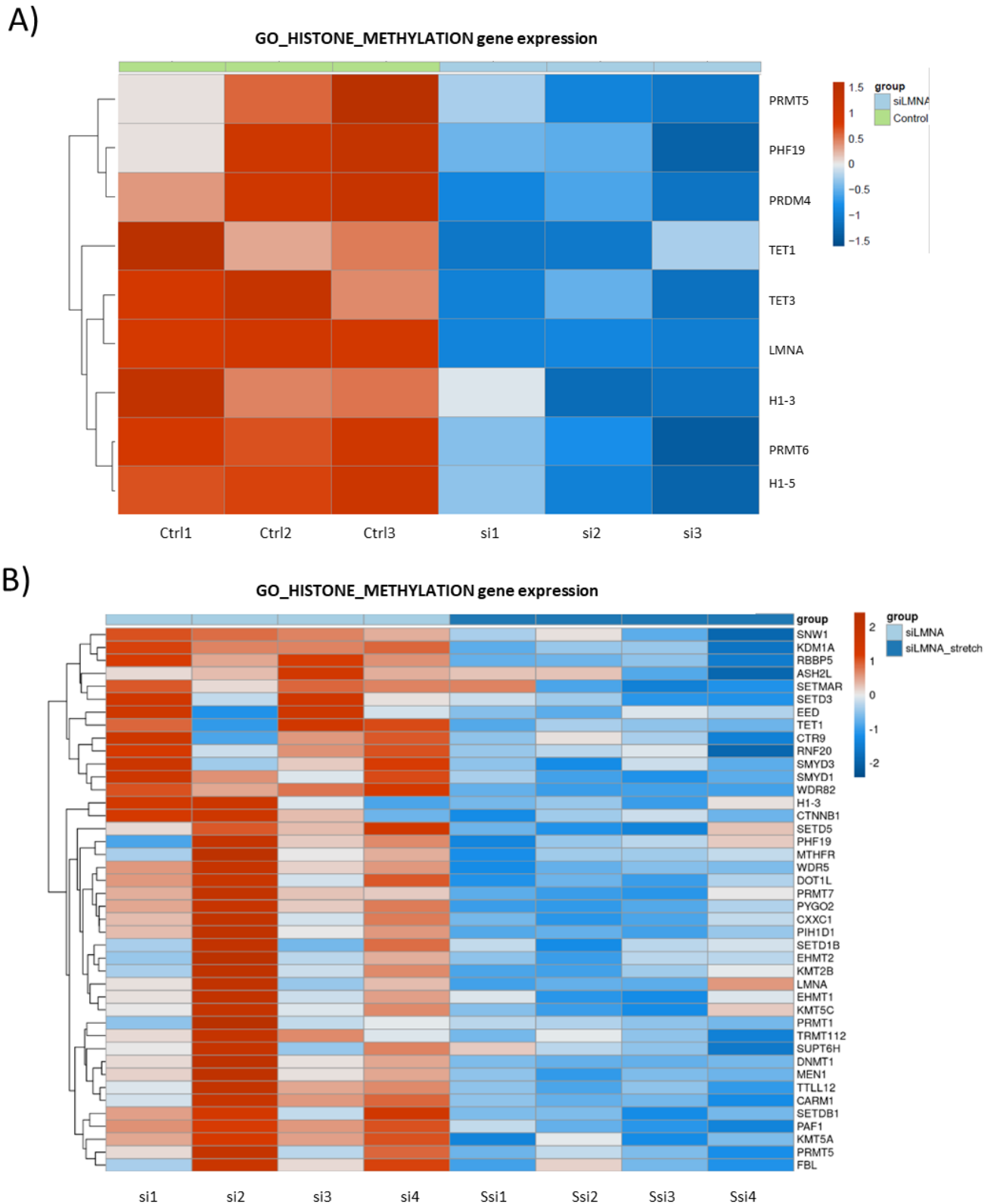


Figure R 12: GO terms enriched in control vs and siLMNA vs stretched siLMNA myotubes.

(A) Heatmap of GO term “Histone methylation gene expression” for Control and siLMNA-treated samples. (B) Heatmap of GO term “Histone methylation gene expression” for siLMNA and stretched siLMNA-treated samples (E) Heatmap of GO term “Nuclear Euchromatin gene expression”. (F) Heatmap of GO term “Transcriptionally active chromatin gene expression”.

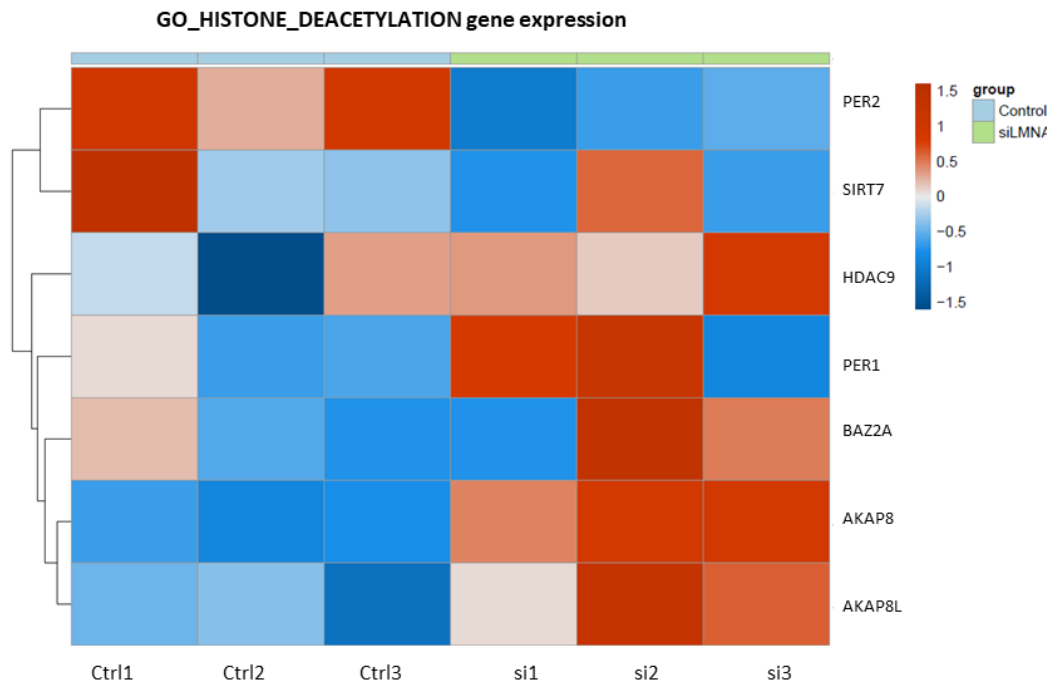
In static condition, *siLMNA* treatment downregulated the expression of genes regulating histone methylation (Figure R 12 A).

In *siLMNA*-treated samples, stretch downregulated the expression of genes regulating histone methylation (Figure R 12 B). Whereas no significant difference was observed in control myotubes.

In addition, genes involved in histone deacetylase complex were upregulated in *siLMNA* versus control myotubes. However, genes involved in histone deacetylase complex were downregulated in stretched *siLMNA* versus static *siLMNA* myotubes (Figure R13 A).

Thus, we show deregulation in both acetylation and methylation in static and stretched *siLMNA*. Overall, *LMNA* deficiency causes an increase in euchromatin and aberrant activation of transcription after stretch (Figure R13 A-B).

A)



B)

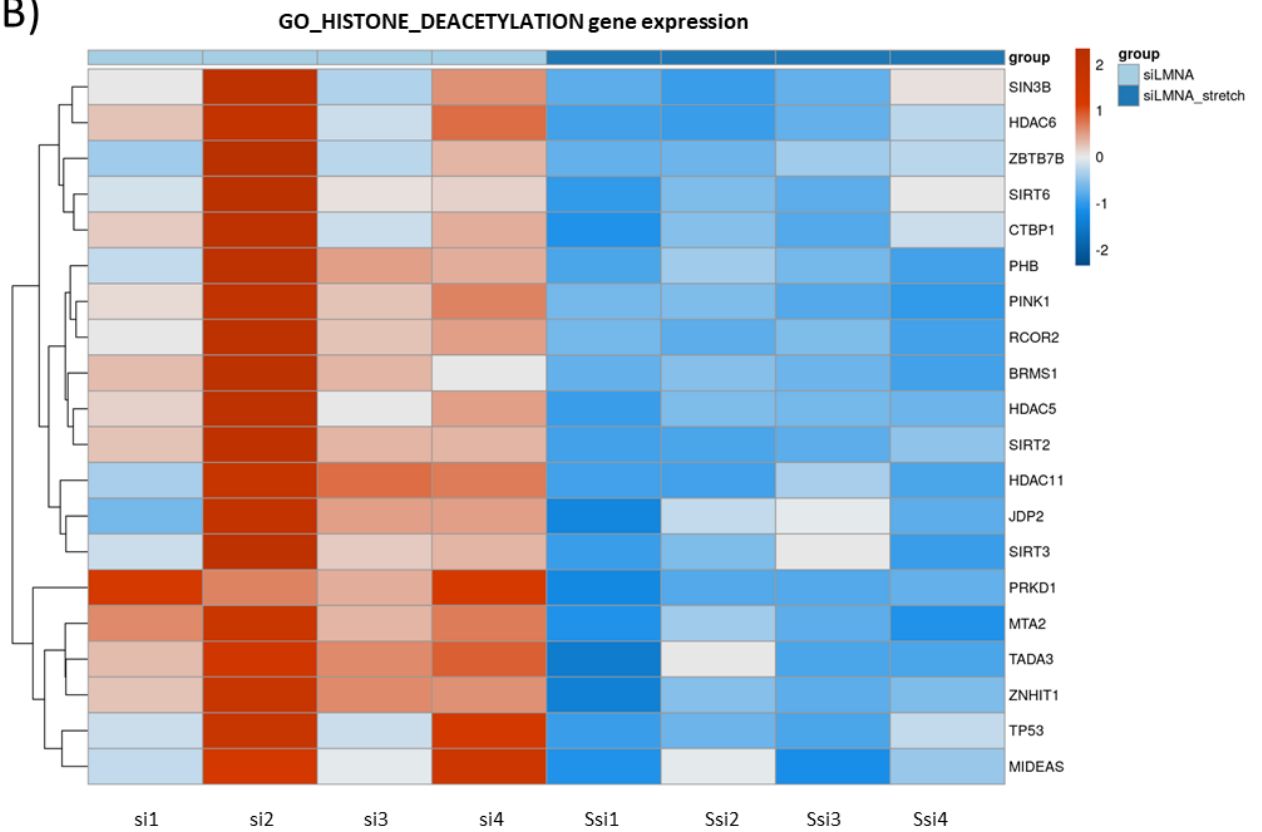
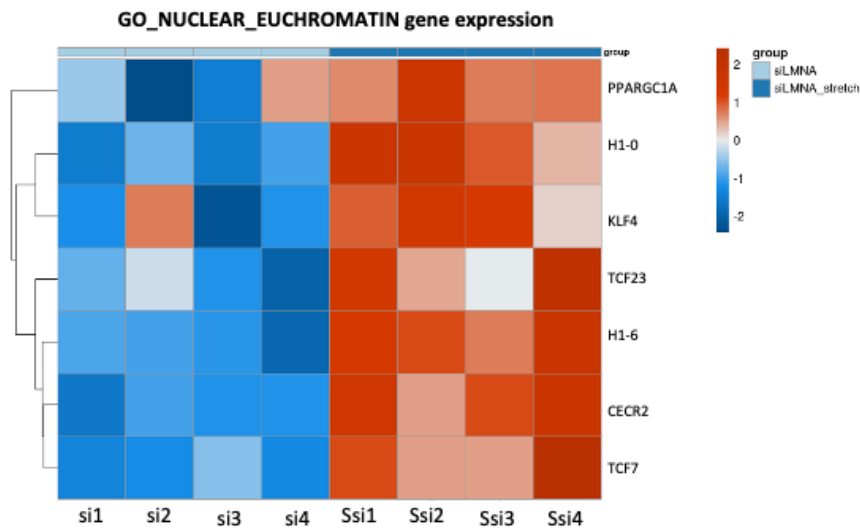


Figure R13: GO terms enriched in control vs siLMNA and siLMNA vs stretched siLMNA myotubes.

(A) Heatmap of GO term "Histone Deacetylation gene expression" for Control and siLMNA-treated samples. (B) Heatmap of GO term "Histone Deacetylation gene expression" for siLMNA and stretched siLMNA-treated sample.

A)



B)

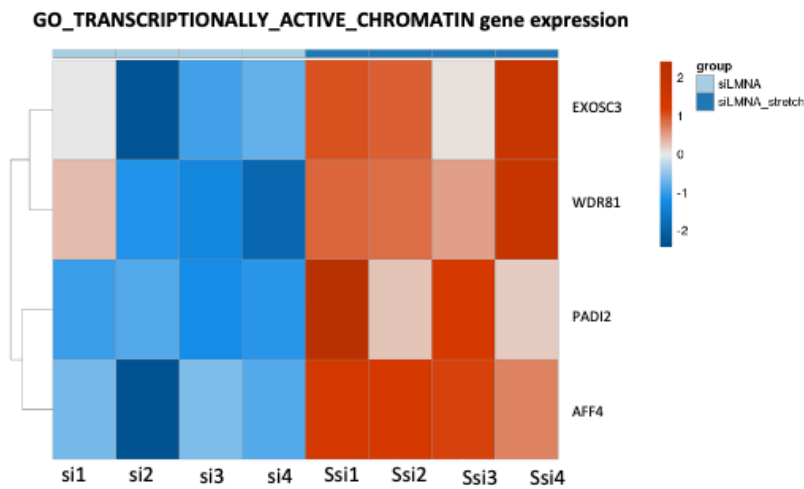


Figure R14: GO terms enriched in control vs siLMNA and siLMNA vs stretched siLMNA myotubes.

(A) Heatmap of GO term “Histone Nuclear Euchromatin gene expression” for Control and siLMNA-treated samples. (B) Heatmap of GO term “Transcriptionally Active Chromatin gene expression” for siLMNA and stretched siLMNA-treated samples.

Overall, our data indicated that mechanical stretch in *LMNA* KO myotubes lead to an aberrant increase in nuclear euchromatin and abnormal transcriptional activation.

IV. Effects of siSUN1 and SUN2

i. Effects of SUN1 or SUN2 silencing on nuclear characteristics

We then investigated the respective roles of nuclear envelope proteins *SUN1* and *SUN2* in myonuclear morphology (Figure R 15). Cells were silenced for *SUN1* or *SUN2* expression using specific siRNA strategies. In static conditions, myonuclei deficient in *SUN1* had significantly higher nuclear area but with no significant change in the myonuclear shape and volume (Figure R 15A-D). Stretch induced significant increase in A/R in myonuclei deficient in *SUN1* (Figure R 15D). In addition, *SUN1* deficiency abolished the stretch-induced increase in nuclear volume.

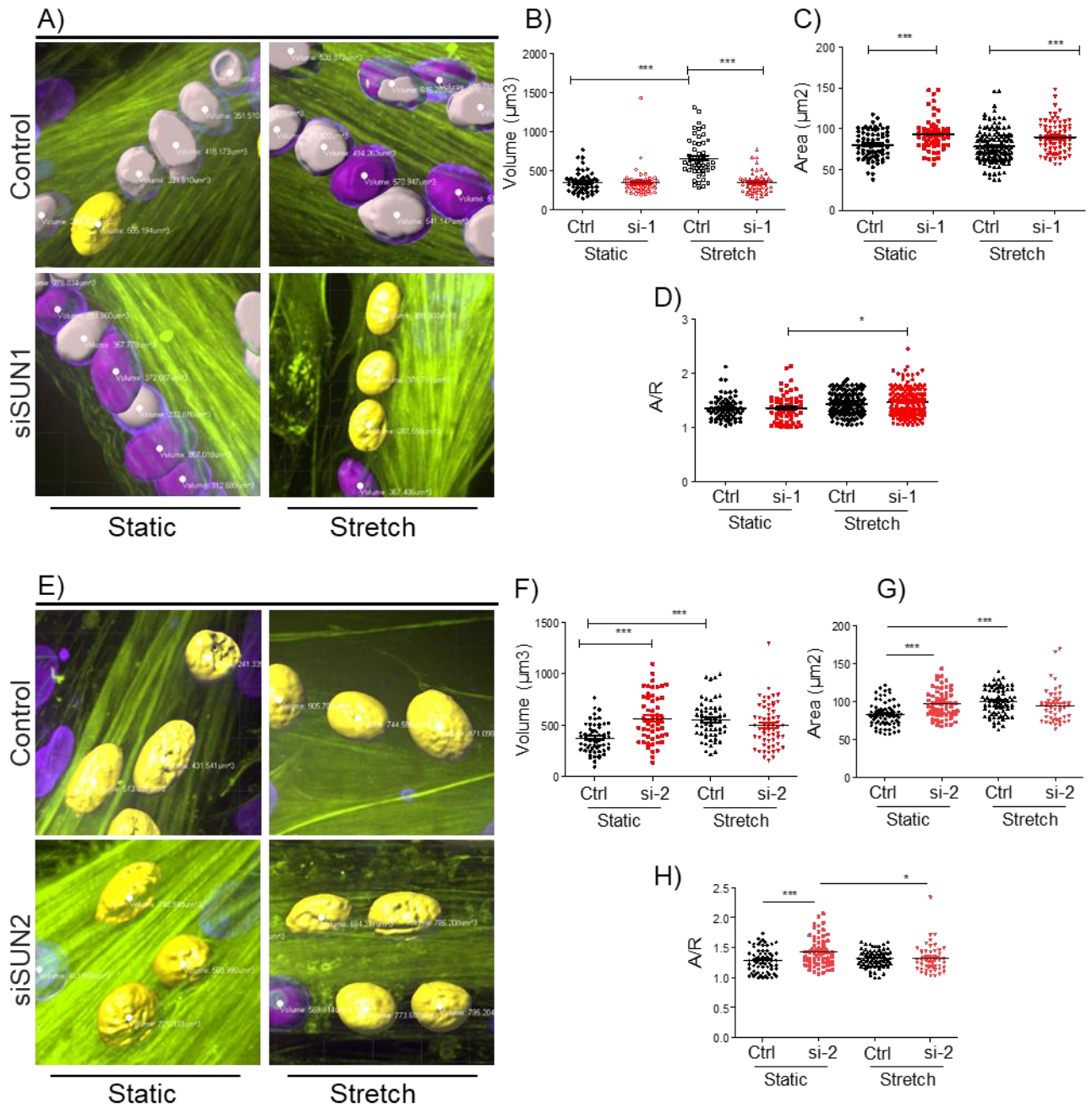


Figure R15: Nuclear segmentation and analysis of nuclear shape after LMNA knockout and cyclic stretch.

A) Left panels: Actin was labeled with Phalloidin (green) and DNA with DAPI (blue). Myonuclei automatically detected by Imaris were in Yellow, whereas manually detected myonuclei were in purple and Gray. (A) Effects of *SUN1* silencing before and after stretch. Right panels (B) Quantification of nuclear Volume, (C) area, (D) and A/R ratio in control and si*SUN1* treated myotubes, before and after stretch.

F) Left panels: Actin was labeled with Phalloidin (green) and DNA with DAPI (blue). Myonuclei automatically detected by Imaris were in Yellow, whereas manually detected myonuclei were in purple and Gray. (A) Effects of *SUN2* silencing before and after stretch. Right panels (B) Quantification of nuclear Volume, (C) area, (D) and A/R ratio in control and si*SUN1* treated myotubes, before and after stretch. n=at least 50 from 3 independent experiments.

In contrast, silencing SUN2 induced major nuclear deformations in static conditions, as attested by significant increase in nuclear volume, area and A/R ratio (Figure R 15E-H). However, no additional differences in nuclear morphology were observed after stretch in SUN2-deficient myonuclei (Figure R 15E-H).

These results suggested that SUN2 played crucial role in maintaining the myonuclear morphology in static conditions.

ii. Effects of SUN1 or SUN2 silencing on histone marks

Both *siSUN1* and *siSUN2* treatment significantly decreased the constitutive heterochromatin marker H3K9me3 (Figures R 16 and 17). Importantly, in static conditions, *siSUN2* treatment induced a large reduction in H3K27me3 and in the euchromatin marker H3K4me3 compared to controls (Figure 17).

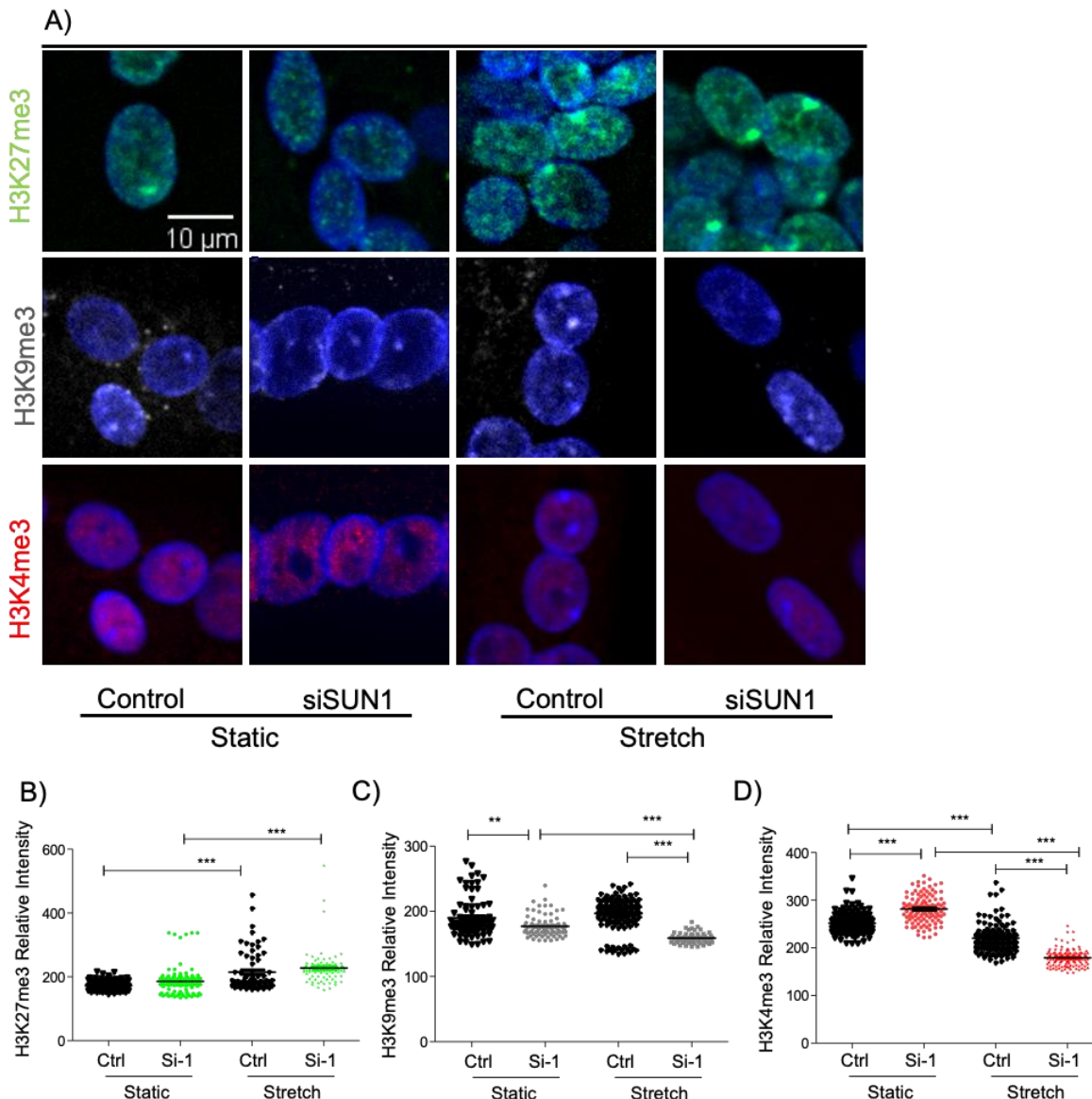


Figure R16: Immunofluorescence and quantification of histone methylation markers in *siSUN1* treated myotubes before and after cyclic stretch.

Confocal images of control myotubes and *siSUN1* treated myotubes before and after stretch. DNA is stained with Dapi (blue), H3K27me3 (in green), H3K9me3 (in white) and H3K4me3 (red). (B) Quantification of the relative intensity of H3K27me3, (C) H3K9me3 and (D) H3K4me3. Ctrl=Control; si-1= *SUN1* knockout myotubes n=at least 60 from 3 independent experiments.

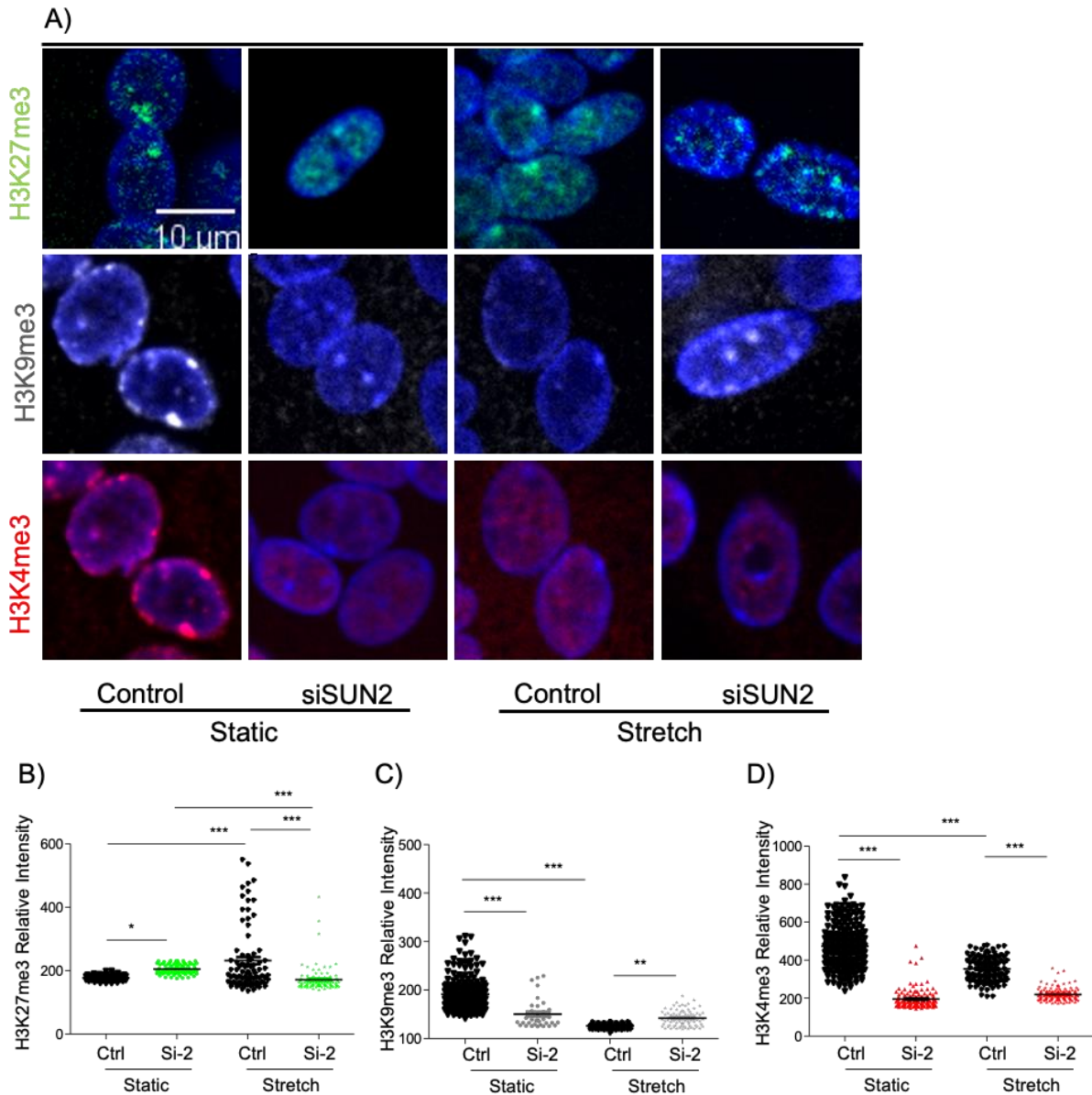


Figure R17: Immunofluorescence and quantification of histone methylation markers in siSUN2 treated myotubes before and after cyclic stretch.

(A) Confocal images of control myotubes and siSUN2 treated myotubes before and after stretch. DNA is stained with Dapi (blue), H3K27me3 (in green), H3K9me3 (in white) and H3K4me3 (red). (B) Quantification of the relative intensity of H3K27me3, (C) H3K9me3 and (D) H3K4me3. Ctrl=Control; si-2= *SUN2* knockout myotubes n=at least 50 from 3 independent experiments.

SUN1 deficiency did not prevent the increased tri-methylation of H3K27me3 after mechanical stretch (Figure R 17). In contrast, *SUN2* deficiency was associated with a stretch-induced reduction in H3K27me3 levels.

There was a major decrease in the euchromatin marker H3K4me3 after *SUN1* knockout after stretch (Figure R 16D) whereas stretch did not modulate H3K4me3 levels in *SUN2* deficient myonuclei (Figure R 17D).

Overall, silencing *SUN1* or *SUN2* was not associated with stretch- induced chromatin decompaction, thus suggesting that lamin-deficiency was directly involved in the abnormal accumulation of H3K4me3-marked chromatin in siLMNA treated myotubes.

V. Cyto-nucleoplasmic exchanges

i. The YAP response

We previously reported that *LMNA* mutations altered the cyto-nucleoplasmic shuttling of the Yes-Associated Protein (YAP), a transcriptional co-regulator that is crucial for mechanotransduction (Bertrand et al 2014; Owens et al 2020). YAP localization was analyzed in control and *LMNA* KO myotubes both in static and stretched conditions (Figure R 18). In static conditions, the nucleo-cytoplasmic ratio was significantly higher in *LMNA* deficiency myotubes compared with controls. As expected, mechanical stretch increased nuclear YAP localization in control myotubes. In contrast, the nucleo-cytoplasmic ratio of YAP significantly decreased after mechanical loading in siLMNA myotubes (Figure R 18 A-B).

Thus, the results in *LMNA* KO myotubes were consistent with those previously reported in *LMNA* mutant myotubes (Bertrand et al, 2014; Owens et al 2020) and strongly supported the role of A-type lamins in the regulation of stretch-induced modulations of the cyto-nucleoplasmic shuttling. In static conditions, nuclear deformations in *LMNA* KO cells could increase YAP nuclear translocation through the nuclear pore complex as reported in other cell types (Elosegui-Artola A et al 2018 ; Elosegui-Artola A). In absence of A-type lamins, cyclic stretch was likely to further impact the NE integrity, thus resulting in NE damage and reduction in active cyto-nucleoplasmic shuttling. Such hypothesis may contribute to the lower nuclear volume after stretch in *LMNA* KO myotubes.

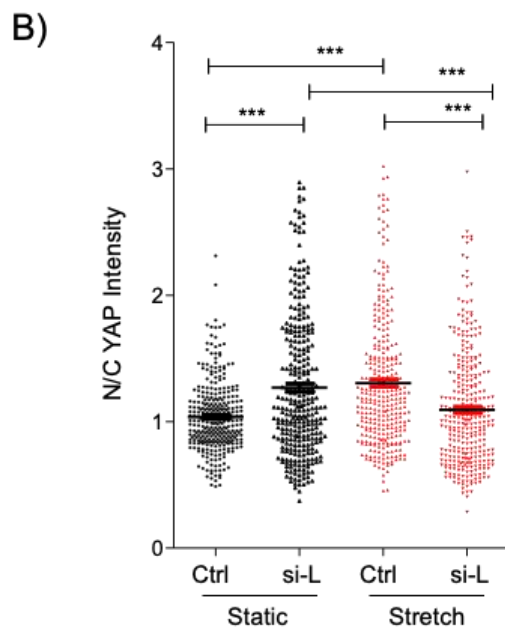
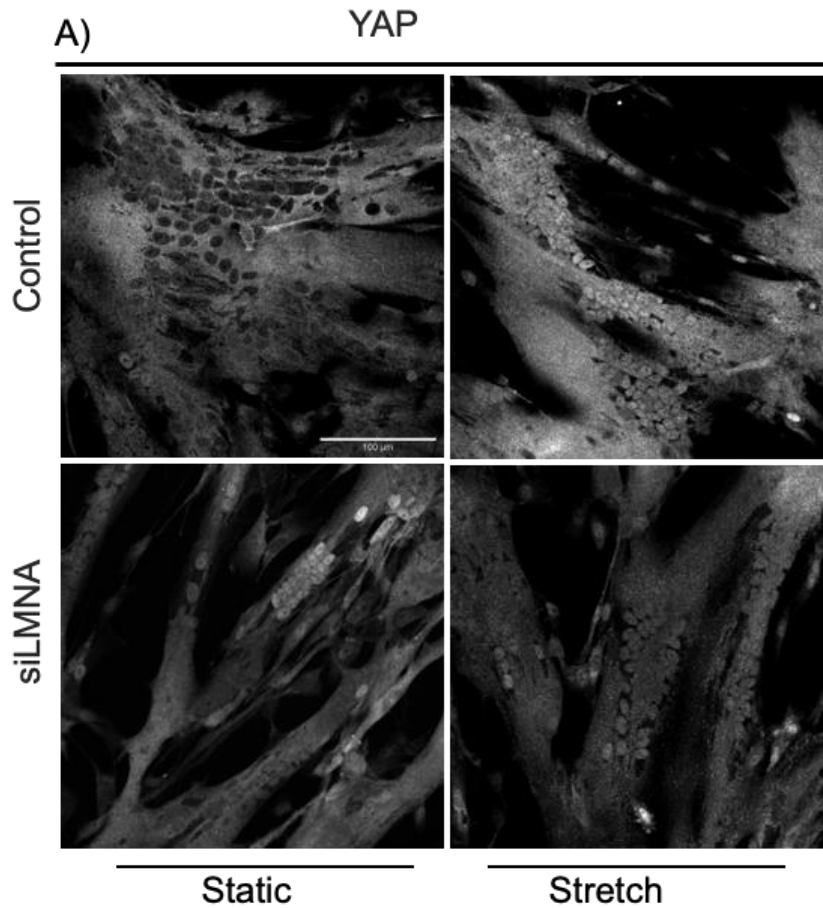


Figure R18: Immunofluorescence and quantification of YAP marker in siLMNA treated myotubes after cyclic stretch.

Confocal images of control myotubes and *LMNA* knockout myotubes before and after stretch. YAP is stained White. (B) Quantification of nuclear over cytoplasmic YAP intensity ratio.

Ctrl=Control; si-L= *LMNA* knockout myotubes. n=at least 314 from 3 independent experiments.

ii. **HDAC modification and acetylation marker intensity: effects of LMNA deficiency and stretch**

Histone acetyltransferases and histone deacetylases (HDACs) are responsible for adding and removing histone acetylation, respectively. In the nucleus, HDACs are generally known to promote transcriptional repression and gene silencing. A-type lamins are known to interact with histone deacetylase 2 (HDAC2) and regulate its activity during stress response (Mattioli E et al 2018 ; Sandi S et al 2020). It has been proposed that i) lamin-HDAC2 complexes in differentiating muscle cells could serve to move HDAC2 away from transcriptionally inactive loci of muscle genes, thus promoting transcription (Sandi S et al 2020) and that ii) *LMNA* mutations could modify the recruitment of HDAC2 to A-type lamins.

To determine whether potential changes in nuclear volume and H3K4ac levels in *LMNA* KO myotubes could be related to HDAC inhibition, we analyzed the effects of Trichostatin-A (TSA), a histone deacetylase (HDAC) inhibitor which results in enhanced acetylation of core histones and chromatin decompaction (Rao et al. 2007) (Bui et al. 2010).

As shown in Figure R 19, TSA treatment (0.1 μ M for 48h) significantly increased the nuclear volume and nuclear area in both myoblasts and myotubes compared with vehicle-treated cells (figure R 19 A-C). HDAC inhibition was associated with a significant increase in H3K4ac in myotubes that mimic the response observed in *LMNA* KO myotubes.

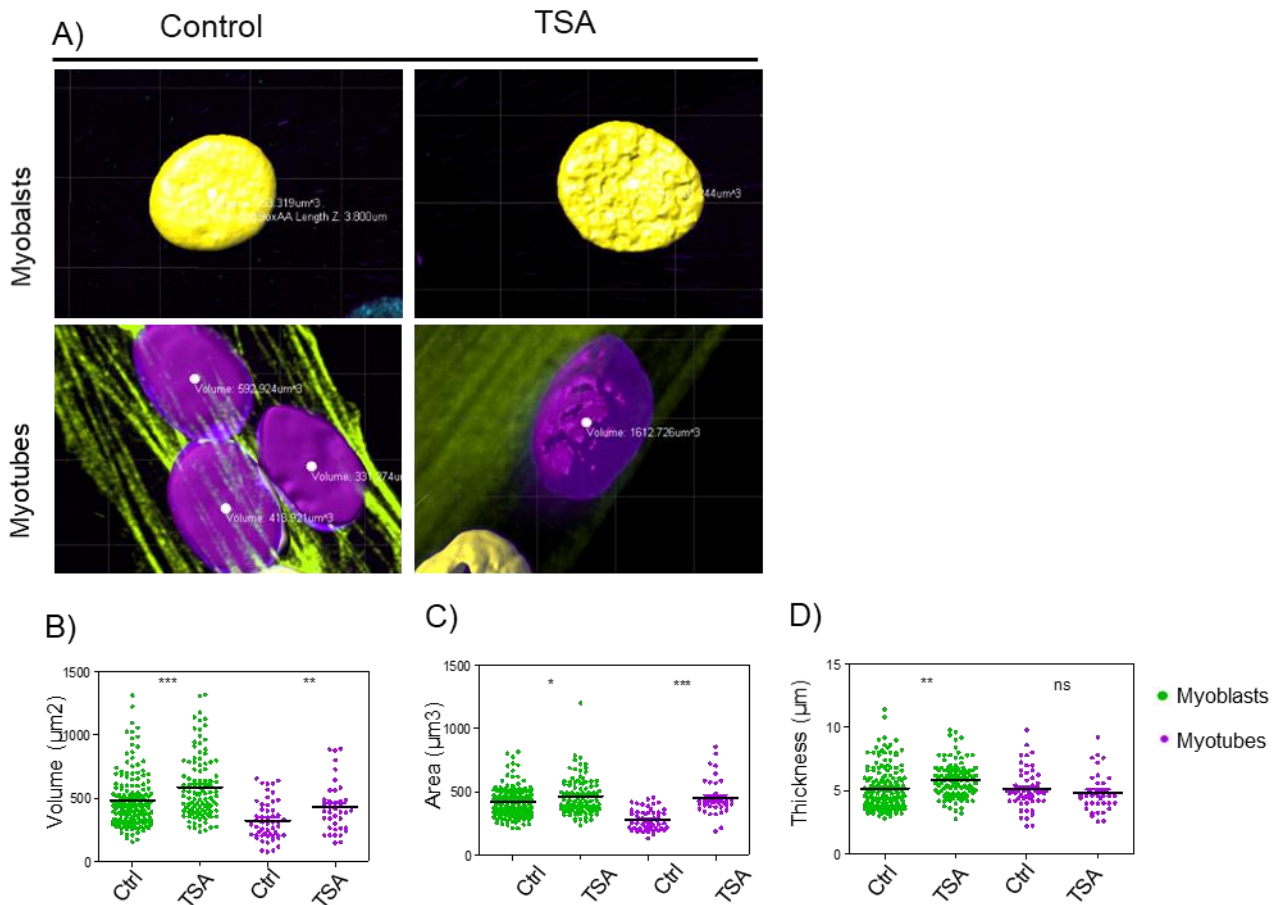


Figure R19: Nuclear segmentation and analysis of nuclear shape and volume after TSA treatment between myoblasts and myotubes.

A) Actin was labeled with Phalloidin (green) and DNA with DAPI (blue). Myonuclei automatically detected by Imaris were in Yellow, whereas manually detected myonuclei were in purple and Gray. Effects of TSA treatment (B) Quantification of nuclear Volume between control and TSA treated myoblasts and myotubes. (C) Quantification of nuclear deformation in control and TSA treated myoblasts and myotubes (C-D) n =at least 60 from 3 independent experiments. Ctrl=Control; TSA= Trichostatin-A

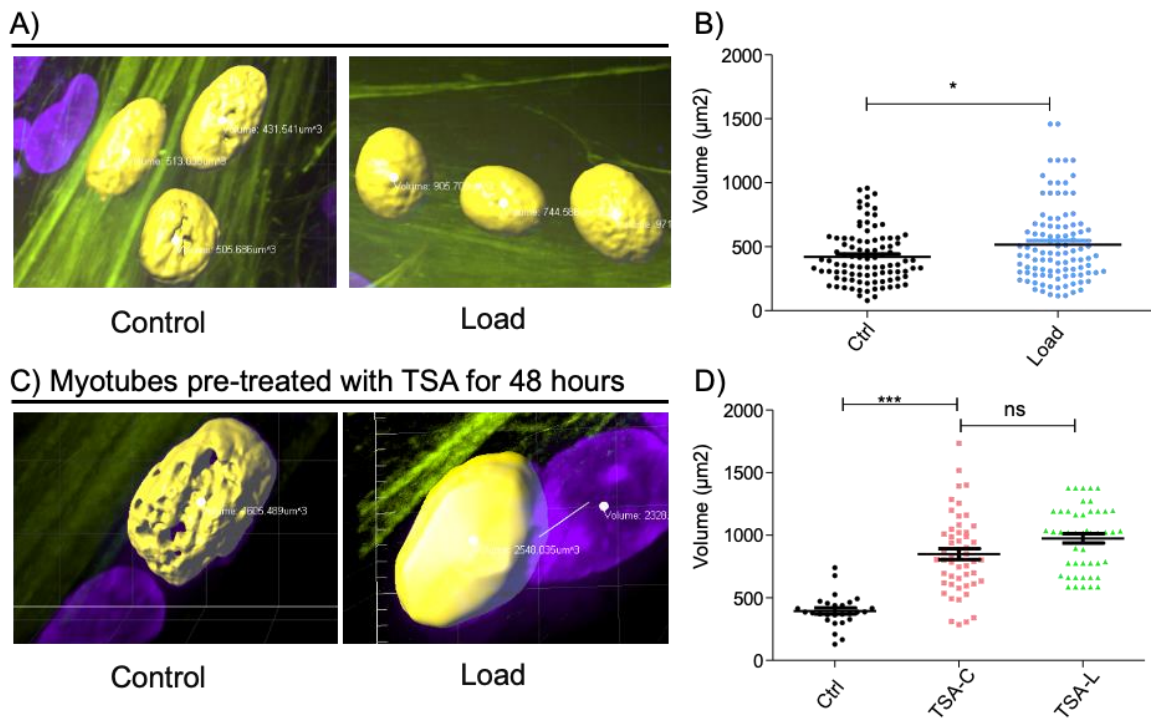


Figure R20: Nuclear segmentation and analysis of nuclear shape after TSA treatment and cyclic stretch.

(A) Phalloidin and DAPI were used to label the actin cytoskeleton (in green) and the nuclei. Automatically detected nucleus (in Yellow) and manually detected nucleus (purple) were quantified using Imaris. Comparison between myotubes in static and load state. (B) Quantification of the nuclear volume (C) Comparison between static 48h TSA treated myotubes and load state. (D) Quantification of the nuclear volume n=at least 50 from 3 independent experiments.

Figure R 21 shows the HDAC changes in TSA treated myotubes before and after mechanical load.

TSA, the HDAC inhibitor treatment was associated with a significant decrease in the HDAC 2 marker, which approved our HDAC inhibition protocol.

Interestingly nuclear HDAC was significantly increased after mechanical stretch (Figure R 21 A-B)

However, the TSA treatment, mechanically stretched myotubes were positive to nuclear HDAC (Figure R 21 A-B).

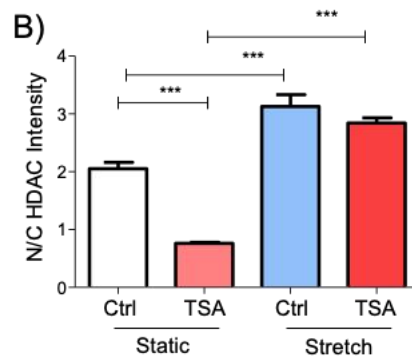
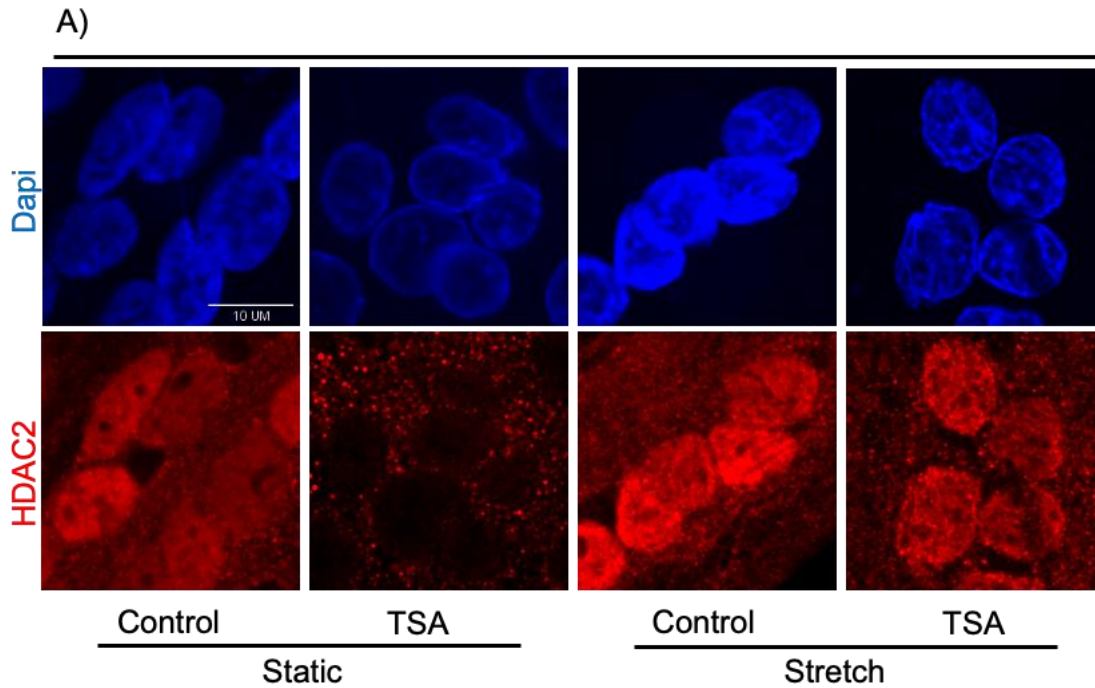


Figure R21: Immunofluorescence and quantification of HDAC marker in TSA treated myotubes after cyclic stretch.

Confocal images of control myotubes and TSA treated myotubes before and after stretch. DNA is stained with Dapi (blue). HDAC 2 in red. (B) Quantification of nuclear over cytoplasmic HDAC intensity ratio.

Ctrl=Control; TSA= myotubes treated for 48hours of TSA. Values are means \pm SEM, n=at least 83 from 2 independent experiments.

In myotubes treated with TSA, stretch induced a slight but significant decrease in H3K4ac level compared to static conditions. However, H3K4ac remained significantly higher after mechanical stretch compared with vehicle-treated myotubes (Figure R 22).

Additional histone mark modifications associated with TSA treatment are depicted in Figure R 23.

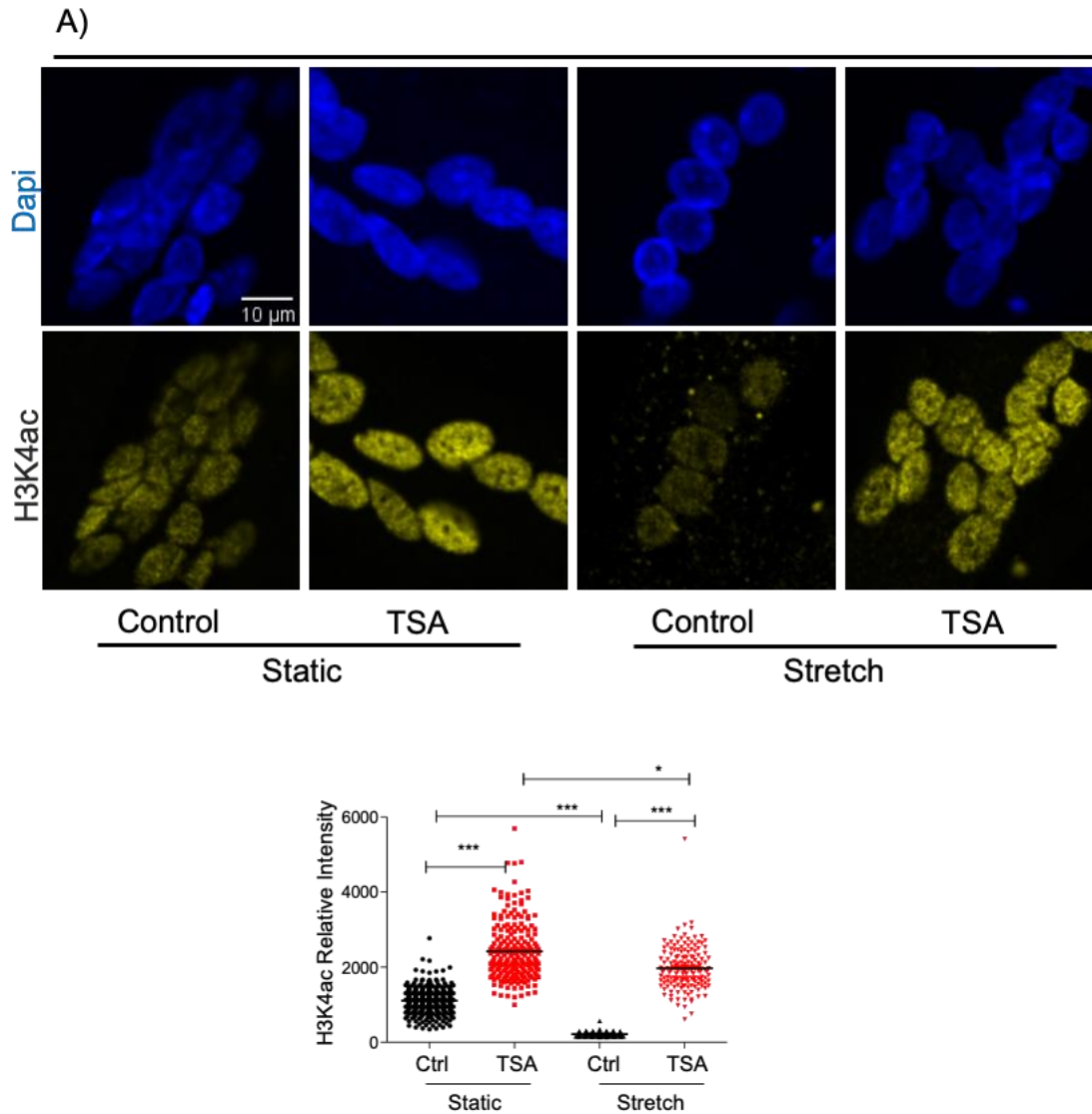


Figure R22: Immunofluorescence and quantification of histone acetylation marker in TSA treated myotubes after cyclic stretch.

Confocal images of control myotubes and TSA treated myotubes before and after stretch. DNA is stained with Dapi (blue). H3K4ac in yellow. (B) Quantification of H3K4ac relative intensity.

Ctrl=Control; TSA= myotubes treated for 48hours of TSA. n=at least 145 from 3 independent experiments.

Global histone hyperacetylation, leading to decondensation of interphase chromatin, was characterized by an increase in H3(K9) and H3(K4) dimethylation and H3(K9) acetylation.

Inhibition of histone deacetylases caused dynamic reorganization of chromatin in parallel with changes in its epigenetic modifications. (Bártová et al. 2005)

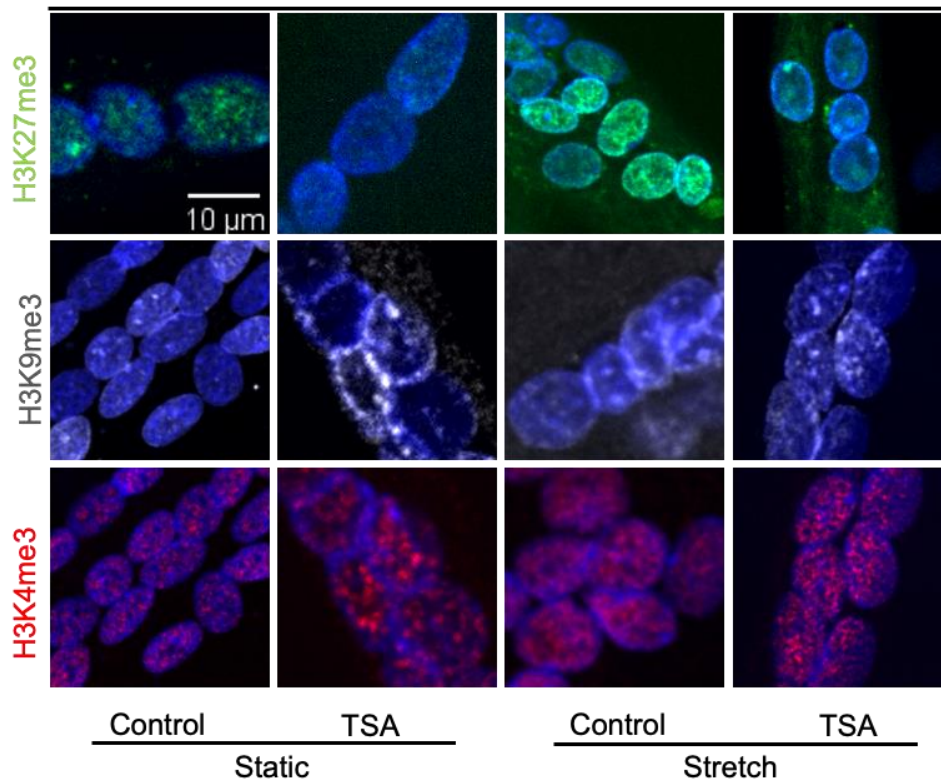
Figure 11 showed the histone changes in TSA treated myotubes before and after mechanical load. HDAC inhibition was associated with a significant decrease in the facultative heterochromatin marker H3K27me3 in static state, associated with a significant increase after

stretch. However, in comparison with control stretched myotubes, TSA treatment has significantly decreased the facultative heterochromatin marker H3K27me3 (Figure R 23 A-B). An increase in the constitutive heterochromatin marker H3K9me3 was associated with TSA treatment on static state, associated with a decrease after stretch. However, in comparison with control stretched myotubes, TSA treatment has significantly increased H3K9me3 (Figure R 23 A and C).

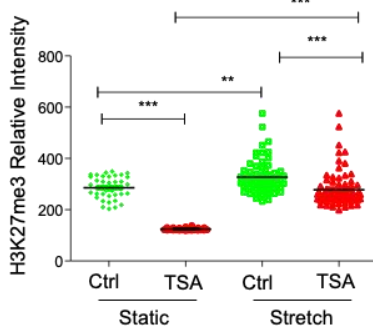
Figure R 23 A and D show an increase in the euchromatin marker H3K4me3 after TSA treatment and the opposite after stretch. No difference were observed between control stretched myotubes and TSA stretched myotubes for H3K4me3.

Our study shows, in skeletal muscle, inhibition of histone deacetylases affected the chromatin reorganization response to mechanical load and its epigenetic modifications response.

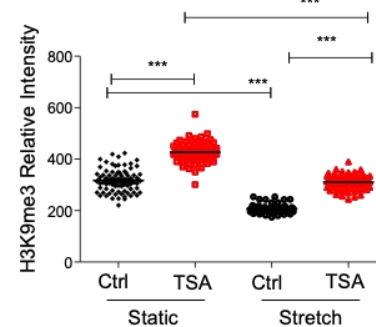
A)



B)



C)



D)

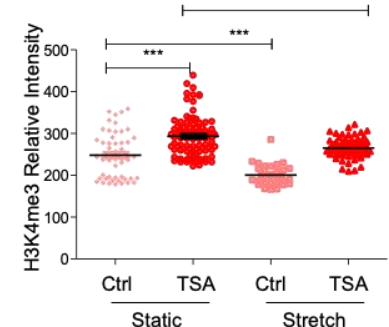


Figure R23: Immunofluorescence and quantification of histone methylation markers in TSA treated myotubes after cyclic stretch.

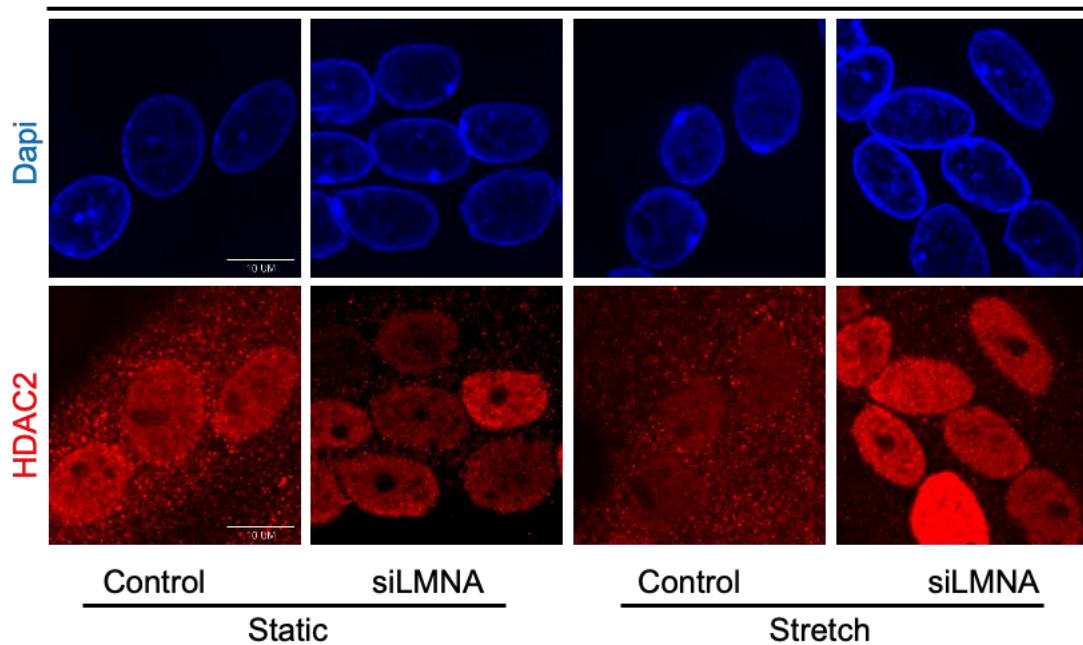
Confocal images of control myotubes and TSA treated myotubes before and after stretch. DNA is stained with Dapi (blue). H3K27me3 was in green, H3K9me3 in white and H3K4me3 was in red. (B) Quantification of the relative intensity of H3K27me3. (C) Quantification of the relative intensity of H3K9me3 (D) Quantification of the relative intensity of H3K4me3. Ctrl=Control; TSA= myotubes treated for 48hours of TSA. n=at least 50 from 3 independent experiments.

We then sought to determine whether there was a link between defective nuclear localization of HDAC2 and increase H3K4ac marker in *LMNA* deficient myonuclei. Figures R 10 and 24 show the HDAC2 and histone acetylation changes in controls and *LMNA* deficient myotubes before and after mechanical load. In controls, the nuclear/cytoplasmic ratio of HDAC2

significantly increased after stretch. Static *LMNA* deficient myotubes had a significant higher level in HDAC 2 but cyclic stretch reduced N/C ratio of HDAC2 compared with static conditions (Figure R 24).

Overall, our data showed that *LMNA* deficiency altered the stretch response of HDAC2.

A)



B)

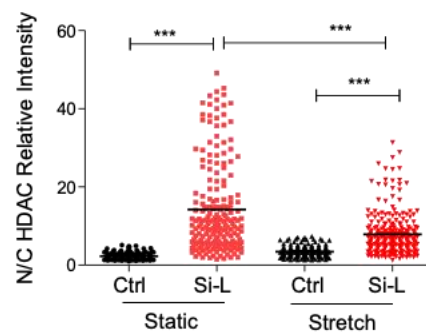


Figure R24: Immunofluorescence and quantification of HDAC and histone acetylation markers in siLMNA treated myotubes after cyclic stretch.

Confocal images of control myotubes and *LMNA* knockout myotubes before and after stretch. DNA is stained with Dapi (blue). HDAC 2 in red, and H3K4ac in yellow (B) Quantification of nuclear over cytoplasmic HDAC intensity ratio, (C) Quantification of H3K4ac relative intensity.

Ctrl=Control; si-L= *LMNA* knockout myotubes. n=at least 175 from 2 independent experiments. One-way Anova benferroni test was done.

VI. Chromatin state modifies transcriptomic response of cells to mechanical stress.

To better understand the role of LMNA in the nucleus mechanoreponse and its effects on the chromatin packaging, assay for transposase-accessible chromatin with sequencing (ATAC-Seq) were performed. ATACseq experiment is a technique that allows to determine chromatin accessibility across the genome.

i. Quality controls

The first step of ATAC-seq analysis involves read alignment to a reference genome, pre- and post-alignment quality controls (QC).

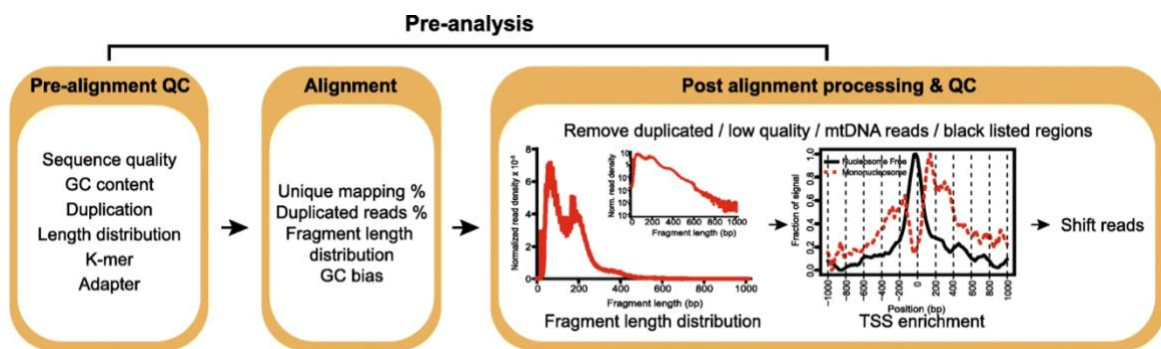


Figure R 25: Pre-analysis step of ATAC-Seq analysis.

Pre-analyses include pre-alignment QC, alignment and post-alignment processing, and QC. Figure reproduced from ref. (Yan et al. 2020)

Figure R25 shows a normal ATAC-Seq profile. The QC package was used to produce individual plots representing the fragment size distribution in the library. First, there is a large proportion of reads with less than 100 bp corresponds to the nucleosome-free region (NFR). Then a periodic distribution of fragment size indicates the occupation of nucleosomes (mononucleosome, dinucleosome, trinucleosome). Most of our samples had a good ATACseq profile. The peak between 50 and 175 bp in Figure R26-A corresponds to the NFR, then the followings represent mononucleosome, dinucleosome and trinucleosome. The complexity of the library is consistent with the NFR peaks (Figure R26-B). Expected distribution of fragment lengths was obtained in all ATAC-seq libraries and included both a nucleosome-free fragment and a single-nucleosome fragment, indicating good data quality.

Profiles of insert size provide valuable indicators of the quality of the ATAC-Seq data. In our samples, the highest peak corresponding to NFR was centered around 50bp (Figure R26-C).

Then, peaks 2 to 4 represent mono-, di- and tri-nucleosomal regions. Overall, profiles of insert size attested to good quality of our samples.

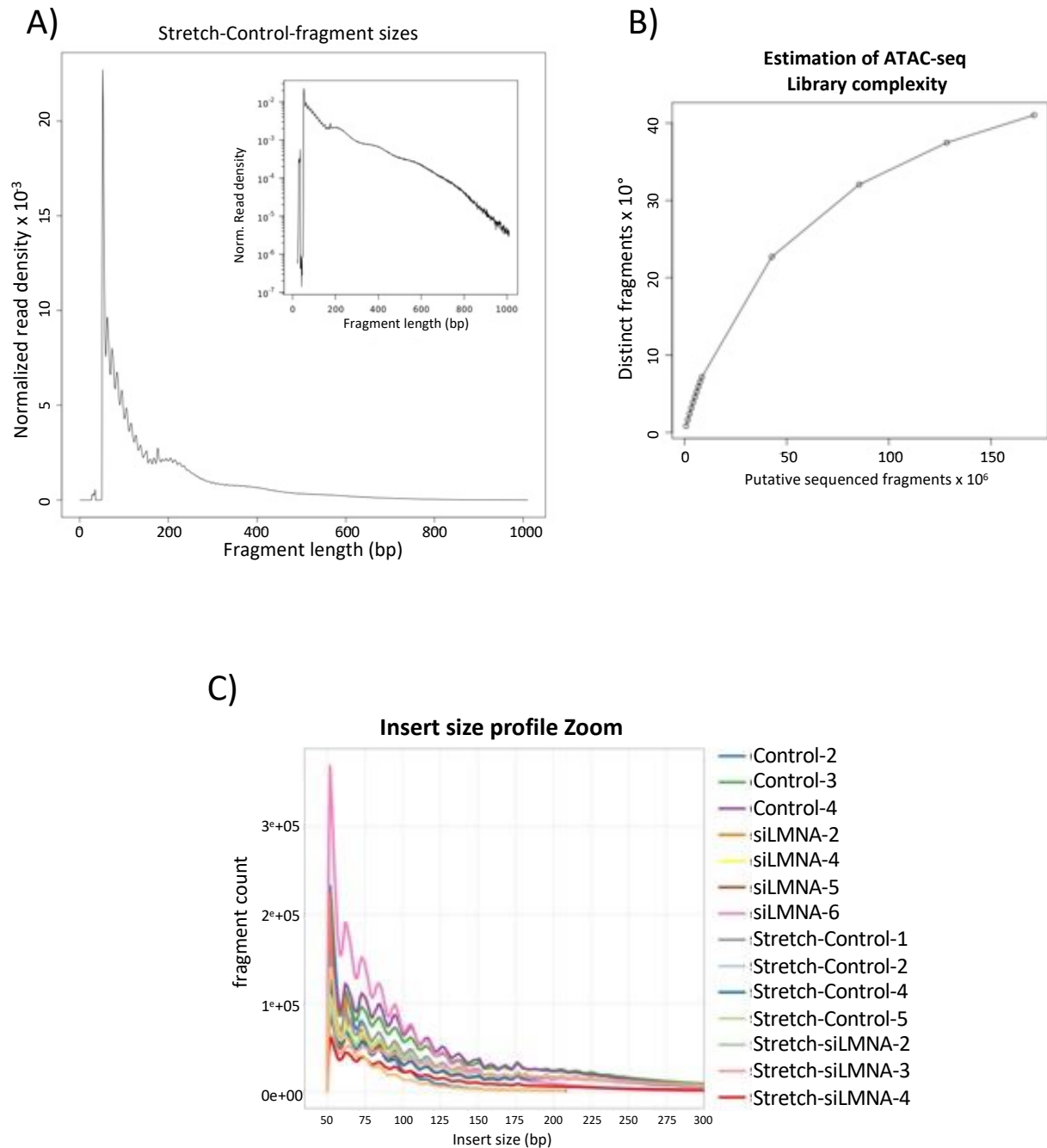


Figure R 26: ATAC-Seq QC profiles.

ATACseqQC package was used to produce individual plots representing the fragment size distribution in the library. A) Typical ATACseq profile first shows a large proportion of reads with less than 100 bp, corresponding to the nucleosome-free region (NFR). Then a periodic distribution of fragment size indicating the occupation of nucleosomes (mononucleosome, dinucleosome, trinucleosome). B) Library complexity. C) Insert size distributions of our samples showing clear nucleosome phasing. The first peak represents the open chromatin, peak 2 to 4 represent mono-, di- and tri-nucleosomal regions. Good ATAC-seq datasets have reads that span nucleosomes (which allows for calling nucleosome positions in addition to open regions of chromatin).

Then, we analyzed the calling peaks, i.e., regions of concentrated ATAC-Seq signal, thus identifying open regions or accessible regions of the chromatin (Figure R27) We used MACS2 that is the default peak caller of the ENCODE ATAC-Seq pipeline. These analysis or peaks show the Transcription Start Site (TSS) enrichment (Figure R27-A) and the promoters' enrichment (Figure R27-B). Typically, in a successful ATAC-Seq experiment, the NFR fragments are expected to be enriched around the TSS of genes. Figure R27-A shows the enrichment around TSS in our samples, which indicate that our ATAC-Seq experiment was successful. Figure R27-B shows the peak annotation of genomic partitions such as promoters, exons, introns, 3' and 5' UTR.

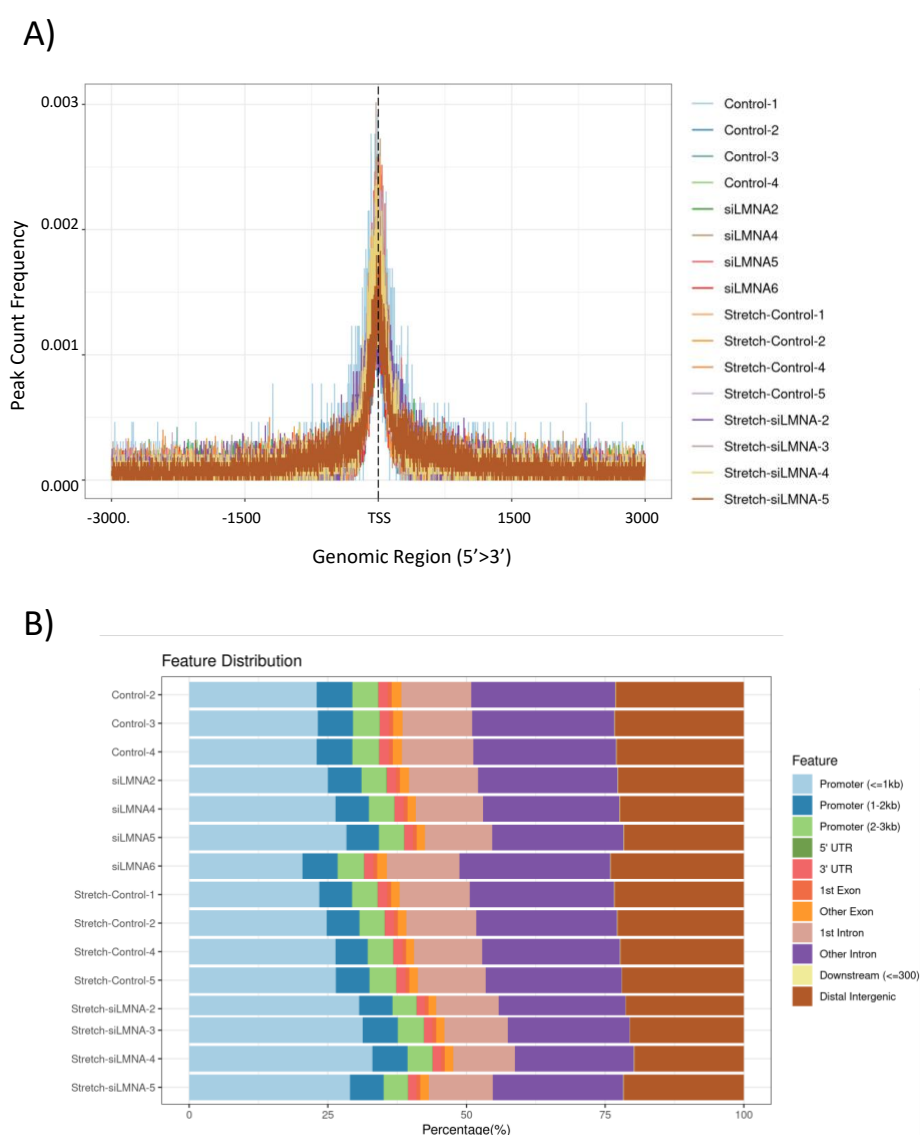


Figure R 27: Peak Call.

distribution feature of ATAC-Seq peaks. A) Peak count frequency of ATAC peaks at the transcription start site. B) Whole genome distribution of differential regions within promoters, UTRs, exons, introns, downstream regions, and distal intergenic. TSS: Transcription start site.

To further confirm the quality of ATAC-seq, Principal Components Analysis (PCA) was performed based on the signals of merged peaks from all samples. The PCA plot sorted the principal components according to the amount of data variability and showed that the samples were clustered by group (Figure R28-A).

ii. Data Analysis

For each group of samples, RNA-seq results were combined with the ATAC-Seq results. (Figure R28 B-F). Heatmaps were made to visualize ATAC peaks on expressed and non-expressed regions/genes in RNAseq (from our previous RNA-seq experiment). The highest 10 000 upregulated and downregulated gene from the RNA-seq data were chosen. We found a good correlation between genes expressed in RNAseq and chromatin accessibility in ATACseq. We visualize a peak on TSS region for the expressed genes, and no peak was visualized for unexpressed genes. Therefor we can continue to analyze our data and go further in our research.

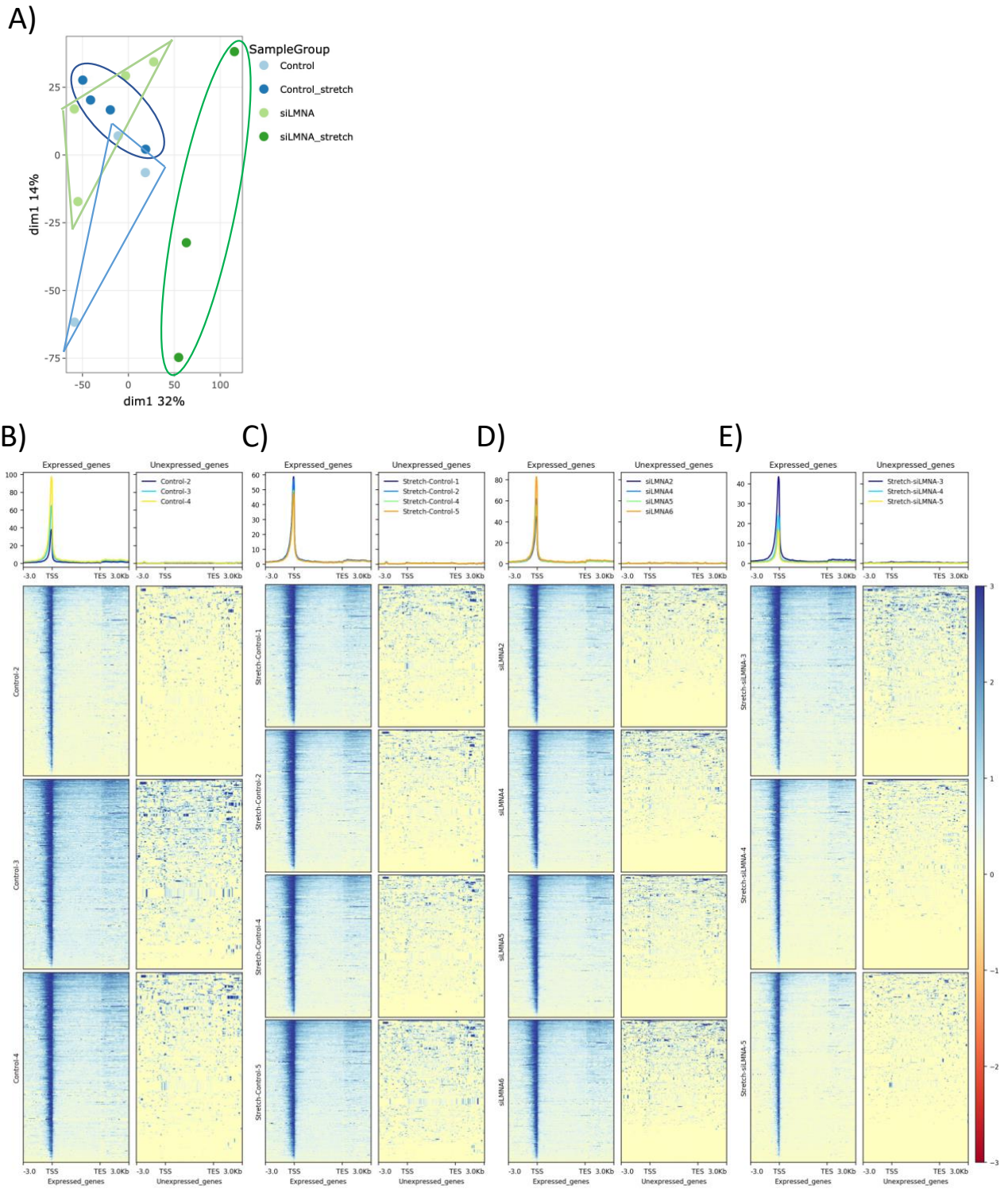


Figure R28: Correlation ATAC-Seq and RNA-seq experiments.

A) First Principal Component Analysis (PCA) without outliers. Results of the assay for transposase accessible chromatin by sequencing (ATAC-seq). (B-E) Mapped reads distributions across gene and peaks. Distributions are presented as an average plot (upper panel) where the X-axis represents the peak length. The Y-axis represents the read enrichment. -3.0 represents 3 kb upstream of TSS, and 3.0 kb represents 3 kb downstream of TES. ATAC-seq read distributions are presented also as heatmaps (downpanel). Heatmap showing the correlation of RNA-seq gene with peaks in a ± 3 -kb. Each panel represents 3 kb upstream and downstream of the TSS. Average plots and heatmaps were done for Control, stretch control, siLMNA and stretch siLMNA samples. TSS = Transcription Start Site, TES = Transcription Stop Site.

From this set of peaks, the differential analysis was done in unpaired or paired mode, with the edgeR and DEseq2 methods (2 statistical methods allowing to do differential analysis). Differential analysis was performed with the following parameters: FDR < 0.05, CF: 0, Deseq2 method.

Figure D5 shows the MA (Minus in the log scale; Average in the log scale) plots for different Differential accessible regions (DARs) between siLMNA vs control (Figure D5-A) and siLMNA stretch vs siLMNA (Figure D5-B).

Negative fold indicates that chromatin has a closed configuration, the positive fold indicates open regions. LMNA deficiency increased chromatin accessibility as attested by an increase number of open regions in siLMNA compared to controls (Figure D5-A).

In control myotubes, stretch was not associated with significant changes in the chromatin state. In contrast, cyclic stretch induced 1559 changed in region in LMNA deficient myotubes (Figure D5-B). This indicates that LMNA deficient increased sensitivity to stretch, with most of genomic regions exhibiting decreased accessibility in stretched compared with static conditions.

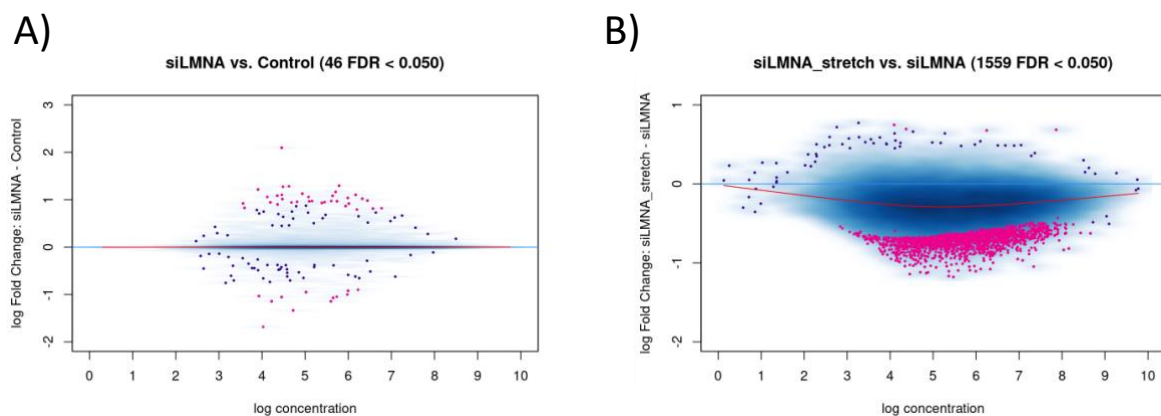


Figure R 29: MA plot of differential accessible regions.

Differential accessible regions (DARs). Differential analysis performed with the following parameters: FDR < 0.05, CF: 0, Deseq2 method. The negative fold means that the chromatin is closed the positive fold is for the open regions. Identified as significantly differentially bound shown in red.

Then the chromatin regions accessibility of some genes that impact histone methylation was analyzed.

Figure R30 shows plots of the average signal profile on genomic loci defined as 3kb upstream of annotated TSS to 3kb downstream of annotated TES (upper panels) and read density heatmaps around the same genomic loci (lower panels), of ARID1B, ARID5B, EHMT1, KDM3B, KDM4A, KDM4B, SMYD4, TCF7, TEAD1, and TLE1 genes respectively, in stretched control and siLMNA samples.

Figure R30 shows that the genomic regions of genes regulating histone methylation. After stretch, higher peaks (upper panel) and higher expression (lower panel) for the TSS region were observed in control versus siLMNA samples. This indicated that the accessibility of the genomic regions regulating histone methylation was lower in siLMNA versus control samples after stretch. Therefore, LMNA deficiency decreased histone methylation and affect the chromatin state during mechanical forces.

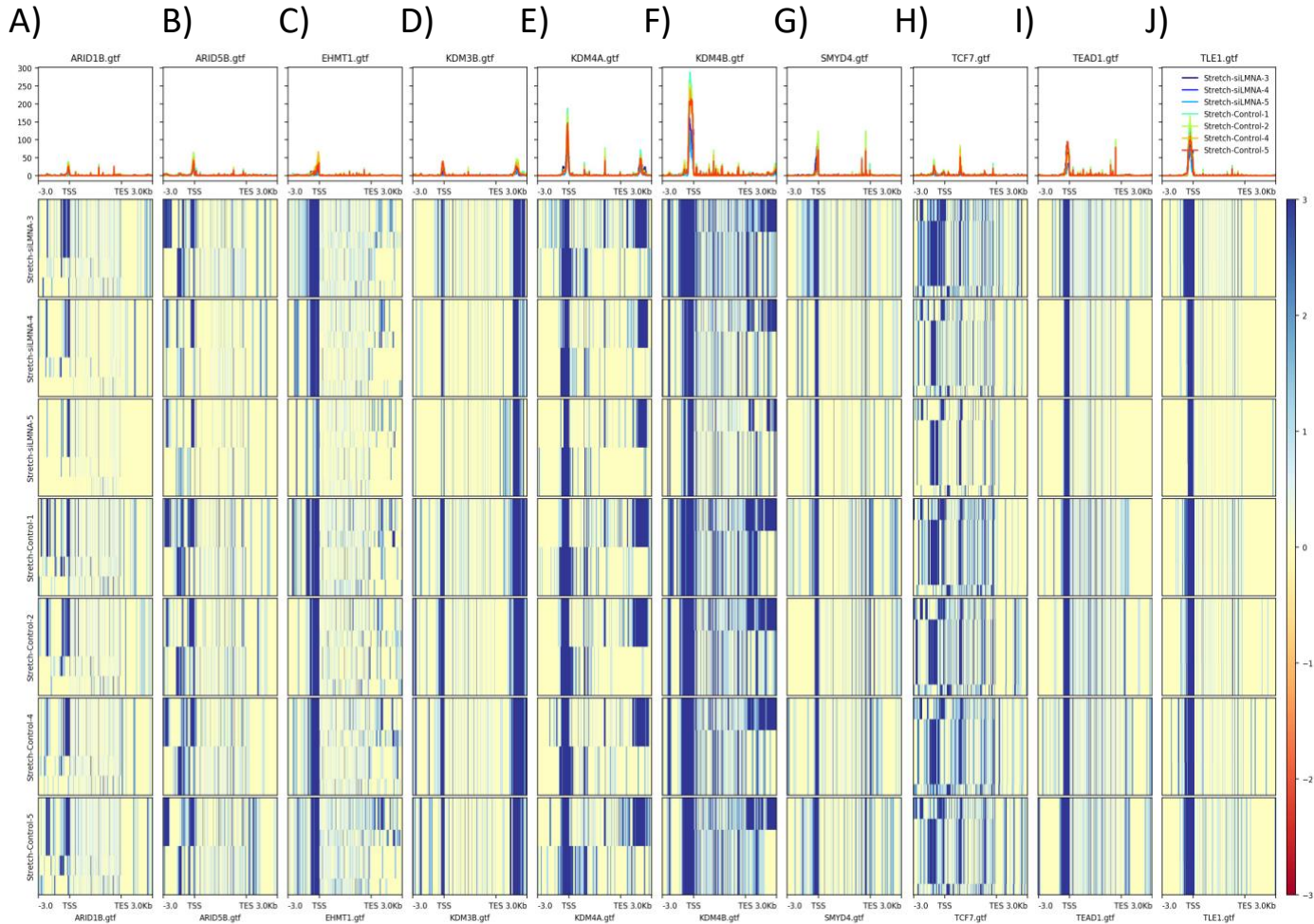


Figure R 30: ATACseq gene enrichment stretch control vs stretch siLMNA.

ATAC-seq results for A) ARID1B B) ARID5B, C) EHMT1, D) KDM3B, E) KDM4A, F) KDM4B, G) SMYD4, H) TCF7, I) TEAD1, and J) TLE1 enrichment around gene loci for Stretch-siLMNA and siLMNA. Upper panels show the average signal profile on genomic loci defined as 3kb upstream of annotated TSS to 3kb downstream of annotated TES. Lower panels show read density heatmaps around the same genomic loci. TSS = Transcription Start Site, TES= Transcription Stop Site

We also analyzed genes enrichment in siLMNA after stretch. We check whether gene downregulation in RNAseq experiments was associated with the closed state of the chromatin.

Figure R31 shows plots of the average signal profile on genomic loci defined as 3kb upstream of annotated TSS to 3kb downstream of annotated TES (upper panels) and read density heatmaps around the same genomic loci (lower panels), of EHMT1, HDAC4, HDAC7, KDM3B, KDM4A, KDM6A and PRMT7 genes respectively, in siLMNA and stretch siLMNA samples.

Figure R31 shows that these genes' genomic regions have higher peaks (upper panel) and higher expression (lower panel) for the TSS region in static versus stretched samples. This means that

these genomic regions are decreasing chromatin accessibility of these genes in siLMNA stretched samples compared to siLMNA samples.

Therefore, LMNA deficiency decreases histone methylation and affect the chromatin state during mechanical forces. Which correlates with our RNAseq data.

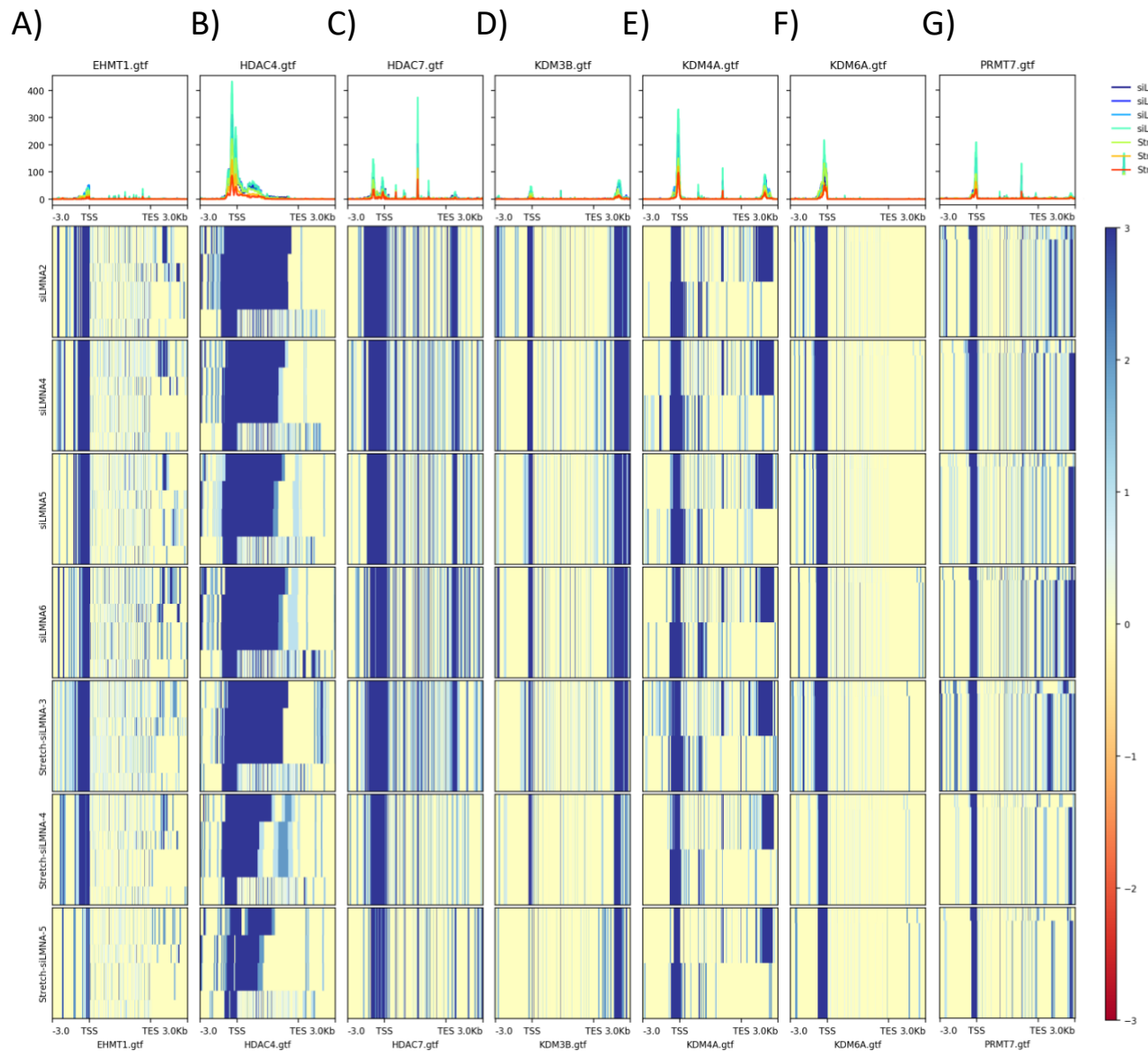


Figure R 31: ATACseq gene enrichment siLMNA vs stretch siLMNA.

ATAC-seq results for A) EHMT1 B) HDAC4, C) HDAC7, D) KDM3B, E) KDM4A, F) KDM6A, and G) PRMT7 enrichment around gene loci for Stretch-siLMNA and siLMNA. Upper panels show the average signal profile on genomic loci defined as 3kb upstream of annotated TSS to 3kb downstream of annotated TES. Lower panels show read density heatmaps around the same genomic loci. TSS = Transcription Start Site, TES= Transcription Stop Site.

Our preliminary ATACseq and RNAseq analyses allow us to gain insight into the chromatin state and how it is affected by A-type lamins during mechanical stress, and how the chromatin state affects pathways related to mechanical stress and A type-lamins in skeletal muscle cells. Additional analysis of ATACseq and RNAseq data is required to complete the interpretation. This will be done in the next future.

Discussion

Skeletal muscle is constantly exposed to high levels of mechanical forces. Mechanical loading include compression, stretch, substrate stiffness and shear stress and is crucial in regulating the skeletal muscle mass. Nuclear mechanotransduction plays important roles in skeletal muscle physiology and adaptation. Stretch is supposed to impact translational events, thereby modulating the rate of protein synthesis leading to changes in myofibrillar protein content.

Nuclear responses involve complex molecular mechanisms and depend on force transmission from the cytoskeleton to the nucleus through the LINC complex (Linker of Nucleoskeleton and Cytoskeleton) and the proteins associated with the NE, including emerin and lamins. The lamina and specifically A-type lamins have been recognized for many years as major contributors to nuclear stiffness and deformations (Dahl et al. 2004; Lammerding et al. 2006). A-type lamins have long been implicated in regulating the three-dimensional (3D) organization of chromatin, particularly via lamin-associated-domains found at the nuclear lamina and that bind to heterochromatin. Together with emerin, A-type lamins trigger the nuclear stiffening in response to mechanical stretch (Guilluy et al. 2014). In addition, mechanical force induces changes in chromatin condensation state and its histone modification state (Le et al ; Heo et al, 2016 ; Stephens et al 2018). All these processes regulate translational capacity and efficiency, nuclear elasticity, and deformability [Kirby et al 2018, Enyedi B., Niethammer P. 2017, Stephens A.D. et al 2018 and 2018, Nava M.M., et al 2020] and in turn, the cell response to mechanical stress.

Prior studies on nuclear mechanotransduction mainly focus on the impact of mechanical cues on nuclear shape and chromatin organization in mesenchymal stem cells (Heo et al. 2016; Stephens et al. 2017; Stephens, Banigan, et Marko 2018). However, differentiation of embryonic stem cells and progenitor cell into mature cells is associated with chromatin condensation and restructuration of the A-type lamin network. These changes not only modulate nuclear size, shape, deformability and stiffness but are also expected to transform the nucleus from a strain sink (an object that easily deform) to a strain concentrator (an object that resist deformation, forcing other components to deform more(Heo et al. 2016).

How A-type lamins and chromatin-mediated mechanoresponse contribute to mechanical load-mediated adaptation in post-mitotic cells such as differentiated muscle cells remain largely unknown.

The main objectives of my PhD project were to determine how mechanical stretch modulate nuclear shape and chromatin organization in control and lamin-deficient differentiated muscle cells.

In control myotubes, our data showed that mechanical loading significant increased nuclear volume and induced nuclear translocation of YAP and HDAC2, all processes which were abolished in A-type lamin deficient myotubes. In addition, compared with static condition, stretching increased the facultative heterochromatin content and reduced euchromatin. Thus, cyclic stretching of control myotubes increased chromatin compaction, a result consistent with previous work in mesenchymal stem cells (Heo et al. 2016; Driscoll et al. 2015; Heo et al. 2016).

A-type lamins have long been implicated in regulating the three-dimensional (3D) organization of chromatin, particularly via lamin-associated-domains found at the nuclear lamina and rich in heterochromatin. Lamins have crucial in regulating the nuclear stiffening in response to mechanical stretch (Guilluy et al. 2014). Not surprisingly, our data showed that A-type lamin deficiency impacts nuclear morphology and altered the organization of chromatin. Importantly, we found higher chromatin active marker levels at baseline and after stretch and abnormal chromatin redistribution after stretch. These defects can result in nuclear rupture, DNA damage, and altered transcription, all of which can contribute to skeletal muscle defects in human laminopathies

In conclusion, A-type lamins appear crucial to preserve the appropriate mechanoresponse and prevent abnormal activation of chromatin active markers in mechanically challenged myotubes. Our results support a model in which extrinsic forces induced lamin-dependent chromatin rearrangement with uncoupling of facultative heterochromatin from the nuclear lamina and global gene silencing. A-type lamins seem to protect the nucleus from large deformations and fine-tune gene expression in response to mechanical challenges.

Perspectives in skeletal muscle cells

It would be interesting to validate our data *in vivo*. To this end, we will perform a chronic mechanical overload on 3-month-old mice carrying a $LMNA^{+\Delta K32}$ mutation (Bertrand et al. 2012).

The $LMNA^{+\Delta K32}$ mouse will be chosen over homozygous mice, as homozygotes display a severe phenotype and die within 3 weeks after birth. Further, we previously show that skeletal muscle from $LMNA^{+\Delta K32}$ mice is unable to hypertrophy in response to functional overload, due to defective fusion of activated MuSCs, defective protein synthesis and defective remodeling of the neuromuscular junction. Whether these defects are related to stretch-induced deregulation of chromatin state remain to be determined *in vivo*.

Alternatively, it would be interesting to analyze the effects of cyclic stretch on human $LMNA$ mutant muscle cell lines and on muscle fibers.

Our research group had access to primary and immortalized muscle cells from L-CMD patients suffering from different $LMNA$ mutations ($LMNA$ p.Lys32del; $LMNA$ p.Arg249Trp, and $LMNA$ p.Leu380Ser) and control cells.

Single intact muscle fibers could be isolated from the skeletal muscle of the $LMNA^{\Delta K32}$ known-in mouse model generated in our laboratory. In order to analyse the nuclear response to mechanical challenges, cultures of myotubes and muscle fibres will be submitted to our stretch protocol described above. In addition, we could also physically separate contributions of nucleus and cytoplasmic mechanotransduction, by submitting isolated nuclei to cyclic stretching.

Finally, FISH detection could be used to reveal additional changes in transcription and DNA damage could also be uncovered (phospho-histone H2A.X).

Uncovering how lamins mediate nuclear processes and mechanosensitive gene expression will provide insights into the pathophysiology of L-CMD with the perspective to open new therapeutic approaches for this incurable disease.

List of tables

TABLE 1: IMMORTALIZED CELL LINES	57
TABLE 2 : SIRNA SEQUENCES LIST.....	58
TABLE 3: PRIMARY ANTIBODIES	62
TABLE 4: SECONDARY ANTIBODIES.....	62
TABLE 5: PRIMERS SEQUENCES.....	65
TABLE 6: INDEX PRIMERS.....	67
TABLE 7: MIX PREPARATION	67

List of Figures

FIGURE 1: THE HUMAN SKELETAL MUSCLE LAYERS OF CONNECTIVE TISSUE.	9
FIGURE 2: STRUCTURAL ORGANIZATION OF A SKELETAL MUSCLE FIBER.	10
FIGURE 3: STRUCTURE AND COMPONENTS OF THE MYOFIBRIL IN SKELETAL MUSCLES.....	11
FIGURE 4: SCHEMATIC OF ADULT MYOGENESIS.	12
FIGURE 5 : THICK MYOFILAMENTS COMPOSITION.	13
FIGURE 6: MUSCLE REGENERATION FOLLOWING INJURY.	14
FIGURE 7: MECHANOTRANSDUCTION.	16
FIGURE 8: MATRIX STIFFNESS IS A CRITICAL DETERMINANT OF STEM CELL LINEAGE SPECIFICATION.	17
FIGURE 9: MECHANICAL PROPERTIES OF DIFFERENT HUMAN TISSUES.	18
FIGURE 10: SCHEMATIC REPRESENTATION OF FORCES EXERTED ON CELLS.	19
FIGURE 11: A MODEL OF FOCAL ADHESION MOLECULAR ARCHITECTURE	21
FIGURE 12: SCHEMATIC ILLUSTRATION OF THE STRESS FIBER NETWORK IN MOTILE CELLS.	23
FIGURE 13: COMPONENTS OF THE PERINUCLEAR ACTIN NETWORK IN MUSCLE CELL PRECURSORS (MCPs).	24
FIGURE 14: SCHEMATIC REPRESENTATION OF CYTOSKELETON AND FORCE TRANSMISSION IN THE MYOBLAST AND MYOFIBRIL.	27
FIGURE 15: SCHEMATIC OVERVIEW OF NUCLEAR ENVELOPE PROTEINS INVOLVED IN FORCE TRANSMISSION TO THE NUCLEUS	30
FIGURE 16: LINC COMPLEXES IN SKELETAL MUSCLE.	31
FIGURE 17: ROLE OF LAMINS AND LAMIN-ASSOCIATED PROTEINS (LAPs) IN NUCLEAR FUNCTION.....	33
FIGURE 18: ASSEMBLY, PROCESSING, AND REGULATION OF LAMINS.	35
FIGURE 19: NUCLEAR LAMINS COMPOSITION.	36
FIGURE 20: ASSEMBLY OF LAMION DIMERS.	37
FIGURE 21: STRUCTURAL COMPARISON OF THE TETRAMERIC STRUCTURES OF THE LAMIN AND VIMENTIN.	38
FIGURE 22: LAMIN-A SCALES WITH TISSUE STIFFNESS.	40
FIGURE 23: SCHEMATIC OF THE LEVELS OF CHROMATIN FOLDING WITHIN THE HIGHER-ORDER 3D GENOME ORGANIZATION.....	42
FIGURE 24: CHROMATIN ORGANIZATION.	43
FIGURE 25: THE FUNCTIONAL ORGANIZATION OF THE GENOME.	46

FIGURE 26: THE MECHANOSENSITIVITY PATHWAY AND THE TENSION-INDUCED REINFORCEMENT RESPONSE.....	48
FIGURE 27: YAP REGULATION.	50
FIGURE 28: SINGLE-POINT MUTATIONS OF THE LMNA GENE.....	53
FIGURE 29: MYOBLAST DIFFERENTIATION IN CULTURED MUSCLE CELLS (ABMAYR ET PAVLATH 2012).	56
FIGURE 30: APPLICATION OF QUIBIAXIAL STRAIN WITH FLEXCELL® TENSION SYSTEMS USING BIOFLEX® CULTURE PLATES.....	59
FIGURE 31: SOLUTION COLOR AS A FUNCTION OF PH.....	66

List of Results Figures

FIGURE R1: NUCLEAR SEGMENTATION AND ANALYSIS OF NUCLEAR SHAPE AND VOLUME IN 2 HUMAN MUSCLE CELL LINES (AB1167 AND WT8220).....	69
FIGURE R2: IMMUNOFLUORESCENCE AND QUANTIFICATION OF HISTONE METHYLATION MARKERS IN MYOBLASTS AND MYOTUBES. ..	70
FIGURE R3: VALIDATION OF SIRNA	71
FIGURE R 4: NUCLEAR SEGMENTATION AND ANALYSIS OF NUCLEAR SHAPE AND VOLUME AFTER LMNA KNOCKOUT.	72
FIGURE R5: IMMUNOFLUORESCENCE AND QUANTIFICATION OF HISTONE METHYLATION MARKERS IN CONTROL AND siLMNA TREATED MYOTUBES.....	73
FIGURE R6: WESTERN BLOT AND QUANTIFICATION OF HISTONE METHYLATION MARKERS IN siLMNA TREATED MYOTUBES BEFORE AND AFTER CYCLIC STRETCH.....	74
FIGURE R 7: PCA ANALYSIS, RT-QPCR, GO TERMS ENRICHED AND DOT PLOT OF GO TERM ENRICHED IN CONTROL AND siLMNA TREATED MYOTUBES.....	76
FIGURE R8: NUCLEAR SEGMENTATION AND ANALYSIS OF NUCLEAR SHAPE AFTER LMNA KNOCKOUT AND CYCLIC STRETCH.....	77
FIGURE R9: IMMUNOFLUORESCENCE AND QUANTIFICATION OF HISTONE METHYLATION MARKERS IN siLMNA TREATED MYOTUBES BEFORE AND AFTER CYCLIC STRETCH.	79
FIGURE R 10: IMMUNOFLUORESCENCE AND QUANTIFICATION OF HISTONE LYSINE 4 ACETYLATION MARKERS IN siLMNA TREATED MYOTUBES BEFORE AND AFTER CYCLIC STRETCH.....	80
FIGURE R 11: RNASEQ SAMPLES DESCRIPTION AND DIFFERENTIAL GENE EXPRESSION IN STATIC siLMNA AND siLMNA STRETCHED MYOTUBES.....	81
FIGURE R 12: GO TERMS ENRICHED IN CONTROL VS AND siLMNA VS STRETCHED siLMNA MYOTUBES.....	82
FIGURE R13: GO TERMS ENRICHED IN CONTROL VS siLMNA AND siLMNA VS STRETCHED siLMNA MYOTUBES.	84
FIGURE R14: GO TERMS ENRICHED IN CONTROL VS siLMNA AND siLMNA VS STRETCHED siLMNA MYOTUBES.	85
FIGURE R15: NUCLEAR SEGMENTATION AND ANALYSIS OF NUCLEAR SHAPE AFTER LMNA KNOCKOUT AND CYCLIC STRETCH.	87
FIGURE R16: IMMUNOFLUORESCENCE AND QUANTIFICATION OF HISTONE METHYLATION MARKERS IN siSUN1 TREATED MYOTUBES BEFORE AND AFTER CYCLIC STRETCH.	89
FIGURE R17: IMMUNOFLUORESCENCE AND QUANTIFICATION OF HISTONE METHYLATION MARKERS IN siSUN2 TREATED MYOTUBES BEFORE AND AFTER CYCLIC STRETCH.	90
FIGURE R18: IMMUNOFLUORESCENCE AND QUANTIFICATION OF YAP MARKER IN siLMNA TREATED MYOTUBES AFTER CYCLIC STRETCH.	92

FIGURE R19: NUCLEAR SEGMENTATION AND ANALYSIS OF NUCLEAR SHAPE AND VOLUME AFTER TSA TREATMENT BETWEEN MYOBLASTS AND MYOTUBES.	94
FIGURE R20: NUCLEAR SEGMENTATION AND ANALYSIS OF NUCLEAR SHAPE AFTER TSA TREATMENT AND CYCLIC STRETCH.	95
FIGURE R21: IMMUNOFLUORESCENCE AND QUANTIFICATION OF HDAC MARKER IN TSA TREATED MYOTUBES AFTER CYCLIC STRETCH.	96
FIGURE R22: IMMUNOFLUORESCENCE AND QUANTIFICATION OF HISTONE ACETYLATION MARKER IN TSA TREATED MYOTUBES AFTER CYCLIC STRETCH.	97
FIGURE R23: IMMUNOFLUORESCENCE AND QUANTIFICATION OF HISTONE METHYLATION MARKERS IN TSA TREATED MYOTUBES AFTER CYCLIC STRETCH.	99
FIGURE R24: IMMUNOFLUORESCENCE AND QUANTIFICATION OF HDAC AND HISTONE ACETYLATION MARKERS IN siLMNA TREATED MYOTUBES AFTER CYCLIC STRETCH.	100

References

Abmayr, Susan M., et Grace K. Pavlath. 2012. « Myoblast Fusion: Lessons from Flies and Mice ». *Development* 139 (4): 641-56. <https://doi.org/10.1242/dev.068353>.

Ahn, Jinsook, Inseong Jo, So-mi Kang, Seokho Hong, Suhyeon Kim, Soyeon Jeong, Yong-Hak Kim, Bum-Joon Park, et Nam-Chul Ha. 2019. « Structural Basis for Lamin Assembly at the Molecular Level ». *Nature Communications* 10 (1): 3757. <https://doi.org/10.1038/s41467-019-11684-x>.

Ait-Si-Ali, Slimane, Valentina Guasconi, Lauriane Fritsch, Hakima Yahi, Redha Sekhri, Irina Naguibneva, Philippe Robin, Florence Cabon, Anna Polesskaya, et Annick Harel-Bellan. 2004. « A Suv39h-dependent mechanism for silencing S-phase genes in differentiating but not in cycling cells ». *The EMBO Journal* 23 (3): 605-15. <https://doi.org/10.1038/sj.emboj.7600074>.

Allis, C. David, Shelley L. Berger, Jacques Cote, Sharon Dent, Thomas Jenuwien, Tony Kouzarides, Lorraine Pillus, et al. 2007. « New Nomenclature for Chromatin-Modifying Enzymes ». *Cell* 131 (4): 633-36. <https://doi.org/10.1016/j.cell.2007.10.039>.

Allis, C. David, et Thomas Jenuwein. 2016. « The Molecular Hallmarks of Epigenetic Control ». *Nature Reviews Genetics* 17 (8): 487-500. <https://doi.org/10.1038/nrg.2016.59>.

Arbach, Hannah E., Marcus Harland-Dunaway, Jessica K. Chang, et Andrea E. Wills. 2018. « Extreme Nuclear Branching in Healthy Epidermal Cells of the *Xenopus* Tail Fin ». *Journal of Cell Science*, janvier, jcs.217513. <https://doi.org/10.1242/jcs.217513>.

Arsenovic, Paul T., Iswarya Ramachandran, Kranthidhar Bathula, Ruijun Zhu, Jiten D.

Narang, Natalie A. Noll, Christopher A. Lemmon, Gregg G. Gundersen, et Daniel E. Conway. 2016. « Nesprin-2G, a Component of the Nuclear LINC Complex, Is Subject to Myosin-Dependent Tension ». *Biophysical Journal* 110 (1): 34-43. <https://doi.org/10.1016/j.bpj.2015.11.014>.

Asp, Patrik, Roy Blum, Vasupradha Vethantham, Fabio Parisi, Mariann Micsinai, Jemie Cheng, Christopher Bowman, Yuval Kluger, et Brian David Dynlacht. 2011. « Genome-Wide Remodeling of the Epigenetic Landscape during Myogenic Differentiation ». *Proceedings of the National Academy of Sciences* 108 (22). <https://doi.org/10.1073/pnas.1102223108>.

Aureille, Julien, Valentin Buffière-Ribot, Ben E Harvey, Cyril Boyault, Lydia Pernet, Tomas Andersen, Gregory Bacola, et al. 2019. « Nuclear Envelope Deformation Controls Cell Cycle Progression in Response to Mechanical Force ». *EMBO Reports* 20 (9). <https://doi.org/10.15252/embr.201948084>.

Aymard, François, Marion Aguirrebengoa, Emmanuelle Guillou, Biola M Javierre, Beatrix Bugler, Coline Arnould, Vincent Rocher, et al. 2017. « Genome-Wide Mapping of Long-Range Contacts Unveils Clustering of DNA Double-Strand Breaks at Damaged Active Genes ». *Nature Structural & Molecular Biology* 24 (4): 353-61. <https://doi.org/10.1038/nsmb.3387>.

Bagley, Bowman. 2020. « 3D Bioprinting Substrate Stiffness – Often Overlooked, But Always at Work », 2020. <https://3dheals.com/substrate-stiffness-often-overlooked-but-always-at-work/>.

Bains, W, P Ponte, H Blau, et L Kedes. 1984. « Cardiac Actin Is the Major Actin Gene Product in Skeletal Muscle Cell Differentiation in Vitro ». *Molecular and Cellular Biology* 4 (8): 1449-53. <https://doi.org/10.1128/mcb.4.8.1449-1453.1984>.

Baker, Brendon M., Britta Trappmann, William Y. Wang, Mahmut S. Sakar, Iris L. Kim, Vivek B. Shenoy, Jason A. Burdick, et Christopher S. Chen. 2015. « Cell-Mediated Fibre Recruitment Drives Extracellular Matrix Mechanosensing in Engineered Fibrillar Microenvironments ». *Nature Materials* 14 (12): 1262-68. <https://doi.org/10.1038/nmat4444>.

Baldini, Enke, Chiara Tuccilli, Natalie Prinzi, Salvatore Sorrenti, Laura Falvo, Corrado De Vito, Antonio Catania, et al. 2015. « Deregulated Expression of Aurora Kinases Is Not a Prognostic Biomarker in Papillary Thyroid Cancer Patients ». Édité par Adriano Angelucci. *PLOS ONE* 10 (3): e0121514. <https://doi.org/10.1371/journal.pone.0121514>.

Barra, H.S., C.A. Arce, J.A. Rodríguez, et R. Caputto. 1974. « Some Common Properties of the Protein That Incorporates Tyrosine as a Single Unit and the Microtubule

Proteins ». *Biochemical and Biophysical Research Communications* 60 (4): 1384-90. [https://doi.org/10.1016/0006-291X\(74\)90351-9](https://doi.org/10.1016/0006-291X(74)90351-9).

Barski, Artem, Suresh Cuddapah, Kairong Cui, Tae-Young Roh, Dustin E. Schones, Zhibin Wang, Gang Wei, Iouri Chepelev, et Keji Zhao. 2007. « High-Resolution Profiling of Histone Methylations in the Human Genome ». *Cell* 129 (4): 823-37. <https://doi.org/10.1016/j.cell.2007.05.009>.

Bártová, Eva, Jiří Pacherník, Andrea Harničarová, Aleš Kovařík, Martina Kovaříková, Jirina Hofmanová, Magdalena Skalníková, Michal Kozubek, et Stanislav Kozubek. 2005. « Nuclear Levels and Patterns of Histone H3 Modification and HP1 Proteins after Inhibition of Histone Deacetylases ». *Journal of Cell Science* 118 (21): 5035-46. <https://doi.org/10.1242/jcs.02621>.

Becker, Robert, Marina Leone, et Felix Engel. 2020. « Microtubule Organization in Striated Muscle Cells ». *Cells* 9 (6): 1395. <https://doi.org/10.3390/cells9061395>.

Beckerle, Mary C. 1997. « Zyxin: Zinc Fingers at Sites of Cell Adhesion ». *BioEssays* 19 (11): 949-57. <https://doi.org/10.1002/bies.950191104>.

Belz, G. G. 1995. « Elastic Properties and Windkessel Function of the Human Aorta ». *Cardiovascular Drugs and Therapy* 9 (1): 73-83. <https://doi.org/10.1007/BF00877747>.

Bera, Manindra, Hema Chandra Kotamarthi, Subarna Dutta, Angana Ray, Saptaparni Ghosh, Dhananjay Bhattacharyya, Sri Rama Koti Ainavarapu, et Kaushik Sengupta. 2014. « Characterization of Unfolding Mechanism of Human Lamin A Ig Fold by Single-Molecule Force Spectroscopy—Implications in EDMD ». *Biochemistry* 53 (46): 7247-58. <https://doi.org/10.1021/bi500726f>.

Bernstein, Bradley E., Tarjei S. Mikkelsen, Xiaohui Xie, Michael Kamal, Dana J. Huebert, James Cuff, Ben Fry, et al. 2006. « A Bivalent Chromatin Structure Marks Key Developmental Genes in Embryonic Stem Cells ». *Cell* 125 (2): 315-26. <https://doi.org/10.1016/j.cell.2006.02.041>.

Bertrand, Anne T., Laure Renou, Aurélie Papadopoulos, Maud Beuvin, Emmanuelle Lacène, Catherine Massart, Chris Ottolenghi, et al. 2012. « DelK32-Lamin A/C Has Abnormal Location and Induces Incomplete Tissue Maturation and Severe Metabolic Defects Leading to Premature Death ». *Human Molecular Genetics* 21 (5): 1037-48. <https://doi.org/10.1093/hmg/ddr534>.

Bertrand, Anne T, Simindokht Ziaei, Camille Ehret, Hélène Duchemin, Kamel Mamchaoui, Anne Bigot, Michèle Mayer, et al. 2014. « Cellular Micro-Environments Reveal Defective Mechanosensing Responses and Elevated YAP Signaling in LMNA-Mutated Muscle

Precursors ». *Journal of Cell Science*, janvier, jcs.144907. <https://doi.org/10.1242/jcs.144907>.

Bestor, Timothy H., John R. Edwards, et Mathieu Boulard. 2015. « Notes on the Role of Dynamic DNA Methylation in Mammalian Development ». *Proceedings of the National Academy of Sciences* 112 (22): 6796-99. <https://doi.org/10.1073/pnas.1415301111>.

Biga, Lindsay, Sierra dawson, Amy Harwell, et Robin Hopkins. s. d. « Anatomy and Physiology ». *Anatomy & Physiology*. [https://open.oregonstate.education/aandp/chapter/10-2-skeletal-muscle/Lindsay M. Biga; Sierra Dawson; Amy Harwell; Robin Hopkins; Joel Kaufmann; Mike LeMaster; Philip Matern; Katie Morrison-Graham; Devon Quick; and Jon Runyeon](https://open.oregonstate.education/aandp/chapter/10-2-skeletal-muscle/Lindsay%20M.%20Biga%20Sierra%20Dawson%20Amy%20Harwell%20Robin%20Hopkins%20Joel%20Kaufmann%20Mike%20LeMaster%20Philip%20Matern%20Katie%20Morrison-Graham%20Devon%20Quick%20and%20Jon%20Runyeon).

Black, Joshua C., Capucine Van Rechem, et Johnathan R. Whetstine. 2012. « Histone Lysine Methylation Dynamics: Establishment, Regulation, and Biological Impact ». *Molecular Cell* 48 (4): 491-507. <https://doi.org/10.1016/j.molcel.2012.11.006>.

Blank, Michael. 2020. « Targeted Regulation of Nuclear Lamins by Ubiquitin and Ubiquitin-Like Modifiers ». *Cells* 9 (6): 1340. <https://doi.org/10.3390/cells9061340>.

Block, Johanna, Viktor Schroeder, Paul Pawelzyk, Norbert Willenbacher, et Sarah Köster. 2015. « Physical Properties of Cytoplasmic Intermediate Filaments ». *Biochimica et Biophysica Acta (BBA) - Molecular Cell Research* 1853 (11): 3053-64. <https://doi.org/10.1016/j.bbamcr.2015.05.009>.

Block, Johanna, Hannes Witt, Andrea Candelli, Erwin J. G. Peterman, Gijs J. L. Wuite, Andreas Janshoff, et Sarah Köster. 2017. « Nonlinear Loading-Rate-Dependent Force Response of Individual Vimentin Intermediate Filaments to Applied Strain ». *Physical Review Letters* 118 (4): 048101. <https://doi.org/10.1103/PhysRevLett.118.048101>.

Bolger, Anthony M., Marc Lohse, et Bjoern Usadel. 2014. « Trimmomatic: A Flexible Trimmer for Illumina Sequence Data ». *Bioinformatics* 30 (15): 2114-20. <https://doi.org/10.1093/bioinformatics/btu170>.

Bone, Courtney R., et Daniel A. Starr. 2016. « Nuclear Migration Events throughout Development ». *Journal of Cell Science* 129 (10): 1951-61. <https://doi.org/10.1242/jcs.179788>.

Bonnans, Caroline, Jonathan Chou, et Zena Werb. 2014. « Remodelling the Extracellular Matrix in Development and Disease ». *Nature Reviews Molecular Cell Biology* 15 (12): 786-801. <https://doi.org/10.1038/nrm3904>.

Bonne, Gisèle, Marina Raffaele Di Barletta, Shaida Varnous, Henri-Marc Bécane, El-Hadi Hammouda, Luciano Merlini, Francesco Muntoni, et al. 1999. « Mutations in the Gene Encoding Lamin A/C Cause Autosomal Dominant Emery-Dreifuss Muscular Dystrophy ». *Nature Genetics* 21 (3): 285-88. <https://doi.org/10.1038/6799>.

Boriek, Aladin M., Y. Capetanaki, Willy Hwang, Todd Officer, Muffasir Badshah, Joe Rodarte, et James G. Tidball. 2001. « Desmin Integrates the Three-Dimensional Mechanical Properties of Muscles ». *American Journal of Physiology-Cell Physiology* 280 (1): C46-52. <https://doi.org/10.1152/ajpcell.2001.280.1.C46>.

Boschetti, Federica, Giancarlo Pennati, Francesca Gervaso, Giuseppe M. Peretti, et Gabriele Dubini. 2004. « Biomechanical Properties of Human Articular Cartilage under Compressive Loads ». *Biorheology* 41 (3-4): 159-66.

Boudriau, S, M Vincent, C H Côté, et P A Rogers. 1993. « Cytoskeletal Structure of Skeletal Muscle: Identification of an Intricate Exosarcomeric Microtubule Lattice in Slow- and Fast-Twitch Muscle Fibers. » *Journal of Histochemistry & Cytochemistry* 41 (7): 1013-21. <https://doi.org/10.1177/41.7.8515044>.

Britten, R. J., et D. E. Kohne. 1968. « Repeated Sequences in DNA: Hundreds of Thousands of Copies of DNA Sequences Have Been Incorporated into the Genomes of Higher Organisms. » *Science* 161 (3841): 529-40. <https://doi.org/10.1126/science.161.3841.529>.

Brown, Karen E, Simon S Guest, Stephen T Smale, Kyungmin Hahm, Matthias Merkenschlager, et Amanda G Fisher. 1997. « Association of Transcriptionally Silent Genes with Ikaros Complexes at Centromeric Heterochromatin ». *Cell* 91 (6): 845-54. [https://doi.org/10.1016/S0092-8674\(00\)80472-9](https://doi.org/10.1016/S0092-8674(00)80472-9).

Buckingham, Margaret, Lola Bajard, Ted Chang, Philippe Daubas, Juliette Hadchouel, Sigolene Meilhac, Didier Montarras, Didier Rocancourt, et Frederic Relaix. 2003. « The Formation of Skeletal Muscle: From Somite to Limb ». *Journal of Anatomy* 202 (1): 59-68. <https://doi.org/10.1046/j.1469-7580.2003.00139.x>.

Buckley, C. D., J. Tan, K. L. Anderson, D. Hanein, N. Volkmann, W. I. Weis, W. J. Nelson, et A. R. Dunn. 2014. « The Minimal Cadherin-Catenin Complex Binds to Actin Filaments under Force ». *Science* 346 (6209): 1254211-1254211. <https://doi.org/10.1126/science.1254211>.

Budday, Silvia, Timothy C. Ovaert, Gerhard A. Holzapfel, Paul Steinmann, et Ellen Kuhl. 2020. « Fifty Shades of Brain: A Review on the Mechanical Testing and Modeling of Brain Tissue ». *Archives of Computational Methods in Engineering* 27 (4): 1187-1230. <https://doi.org/10.1007/s11831-019-09352-w>.

Bui, Hong-Thuy, Sayaka Wakayama, Satoshi Kishigami, Keun-Kyu Park, Jin-Hoi Kim, Nguyen Van Thuan, et Teruhiko Wakayama. 2010. « Effect of Trichostatin A on Chromatin Remodeling, Histone Modifications, DNA Replication, and Transcriptional Activity in Cloned Mouse Embryos1 ». *Biology of Reproduction* 83 (3): 454-63.

<https://doi.org/10.1095/biolreprod.109.083337>.

Burke, Brian, et Colin L. Stewart. 2013. « The Nuclear Lamins: Flexibility in Function ». *Nature Reviews Molecular Cell Biology* 14 (1): 13-24. <https://doi.org/10.1038/nrm3488>.

Burridge, Keith. 2017. « Focal Adhesions: A Personal Perspective on a Half Century of Progress ». *The FEBS Journal* 284 (20): 3355-61. <https://doi.org/10.1111/febs.14195>.

Buxboim, Amnon, Jerome Irianto, Joe Swift, Avathamsa Athirasala, Jae-Won Shin, Florian Rehfeldt, et Dennis E. Discher. 2017. « Coordinated Increase of Nuclear Tension and Lamin-A with Matrix Stiffness Outcompetes Lamin-B Receptor That Favors Soft Tissue Phenotypes ». Édité par Yixian Zheng. *Molecular Biology of the Cell* 28 (23): 3333-48. <https://doi.org/10.1091/mbc.e17-06-0393>.

Buxboim, Amnon, Joe Swift, Jerome Irianto, Kyle R. Spinler, P.C. Dave P. Dingal, Avathamsa Athirasala, Yun-Ruei C. Kao, et al. 2014. « Matrix Elasticity Regulates Lamin-A,C Phosphorylation and Turnover with Feedback to Actomyosin ». *Current Biology* 24 (16): 1909-17. <https://doi.org/10.1016/j.cub.2014.07.001>.

Campbell, I. D., et M. J. Humphries. 2011. « Integrin Structure, Activation, and Interactions ». *Cold Spring Harbor Perspectives in Biology* 3 (3): a004994-a004994. <https://doi.org/10.1101/cshperspect.a004994>.

Campellone, Kenneth G., et Matthew D. Welch. 2010. « A Nucleator Arms Race: Cellular Control of Actin Assembly ». *Nature Reviews Molecular Cell Biology* 11 (4): 237-51. <https://doi.org/10.1038/nrm2867>.

Capetanaki, Y. 2002. « Desmin Cytoskeleton A Potential Regulator of Muscle Mitochondrial Behavior and Function ». *Trends in Cardiovascular Medicine* 12 (8): 339-48. [https://doi.org/10.1016/S1050-1738\(02\)00184-6](https://doi.org/10.1016/S1050-1738(02)00184-6).

Capetanaki, Yassemi, Robert J. Bloch, Asimina Kouloumenta, Manolis Mavroidis, et Stelios Psarras. 2007. « Muscle Intermediate Filaments and Their Links to Membranes and Membranous Organelles ». *Experimental Cell Research* 313 (10): 2063-76. <https://doi.org/10.1016/j.yexcr.2007.03.033>.

Chambliss, Allison B., Shyam B. Khatau, Nicholas Erdenberger, D. Kyle Robinson, Didier Hodzic, Gregory D. Longmore, et Denis Wirtz. 2013. « The LINC-Anchored Actin Cap Connects the Extracellular Milieu to the Nucleus for Ultrafast Mechanotransduction ». *Scientific Reports* 3 (1): 1087. <https://doi.org/10.1038/srep01087>.

Chapman, Mark A., Jianlin Zhang, Indroneal Banerjee, Ling T. Guo, Zhiwei Zhang, G. Diane Shelton, Kunfu Ouyang, Richard L. Lieber, et Ju Chen. 2014. « Disruption of Both

Nesprin 1 and Desmin Results in Nuclear Anchorage Defects and Fibrosis in Skeletal Muscle ». *Human Molecular Genetics* 23 (22): 5879-92. <https://doi.org/10.1093/hmg/ddu310>.

Charrier, Elisabeth E., Lorraine Montel, Atef Asnacios, Florence Delort, Patrick Vicart, François Gallet, Sabrina Battonnet-Pichon, et Sylvie Hénon. 2018. « The Desmin Network Is a Determinant of the Cytoplasmic Stiffness of Myoblasts: Desmin Network: A Determinant of the Cytoplasmic Stiffness of Myoblasts ». *Biology of the Cell* 110 (4): 77-90. <https://doi.org/10.1111/boc.201700040>.

Choi, Jinmi, Hyonchol Jang, Hyunsoo Kim, Seong-Tae Kim, Eun-Jung Cho, et Hong-Duk Youn. 2010. « Histone Demethylase LSD1 Is Required to Induce Skeletal Muscle Differentiation by Regulating Myogenic Factors ». *Biochemical and Biophysical Research Communications* 401 (3): 327-32. <https://doi.org/10.1016/j.bbrc.2010.09.014>.

Chow, Kin-Hoe, Rachel E. Factor, et Katharine S. Ullman. 2012. « The Nuclear Envelope Environment and Its Cancer Connections ». *Nature Reviews Cancer* 12 (3): 196-209. <https://doi.org/10.1038/nrc3219>.

Coffinier, Catherine, Hea-Jin Jung, Chika Nobumori, Sandy Chang, Yiping Tu, Richard H. Barnes, Yuko Yoshinaga, et al. 2011. « Deficiencies in Lamin B1 and Lamin B2 Cause Neurodevelopmental Defects and Distinct Nuclear Shape Abnormalities in Neurons ». Édité par Thomas Michael Magin. *Molecular Biology of the Cell* 22 (23): 4683-93. <https://doi.org/10.1091/mbc.e11-06-0504>.

Collinet, Claudio, et Thomas Lecuit. 2021. « Programmed and Self-Organized Flow of Information during Morphogenesis ». *Nature Reviews Molecular Cell Biology* 22 (4): 245-65. <https://doi.org/10.1038/s41580-020-00318-6>.

Collinson, Adam, Amanda J. Collier, Natasha P. Morgan, Arnold R. Sienerth, Tamir Chandra, Simon Andrews, et Peter J. Rugg-Gunn. 2016. « Deletion of the Polycomb-Group Protein EZH2 Leads to Compromised Self-Renewal and Differentiation Defects in Human Embryonic Stem Cells ». *Cell Reports* 17 (10): 2700-2714. <https://doi.org/10.1016/j.celrep.2016.11.032>.

Cooper, John A, et Dorothy A Schafer. 2000. « Control of Actin Assembly and Disassembly at Filament Ends ». *Current Opinion in Cell Biology* 12 (1): 97-103. [https://doi.org/10.1016/S0955-0674\(99\)00062-9](https://doi.org/10.1016/S0955-0674(99)00062-9).

Cornelison, D.D.W., Bradley B. Olwin, Michael A. Rudnicki, et Barbara J. Wold. 2000. « MyoD^{-/-} Satellite Cells in Single-Fiber Culture Are Differentiation Defective and MRF4 Deficient ». *Developmental Biology* 224 (2): 122-37. <https://doi.org/10.1006/dbio.2000.9682>.

Croft, Jenny A., Joanna M. Bridger, Shelagh Boyle, Paul Perry, Peter Teague, et Wendy

A. Bickmore. 1999. « Differences in the Localization and Morphology of Chromosomes in the Human Nucleus ». *Journal of Cell Biology* 145 (6): 1119-31. <https://doi.org/10.1083/jcb.145.6.1119>.

Dahl, Kris Noel, Samuel M. Kahn, Katherine L. Wilson, et Dennis E. Discher. 2004. « The Nuclear Envelope Lamina Network Has Elasticity and a Compressibility Limit Suggestive of a Molecular Shock Absorber ». *Journal of Cell Science* 117 (20): 4779-86. <https://doi.org/10.1242/jcs.01357>.

Deaton, Aimée M., et Adrian Bird. 2011. « CpG Islands and the Regulation of Transcription ». *Genes & Development* 25 (10): 1010-22. <https://doi.org/10.1101/gad.2037511>.

Dechat, T. 1998. « Detergent-salt resistance of LAP2alpha in interphase nuclei and phosphorylation-dependent association with chromosomes early in nuclear assembly implies functions in nuclear structure dynamics ». *The EMBO Journal* 17 (16): 4887-4902. <https://doi.org/10.1093/emboj/17.16.4887>.

Dechat, T., K. Gesson, et R. Foisner. 2010. « Lamina-Independent Lamins in the Nuclear Interior Serve Important Functions ». *Cold Spring Harbor Symposia on Quantitative Biology* 75 (0): 533-43. <https://doi.org/10.1101/sqb.2010.75.018>.

Dechat, Thomas, Katrin Pflieger, Kaushik Sengupta, Takeshi Shimi, Dale K. Shumaker, Liliana Solimando, et Robert D. Goldman. 2008. « Nuclear Lamins: Major Factors in the Structural Organization and Function of the Nucleus and Chromatin ». *Genes & Development* 22 (7): 832-53. <https://doi.org/10.1101/gad.1652708>.

Dewey, C. F., S. R. Bussolari, M. A. Gimbrone, et P. F. Davies. 1981. « The Dynamic Response of Vascular Endothelial Cells to Fluid Shear Stress ». *Journal of Biomechanical Engineering* 103 (3): 177-85. <https://doi.org/10.1115/1.3138276>.

Dilworth, FJeffrey, et Alexandre Blais. 2011. « Epigenetic Regulation of Satellite Cell Activation during Muscle Regeneration ». *Stem Cell Research & Therapy* 2 (2): 18. <https://doi.org/10.1186/scrt59>.

Donnaloja, Francesca, Federica Carnevali, Emanuela Jacchetti, et Manuela Teresa Raimondi. 2020. « Lamin A/C Mechanotransduction in Laminopathies ». *Cells* 9 (5): 1306. <https://doi.org/10.3390/cells9051306>.

Driscoll, Tristan P., Brian D. Cosgrove, Su-Jin Heo, Zach E. Shurden, et Robert L. Mauck. 2015. « Cytoskeletal to Nuclear Strain Transfer Regulates YAP Signaling in Mesenchymal Stem Cells ». *Biophysical Journal* 108 (12): 2783-93. <https://doi.org/10.1016/j.bpj.2015.05.010>.

Dunlevy, Kelly L., Valentina Medvedeva, Jade E. Wilson, Mohammed Hoque, Trinity

Pellegrin, Adam Maynard, Madison M. Kremp, Jason S. Wasserman, Andrey Poleshko, et Richard A. Katz. 2020. « The PRR14 Heterochromatin Tether Encodes Modular Domains That Mediate and Regulate Nuclear Lamina Targeting ». *Journal of Cell Science*, janvier, jcs.240416. <https://doi.org/10.1242/jcs.240416>.

Dutour-Provenzano, Gaëlle, et Sandrine Etienne-Manneville. 2021. « Intermediate Filaments ». *Current Biology* 31 (10): R522-29. <https://doi.org/10.1016/j.cub.2021.04.011>.

Eibauer, Matthias, Mauro Pellanda, Yagmur Turgay, Anna Dubrovsky, Annik Wild, et Ohad Medalia. 2015. « Structure and Gating of the Nuclear Pore Complex ». *Nature Communications* 6 (1): 7532. <https://doi.org/10.1038/ncomms8532>.

Elosegui-Artola, Alberto, Xavier Trepast, et Pere Roca-Cusachs. 2018. « Control of Mechanotransduction by Molecular Clutch Dynamics ». *Trends in Cell Biology* 28 (5): 356-67. <https://doi.org/10.1016/j.tcb.2018.01.008>.

Engler, Adam J., Shamik Sen, H. Lee Sweeney, et Dennis E. Discher. 2006. « Matrix Elasticity Directs Stem Cell Lineage Specification ». *Cell* 126 (4): 677-89. <https://doi.org/10.1016/j.cell.2006.06.044>.

Enyedi, Balázs, et Philipp Niethammer. 2017. « Nuclear Membrane Stretch and Its Role in Mechanotransduction ». *Nucleus* 8 (2): 156-61. <https://doi.org/10.1080/19491034.2016.1263411>.

Ervasti, James M. 2003. « Costameres: The Achilles' Heel of Herculean Muscle ». *Journal of Biological Chemistry* 278 (16): 13591-94. <https://doi.org/10.1074/jbc.R200021200>.

Etienne-Manneville, Sandrine. 2018. « Cytoplasmic Intermediate Filaments in Cell Biology ». *Annual Review of Cell and Developmental Biology* 34 (1): 1-28. <https://doi.org/10.1146/annurev-cellbio-100617-062534>.

Falk, Martin, et Michael Hausmann. 2020. « A Paradigm Revolution or Just Better Resolution—Will Newly Emerging Superresolution Techniques Identify Chromatin Architecture as a Key Factor in Radiation-Induced DNA Damage and Repair Regulation? » *Cancers* 13 (1): 18. <https://doi.org/10.3390/cancers13010018>.

Fischer, Martina, Paul Rikeit, Petra Knaus, et Catherine Coirault. 2016. « YAP-Mediated Mechanotransduction in Skeletal Muscle ». *Frontiers in Physiology* 7 (février). <https://doi.org/10.3389/fphys.2016.00041>.

Fouse, Shaun D., Yin Shen, Matteo Pellegrini, Steve Cole, Alexander Meissner, Leander Van Neste, Rudolf Jaenisch, et Guoping Fan. 2008. « Promoter CpG Methylation Contributes to ES Cell Gene Regulation in Parallel with Oct4/Nanog, PcG Complex, and Histone H3 K4/K27 Trimethylation ». *Cell Stem Cell* 2 (2): 160-69.

<https://doi.org/10.1016/j.stem.2007.12.011>.

Francastel, Claire, Dirk Schübeler, David I. K. Martin, et Mark Groudine. 2000. « Nuclear Compartmentalization and Gene Activity ». *Nature Reviews Molecular Cell Biology* 1 (2): 137-43. <https://doi.org/10.1038/35040083>.

Fudge, Douglas S., Kenn H. Gardner, V. Trevor Forsyth, Christian Riekkel, et John M. Gosline. 2003. « The Mechanical Properties of Hydrated Intermediate Filaments: Insights from Hagfish Slime Threads ». *Biophysical Journal* 85 (3): 2015-27. [https://doi.org/10.1016/S0006-3495\(03\)74629-3](https://doi.org/10.1016/S0006-3495(03)74629-3).

Galbraith, C.G., R. Skalak, et S. Chien. 1998. « Shear Stress Induces Spatial Reorganization of the Endothelial Cell Cytoskeleton ». *Cell Motility and the Cytoskeleton* 40 (4): 317-30. [https://doi.org/10.1002/\(SICI\)1097-0169\(1998\)40:4<317::AID-CM1>3.0.CO;2-8](https://doi.org/10.1002/(SICI)1097-0169(1998)40:4<317::AID-CM1>3.0.CO;2-8).

Galou, Maria, Jie Gao, Jeanne Humbert, Mathias Mericskay, Zhenlin Li, Denise Paulin, et Patrick Vicart. 1997. « The Importance of Intermediate Filaments in the Adaptation of Tissues to Mechanical Stress: Evidence from Gene Knockout Studies ». *Biology of the Cell* 89 (2): 85-97. <https://doi.org/10.1111/j.1768-322X.1997.tb00997.x>.

Gao, Quan Q., Eugene Wyatt, Jeff A. Goldstein, Peter LoPresti, Lisa M. Castillo, Alec Gazda, Natalie Petrossian, et al. 2015. « Reengineering a Transmembrane Protein to Treat Muscular Dystrophy Using Exon Skipping ». *Journal of Clinical Investigation* 125 (11): 4186-95. <https://doi.org/10.1172/JCI82768>.

Gerace, Larry, et Günter Blobel. 1980. « The Nuclear Envelope Lamina Is Reversibly Depolymerized during Mitosis ». *Cell* 19 (1): 277-87. [https://doi.org/10.1016/0092-8674\(80\)90409-2](https://doi.org/10.1016/0092-8674(80)90409-2).

Gesson, Kevin, Philipp Rescheneder, Michael P. Skoruppa, Arndt von Haeseler, Thomas Dechat, et Roland Foisner. 2016. « A-Type Lamins Bind Both Hetero- and Euchromatin, the Latter Being Regulated by Lamina-Associated Polypeptide 2 Alpha ». *Genome Research* 26 (4): 462-73. <https://doi.org/10.1101/gr.196220.115>.

Gimpel, Petra, Yin Loon Lee, Radoslaw M. Sobota, Alessandra Calvi, Victoria Koullourou, Rutti Patel, Kamel Mamchaoui, et al. 2017. « Nesprin-1 α -Dependent Microtubule Nucleation from the Nuclear Envelope via Akap450 Is Necessary for Nuclear Positioning in Muscle Cells ». *Current Biology* 27 (19): 2999-3009.e9. <https://doi.org/10.1016/j.cub.2017.08.031>.

Gittes, F, B Mickey, J Nettleton, et J Howard. 1993. « Flexural Rigidity of Microtubules and Actin Filaments Measured from Thermal Fluctuations in Shape. » *Journal of Cell Biology* 120 (4): 923-34. <https://doi.org/10.1083/jcb.120.4.923>.

Grewal, Shiv I. S., et Danesh Moazed. 2003. « Heterochromatin and Epigenetic Control of Gene Expression ». *Science* 301 (5634): 798-802. <https://doi.org/10.1126/science.1086887>.

Gruenbaum, Yosef, et Ueli Aebi. 2014. « Intermediate filaments: a dynamic network that controls cell mechanics ». *F1000Prime Reports* 6 (juillet). <https://doi.org/10.12703/P6-54>.

Guilluy, Christophe, Lukas D. Osborne, Laurianne Van Landeghem, Lisa Sharek, Richard Superfine, Rafael Garcia-Mata, et Keith Burrige. 2014. « Isolated Nuclei Adapt to Force and Reveal a Mechanotransduction Pathway in the Nucleus ». *Nature Cell Biology* 16 (4): 376-81. <https://doi.org/10.1038/ncb2927>.

Hall, Christopher S., Michael J. Scott, Gregory M. Lanza, James G. Miller, et Samuel A. Wickline. 2000. « The Extracellular Matrix Is an Important Source of Ultrasound Backscatter from Myocardium ». *The Journal of the Acoustical Society of America* 107 (1): 612-19. <https://doi.org/10.1121/1.428327>.

Hansen, Carsten Gram, Toshiro Moroishi, et Kun-Liang Guan. 2015. « YAP and TAZ: A Nexus for Hippo Signaling and Beyond ». *Trends in Cell Biology* 25 (9): 499-513. <https://doi.org/10.1016/j.tcb.2015.05.002>.

Haque, Farhana, David J. Lloyd, Dawn T. Smallwood, Carolyn L. Dent, Catherine M. Shanahan, Andrew M. Fry, Richard C. Trembath, et Sue Shackleton. 2006. « SUN1 Interacts with Nuclear Lamin A and Cytoplasmic Nesprins To Provide a Physical Connection between the Nuclear Lamina and the Cytoskeleton ». *Molecular and Cellular Biology* 26 (10): 3738-51. <https://doi.org/10.1128/MCB.26.10.3738-3751.2006>.

Harada, Akihito, Kazumitsu Maehara, Yuko Sato, Daijiro Konno, Taro Tachibana, Hiroshi Kimura, et Yasuyuki Ohkawa. 2015. « Incorporation of Histone H3.1 Suppresses the Lineage Potential of Skeletal Muscle ». *Nucleic Acids Research* 43 (2): 775-86. <https://doi.org/10.1093/nar/gku1346>.

Harr, Jennifer C., Teresa Romeo Luperchio, Xianrong Wong, Erez Cohen, Sarah J. Wheelan, et Karen L. Reddy. 2015. « Directed Targeting of Chromatin to the Nuclear Lamina Is Mediated by Chromatin State and A-Type Lamins ». *Journal of Cell Biology* 208 (1): 33-52. <https://doi.org/10.1083/jcb.201405110>.

Harris, A. K., P. Wild, et D. Stopak. 1980. « Silicone Rubber Substrata: A New Wrinkle in the Study of Cell Locomotion ». *Science (New York, N.Y.)* 208 (4440): 177-79. <https://doi.org/10.1126/science.6987736>.

Hart, Gerald W., Chad Slawson, Genaro Ramirez-Correa, et Olof Lagerlof. 2011. « Cross Talk Between O-GlcNAcylation and Phosphorylation: Roles in Signaling, Transcription, and Chronic Disease ». *Annual Review of Biochemistry* 80 (1): 825-58.

<https://doi.org/10.1146/annurev-biochem-060608-102511>.

Heath, J.P. 1983. « Behaviour and Structure of the Leading Lamella in Moving Fibroblasts. I. Occurrence and Centripetal Movement of Arc-Shaped Microfilament Bundles beneath the Dorsal Cell Surface ». *Journal of Cell Science* 60 (1): 331-54. <https://doi.org/10.1242/jcs.60.1.331>.

Heffler, Julie, Parisha P. Shah, Patrick Robison, Sai Phyo, Kimberly Veliz, Keita Uchida, Alexey Bogush, Joshua Rhoades, Rajan Jain, et Benjamin L. Prosser. 2020. « A Balance Between Intermediate Filaments and Microtubules Maintains Nuclear Architecture in the Cardiomyocyte ». *Circulation Research* 126 (3). <https://doi.org/10.1161/CIRCRESAHA.119.315582>.

Heinz, Sven, Christopher Benner, Nathanael Spann, Eric Bertolino, Yin C. Lin, Peter Laslo, Jason X. Cheng, Cornelis Murre, Harinder Singh, et Christopher K. Glass. 2010. « Simple Combinations of Lineage-Determining Transcription Factors Prime Cis-Regulatory Elements Required for Macrophage and B Cell Identities ». *Molecular Cell* 38 (4): 576-89. <https://doi.org/10.1016/j.molcel.2010.05.004>.

Heo, Su-Jin, Tristan P Driscoll, Stephen D Thorpe, Nandan L Nerurkar, Brendon M Baker, Michael T Yang, Christopher S Chen, David A Lee, et Robert L Mauck. 2016. « Differentiation Alters Stem Cell Nuclear Architecture, Mechanics, and Mechano-Sensitivity ». *ELife* 5 (novembre): e18207. <https://doi.org/10.7554/eLife.18207>.

Hernandez, Marylens, Julia Patzig, Sonia R. Mayoral, Kevin D. Costa, Jonah R. Chan, et Patrizia Casaccia. 2016. « Mechanostimulation Promotes Nuclear and Epigenetic Changes in Oligodendrocytes ». *The Journal of Neuroscience* 36 (3): 806-13. <https://doi.org/10.1523/JNEUROSCI.2873-15.2016>.

Hirano, Yasuhiro, Kohji Hizume, Hiroshi Kimura, Kunio Takeyasu, Tokuko Haraguchi, et Yasushi Hiraoka. 2012. « Lamin B Receptor Recognizes Specific Modifications of Histone H4 in Heterochromatin Formation ». *Journal of Biological Chemistry* 287 (51): 42654-63. <https://doi.org/10.1074/jbc.M112.397950>.

Hirata, Hiroaki, Hitoshi Tatsumi, Chwee Teck Lim, et Masahiro Sokabe. 2014. « Force-Dependent Vinculin Binding to Talin in Live Cells: A Crucial Step in Anchoring the Actin Cytoskeleton to Focal Adhesions ». *American Journal of Physiology-Cell Physiology* 306 (6): C607-20. <https://doi.org/10.1152/ajpcell.00122.2013>.

Hirokawa, N, L G Tilney, K Fujiwara, et J E Heuser. 1982. « Organization of Actin, Myosin, and Intermediate Filaments in the Brush Border of Intestinal Epithelial Cells. » *Journal of Cell Biology* 94 (2): 425-43. <https://doi.org/10.1083/jcb.94.2.425>.

Hoffman, Brenton D., Carsten Grashoff, et Martin A. Schwartz. 2011. « Dynamic Molecular Processes Mediate Cellular Mechanotransduction ». *Nature* 475 (7356): 316-23. <https://doi.org/10.1038/nature10316>.

Holmer, L., et H.J. Worman. 2001. « Inner Nuclear Membrane Proteins: Functions and Targeting ». *Cellular and Molecular Life Sciences* 58 (12): 1741-47. <https://doi.org/10.1007/PL00000813>.

Holt, Ian, Heidi R. Fuller, Le Thanh Lam, Caroline A. Sewry, Sally L. Shirran, Qiuping Zhang, Catherine M. Shanahan, et Glenn E. Morris. 2019. « Nesprin-1-Alpha2 Associates with Kinesin at Myotube Outer Nuclear Membranes, but Is Restricted to Neuromuscular Junction Nuclei in Adult Muscle ». *Scientific Reports* 9 (1): 14202. <https://doi.org/10.1038/s41598-019-50728-6>.

Hotulainen, Pirta, et Pekka Lappalainen. 2006. « Stress Fibers Are Generated by Two Distinct Actin Assembly Mechanisms in Motile Cells ». *Journal of Cell Biology* 173 (3): 383-94. <https://doi.org/10.1083/jcb.200511093>.

Hsu, T.C. 1962. « Chromosomal Evolution in Cell Populations ». In *International Review of Cytology*, 12:69-161. Elsevier. [https://doi.org/10.1016/S0074-7696\(08\)60539-2](https://doi.org/10.1016/S0074-7696(08)60539-2).

Hu, Jiliang, Yiwei Li, Yukun Hao, Tianqi Zheng, Satish K. Gupta, German Alberto Parada, Huayin Wu, et al. 2019. « High Stretchability, Strength, and Toughness of Living Cells Enabled by Hyperelastic Vimentin Intermediate Filaments ». *Proceedings of the National Academy of Sciences* 116 (35): 17175-80. <https://doi.org/10.1073/pnas.1903890116>.

Hynes, R. O., et A. Naba. 2012. « Overview of the Matrisome--An Inventory of Extracellular Matrix Constituents and Functions ». *Cold Spring Harbor Perspectives in Biology* 4 (1): a004903-a004903. <https://doi.org/10.1101/cshperspect.a004903>.

Hynes, Richard O. 2002. « Integrins ». *Cell* 110 (6): 673-87. [https://doi.org/10.1016/S0092-8674\(02\)00971-6](https://doi.org/10.1016/S0092-8674(02)00971-6).

Irianto, Jerome, Charlotte R. Pfeifer, Irena L. Ivanovska, Joe Swift, et Dennis E. Discher. 2016. « Nuclear Lamins in Cancer ». *Cellular and Molecular Bioengineering* 9 (2): 258-67. <https://doi.org/10.1007/s12195-016-0437-8>.

Jabre, Saline, Walid Hleihel, et Catherine Coirault. 2021. « Nuclear Mechanotransduction in Skeletal Muscle ». *Cells* 10 (2): 318. <https://doi.org/10.3390/cells10020318>.

Jaenisch, Rudolf, et Adrian Bird. 2003. « Epigenetic Regulation of Gene Expression: How the Genome Integrates Intrinsic and Environmental Signals ». *Nature Genetics* 33 (S3): 245-54. <https://doi.org/10.1038/ng1089>.

Jahed, Zeinab, Hengameh Shams, et Mohammad R.K. Mofrad. 2015. « A Disulfide Bond Is Required for the Transmission of Forces through SUN-KASH Complexes ». *Biophysical Journal* 109 (3): 501-9. <https://doi.org/10.1016/j.bpj.2015.06.057>.

Jansen, Karin A., Dominique M. Donato, Hayri E. Balcioglu, Thomas Schmidt, Erik H.J. Danen, et Gijsje H. Koenderink. 2015. « A Guide to Mechanobiology: Where Biology and Physics Meet ». *Biochimica et Biophysica Acta (BBA) - Molecular Cell Research* 1853 (11): 3043-52. <https://doi.org/10.1016/j.bbamcr.2015.05.007>.

Jones, Peter A. 2012. « Functions of DNA Methylation: Islands, Start Sites, Gene Bodies and Beyond ». *Nature Reviews Genetics* 13 (7): 484-92. <https://doi.org/10.1038/nrg3230>.

Juan, Aster H., Assia Derfoul, Xuesong Feng, James G. Ryall, Stefania Dell'Orso, Alessandra Pasut, Hossein Zare, James M. Simone, Michael A. Rudnicki, et Vittorio Sartorelli. 2011. « Polycomb EZH2 Controls Self-Renewal and Safeguards the Transcriptional Identity of Skeletal Muscle Stem Cells ». *Genes & Development* 25 (8): 789-94. <https://doi.org/10.1101/gad.2027911>.

Kapinos, Larisa E., Jens Schumacher, Norbert Mücke, Gia Machaidze, Peter Burkhard, Ueli Aebi, Sergei V. Strelkov, et Harald Herrmann. 2010. « Characterization of the Head-to-Tail Overlap Complexes Formed by Human Lamin A, B1 and B2 “Half-Minilamin” Dimers ». *Journal of Molecular Biology* 396 (3): 719-31. <https://doi.org/10.1016/j.jmb.2009.12.001>.

Kaunas, Roland, Phu Nguyen, Shunichi Usami, et Shu Chien. 2005. « Cooperative Effects of Rho and Mechanical Stretch on Stress Fiber Organization ». *Proceedings of the National Academy of Sciences* 102 (44): 15895-900. <https://doi.org/10.1073/pnas.0506041102>.

Kharchenko, Peter V., Artyom A. Alekseyenko, Yuri B. Schwartz, Aki Minoda, Nicole C. Riddle, Jason Ernst, Peter J. Sabo, et al. 2011. « Comprehensive Analysis of the Chromatin Landscape in *Drosophila Melanogaster* ». *Nature* 471 (7339): 480-85. <https://doi.org/10.1038/nature09725>.

Khatau, Shyam B., Christopher M. Hale, P. J. Stewart-Hutchinson, Meet S. Patel, Colin L. Stewart, Peter C. Searson, Didier Hodzic, et Denis Wirtz. 2009. « A Perinuclear Actin Cap Regulates Nuclear Shape ». *Proceedings of the National Academy of Sciences* 106 (45): 19017-22. <https://doi.org/10.1073/pnas.0908686106>.

Khatau, Shyam B., Sravanti Kusuma, Donny Hanjaya-Putra, Prashant Mali, Linzhao Cheng, Jerry S. H. Lee, Sharon Gerecht, et Denis Wirtz. 2012. « The Differential Formation of the LINC-Mediated Perinuclear Actin Cap in Pluripotent and Somatic Cells ». Édité par Laurent Kreplak. *PLoS ONE* 7 (5): e36689. <https://doi.org/10.1371/journal.pone.0036689>.

Khurana, Seema, et Sudeep P. George. 2011. « The Role of Actin Bundling Proteins in the Assembly of Filopodia in Epithelial Cells ». *Cell Adhesion & Migration* 5 (5): 409-20. <https://doi.org/10.4161/cam.5.5.17644>.

Kim, Dong-Hwee, Allison B. Chambliss, et Denis Wirtz. 2013. « The Multi-Faceted Role of the Actin Cap in Cellular Mechanosensation and Mechanotransduction ». *Soft Matter* 9 (23): 5516. <https://doi.org/10.1039/c3sm50798j>.

Kim, Dong-Hwee, et Denis Wirtz. 2015. « Cytoskeletal Tension Induces the Polarized Architecture of the Nucleus ». *Biomaterials* 48 (avril): 161-72. <https://doi.org/10.1016/j.biomaterials.2015.01.023>.

Kim, Seyun, et Pierre A. Coulombe. 2007. « Intermediate Filament Scaffolds Fulfill Mechanical, Organizational, and Signaling Functions in the Cytoplasm ». *Genes & Development* 21 (13): 1581-97. <https://doi.org/10.1101/gad.1552107>.

Kirby, Tyler J., et Jan Lammerding. 2018. « Emerging Views of the Nucleus as a Cellular Mechanosensor ». *Nature Cell Biology* 20 (4): 373-81. <https://doi.org/10.1038/s41556-018-0038-y>.

Kittisopikul, Mark, Takeshi Shimi, Meltem Tatli, Joseph Riley Tran, Yixian Zheng, Ohad Medalia, Khuloud Jaqaman, Stephen A. Adam, et Robert D. Goldman. 2021. « Computational Analyses Reveal Spatial Relationships between Nuclear Pore Complexes and Specific Lamins ». *Journal of Cell Biology* 220 (4): e202007082. <https://doi.org/10.1083/jcb.202007082>.

Kooistra, Susanne Marije, et Kristian Helin. 2012. « Molecular Mechanisms and Potential Functions of Histone Demethylases ». *Nature Reviews Molecular Cell Biology* 13 (5): 297-311. <https://doi.org/10.1038/nrm3327>.

Kouzarides, Tony. 2007. « Chromatin Modifications and Their Function ». *Cell* 128 (4): 693-705. <https://doi.org/10.1016/j.cell.2007.02.005>.

Kreitzer, Geri, Guojuan Liao, et Gregg G. Gundersen. 1999. « Detyrosination of Tubulin Regulates the Interaction of Intermediate Filaments with Microtubules In Vivo via a Kinesin-Dependent Mechanism ». Édité par Marc W. Kirschner. *Molecular Biology of the Cell* 10 (4): 1105-18. <https://doi.org/10.1091/mbc.10.4.1105>.

Kreplak, Laurent, Harald Herrmann, et Ueli Aebi. 2008. « Tensile Properties of Single Desmin Intermediate Filaments ». *Biophysical Journal* 94 (7): 2790-99. <https://doi.org/10.1529/biophysj.107.119826>.

Kutscheidt, Stefan, Ruijun Zhu, Susumu Antoku, G. W. Gant Luxton, Igor Stagljar, Oliver T. Fackler, et Gregg G. Gundersen. 2014. « FHOD1 Interaction with Nesprin-2G

Mediates TAN Line Formation and Nuclear Movement ». *Nature Cell Biology* 16 (7): 708-15. <https://doi.org/10.1038/ncb2981>.

Lammerding, Jan, Loren G. Fong, Julie Y. Ji, Karen Reue, Colin L. Stewart, Stephen G. Young, et Richard T. Lee. 2006. « Lamins A and C but Not Lamin B1 Regulate Nuclear Mechanics ». *Journal of Biological Chemistry* 281 (35): 25768-80. <https://doi.org/10.1074/jbc.M513511200>.

Lancaster, Oscar M., Maël Le Berre, Andrea Dimitracopoulos, Daria Bonazzi, Ewa Zlotek-Zlotkiewicz, Remigio Picone, Thomas Duke, Matthieu Piel, et Buzz Baum. 2013. « Mitotic Rounding Alters Cell Geometry to Ensure Efficient Bipolar Spindle Formation ». *Developmental Cell* 25 (3): 270-83. <https://doi.org/10.1016/j.devcel.2013.03.014>.

Langer, Henning Tim, Shoaib Afzal, Stefan Kempa, et Simone Spuler. 2020. « Nerve Damage Induced Skeletal Muscle Atrophy Is Associated with Increased Accumulation of Intramuscular Glucose and Polyol Pathway Intermediates ». *Scientific Reports* 10 (1): 1908. <https://doi.org/10.1038/s41598-020-58213-1>.

Langmead, Ben, et Steven L Salzberg. 2012. « Fast Gapped-Read Alignment with Bowtie 2 ». *Nature Methods* 9 (4): 357-59. <https://doi.org/10.1038/nmeth.1923>.

Langmead, Ben, Cole Trapnell, Mihai Pop, et Steven L Salzberg. 2009. « Ultrafast and Memory-Efficient Alignment of Short DNA Sequences to the Human Genome ». *Genome Biology* 10 (3): R25. <https://doi.org/10.1186/gb-2009-10-3-r25>.

Lazarides, E. 1976. « Actin, Alpha-Actinin, and Tropomyosin Interaction in the Structural Organization of Actin Filaments in Nonmuscle Cells. » *Journal of Cell Biology* 68 (2): 202-19. <https://doi.org/10.1083/jcb.68.2.202>.

Lazarides, Elias. 1980. « Intermediate Filaments as Mechanical Integrators of Cellular Space ». *Nature* 283 (5744): 249-55. <https://doi.org/10.1038/283249a0>.

Le Grand, Fabien, et Michael A Rudnicki. 2007. « Skeletal Muscle Satellite Cells and Adult Myogenesis ». *Current Opinion in Cell Biology* 19 (6): 628-33. <https://doi.org/10.1016/j.ceb.2007.09.012>.

Leggett, Richard M., Ricardo H. Ramirez-Gonzalez, Bernardo J. Clavijo, Darren Waite, et Robert P. Davey. 2013. « Sequencing quality assessment tools to enable data-driven informatics for high throughput genomics ». *Frontiers in Genetics* 4. <https://doi.org/10.3389/fgene.2013.00288>.

Lei, Kai, Xiaoqiang Zhu, Renner Xu, Chunlin Shao, Tian Xu, Yuan Zhuang, et Min Han. 2012. « Inner Nuclear Envelope Proteins SUN1 and SUN2 Play a Prominent Role in the DNA Damage Response ». *Current Biology* 22 (17): 1609-15.

<https://doi.org/10.1016/j.cub.2012.06.043>.

Lessey, Elizabeth C., Christophe Guilluy, et Keith Burridge. 2012. « From Mechanical Force to RhoA Activation ». *Biochemistry* 51 (38): 7420-32. <https://doi.org/10.1021/bi300758e>.

Letort, Gaëlle, Hajer Ennomani, Laurène Gressin, Manuel Théry, et Laurent Blanchoin. 2015. « Dynamic Reorganization of the Actin Cytoskeleton ». *F1000Research* 4 (octobre): 940. <https://doi.org/10.12688/f1000research.6374.1>.

Li, Guohong, et Danny Reinberg. 2011. « Chromatin Higher-Order Structures and Gene Regulation ». *Current Opinion in Genetics & Development* 21 (2): 175-86. <https://doi.org/10.1016/j.gde.2011.01.022>.

Li, Yuan, David Lovett, Qiao Zhang, Srujana Neelam, Ram Anirudh Kuchibhotla, Ruijun Zhu, Gregg G. Gundersen, Tanmay P. Lele, et Richard B. Dickinson. 2015. « Moving Cell Boundaries Drive Nuclear Shaping during Cell Spreading ». *Biophysical Journal* 109 (4): 670-86. <https://doi.org/10.1016/j.bpj.2015.07.006>.

Li, Zhenlin, Emma Colucci-Guyon, Martine Pinçon-Raymond, Mathias Mericskay, Sandrine Pournin, Denise Paulin, et Charles Babinet. 1996. « Cardiovascular Lesions and Skeletal Myopathy in Mice Lacking Desmin ». *Developmental Biology* 175 (2): 362-66. <https://doi.org/10.1006/dbio.1996.0122>.

Lin, F., et H.J. Worman. 1993. « Structural Organization of the Human Gene Encoding Nuclear Lamin A and Nuclear Lamin C ». *Journal of Biological Chemistry* 268 (22): 16321-26. [https://doi.org/10.1016/S0021-9258\(19\)85424-8](https://doi.org/10.1016/S0021-9258(19)85424-8).

Lin, Feng, et Howard J. Worman. 1995. « Structural Organization of the Human Gene (LMNB1) Encoding Nuclear Lamin B1 ». *Genomics* 27 (2): 230-36. <https://doi.org/10.1006/geno.1995.1036>.

Lin, J J, et J L Lin. 1986. « Assembly of Different Isoforms of Actin and Tropomyosin into the Skeletal Tropomyosin-Enriched Microfilaments during Differentiation of Muscle Cells in Vitro. » *The Journal of Cell Biology* 103 (6): 2173-83. <https://doi.org/10.1083/jcb.103.6.2173>.

Liu, Ling, Tom H. Cheung, Gregory W. Charville, Bernadette Marie Ceniza Hurgo, Tripp Leavitt, Johnathan Shih, Anne Brunet, et Thomas A. Rando. 2013. « Chromatin Modifications as Determinants of Muscle Stem Cell Quiescence and Chronological Aging ». *Cell Reports* 4 (1): 189-204. <https://doi.org/10.1016/j.celrep.2013.05.043>.

Lloyd, C.M, M Berendse, D.G Lloyd, G Schevzov, et M.D Grounds. 2004. « A Novel Role for Non-Muscle γ -Actin in Skeletal Muscle Sarcomere Assembly ». *Experimental Cell*

Research 297 (1): 82-96. <https://doi.org/10.1016/j.yexcr.2004.02.012>.

Lotterberger, Francisca, Roos Anna Karssemeijer, Nadya Dimitrova, et Titia de Lange. 2015. « 53BP1 and the LINC Complex Promote Microtubule-Dependent DSB Mobility and DNA Repair ». *Cell* 163 (4): 880-93. <https://doi.org/10.1016/j.cell.2015.09.057>.

Love, Michael I, Wolfgang Huber, et Simon Anders. 2014. « Moderated Estimation of Fold Change and Dispersion for RNA-Seq Data with DESeq2 ». *Genome Biology* 15 (12): 550. <https://doi.org/10.1186/s13059-014-0550-8>.

Luxton, G.W. Gant, Edgar R. Gomes, Eric S. Folker, Howard Worman, et Gregg G. Gundersen. 2011. « TAN Lines: A Novel Nuclear Envelope Structure Involved in Nuclear Positioning ». *Nucleus* 2 (3): 173-81. <https://doi.org/10.4161/nucl.2.3.16243>.

Lyman, Susan K., Tinglu Guan, Janna Bednenko, Harald Wodrich, et Larry Gerace. 2002. « Influence of Cargo Size on Ran and Energy Requirements for Nuclear Protein Import ». *Journal of Cell Biology* 159 (1): 55-67. <https://doi.org/10.1083/jcb.200204163>.

Machowska, Magdalena, Katarzyna Piekarowicz, et Ryszard Rzepecki. 2015. « Regulation of Lamin Properties and Functions: Does Phosphorylation Do It All? » *Open Biology* 5 (11): 150094. <https://doi.org/10.1098/rsob.150094>.

Mackey, Abigail L., et Michael Kjaer. 2017. « The Breaking and Making of Healthy Adult Human Skeletal Muscle in Vivo ». *Skeletal Muscle* 7 (1): 24. <https://doi.org/10.1186/s13395-017-0142-x>.

Maganaris, C. N. 2001. « Force-Length Characteristics of *in Vivo* Human Skeletal Muscle: In Vivo Muscle Force-Length Relation ». *Acta Physiologica Scandinavica* 172 (4): 279-85. <https://doi.org/10.1046/j.1365-201x.2001.00799.x>.

Makarov, Alex A., Juan Zou, Douglas R. Houston, Christos Spanos, Alexandra S. Solovyova, Cristina Cardenal-Peralta, Juri Rappsilber, et Eric C. Schirmer. 2019. « Lamin A Molecular Compression and Sliding as Mechanisms behind Nucleoskeleton Elasticity ». *Nature Communications* 10 (1): 3056. <https://doi.org/10.1038/s41467-019-11063-6>.

Mal, Asoke, et Marian L. Harter. 2003. « MyoD Is Functionally Linked to the Silencing of a Muscle-Specific Regulatory Gene Prior to Skeletal Myogenesis ». *Proceedings of the National Academy of Sciences* 100 (4): 1735-39. <https://doi.org/10.1073/pnas.0437843100>.

Mal, Asoke K. 2006. « Histone methyltransferase Suv39h1 represses MyoD-stimulated myogenic differentiation ». *The EMBO Journal* 25 (14): 3323-34. <https://doi.org/10.1038/sj.emboj.7601229>.

Mamchaoui, Kamel, Capucine Trollet, Anne Bigot, Elisa Negroni, Soraya Chaouch, Annie Wolff, Prashanth K Kandalla, et al. 2011. « Immortalized Pathological Human

Myoblasts: Towards a Universal Tool for the Study of Neuromuscular Disorders ». *Skeletal Muscle* 1 (1): 34. <https://doi.org/10.1186/2044-5040-1-34>.

Marchand, Marion, Catherine Monnot, Laurent Muller, et Stéphane Germain. 2019. « Extracellular Matrix Scaffolding in Angiogenesis and Capillary Homeostasis ». *Seminars in Cell & Developmental Biology* 89 (mai): 147-56. <https://doi.org/10.1016/j.semcdb.2018.08.007>.

Margueron, Raphael, Guohong Li, Kavitha Sarma, Alexandre Blais, Jiri Zavadil, Christopher L. Woodcock, Brian D. Dynlacht, et Danny Reinberg. 2008. « Ezh1 and Ezh2 Maintain Repressive Chromatin through Different Mechanisms ». *Molecular Cell* 32 (4): 503-18. <https://doi.org/10.1016/j.molcel.2008.11.004>.

Marjoram, R.J., E.C. Lessey, et K. Burridge. 2014. « Regulation of RhoA Activity by Adhesion Molecules and Mechanotransduction ». *Current Molecular Medicine* 14 (2): 199-208. <https://doi.org/10.2174/1566524014666140128104541>.

Marshall, Owen J., et Andrea H. Brand. 2017. « Chromatin State Changes during Neural Development Revealed by in Vivo Cell-Type Specific Profiling ». *Nature Communications* 8 (1): 2271. <https://doi.org/10.1038/s41467-017-02385-4>.

Martel, Véronique, Claire Racaud-Sultan, Sandra Dupe, Christiane Marie, Frédérique Paulhe, Antoine Galmiche, Marc R. Block, et Corinne Albiges-Rizo. 2001. « Conformation, Localization, and Integrin Binding of Talin Depend on Its Interaction with Phosphoinositides ». *Journal of Biological Chemistry* 276 (24): 21217-27. <https://doi.org/10.1074/jbc.M102373200>.

Mauro, Alexander. 1961. « SATELLITE CELL OF SKELETAL MUSCLE FIBERS ». *The Journal of Biophysical and Biochemical Cytology* 9 (2): 493-95. <https://doi.org/10.1083/jcb.9.2.493>.

McBeath, Rowena, Dana M Pirone, Celeste M Nelson, Kiran Bhadriraju, et Christopher S Chen. 2004. « Cell Shape, Cytoskeletal Tension, and RhoA Regulate Stem Cell Lineage Commitment ». *Developmental Cell* 6 (4): 483-95. [https://doi.org/10.1016/S1534-5807\(04\)00075-9](https://doi.org/10.1016/S1534-5807(04)00075-9).

Meier, J., et S. D. Georgatos. 1994. « Type B Lamins Remain Associated with the Integral Nuclear Envelope Protein P58 during Mitosis: Implications for Nuclear Reassembly ». *The EMBO Journal* 13 (8): 1888-98. <https://doi.org/10.1002/j.1460-2075.1994.tb06458.x>.

Mermelstein, Cláudia S., Leonardo R. Andrade, Debora M. Portilho, et Manoel L. Costa. 2006. « Desmin Filaments Are Stably Associated with the Outer Nuclear Surface in Chick Myoblasts ». *Cell and Tissue Research* 323 (2): 351-57. <https://doi.org/10.1007/s00441-005-0063-6>.

Miyamoto, Tadashi, Chikara Furusawa, et Kunihiko Kaneko. 2015. « Pluripotency, Differentiation, and Reprogramming: A Gene Expression Dynamics Model with Epigenetic Feedback Regulation ». Édité par John C Marioni. *PLOS Computational Biology* 11 (8): e1004476. <https://doi.org/10.1371/journal.pcbi.1004476>.

Mofrad, kAAZEMPUR. 2004. « Force-induced Unfolding of the Focal Adhesion Targeting Domain and the Influence of Paxillin Binding ». *Tech Science Press*, 2004.

Moir, Robert D., Miri Yoon, Satya Khuon, et Robert D. Goldman. 2000. « Nuclear Lamins a and B1 ». *Journal of Cell Biology* 151 (6): 1155-68. <https://doi.org/10.1083/jcb.151.6.1155>.

Mouw, Janna K., Guanqing Ou, et Valerie M. Weaver. 2014. « Extracellular Matrix Assembly: A Multiscale Deconstruction ». *Nature Reviews Molecular Cell Biology* 15 (12): 771-85. <https://doi.org/10.1038/nrm3902>.

Mücke, N., R. Kirmse, T. Wedig, J.F. Leterrier, et L. Kreplak. 2005. « Investigation of the Morphology of Intermediate Filaments Adsorbed to Different Solid Supports ». *Journal of Structural Biology* 150 (3): 268-76. <https://doi.org/10.1016/j.jsb.2005.02.012>.

Mullins, R. Dyche, John A. Heuser, et Thomas D. Pollard. 1998. « The Interaction of Arp2/3 Complex with Actin: Nucleation, High Affinity Pointed End Capping, and Formation of Branching Networks of Filaments ». *Proceedings of the National Academy of Sciences* 95 (11): 6181-86. <https://doi.org/10.1073/pnas.95.11.6181>.

Musa, H., C. Orton, E. E. Morrison, et M. Peckham. 2003. « Microtubule Assembly in Cultured Myoblasts and Myotubes Following Nocodazole Induced Microtubule Depolymerisation ». *Journal of Muscle Research and Cell Motility* 24 (4-6): 301-8.

Musselman, Catherine A, Marie-Eve Lalonde, Jacques Côté, et Tatiana G Kutateladze. 2012. « Perceiving the Epigenetic Landscape through Histone Readers ». *Nature Structural & Molecular Biology* 19 (12): 1218-27. <https://doi.org/10.1038/nsmb.2436>.

Naetar, Nana, Simona Ferraioli, et Roland Foisner. 2017. « Lamins in the Nuclear Interior – Life Outside the Lamina ». *Journal of Cell Science* 130 (13): 2087-96. <https://doi.org/10.1242/jcs.203430>.

Nguyen, John H., Jin D. Chung, Gordon S. Lynch, et James G. Ryall. 2019. « The Microenvironment Is a Critical Regulator of Muscle Stem Cell Activation and Proliferation ». *Frontiers in Cell and Developmental Biology* 7 (octobre): 254. <https://doi.org/10.3389/fcell.2019.00254>.

Ojima, Koichi. 2019. « Myosin: Formation and Maintenance of Thick Filaments ». *Animal Science Journal* 90 (7): 801-7. <https://doi.org/10.1111/asj.13226>.

Olguin, Hugo C., Zhihong Yang, Stephen J. Tapscott, et Bradley B. Olwin. 2007. « Reciprocal Inhibition between Pax7 and Muscle Regulatory Factors Modulates Myogenic Cell Fate Determination ». *Journal of Cell Biology* 177 (5): 769-79. <https://doi.org/10.1083/jcb.200608122>.

Osmanagic-Myers, Selma, Thomas Dechat, et Roland Foisner. 2015. « Lamins at the Crossroads of Mechanosignaling ». *Genes & Development* 29 (3): 225-37. <https://doi.org/10.1101/gad.255968.114>.

Owens, Daniel J., Martina Fischer, Saline Jabre, Sophie Moog, Kamel Mamchaoui, Gillian Butler-Browne, et Catherine Coirault. 2020. « Lamin Mutations Cause Increased YAP Nuclear Entry in Muscle Stem Cells ». *Cells* 9 (4): 816. <https://doi.org/10.3390/cells9040816>.

Pajerowski, J. David, Kris Noel Dahl, Franklin L. Zhong, Paul J. Sannak, et Dennis E. Discher. 2007. « Physical Plasticity of the Nucleus in Stem Cell Differentiation ». *Proceedings of the National Academy of Sciences* 104 (40): 15619-24. <https://doi.org/10.1073/pnas.0702576104>.

Palacios, Daniela, Dennis Summerbell, Peter W. J. Rigby, et Joan Boyes. 2010. « Interplay between DNA Methylation and Transcription Factor Availability: Implications for Developmental Activation of the Mouse *Myogenin* Gene ». *Molecular and Cellular Biology* 30 (15): 3805-15. <https://doi.org/10.1128/MCB.00050-10>.

Pancier, Tito, Luca Azzolin, Michelangelo Cordenonsi, et Stefano Piccolo. 2017. « Mechanobiology of YAP and TAZ in Physiology and Disease ». *Nature Reviews Molecular Cell Biology* 18 (12): 758-70. <https://doi.org/10.1038/nrm.2017.87>.

Pardo, J V, J D Siliciano, et S W Craig. 1983. « A Vinculin-Containing Cortical Lattice in Skeletal Muscle: Transverse Lattice Elements (“costameres”) Mark Sites of Attachment between Myofibrils and Sarcolemma. » *Proceedings of the National Academy of Sciences* 80 (4): 1008-12. <https://doi.org/10.1073/pnas.80.4.1008>.

Parmar, Jyotsana J, et Ranjith Padinhateeri. 2020. « Nucleosome Positioning and Chromatin Organization ». *Current Opinion in Structural Biology* 64 (octobre): 111-18. <https://doi.org/10.1016/j.sbi.2020.06.021>.

Pascual-Reguant, Laura, Enrique Blanco, Silvia Galan, François Le Dily, Yasmina Cuartero, Gemma Serra-Bardenys, Valerio Di Carlo, et al. 2018. « Lamin B1 Mapping Reveals the Existence of Dynamic and Functional Euchromatin Lamin B1 Domains ». *Nature Communications* 9 (1): 3420. <https://doi.org/10.1038/s41467-018-05912-z>.

Pasini, Diego, Paul A. C. Cloos, Julian Walfridsson, Linda Olsson, John-Paul Bukowski, Jens V. Johansen, Mads Bak, Niels Tommerup, Juri Rappsilber, et Kristian Helin.

2010. « JARID2 Regulates Binding of the Polycomb Repressive Complex 2 to Target Genes in ES Cells ». *Nature* 464 (7286): 306-10. <https://doi.org/10.1038/nature08788>.

Patteson, Alison E., Amir Vahabikashi, Katarzyna Pogoda, Stephen A. Adam, Kalpana Mandal, Mark Kittisopikul, Suganya Sivagurunathan, Anne Goldman, Robert D. Goldman, et Paul A. Janmey. 2019. « Vimentin Protects Cells against Nuclear Rupture and DNA Damage during Migration ». *Journal of Cell Biology* 218 (12): 4079-92. <https://doi.org/10.1083/jcb.201902046>.

Paulin, D, et Z Li. 2004. « Desmin: A Major Intermediate Filament Protein Essential for the Structural Integrity and Function of Muscle ». *Experimental Cell Research* 301 (1): 1-7. <https://doi.org/10.1016/j.yexcr.2004.08.004>.

Paulin, Denise, Yeranuhi Hovhannisyan, Serdar Kasakyan, Onnik Agbulut, Zhenlin Li, et Zhigang Xue. 2020. « Synemin-Related Skeletal and Cardiac Myopathies: An Overview of Pathogenic Variants ». *American Journal of Physiology-Cell Physiology* 318 (4): C709-18. <https://doi.org/10.1152/ajpcell.00485.2019>.

Pearson education 2015, et Elaine Marieb. 2015. « Essentials of human anatomy and physiology ». In . <https://slideplayer.com/slide/13202814/>.

Pegoraro, Adrian F., Paul Janmey, et David A. Weitz. 2017. « Mechanical Properties of the Cytoskeleton and Cells ». *Cold Spring Harbor Perspectives in Biology* 9 (11): a022038. <https://doi.org/10.1101/cshperspect.a022038>.

Peng, Jamy C., Anton Valouev, Tomek Swigut, Junmei Zhang, Yingming Zhao, Arend Sidow, et Joanna Wysocka. 2009. « Jarid2/Jumonji Coordinates Control of PRC2 Enzymatic Activity and Target Gene Occupancy in Pluripotent Cells ». *Cell* 139 (7): 1290-1302. <https://doi.org/10.1016/j.cell.2009.12.002>.

Pindyurin, Alexey V., Artem A. Ilyin, Anton V. Ivankin, Mikhail V. Tselebrovsky, Valentina V. Nenasheva, Elena A. Mikhaleva, Ludo Pagie, Bas van Steensel, et Yuri Y. Shevelyov. 2018. « The Large Fraction of Heterochromatin in Drosophila Neurons Is Bound by Both B-Type Lamin and HP1a ». *Epigenetics & Chromatin* 11 (1): 65. <https://doi.org/10.1186/s13072-018-0235-8>.

Pizon, Véronique, Fabien Gerbal, Carmen Cifuentes Diaz, et Eric Karsenti. 2005. « Microtubule-dependent transport and organization of sarcomeric myosin during skeletal muscle differentiation ». *The EMBO Journal* 24 (21): 3781-92. <https://doi.org/10.1038/sj.emboj.7600842>.

Polioudaki, Hara, Niki Kourmouli, Victoria Drosou, Alexandra Bakou, Panayiotis A Theodoropoulos, Prim B Singh, Thomas Giannakouros, et Spyros D Georgatos. 2001.

« Histones H3/H4 Form a Tight Complex with the Inner Nuclear Membrane Protein LBR and Heterochromatin Protein 1 ». *EMBO Reports* 2 (10): 920-25. <https://doi.org/10.1093/embo-reports/kve199>.

Pollard, Thomas D. 2016. « Actin and Actin-Binding Proteins ». *Cold Spring Harbor Perspectives in Biology* 8 (8): a018226. <https://doi.org/10.1101/cshperspect.a018226>.

Prasanth, Kannanganattu V., Supriya G. Prasanth, Zhenyu Xuan, Stephen Hearn, Susan M. Freier, C. Frank Bennett, Michael Q. Zhang, et David L. Spector. 2005. « Regulating Gene Expression through RNA Nuclear Retention ». *Cell* 123 (2): 249-63. <https://doi.org/10.1016/j.cell.2005.08.033>.

Price, M. G. 1984. « Molecular Analysis of Intermediate Filament Cytoskeleton--a Putative Load-Bearing Structure ». *American Journal of Physiology-Heart and Circulatory Physiology* 246 (4): H566-72. <https://doi.org/10.1152/ajpheart.1984.246.4.H566>.

Przybyla, Laralynne, Johnathon N. Lakins, et Valerie M. Weaver. 2016. « Tissue Mechanics Orchestrate Wnt-Dependent Human Embryonic Stem Cell Differentiation ». *Cell Stem Cell* 19 (4): 462-75. <https://doi.org/10.1016/j.stem.2016.06.018>.

Rampalli, Shravanti, LiFang Li, Esther Mak, Kai Ge, Marjorie Brand, Stephen J Tapscott, et F Jeffrey Dilworth. 2007. « P38 MAPK Signaling Regulates Recruitment of Ash2L-Containing Methyltransferase Complexes to Specific Genes during Differentiation ». *Nature Structural & Molecular Biology* 14 (12): 1150-56. <https://doi.org/10.1038/nsmb1316>.

Randles, K. Natalie, Le Thanh Lam, Caroline A. Sewry, Megan Puckelwartz, Denis Furling, Manfred Wehnert, Elizabeth M. McNally, et Glenn E. Morris. 2010. « Nesprins, but Not Sun Proteins, Switch Isoforms at the Nuclear Envelope during Muscle Development ». *Developmental Dynamics* 239 (3): 998-1009. <https://doi.org/10.1002/dvdy.22229>.

Rao, Jyothsna, Dipanjan Bhattacharya, Bidisha Banerjee, Apurva Sarin, et G.V. Shivashankar. 2007. « Trichostatin-A Induces Differential Changes in Histone Protein Dynamics and Expression in HeLa Cells ». *Biochemical and Biophysical Research Communications* 363 (2): 263-68. <https://doi.org/10.1016/j.bbrc.2007.08.120>.

Reipert, S. 1999. « Association of Mitochondria with Plectin and Desmin Intermediate Filaments in Striated Muscle ». *Experimental Cell Research* 252 (2): 479-91. <https://doi.org/10.1006/excr.1999.4626>.

Relaix, Frédéric, Didier Rocancourt, Ahmed Mansouri, et Margaret Buckingham. 2005. « A Pax3/Pax7-Dependent Population of Skeletal Muscle Progenitor Cells ». *Nature* 435 (7044): 948-53. <https://doi.org/10.1038/nature03594>.

Rho, Jae-Young, Marcel E. Roy, Ting Y. Tsui, et George M. Pharr. 1999. « Elastic

Properties of Microstructural Components of Human Bone Tissue as Measured by Nanoindentation ». *Journal of Biomedical Materials Research* 45 (1): 48-54. [https://doi.org/10.1002/\(SICI\)1097-4636\(199904\)45:1<48::AID-JBM7>3.0.CO;2-5](https://doi.org/10.1002/(SICI)1097-4636(199904)45:1<48::AID-JBM7>3.0.CO;2-5).

Ridley, Anne J., et Alan Hall. 1992. « The Small GTP-Binding Protein Rho Regulates the Assembly of Focal Adhesions and Actin Stress Fibers in Response to Growth Factors ». *Cell* 70 (3): 389-99. [https://doi.org/10.1016/0092-8674\(92\)90163-7](https://doi.org/10.1016/0092-8674(92)90163-7).

Robelin, J. 1990. « Différenciation, croissance et développement cellulaire du tissu musculaire » 3 (4): 253_263.

Roman, William, João P. Martins, Filomena A. Carvalho, Raphael Voituriez, Jasmine V. G. Abella, Nuno C. Santos, Bruno Cadot, Michael Way, et Edgar R. Gomes. 2017. « Myofibril Contraction and Crosslinking Drive Nuclear Movement to the Periphery of Skeletal Muscle ». *Nature Cell Biology* 19 (10): 1189-1201. <https://doi.org/10.1038/ncb3605>.

Rybakova, Inna N., Jitandrakumar R. Patel, et James M. Ervasti. 2000. « The Dystrophin Complex Forms a Mechanically Strong Link between the Sarcolemma and Costameric Actin ». *Journal of Cell Biology* 150 (5): 1209-14. <https://doi.org/10.1083/jcb.150.5.1209>.

Sanger, Joseph W., Jushuo Wang, Yingli Fan, Jennifer White, Lei Mi-Mi, Dipak K. Dube, Jean M. Sanger, et David Pruyne. 2016. « Assembly and Maintenance of Myofibrils in Striated Muscle ». In *The Actin Cytoskeleton*, édité par Brigitte M. Jockusch, 235:39-75. Handbook of Experimental Pharmacology. Cham: Springer International Publishing. https://doi.org/10.1007/164_2016_53.

Schiaffino, S., et C. Reggiani. 1994. « Myosin Isoforms in Mammalian Skeletal Muscle ». *Journal of Applied Physiology* 77 (2): 493-501. <https://doi.org/10.1152/jappl.1994.77.2.493>.

Schübeler, Dirk. 2015. « Function and Information Content of DNA Methylation ». *Nature* 517 (7534): 321-26. <https://doi.org/10.1038/nature14192>.

Seetharaman, Shailaja, et Sandrine Etienne-Manneville. 2018. « Integrin Diversity Brings Specificity in Mechanotransduction: Integrin Diversity Brings Specificity in Mechanotransduction ». *Biology of the Cell* 110 (3): 49-64. <https://doi.org/10.1111/boc.201700060>.

Sejersen, T., et U. Lendahl. 1993. « Transient Expression of the Intermediate Filament Nestin during Skeletal Muscle Development ». *Journal of Cell Science* 106 (4): 1291-1300. <https://doi.org/10.1242/jcs.106.4.1291>.

Shimi, Takeshi, Mark Kittisopikul, Joseph Tran, Anne E. Goldman, Stephen A. Adam,

Yixian Zheng, Khuloud Jaqaman, et Robert D. Goldman. 2015. « Structural Organization of Nuclear Lamins A, C, B1, and B2 Revealed by Superresolution Microscopy ». Édité par Karsten Weis. *Molecular Biology of the Cell* 26 (22): 4075-86. <https://doi.org/10.1091/mbc.E15-07-0461>.

Shimi, Takeshi, Katrin Pflgebraar, Shin-ichiro Kojima, Chan-Gi Pack, Irina Solovei, Anne E. Goldman, Stephen A. Adam, et al. 2008. « The A- and B-Type Nuclear Lamin Networks: Microdomains Involved in Chromatin Organization and Transcription ». *Genes & Development* 22 (24): 3409-21. <https://doi.org/10.1101/gad.1735208>.

Shiu, Jau-Ye, Lina Aires, Zhe Lin, et Viola Vogel. 2018. « Nanopillar Force Measurements Reveal Actin-Cap-Mediated YAP Mechanotransduction ». *Nature Cell Biology* 20 (3): 262-71. <https://doi.org/10.1038/s41556-017-0030-y>.

Shvedunova, Maria, et Asifa Akhtar. 2022. « Modulation of Cellular Processes by Histone and Non-Histone Protein Acetylation ». *Nature Reviews Molecular Cell Biology* 23 (5): 329-49. <https://doi.org/10.1038/s41580-021-00441-y>.

Smoler, Mariano, Giovanna Coceano, Ilaria Testa, Luciana Bruno, et Valeria Levi. 2020. « Apparent Stiffness of Vimentin Intermediate Filaments in Living Cells and Its Relation with Other Cytoskeletal Polymers ». *Biochimica et Biophysica Acta (BBA) - Molecular Cell Research* 1867 (8): 118726. <https://doi.org/10.1016/j.bbamcr.2020.118726>.

Snider, Natasha T., et M. Bishr Omary. 2014. « Post-Translational Modifications of Intermediate Filament Proteins: Mechanisms and Functions ». *Nature Reviews Molecular Cell Biology* 15 (3): 163-77. <https://doi.org/10.1038/nrm3753>.

Song, Yuyu, et Scott T. Brady. 2015. « Post-Translational Modifications of Tubulin: Pathways to Functional Diversity of Microtubules ». *Trends in Cell Biology* 25 (3): 125-36. <https://doi.org/10.1016/j.tcb.2014.10.004>.

Starr, Daniel A., et Heidi N. Fridolfsson. 2010. « Interactions Between Nuclei and the Cytoskeleton Are Mediated by SUN-KASH Nuclear-Envelope Bridges ». *Annual Review of Cell and Developmental Biology* 26 (1): 421-44. <https://doi.org/10.1146/annurev-cellbio-100109-104037>.

Stephens, Andrew D., Edward J. Banigan, Stephen A. Adam, Robert D. Goldman, et John F. Marko. 2017. « Chromatin and Lamin A Determine Two Different Mechanical Response Regimes of the Cell Nucleus ». Édité par Dunn Alex R. *Molecular Biology of the Cell* 28 (14): 1984-96. <https://doi.org/10.1091/mbc.e16-09-0653>.

Stephens, Andrew D., Edward J. Banigan, et John F. Marko. 2018. « Separate Roles for Chromatin and Lamins in Nuclear Mechanics ». *Nucleus* 9 (1): 119-24.

<https://doi.org/10.1080/19491034.2017.1414118>.

Stewart, Martin P., Adrian W. Hodel, Andreas Spielhofer, Cedric J. Cattin, Daniel J. Müller, et Jonne Helenius. 2013. « Wedged AFM-Cantilevers for Parallel Plate Cell Mechanics ». *Methods (San Diego, Calif.)* 60 (2): 186-94. <https://doi.org/10.1016/j.ymeth.2013.02.015>.

Stuurman, Nico, Susanne Heins, et Ueli Aebi. 1998. « Nuclear Lamins: Their Structure, Assembly, and Interactions ». *Journal of Structural Biology* 122 (1-2): 42-66. <https://doi.org/10.1006/jsbi.1998.3987>.

Sun, Zhiqi, Shengzhen S. Guo, et Reinhard Fässler. 2016. « Integrin-Mediated Mechanotransduction ». *Journal of Cell Biology* 215 (4): 445-56. <https://doi.org/10.1083/jcb.201609037>.

Sutherland, Robert M. 1988. « Cell and Environment Interactions in Tumor Microregions: The Multicell Spheroid Model ». *Science* 240 (4849): 177-84. <https://doi.org/10.1126/science.2451290>.

Svitkina, Tatyana M., et Gary G. Borisy. 1999. « Arp2/3 Complex and Actin Depolymerizing Factor/Cofilin in Dendritic Organization and Treadmilling of Actin Filament Array in Lamellipodia ». *Journal of Cell Biology* 145 (5): 1009-26. <https://doi.org/10.1083/jcb.145.5.1009>.

Swift, Joe, Irena L. Ivanovska, Amnon Buxboim, Takamasa Harada, P. C. Dave P. Dingal, Joel Pinter, J. David Pajerowski, et al. 2013a. « Nuclear Lamin-A Scales with Tissue Stiffness and Enhances Matrix-Directed Differentiation ». *Science* 341 (6149): 1240104. <https://doi.org/10.1126/science.1240104>.

2013b. « Nuclear Lamin-A Scales with Tissue Stiffness and Enhances Matrix-Directed Differentiation ». *Science* 341 (6149): 1240104. <https://doi.org/10.1126/science.1240104>.

Sylvius, N, A Hathaway, E Boudreau, P Gupta, S Labib, P Bolongo, P Rippstein, H McBride, Z Bilinska, et F Tesson. 2008. « Specific Contribution of Lamin A and Lamin C in the Development of Laminopathies ». *Experimental Cell Research* 314 (13): 2362-75. <https://doi.org/10.1016/j.yexcr.2008.04.017>.

Tajik, Arash, Yuejin Zhang, Fuxiang Wei, Jian Sun, Qiong Jia, Wenwen Zhou, Rishi Singh, Nimish Khanna, Andrew S. Belmont, et Ning Wang. 2016. « Transcription Upregulation via Force-Induced Direct Stretching of Chromatin ». *Nature Materials* 15 (12): 1287-96. <https://doi.org/10.1038/nmat4729>.

Tatli, Meltem, et Ohad Medalia. 2018. « Insight into the Functional Organization of Nuclear Lamins in Health and Disease ». *Current Opinion in Cell Biology* 54 (octobre): 72-79.

<https://doi.org/10.1016/j.ceb.2018.05.001>.

Tojkander, Sari, Gergana Gateva, et Pekka Lappalainen. 2012. « Actin Stress Fibers – Assembly, Dynamics and Biological Roles ». *Journal of Cell Science*, janvier, jcs.098087. <https://doi.org/10.1242/jcs.098087>.

Tolstonog, Genrich V., Michael Sabasch, et Peter Traub. 2002. « Cytoplasmic Intermediate Filaments Are Stably Associated with Nuclear Matrices and Potentially Modulate Their DNA-Binding Function ». *DNA and Cell Biology* 21 (3): 213-39. <https://doi.org/10.1089/10445490252925459>.

Tsukada, Yu-ichi, Jia Fang, Hediye Erdjument-Bromage, Maria E. Warren, Christoph H. Borchers, Paul Tempst, et Yi Zhang. 2006. « Histone Demethylation by a Family of JmjC Domain-Containing Proteins ». *Nature* 439 (7078): 811-16. <https://doi.org/10.1038/nature04433>.

Turgay, Yagmur, Lysie Champion, Csaba Balazs, Michael Held, Alberto Toso, Daniel W. Gerlich, Patrick Meraldi, et Ulrike Kutay. 2014. « SUN Proteins Facilitate the Removal of Membranes from Chromatin during Nuclear Envelope Breakdown ». *Journal of Cell Biology* 204 (7): 1099-1109. <https://doi.org/10.1083/jcb.201310116>.

Turgay, Yagmur, Matthias Eibauer, Anne E. Goldman, Takeshi Shimi, Maayan Khayat, Kfir Ben-Harush, Anna Dubrovsky-Gaup, K. Tanuj Sapra, Robert D. Goldman, et Ohad Medalia. 2017. « The Molecular Architecture of Lamins in Somatic Cells ». *Nature* 543 (7644): 261-64. <https://doi.org/10.1038/nature21382>.

Uhler, Caroline, et G. V. Shivashankar. 2017. « Regulation of Genome Organization and Gene Expression by Nuclear Mechanotransduction ». *Nature Reviews Molecular Cell Biology* 18 (12): 717-27. <https://doi.org/10.1038/nrm.2017.101>.

Upton, John-Paul, Likun Wang, Dan Han, Eric S. Wang, Noelle E. Huskey, Lionel Lim, Morgan Truitt, et al. 2012. « IRE1 α Cleaves Select MicroRNAs During ER Stress to Derepress Translation of Proapoptotic Caspase-2 ». *Science* 338 (6108): 818-22. <https://doi.org/10.1126/science.1226191>.

Vastenhouw, Nadine L, et Alexander F Schier. 2012. « Bivalent Histone Modifications in Early Embryogenesis ». *Current Opinion in Cell Biology* 24 (3): 374-86. <https://doi.org/10.1016/j.ceb.2012.03.009>.

Verrier, Laure, Marie Vandromme, et Didier Trouche. 2011. « Histone Demethylases in Chromatin Cross-Talks ». *Biology of the Cell* 103 (8): 381-401. <https://doi.org/10.1042/BC20110028>.

Vining, Kyle H., et David J. Mooney. 2017. « Mechanical Forces Direct Stem Cell

Behaviour in Development and Regeneration ». *Nature Reviews Molecular Cell Biology* 18 (12): 728-42. <https://doi.org/10.1038/nrm.2017.108>.

Wagner, Oliver I., Sebastian Rammensee, Neha Korde, Qi Wen, Jean-Francois Leterrier, et Paul A. Janmey. 2007. « Softness, Strength and Self-Repair in Intermediate Filament Networks ». *Experimental Cell Research* 313 (10): 2228-35. <https://doi.org/10.1016/j.yexcr.2007.04.025>.

Wang, Jingqiang, et Cory Abate-Shen. 2012. « The Msx1 Homeoprotein Recruits G9a Methyltransferase to Repressed Target Genes in Myoblast Cells ». Édité par Charalampos Babis Spilianakis. *PLoS ONE* 7 (5): e37647. <https://doi.org/10.1371/journal.pone.0037647>.

Wang, Weiyi, Ting Shen, Raphael Guerois, Fuming Zhang, Hureshitanmu Kuerban, Yuncong Lv, Benoît Gigant, Marcel Knossow, et Chunguang Wang. 2015. « New Insights into the Coupling between Microtubule Depolymerization and ATP Hydrolysis by Kinesin-13 Protein Kif2C ». *Journal of Biological Chemistry* 290 (30): 18721-31. <https://doi.org/10.1074/jbc.M115.646919>.

Webster, Micah, Keren L. Witkin, et Orna Cohen-Fix. 2009. « Sizing up the Nucleus: Nuclear Shape, Size and Nuclear-Envelope Assembly ». *Journal of Cell Science* 122 (10): 1477-86. <https://doi.org/10.1242/jcs.037333>.

« White, Jennifer, Marietta V. Barro, Helen P. Makarenkova, Joseph W. Sanger, et Jean M. Sanger. 2014. « Localization of Sarcomeric Proteins during Myofibril Assembly in Cultured Mouse Primary Skeletal Myotubes ». *Anatomical Record* ». s. d.

Wilhelmsen, Kevin, Sandy H.M. Litjens, Ingrid Kuikman, Ntambua Tshimbalanga, Hans Janssen, Iman van den Bout, Karine Raymond, et Arnoud Sonnenberg. 2005. « Nesprin-3, a Novel Outer Nuclear Membrane Protein, Associates with the Cytoskeletal Linker Protein Plectin ». *Journal of Cell Biology* 171 (5): 799-810. <https://doi.org/10.1083/jcb.200506083>.

Wilson, K. L., et R. Foisner. 2010. « Lamin-Binding Proteins ». *Cold Spring Harbor Perspectives in Biology* 2 (4): a000554-a000554. <https://doi.org/10.1101/cshperspect.a000554>.

Wilson, Meredith H., et Erika L. F. Holzbaur. 2015. « Nesprins Anchor Kinesin-1 Motors to the Nucleus to Drive Nuclear Distribution in Muscle Cells ». *Development* 142 (1): 218-28. <https://doi.org/10.1242/dev.114769>.

Winter, Daniel L., Denise Paulin, Mathias Mericskay, et Zhenlin Li. 2014. « Posttranslational Modifications of Desmin and Their Implication in Biological Processes and Pathologies ». *Histochemistry and Cell Biology* 141 (1): 1-16. <https://doi.org/10.1007/s00418-013-1148-z>.

Wong, Xianrong, Ashley J. Melendez-Perez, et Karen L. Reddy. 2022. « The Nuclear

Lamina ». *Cold Spring Harbor Perspectives in Biology* 14 (2): a040113. <https://doi.org/10.1101/cshperspect.a040113>.

Worman, Howard J. 2012. « Nuclear Lamins and Laminopathies ». *The Journal of Pathology* 226 (2): 316-25. <https://doi.org/10.1002/path.2999>.

Wydner, Karen L., John A. McNeil, Feng Lin, Howard J. Worman, et Jeanne B. Lawrence. 1996. « Chromosomal Assignment of Human Nuclear Envelope Protein Genes LMNA, LMNB1, and LBR by Fluorescence in Situ Hybridization ». *Genomics* 32 (3): 474-78. <https://doi.org/10.1006/geno.1996.0146>.

Yan, Feng, David R. Powell, David J. Curtis, et Nicholas C. Wong. 2020. « From Reads to Insight: A Hitchhiker's Guide to ATAC-Seq Data Analysis ». *Genome Biology* 21 (1): 22. <https://doi.org/10.1186/s13059-020-1929-3>.

Yeh, Chung-Hsin, Pao-Lin Kuo, Ya-Yun Wang, Ying-Yu Wu, Mei-Feng Chen, Ding-Yen Lin, Tsung-Hsuan Lai, Han-Sun Chiang, et Ying-Hung Lin. 2015. « SEPT12/SPAG4/LAMINB1 Complexes Are Required for Maintaining the Integrity of the Nuclear Envelope in Postmeiotic Male Germ Cells ». Édité par Joël R Drevet. *PLOS ONE* 10 (3): e0120722. <https://doi.org/10.1371/journal.pone.0120722>.

Yi, Jinseong, Susanne Kloeker, Christopher C. Jensen, Susanne Bockholt, Hiroaki Honda, Hisamura Hirai, et Mary C. Beckerle. 2002. « Members of the Zyxin Family of LIM Proteins Interact with Members of the P130Cas Family of Signal Transducers ». *Journal of Biological Chemistry* 277 (11): 9580-89. <https://doi.org/10.1074/jbc.M106922200>.

Yu, Guangchuang, Li-Gen Wang, Yanyan Han, et Qing-Yu He. 2012. « ClusterProfiler: An R Package for Comparing Biological Themes Among Gene Clusters ». *OMICS: A Journal of Integrative Biology* 16 (5): 284-87. <https://doi.org/10.1089/omi.2011.0118>.

Zhang, Qiuping, Jeremy N. Skepper, Fangtang Yang, John D. Davies, Laszlo Hegyi, Roland G. Roberts, Peter L. Weissberg, Juliet A. Ellis, et Catherine M. Shanahan. 2001. « Nesprins: A Novel Family of Spectrin-Repeat-Containing Proteins That Localize to the Nuclear Membrane in Multiple Tissues ». *Journal of Cell Science* 114 (24): 4485-98. <https://doi.org/10.1242/jcs.114.24.4485>.

Zhang, Yong, Tao Liu, Clifford A Meyer, Jérôme Eeckhoute, David S Johnson, Bradley E Bernstein, Chad Nusbaum, et al. 2008. « Model-Based Analysis of ChIP-Seq (MACS) ». *Genome Biology* 9 (9): R137. <https://doi.org/10.1186/gb-2008-9-9-r137>.

Zhang, Yu-Qian, et Kevin D. Sarge. 2008. « Sumoylation Regulates Lamin A Function and Is Lost in Lamin A Mutants Associated with Familial Cardiomyopathies ». *Journal of Cell Biology* 182 (1): 35-39. <https://doi.org/10.1083/jcb.200712124>.

Abbreviations

ATP: Adenosine triphosphate
MHC: Myosin heavy chains
MLC: Myosin light chains
ELC: Essential light chains
RLC: Regulatory light chains
Myf5: Myogenic factor 5
MyoD: Myogenic Differentiation 1
MyoG: Myogenin
Mef2: Myocyte enhancer factor-2
ECM: Extracellular matrix
MMPs : Matrix metalloproteinases
PTMs: post-translational modifications
MCPs: Components of the perinuclear actin network in muscle cell precursors
TAN: Transmembrane actin-associated nuclear lines.
MT: Microtubules
MAPs: Microtubules-associated proteins
IF: Cytoplasmic intermediate filaments
ULFs: Unit length filaments
LINC: Linker of Nucleoskeleton and Cytoskeleton
NE: The nuclear envelope
INM: Inner nuclear membrane
ONM: Outer nuclear membrane
NPCs: Nuclear pore complexes
Nups: Nucleoporins
KASH: Klarsicht-ANC1-Syne homology
SUN: Sad1 and Unc-84
LRMP: Lymphoid-restricted membrane protein
NETs: Nuclear envelop transmembrane proteins
LAPs: lamin-associated proteins
NLS: nuclear localization signal
PTMs: posttranslational modifications

CDK1: cyclin-dependent kinase 1
NLS: nuclear localization signal
cryo-ET: Cryo-electron tomography
FACE1: zinc metalloendoprotease Zmpste24
SUMO: small ubiquitin-like modifier
GlcNAc: β -N-acetylglucosamine
OGT: O-GlcNAc transferase
BAF: Barrier to autointegration factor
LAP2: Lamin-associated polypeptide 2
HP1: Heterochromatin protein 1
PRR14: Proline-rich protein 14
LADs: Lamin Associated domain
PTMs: Posttranslational modifications
TADs: Topologically associated domains
CTCF: CCCTC-binding factor
H3K9me2: H3 lysine 9 dimethylation
H3K9me3: H3 lysine 9 trimethylation
H3K4me3: H3 lysine 4 trimethylation
H3K27me3: H3 lysine 27 trimethylation
dsDNA: Double-stranded DNA
HATs: Histone acetyltransferases
HDACs: Histone deacetylases
acetyl-CoA: Acetyl co-enzyme A
PcG: Polycomb group
PRC2: polycomb repressor complex 2
YAP: Yes-associated Protein
AMOT: Angiomotin
NF2: Neurofibromin 2
miR-29: microRNA
NET: Nuclear envelope transmembrane
EDMD: Emery-Dreifuss muscular dystrophy
LGMD1B: Limb-Girdle dystrophy type 1B
AD-SMA: Autosomal dominant spinal muscular dystrophy
L-CMD: Lamin-related congenital muscular dystrophy

CMDA: Dilated cardiomyopathy

TSA: Trichostatin-A

hTERT: Telomerase- expressing

CDK4: Cyclin dependent kinase 4-expressing vectors

DZNep: 3-Dezaneplanocin A

siRNA: Small-interfering ribonucleic acid

Résumé en français

La réponse du noyau aux contraintes mécaniques impliquent les lamines de type A mais aussi la chromatine et les modifications post-traductionnelles des histones. Cette réponse est essentielle à l'adaptation des cellules aux contraintes mécaniques, notamment dans les tissus soumis à des contraintes mécaniques importantes comme le muscle squelettique. Cependant les mécanismes impliqués restent mal connus.

Le premier objectif de ma thèse était de déterminer l'impact de la différenciation musculaire sur les caractéristiques nucléaires de cellules musculaires. Les objectifs suivants étaient d'analyser l'effet de l'expression des protéines de l'enveloppe nucléaire (lamines A/C, SUN1 et SUN2) et de la compaction de la chromatine sur la réponse nucléaire aux contraintes mécaniques. J'ai caractérisé la forme nucléaire et des marqueurs d'histone dans des cellules précurseurs musculaires (MuSC) immortalisées obtenus chez des patients sains et dans des myotubes (72h de différenciation). Les marqueurs d'histones suivants ont été analysés : 1-La tri-méthylation de la lysine4 de l'histone H3 (H3K4me3) et l'acétylation de H3K4 (H3K4ac), associés aux gènes activement transcrits 2- H3K27me3, un marqueur de l'hétérochromatine facultative, régulé par le développement 3- et H3K9me3, un marqueur de l'hétérochromatine constitutive. La différenciation en myotubes est associée à une élongation et à une réduction significative du volume nucléaire. De plus, l'intensité du marquage nucléaire H3K27me3 est significativement plus faible dans les myotubes par rapport aux MuSC alors que les intensités nucléaires H3K9me3 et H3K4me3 sont plus élevées. Ces résultats sont compatibles avec les modifications attendues de l'accessibilité de la machinerie transcriptionnelle avec la différenciation myogénique.

Dans les myotubes, la déficience en lamines A/C entraîne une déformation nucléaire qui est majorée par le stretch mécanique (étirement cyclique de 10%, 4h) Le stretch est associé à une

augmentation significative du volume nucléaire dans les myotubes témoins, qui est abolie dans les myotubes déficients en lamines A/C. Dans les myotubes témoins, le stretch augmente l'intensité du marquage H3K27me3 et réduit l'intensité du marquage H3K4me3 et H3K4ac. Dans les myotubes déficients en lamines A/C, l'intensité des marqueurs actifs de la chromatine est plus élevée en conditions statiques et stretch s'accompagne d'une augmentation paradoxale de H3K4me3 après. L'inhibition spécifique des histones désacétylases de classe I et II par la trichostatine A induit également une augmentation de H3K4ac en conditions statique et après stretch par rapport au myotubes témoins. A l'inverse, dans les myotubes déficients en SUN2 ou SUN1, l'étirement réduit l'intensité de H3K4me3, alors que l'augmentation de l'intensité nucléaire de H3K27me3 est abolie dans les myotubes déficients en SUN2 étirés. Par ailleurs, la déficience en lamines A/C s'accompagne d'une dérégulation majeure des gènes régulant les marqueurs d'histone.

Dans l'ensemble, notre étude met en évidence des modifications importantes des marqueurs post-traductionnels des histones au cours de la différenciation musculaire et lors d'un stress mécanique. Les lamines de type A semblent cruciales pour prévenir l'activation anormale des marqueurs actifs de la chromatine dans les myotubes soumis à un défi mécanique. Nos résultats suggèrent que la mécano-réponse chromatinienne est étroitement régulée par les protéines de l'enveloppe nucléaire dans le muscle squelettique.

Abstract in english

The lamina, and specifically A-type lamins, are major contributors to nuclear stiffness and deformations. However, chromatin and its histone modification states also contribute to nuclear mechanics independently of A-type lamins. How A-type lamins and chromatin-mediated mechanoresponse contribute to mechanical load-mediated adaptation in normal and pathological skeletal muscle remains unknown.

We sought to determine how muscle differentiation impacts nuclear characteristics in muscle cell precursors (MuSCs) and myotubes. Then, we investigated the respective roles of nuclear envelope proteins (lamin A/C, SUN1 and SUN2) and drug-modulated chromatin compaction on the mechanical load-mediated nuclear response in myonuclei.

We used immortalized MuSCs obtained from healthy patients and analyzed nuclear shape and chromatin characteristics in MuSCs and myotubes obtained after 72h of differentiation. Histone

modifications were analyzed: a) histone H3 lysine4 tri-methylation (H3K4me3) and H3K4 acetylation (H3K4ac), associated with transcriptionally active genes, b) H3K27 tri-methylation (H3K27me3), a chromatin repression marker, associated with facultative heterochromatin and c) H3K9 tri-methylation (H3K9me3), a chromatin repression marker associated with constitutive heterochromatin and mainly located at the nuclear periphery. Myotube differentiation was associated with nuclear elongation and significant reduction in nuclear volume. In addition, the relative intensity of nuclear H3K27me3 (chromatin repression marker) labelling was significantly lower in myotubes compared to MuSCs, whereas nuclear H3K9me3 and H3K4me3 (chromatin active marker) intensities were higher in myotubes compared to MuSCs, thereby showing that myogenic differentiation is modulating the accessibility of the transcriptional machinery.

Myotubes were silenced for LMNA expression with silencing mRNA strategies and submitted to a cyclic stretch (10%,4hours) to investigate A-type lamin' roles in nuclear shape and chromatin organization during mechanical stress. A-type lamin deficient myotubes had abnormal nuclear shape in static conditions and nuclear deformations further increased after cyclic stretch. Cyclic stretch was associated with a significant increase in nuclear volume in control myotubes that was abolished in A-type lamin deficient myotubes. In addition, stretching increased the intensity of the H3K27me3 and reduced H3K4me3 and H3K4ac intensities of labelling in nuclei from control myotubes. Importantly, A-type lamin deficiency was associated with higher intensity in chromatin active markers at baseline and a paradoxical increase in H3K4me3 after stretch. Consistent modifications in histone modifications were obtained by western-blot in control and A-type deficient myotubes. Interestingly, stretch reduced H3K4me3 intensity both in SUN2 or SUN1-deficient myotubes while the increase in the nuclear intensity of the H3K27me3 was abolished in stretched SUN2-deficient myotubes. Transcriptomic changes associated with A-type lamin deficiency support these results.

Trichostatin A (TSA) is a powerful and specific Class I and II histone deacetylase inhibitor (HDACi), widely used to increase the expression of genes silenced by chromatin condensation, thereby favoring chromatin decompaction. TSA increased nuclear volume without affecting nuclear shape both in static and stretched conditions. In addition, TSA decreased H3K27me3 and H3K9me3 intensities in static myotubes but did not prevent the stretch-induced increase in H3K27me3 intensity.


Overall, our study highlights crucial changes of histone post-translational markers during muscle differentiation and upon mechanical challenge. A-type lamins appear crucial to prevent

abnormal activation of chromatin active markers in mechanically challenged myotubes. Moreover, our results suggest that the nuclear mechano-response is tightly regulated by nuclear envelope proteins in skeletal muscle.

Publications

Review

Nuclear Mechanotransduction in Skeletal Muscle

Saline Jabre^{1,2}, Walid Hleihel^{2,3} and Catherine Coirault^{1,*} 

¹ Sorbonne Université, INSERM UMRS-974 and Institut de Myologie, 75013 Paris, France; saline.jabr@net.usek.edu.lb

² Department of Biology, Faculty of Arts and Sciences, Holy Spirit University of Kasik (USEK), Jounieh 446, Lebanon; walidhleihel@usek.edu.lb

³ Department of Basic Health Sciences, Faculty of Medicine, Holy Spirit University of Kaslik (USEK), Jounieh 446, Lebanon

* Correspondence: catherine.coirault@inserm.fr

Abstract: Skeletal muscle is composed of multinucleated, mature muscle cells (myofibers) responsible for contraction, and a resident pool of mononucleated muscle cell precursors (MCPs), that are maintained in a quiescent state in homeostatic conditions. Skeletal muscle is remarkable in its ability to adapt to mechanical constraints, a property referred as muscle plasticity and mediated by both MCPs and myofibers. An emerging body of literature supports the notion that muscle plasticity is critically dependent upon nuclear mechanotransduction, which is transduction of exterior physical forces into the nucleus to generate a biological response. Mechanical loading induces nuclear deformation, changes in the nuclear lamina organization, chromatin condensation state, and cell signaling, which ultimately impacts myogenic cell fate decisions. This review summarizes contemporary insights into the mechanisms underlying nuclear force transmission in MCPs and myofibers. We discuss how the cytoskeleton and nuclear reorganizations during myogenic differentiation may affect force transmission and nuclear mechanotransduction. We also discuss how to apply these findings in the context of muscular disorders. Finally, we highlight current gaps in knowledge and opportunities for further research in the field.

Keywords: mechanotransduction; muscle disorders; nucleus; nucleo-cytoplasmic coupling; mechanics



Citation: Jabre, S.; Hleihel, W.; Coirault, C. Nuclear Mechanotransduction in Skeletal Muscle. *Cells* **2021**, *10*, 318. <https://doi.org/10.3390/10020318>

Academic Editor: Rudolf Leube
Received: 8 December 2020
Accepted: 1 February 2021
Published: 4 February 2021

Publisher's Note: MDPI stays neutral with regard to jurisdictional claims in published maps and institutional affiliations.



Copyright: © 2021 by the authors. Licensee MDPI, Basel, Switzerland. This article is an open access article distributed under the terms and conditions of the Creative Commons Attribution (CC BY) license (<https://creativecommons.org/licenses/by/4.0/>).

1. Introduction

Skeletal muscle is a highly organized tissue designed to produce force and movement. It is composed of differentiated, multinucleated and aligned myofibers responsible for contraction, and also contains a population of mononucleated muscle cell precursors (MCPs), that are maintained in a quiescent state under homeostatic conditions. Fusion of tens of thousands of differentiated MCPs (myocytes) produces multinucleated myotubes which mature into myofibers, composed of a regular array of contractile elements, the sarcomere [1]. Skeletal muscle is remarkable in its ability to adapt in response to the demands imposed on it, a property referred to as muscle plasticity. Low physical activity and some disease conditions lead to the reduction in myofiber size, called atrophy, whereas hypertrophy refers to the increase in myofiber size induced by high physical activity or intrinsic factors such as anabolic hormones/drugs. Molecular mechanisms that regulate changes in skeletal muscle mass in response to mechanical load have been detailed [2–5]. In post-mitotic muscle cells, mechanical loading impacts translational events, thereby regulating the rate of protein synthesis leading to changes in myofibrillar protein content [2]. In addition, mechanical loading triggers changes in the cell cycle rate [6,7] and MCP proliferation [5]. The fusion of MCPs to the growing fiber allows the addition of new myonuclei, which are likely to contribute to sustained and harmonious muscle growth [8]. Finally, the nucleus triggers diverse cell responses in response to nuclear envelope deformation: nuclear accumulation of the transcription factors yes-associated protein (YAP)/transcriptional co-activator with PDZ-binding motif (TAZ) [6,9,10], activation

of the ataxia telangiectasia and Rad3-related protein kinase [11,12], calcium release [13], activation of the calcium-dependent cytosolic phospholipase A2 [14] and rupture of the nuclear envelope (NE) associated with DNA damage [15,16].

The nucleus is generally the stiffest element of all eukaryotic cells [17]. In addition to being the site for storage of genetic material and gene transcription, the nucleus plays crucial roles in mechanotransduction, which is the transduction of exterior physical forces to generate a biological response [18]. Nuclear mechanotransduction is likely to play important roles in skeletal muscle physiology and adaptation. Force transmission from the cell periphery to the nucleus involves the cytoskeleton, the LINC complex (Linker of Nucleoskeleton and Cytoskeleton) and the proteins associated with the NE, including emerin and lamins. Mechanical force induces changes in nuclear lamina polymerization and chromatin condensation state, thereby regulating translational capacity and efficiency, nuclear elasticity, and deformability [2,19–23] and in turn, the cell response to mechanical stress.

Nuclear mechanotransduction is essential to help the muscle to adapt in response to changes in physical activity [4,24] or in mechanical stimuli arising from the surrounding extracellular matrix or from neighboring cells [25]. Numerous studies have gained insights into the molecular mechanisms associated with muscle mechanotransduction and their role in skeletal muscle growth [26–31]. The role of the cytoskeleton in regulating nuclear shape via interaction with the NE has been detailed in different cell types including muscle cells [32–34]. Interestingly, cytoskeleton and nuclear architectures are dynamically regulated. They respond to the mechanical environment and differ according to the myogenic state [34]. In addition, signaling molecules and transcription factors such as YAP, TAZ, and serum responsive factor have emerged as important signaling pathways to relay mechanical signals and regulate dynamics of cytoskeleton, gene expression, and in turn myogenic development of striated muscle [28,31,35–38]. Importantly, because intracellular structures and signaling pathways are developmentally regulated, the myogenic process is likely to modulate in turn the nuclear mechanotransduction, thus differentially modulating the force response on MCPs, myotubes and terminally differentiated myofibers. Finally, direct or indirect mechanisms responsible for defective cytoskeleton and nuclear architectures are likely to impact the nuclear response and contribute to muscle dysfunction in muscle diseases.

In this review, the cellular and molecular mechanisms regulating nuclear mechanotransduction in skeletal muscle are updated, and findings regarding nuclear force transmission and nuclear response to mechanical forces in MCPs and multinucleated myofibers are summarized. Based on data from diverse cell types including myogenic cells, we will focus on how myogenic differentiation can affect force transmission to the nucleus. Finally, we will discuss how to apply these findings in the context of muscular disorders.

2. Cytoskeletal Components Relevant for Force Transmission to the Nucleus

The cytoskeletal components relevant for force transmission to the nucleus include actin filaments (F-actin), microtubules (MTs) and intermediate filaments (IFs), whose structural and functional organization, including assembly sites, dynamics, turnover and integration with other cell components, determine function [39–41]. The perinuclear cytoskeleton provides a structural network to transmit and focus pushing or pulling forces onto the nucleus [40,42] through specialized proteins that comprise the LINC complex [43–45]. The amount and organization of the cytoskeletal and LINC components are tissue-specific and developmentally regulated (see below).

Major reorganization of the cytoskeleton network occurs during the process of muscle differentiation (Figure 1), with functional consequences on force transmission to the nuclear envelope and thus on the nuclear response. Although force transmission to the nucleus is crucial for MCP fate, a major contribution of the distribution of the cytoskeleton in mature striated muscle fibers could be to transmit force to the extracellular matrix (ECM) while protecting myonuclei from the axial contractile force generated by the contractile apparatus.

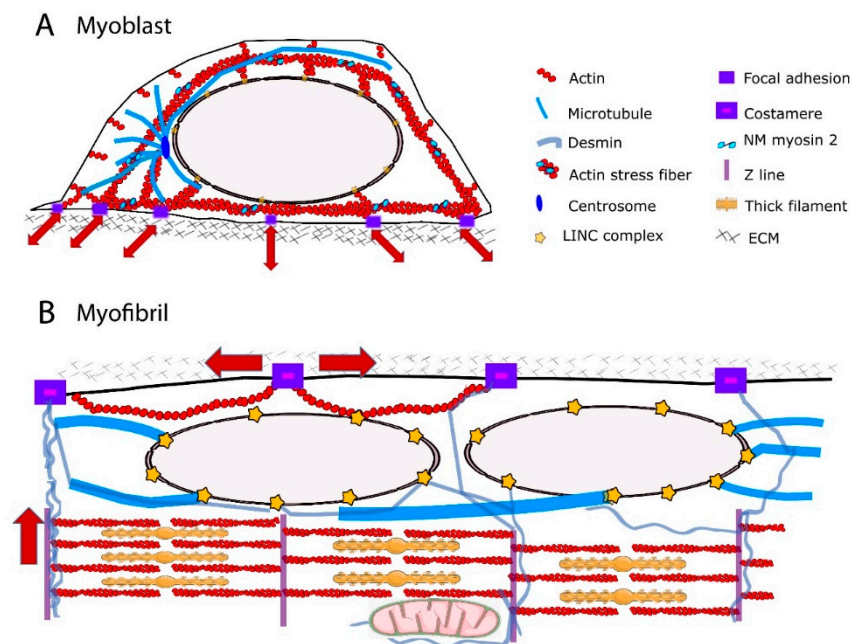


Figure 1. Schematic representation of cytoskeleton and force transmission in the myoblast and myofibril. **(A)** Radial distribution of the actin, microtubule and intermediate filament (IF) networks in myoblast favors the transmission of extra- and intra-cellular forces (red arrows) to the nucleus. Direct connections between focal adhesions and the actin cytoskeleton transmit the force along actin fibers towards the nucleus. Reciprocally, intracellular forces can be transmitted from the cell interior to the extracellular matrix (ECM). Perinuclear cytoskeleton is tethered to the nucleus via Linker of Nucleoskeleton and Cytoskeleton (LINC) complex. **(B)** Paraxial arrays of F-actin, microtubules and IFs in myofibrils. Main directions of force transmission from the contractile apparatus to the ECM are indicated (red arrows). In skeletal muscle, contractile force can be transmitted laterally between the z-disks of neighboring myofibrils to the ECM through specific cell–matrix adhesions called costameres.

2.1. The Perinuclear Actin Network and Muscle Differentiation

In different cell types, perinuclear actin emerges as a critical component for proper nucleo-cytoskeletal connections [39,40,46]. On the dorsal side of the nucleus of cells grown in 2D culture, perinuclear actin comprises the actin cap formed by dorsal stress fibers [47] (Figure 2A) and the so-called transmembrane actin-associated nuclear (TAN) lines [48] (Figure 2B,C). The actin cap is composed of thick parallel and highly contractile acto-myosin filaments, tightly connected to the nucleus, and attached to basal focal adhesion sites on both extremities [47,49–51]. The perinuclear actin cap accumulates upon mechanical stimulation [49,50] and has important roles in nuclear mechanotransduction [50,52].

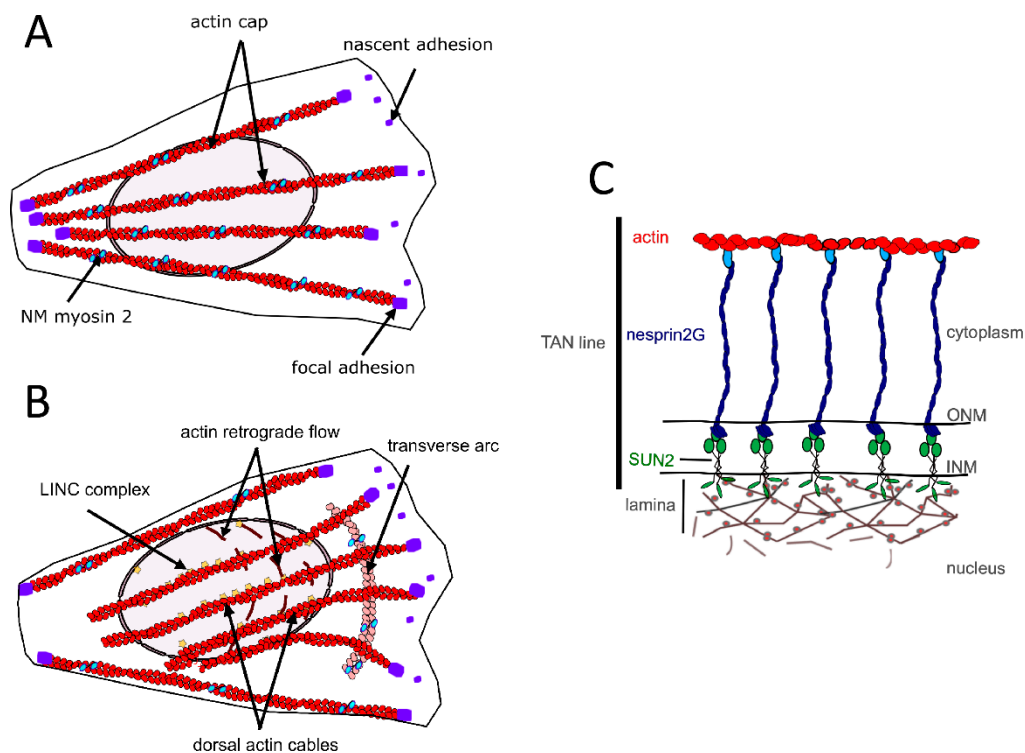


Figure 2. Components of the perinuclear actin network in muscle cell precursors (MCPs). **(A)** Actin cap formed by dorsal stress fibers. **(B)** transmembrane actin-associated nuclear (TAN) lines. **(C)** Illustration of the molecular composition of a TAN line.

The actin cap is developmentally regulated, being present in myoblasts but absent in undifferentiated embryonic stem cells [53] and terminally differentiated muscle cells [27]. The structural and functional organization of actin cytoskeleton in the perinuclear region of myotubes remain partly unknown. During skeletal myofiber formation, nuclei are initially in the center of the myofiber and then move towards to myofiber periphery [54]. It has been shown that amphiphysin-2/BIN1, which is mutated in centronuclear myopathies, triggers peripheral nuclear positioning to the periphery of myofibers via N-WASP and actin, thus implicating the actin cytoskeleton in nuclear movement [55]. In addition, perinuclear actin may significantly alter the nuclear shape [27]. However, nuclear positioning to the myofiber periphery is mediated by centripetal forces arising from myofibril contraction around the nucleus [27]. Furthermore, it has been proposed that a nucleus–cytoskeleton connection is not required for peripheral nuclear movement [27]. Future work should address how structural and functional connections between perinuclear actin network and nuclei are modified during skeletal myofiber formation. In addition to extensive cytoskeletal reorganization, shifts in expression of actin components from non-muscle to muscle isoforms occur during skeletal myogenesis [56–58]. The muscle-specific isoform α -actin becomes the predominant actin in terminally differentiated myofibers and localizes to the sarcomeric thin filaments, where it interacts with myosin to produce a contractile force [59,60]. The non-muscle actins γ and β that are present around the nucleus in myoblasts [61] are downregulated during terminal differentiation of myoblasts into myotubes. In terminally differentiated myofibers, γ - and β -actins reside in the cortical cytoskeleton and at costameres [62–65]. The costameric F-actin network is thought to contribute with other proteins to the radial transmission of contractile force outward from the sarcomere to the extracellular matrix, adjacent muscle fibers, and beyond [64]. Therefore, non-muscle F-actin could serve opposite force transmission direction according to the state of myogenic differentiation. The direction could be predominantly external to internal, toward NE in

myoblasts, but predominantly internal and sarcomeric to external, toward extracellular matrix, in myofibers (Figure 1).

2.2. The MTs

MTs are three orders of magnitude stiffer than actin, IFs being the softness among the three major types of cytoskeleton filaments [65]. Their radial, centrosome-dominated distribution in myoblasts [66,67] may favor the transmission of external mechanical forces to the NE and influence nuclear shape [68] and function [69] (Figure 1A). During the differentiation process, there is a large reorganization of the centrosome proteins: myoblasts possess a morphologically recognizable centrosome with characteristic marker proteins concentrated in the pericentriolar material, whereas myotube differentiation requires relocalization of centrosome proteins to the surface of the nucleus [67,70,71]. Centrosome proteins are critical for MT nucleation and/or anchoring; therefore, MT orientation is extensively redistributed into a more ordered paraxial array in myotubes [66,67,72,73] (Figure 1B). Mature myofibers also exhibit a perinuclear network of MTs, comprising a cage-like structure of a high-density meshwork that may be responsible for nuclear shaping and mechanical protection, and a circular and radial-anisotropic MTs, which are either polarized in the direction of contraction or in the lateral direction [74]. MT post-translational modifications such as increased detyrosinated [75,76] and binding of MTs to MT-associated proteins (MAPs), including EB1 and spectraplakain [74], confers stability to the MTs and has been shown to be essential for maintaining myonuclear morphology [74]. Additionally, it has been proposed that the spectrin domains of nesprin confers elastic features of the MT-spectraplakain-EB1 perinuclear network during the contraction of striated muscle [74]. As a consequence, primary defects in the nuclear-associated networks of MTs have been implicated in strain-induced myonuclear damage [27,74,77].

2.3. Cytoplasmic IFs

IFs have emerged as a perfect candidate for maintaining proper nuclear mechano-response because they are able to resist high mechanical stresses, i.e., bending and stretching, to a considerable degree [65]. IFs are surprisingly flexible [78–82] and can undergo strain-stiffening [83–85]. This is due to the short persistence length of intermediate filaments (1–3 μm) [65]. In the cytoplasm, they can form mechanically relevant links to each other, to other cytoskeletal filaments, to membrane complexes, and to internal organelles including the nucleus [82,86] (Figure 1). These mechanical properties and interconnections enable the IFs to serve as mechanical stress absorbers that protect the cytoplasm and organelles, including the nucleus, against large deformations [51,87,88]. This idea is supported by the fact that IFs can withstand deformations of up to 300% of their initial length without rupturing [89]. Several IFs are expressed and developmentally regulated in human skeletal muscle cells [90–93]. Non muscle-specific proteins vimentin and nestin are expressed in MCPs and myoblasts and are downregulated during later differentiation [94]. Desmin, the muscle-specific IF protein, is expressed at low levels in MCPs and its expression continuously increases to become the prominent IF in mature myofibers [94,95]. It can form copolymers with synemin, another non-muscle specific IF, around the α -actinin-rich Z-lines [92]. In undifferentiated myoblasts, vimentin and desmin are stably linked to the outer nuclear membrane [96] via plectin [97], thus contributing to the perinuclear cage-like structure. During terminal muscle differentiation, desmin accumulates and forms a three-dimensional network between the contractile apparatus, the extracellular matrix, and other cell organelles such as mitochondria, T-tubules, and nuclei [95,98–100] (Figure 1). Close to the nucleus, desmin filaments extend from the Z-lines of striated muscles towards the NE, where they interact with plectin. Terminal differentiation-induced desmin redistribution is associated with post-translational modifications such as phosphorylation and ADP-ribosylation [101], which in turn regulate IF assembly and disassembly as well as interactions between IFs and other cell components and structures [102]. In mature muscle fibers, the primary role of desmin is to link adjacent myofibrils to each

other and to the extracellular matrix, via costameres [39,103–105]. Consequently, a functional reduction in desmin is associated with structural instability of the sarcomeres [106]. Accumulating evidence indicates that desmin is also crucial as a stress-transmitting and stress-signaling network [98,107–110]. Desmin interactions with the nucleus are required to maintain nuclear architecture in cardiomyocytes [111] and to prevent nuclear and muscle damage in response to mechanical challenges [111,112]. Future studies will determine the contribution of desmin scaffolds in myonucleus architecture and function.

3. Mechanical Linkages between the Cytoskeleton and the Nucleoskeleton

LINC complexes provide direct physical nucleo-cytoskeletal coupling between the cytoskeleton network and the NE [113,114] (Figure 3). The LINC complexes comprise outer nuclear transmembrane proteins, called nesprins (NE Spectrin-Repeat Proteins) defined by the Klarsicht-ANC1-Syne-homology (KASH) domain. This domain directly interacts with the luminal domain of the inner nuclear membrane proteins Sad1 and UNC-84 (SUN) proteins 1 (SUN1) or 2 (SUN2) [44,113] within the perinuclear space of the nuclear envelope. SUN proteins form trimers and span the inner nuclear membrane, with their N-amino-terminal nucleoplasmic domains interacting with lamins and lamin-associated proteins within the nucleoplasm [115]. By crossing the outer nuclear membrane, nesprins provide a mechanical link from the cytoskeleton to the nucleoskeleton.

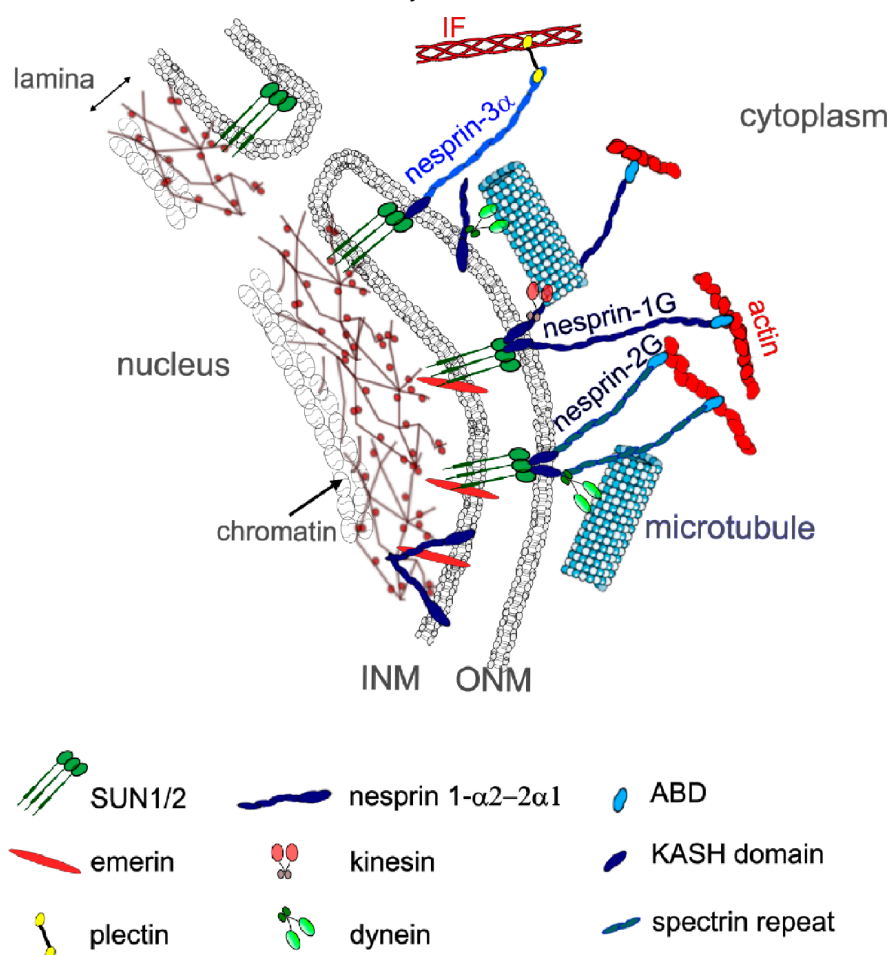


Figure 3. LINC complexes in skeletal muscle. LINC is a complex of proteins including SUN1/2 and nesprins that connect the cytoskeleton to the nucleoskeleton. Different nesprin isoforms are expressed during myogenesis: in MCPs, nesprin-1G and -2G can interact with actin and microtubules in the cytoplasm and with SUN1/2 proteins, emerin and lamins, on the inner nuclear membrane. Shorter nesprin-1α2 and nesprin-2α1 are expressed during myotube differentiation and can bind with microtubules in the cytoplasm via kinesin and other proteins such as A-kinase anchoring protein. Short nesprin-1α2 can also interact with intranuclear proteins such as lamins and emerin. INN: inner nuclear membrane; ONM: outer nuclear membrane.

To date, six genes encoding for different nesprins (-1,-2,-3,-4, lymphoid-restricted membrane protein (LRMP) and KASH5) have been identified in mammals [97,116,117]. Giant nesprins-1 and -2 are ubiquitously expressed with highest representation in striated muscle [118,119]. The *SYNE-1* and *SYNE-2* genes encode the nesprin-1G (1008 kD) and nesprin-2G (792 kD), respectively, with calponin domains at their N-termini that bind the actin cytoskeleton [116]. Nesprins-1G and -2G also bind to the MT motors dynein and kinesin via their C-terminal cytoplasmic stretch [113,120–122]. Kinesin-1 interacts with nesprin-1G and -2 via their LEWD motifs [119,120].

SYNE-1 and *SYNE-2* have multiple internal promoters giving rise to shorter nesprin isoforms which lack the actin-binding domain [119,123] (Figure 3). Alternative splicing also generates short isoforms that lack the C-terminal KASH domain as well as short isoforms that lack both the KASH domain and CH domains [124].

In contrast to SUN proteins, nesprins-1 and -2 switch localizations and isoforms during myogenesis [118,119]. Nesprin-1 increases at the nuclear rim during early myogenesis but is partially replaced by nesprin-2 at later stages of muscle development [118,119]. However, nesprin-1 appears to be critical in synaptic and non-synaptic myonuclear anchoring in skeletal muscle [125,126], due to its ability to form interactions between myonuclei and actin cytoskeleton [125–127]. Expression of two shorter α isoforms, nesprin-1 α 2 and nesprin-2 α 1, is switched on during myogenesis [121,122,128] and becomes dominant in mature skeletal muscle [118]. They are found almost exclusively in skeletal and cardiac muscle [122,128] and form a complex with emerin and A-type lamins at the inner nuclear membrane [129,130]. At the outer nuclear membrane, nesprin-1 α 2 and nesprin-2 α 1 can interact with kinesin and microtubules [119,123] (Figure 3). Nesprin1- α 2 is the main short form of nesprin-1 in skeletal muscle [131]. It is located mainly at the nuclear rim in early myotubes and immature muscle fibers, but then declines in most mature, adult muscle fibers [131], being restricted to neuromuscular junction nuclei [116,119]. Nesprin1- α 2 is required for the correct positioning of myonuclei [77,120,132,133] and MT nucleation from the NE [119], by recruiting A-Kinase Anchoring Protein-450 to the NE [77]. Nesprin-3 lacks actin-binding domains but can indirectly connect to the cytoskeleton by binding to another protein with tandem actin-binding calponin homology domain [134]. Although nesprin-3 exists as two isoforms, nesprin-3 α and nesprin-3 β , only nesprin-3 α can attach to the cytoskeleton. For instance, nesprin-3 α can anchor IFs to the NE through plectin [121–123,126], a plakin family member that can also interact with actin filaments and MTs [97,135–137]. This plectin–nesprin interaction requires the dimerization of plectin and takes place between the N-terminal actin-binding domain of plectin and the first spectrin repeat of nesprin-3 α [135]. Nesprin-3 β does not interact with IFs because it lacks this spectrin-like repeat of nesprin-3 α [135].

The different components of the LINC complexes have been associated with a number of pathogenic modifications in humans as well as in animal models. Perturbation of LINC complexes induces defective signal transduction across the NE [138,139], and prevents centrosome reorientation [48], chromatin organization [77,140–143], and abnormal nuclear positioning [116,121,131,144–146]. It has been shown that mutations in nesprins-1 and -2 cause Emery–Dreifuss muscular dystrophy [77,125,147–150] and dilated cardiomyopathy [149]. It has been proposed that the giant nesprin-1 regulates a feedback loop by which MCPs adapt their intracellular tension to the softness of their native extracellular microenvironment through nucleo-cytoskeletal connections [150]. In addition, nesprin mutations can impair the interaction of nesprin with lamins, emerin and/or SUN proteins, thus affecting diverse functions including gene expression, nuclear shape and positioning [149]. As yet, no mutation in nesprin-3 has been found to be responsible for skeletal muscle diseases. However, acute depletion of nesprin-3 does lead to rapid shrinkage and unfolding of nuclei in a microtubule-dependent manner in rat ventricular cardiomyocytes [111]. Loss of nuclear integrity is concomitant with compromised contractile function and has been proposed to contribute to the pathophysiological changes observed in desmin-related myopathies [111]. Further investigations are required to elucidate the complex mecha-

nisms behind LINC-mediated nucleo-cytoskeletal linkages in skeletal muscle. Finally, although LINC complexes are critical for force transmission across the NE, alternative LINC-independent mechanisms have also been proposed [151]. For instance, it has been proposed that cell boundaries can drive nuclear flattening during cell spreading on rigid substrates [152]. It was shown that a direct compressive force by LINC-anchored apical actin cables is not required for nuclear flattening [152]. According to this model, the overall nuclear shape is primarily dictated by passive forces generated within the actin cytoskeleton, with cell spreading and forces transmitted by the actin cap or LINC complexes contribute to a lesser degree [151,153].

4. The Nuclear Lamina

The nuclear lamina is a filamentous network of proteins mainly composed of the type V IF lamin proteins that assemble into a meshwork underneath the inner nuclear membrane [154,155]. The lamina is composed of lamins and lamin-associated proteins and provides structural support to the NE [156]. Lamins can be categorized as A-type (lamin A/C) or B-type (lamin B1, B2) lamins. They are key components of the nuclear environment and interact with a large number of proteins [140,157–159], the nuclear membrane, and chromatin [157,160] to influence mechanical cues and signaling pathways crucial for cellular proliferation and differentiation [161]. In addition, lamins are involved in the epigenetic regulation of chromatin with drastic consequences for gene regulation [162].

The B-type lamins, lamins B1 and B2, coded for by the *LMNB1* and *LMNB2* genes, are expressed in all somatic cells. B-type lamins have an important role in nuclear shape [86,163] and structure [155,164,165] and may provide nuclear elastic resistance [164], particularly in cells with low A-type lamins [86,163,166]. However, B-type lamin expression differs minimally across solid tissues or in response to matrix stiffness [167] and does not appear to play a major role in nuclear stiffness [86]. In contrast, A-type lamins, encoded for by the *LMNA* gene, are critical for the appropriate nucleus stiffening [166] and dictate the nuclear strain stiffening that dominates nuclear resistance to large deformations [20]. Indeed, upon nuclear mechanostimulation, nucleoplasmic domain of the inner nuclear membrane protein emerin becomes phosphorylated by the protein proto-oncogene tyrosine protein kinase Sarcoma (Src) [168,169]. The Ig fold domain of lamin A is able to partially unfold, leading to stretching of the protein [170]. A-type lamins undergoes dephosphorylation of the S22 residue, associated with relocalization of the nucleoplasmic fraction to the nuclear lamina [166,168,171]. This in turn reinforces the nuclear lamina by stabilization and assembly of A-type lamins and increases nuclear stiffness [161,166]. Conversely, in reduced mechanical constraints, the mobility and turnover of A-type lamins increases [166,171,172]. It has also been shown that, under compression, the coiled coils in the rod domains of A-type lamin polymers are able to slide over each other to contract the length of the rod, behaving as a compression spring able to absorb pressure [173]. The expression of A-type lamins can be correlated with tissue stiffness [166], stiff tissues such as muscle having higher A-type lamin expression and stiffer nuclei than those in softer tissues such as brain [166]. Moreover, the expression and stability of A-type lamins increase during myogenic differentiation [86], leading to nuclear stiffening [174].

Importantly, force-induced remodeling of the nuclear lamina may affect gene transcription by changing the binding properties of NE proteins and transcription factors. Indeed, it is known that chromatin containing actively transcribed genes exists in a less condensed state (i.e., euchromatin) compared to the more compact regions (i.e., heterochromatin) that contain silent genes. Chromatin contained in lamin-associated domains (LADs) is generally heterochromatin [175]. Force changes trigger rapid reorganization of the heterochromatin at the nuclear lamina and are associated with changes in global patterns of gene expression [176]. Nuclear stretch decreases the levels of repressive histone H3K9me3 at the nuclear periphery and increases chromatin mobility [177]. According to studies from Wickström's lab, this chromatin response relies on ER Ca²⁺ release [22]. A-type lamin levels and nuclear stiffness determine the sensitivity of the ER calcium release, where

stiffer nuclei are more prone to respond [22]. Interestingly, myogenic differentiation is associated with specific developmental gene repositioning to and from the nuclear periphery, generally associated with the repression of genes inhibitory to myogenesis and the activation of genes required for myotube differentiation [178]. Muscle-specific NE transmembrane proteins (NETs), including NET39, Transmembrane Protein 38A, and wolframin ER transmembrane glycoprotein, direct specific myogenic genes to the nuclear periphery to facilitate their repression and their combined knockdown almost completely blocks myotube formation [178]. There is also evidence that the disrupted tethering of myogenic genes with NE [169,170] and muscle-specific NETs [178] could underlie muscle pathology in NE-linked diseases. Alternatively, NET-directed gene repositioning may contribute to nuclear stiffening during differentiation.

In line with these physiological roles of A-type lamins, mutations in the *LMNA* gene cause laminopathies, a heterogeneous group of disorders, including skeletal muscle dystrophies and cardiomyopathies [156,179–182]. The severity of the muscle disease is highly variable, the most severe form being the *LMNA*-related congenital muscular dystrophy [183,184]. Although the physiopathology of the disease still requires further studies, there is clear evidence that impaired integrity of the nucleus [184–188], aberrant positioning of myogenic genes [178,189,190] and defective mechanotransduction signaling [29,31,185,191,192] all contribute to the muscle diseases related to *LMNA* mutations. Future studies will precisely determine how the combination of mechanical uncoupling/epigenetic factors and a signaling defect could drive these skeletal muscle disorders.

5. Chromatin-Mediated Mechanoresponse

Whereas the lamina has been recognized for many years as a major contributor to nuclear stiffness, there is now evidence that chromatin and its histone modification state also contribute to nuclear mechanics independently of A-type lamins [20,23,193–196]. It has been proposed that chromatin dominates nuclear force responses at short extensions of <30% strain [20]. Chromatin-based nuclear rigidity operates by inducing changes in histone modification state. Alterations that produce more euchromatin or heterochromatin result in decreased or increased small extension nuclear stiffness, respectively [20].

Upon mechanical stimulation, untethering LADs from the nuclear lamina could initiate gene repositioning and transcription. Mechanical forces could also decondense gene loci at the nuclear periphery, thus allowing better access for transcription machinery and increased transcription. However, it is important to remember that genes located at the nuclear envelope are not necessarily silent [197–199], and that untethering from the lamina is not sufficient to induce changes in gene transcription [200,201]. Taking into account these limitations, there is evidence that force can induce chromatin rearrangement and gene activation. Indeed, the activation and transcription of many genes has been associated with effective force transmission to the nucleus and/or to nuclear deformations [184,202–205]. In addition, force-induced chromatin reorganization could play a critical role in stem cell differentiation [178,206,207]. Interestingly, data show that forces propagate through lamina–chromatin interactions to directly stretch the chromatin and induce transcription upregulation in a living cell [208]. How the altered chromatin-mediated mechanoresponse contributes to mechanical load-mediated adaptation in normal and pathological skeletal muscle remains open for future studies.

6. Nuclear Positioning and Mechanotransduction

Skeletal muscle fibers contain hundreds of flattened myonuclei evenly distributed at the periphery of each cell, with 3–8 nuclei (synaptic nuclei) anchored beneath the neuromuscular junction. How nuclei properly position themselves within each muscle fiber remains partly obscured, especially in tissues. Myonuclear positioning in skeletal muscle cells is an active process that occurs during the differentiation and maturation process, as well as during regeneration [209]. It involves the cytoskeletal network of MTs, F-actin and/or IFs as follows: MTs in the initial translocation/spacing of nu-

clei along the fiber [54,55,77,138,210], and F-actin and desmin in their movement to the fiber periphery [27]. Mislocalization of myonuclei has been associated with a variety of muscle disorders, characterized by muscle atrophy, muscle weakness, and reduced muscle performance [209,211].

The unique distribution of myonuclei at the muscle fiber periphery raises questions about the amount of intracellular force transmitted from the cytoskeleton to NE. Mispositioned myonuclei within individual multinucleated muscle fibers are a hallmark of many muscle diseases, including congenital myopathies and muscular dystrophies [55,125,138,210,212]. Abnormal nuclear positioning is likely to affect individual myonuclear activity by affecting force and strain transmission across the NE [74]. It has been proposed that centrally located myonuclei may experience higher contractile forces exerted by the myofibrils around the nucleus than peripheral nuclei which could disturb nuclear stability. However, whether or not mispositioned myonuclei are a cause or consequence of muscle disease states still remains to be determined.

7. Conclusions and Future Directions

An increasing number of studies focusing on the importance of appropriate nuclear mechanotransduction for muscle homeostasis, regeneration, and plasticity have appeared in the literature since 2010. Advances in deciphering the molecular mechanisms contributing to nuclear mechanotransduction strongly support the idea that defects in nuclear mechanotransduction contribute to human muscle disorders. However, an understanding of the mechanistic and physiological outcomes for nuclear mechanical stress response mainly arises from studies conducted in embryonic and/or mononucleated cells and may depend on the specific cell lines used. The majority of nuclear and cytoskeletal components involved in nuclear mechanotransduction are developmentally regulated and largely reorganized during muscle differentiation, which complicates the understanding of nuclear mechanotransduction defects in muscle disorders.

We anticipate that future research efforts will provide new insights into how the terminal differentiation of MCPs into multinucleated muscle fibers affects nuclear mechanotransduction. In addition, we foresee the elucidation of the contributive role of stress- and strain-induced nuclear response in normal and diseased striated muscles in the future.

Author Contributions: Conceptualization, C.C.; writing—original draft preparation, C.C.; writing—review and editing, S.J. and W.H.; supervision, C.C. All authors have read and agreed to the published version of the manuscript.

Funding: This research received no external funding. The authors acknowledge the Association Institute of Myology, Paris, France, the USEK, the AUF and Lebanon CNRS for financial support to S.J.

Acknowledgments: The authors acknowledge Gillian Butler-Browne for discussion and careful reading.

Conflicts of Interest: The authors declare no conflict of interest.

References

1. Abmayr, S.M.; Pavlath, G.K. Myoblast fusion: Lessons from flies and mice. *Development* **2012**, *139*, 641–656. [[CrossRef](#)]
2. Kirby, T.J.; Lammerding, J. Emerging views of the nucleus as a cellular mechanosensor. *Nat. Cell Biol.* **2018**, *20*, 373–381. [[CrossRef](#)]
3. Ato, S.; Kido, K.; Sase, K.; Fujita, S. Response of resistance exercise-induced muscle protein synthesis and skeletal muscle hypertrophy are not enhanced after disuse muscle atrophy in rat. *Front. Physiol.* **2020**, *11*, 469. [[CrossRef](#)] [[PubMed](#)]
4. Burkholder, T.J. Mechanotransduction in skeletal muscle. *Front. Biosci. A J. Virtual Libr.* **2007**, *12*, 174–191. [[CrossRef](#)] [[PubMed](#)]
5. Masschelein, E.; D’Hulst, G.; Zvick, J.; Hinte, L.; Soro-Arnaiz, I.; Gorski, T.; von Meyenn, F.; Bar-Nur, O.; De Bock, K. Exercise promotes satellite cell contribution to myofibers in a load-dependent manner. *Skelet. Muscle* **2020**, *10*, 21. [[CrossRef](#)] [[PubMed](#)]
6. Aureille, J.; Buffière-Ribot, V.; Harvey, B.E.; Boyault, C.; Pernet, L.; Andersen, T.; Bacola, G.; Balland, M.; Fraboulet, S.; Van Landeghem, L.; et al. Nuclear envelope deformation controls cell cycle progression in response to mechanical force. *EMBO Rep.* **2019**, *20*. [[CrossRef](#)]
7. Uroz, M.; Wistorf, S.; Serra-Picamal, X.; Conte, V.; Sales-Pardo, M.; Roca-Cusachs, P.; Guimerà, R.; Trepac, X. Regulation of cell cycle progression by cell-cell and cell-matrix forces. *Nat. Cell Biol.* **2018**, *20*, 646–654. [[CrossRef](#)] [[PubMed](#)]

8. Fukuda, S.; Kaneshige, A.; Kaji, T.; Noguchi, Y.-T.; Takemoto, Y.; Zhang, L.; Tsujikawa, K.; Kokubo, H.; Uezumi, A.; Maehara, K.; et al. Sustained expression of HeyL is critical for the proliferation of muscle stem cells in overloaded muscle. *eLife* **2019**, *8*, e48284. [[CrossRef](#)] [[PubMed](#)]
9. Dupont, S.; Morsut, L.; Aragona, M.; Enzo, E.; Giulitti, S.; Cordenonsi, M.; Zanconato, F.; Le Digabel, J.; Forcato, M.; Bicciato, S.; et al. Role of YAP/TAZ in mechanotransduction. *Nature* **2011**, *474*, 179–183. [[CrossRef](#)]
10. Elosegui-Artola, A.; Andreu, I.; Beedle, A.E.M.; Lezamiz, A.; Uroz, M.; Kosmalska, A.J.; Oria, R.; Kechagia, J.Z.; Rico-Lastres, P.; Le Roux, A.-L.; et al. Force triggers YAP Nuclear entry by regulating transport across nuclear pores. *Cell* **2017**, *171*, 1397–1410.e14. [[CrossRef](#)] [[PubMed](#)]
11. Kumar, A.; Mazzanti, M.; Mistrik, M.; Kosar, M.; Beznoussenko, G.V.; Mironov, A.A.; Garrè, M.; Parazzoli, D.; Shivashankar, G.V.; Mironov, A.A.; et al. ATR Mediates a checkpoint at the nuclear envelope in response to mechanical stress. *Cell* **2014**, *158*, 633–646. [[CrossRef](#)]
12. Kidiyoor, G.R.; Li, Q.; Bastianello, G.; Bruhn, C.; Giovannetti, I.; Mohamood, A.; Beznoussenko, G.V.; Mironov, A.; Raab, M.; Piel, M.; et al. ATR is essential for preservation of cell mechanics and nuclear integrity during interstitial migration. *Nat. Commun.* **2020**, *11*, 4828. [[CrossRef](#)]
13. Itano, N.; Okamoto, S.-I.; Zhang, D.; Lipton, S.A.; Ruoslahti, E. Cell spreading controls endoplasmic and nuclear calcium: A physical gene regulation pathway from the cell surface to the nucleus. *Proc. Natl. Acad. Sci. USA* **2003**, *100*, 5181–5186. [[CrossRef](#)]
14. Enyedi, B.; Jelcic, M.; Niethammer, P. The Cell nucleus serves as a mechanotransducer of tissue damage-induced inflammation. *Cell* **2016**, *165*, 1160–1170. [[CrossRef](#)] [[PubMed](#)]
15. Raab, M.; Gentili, M.; de Belly, H.; Thiam, H.-R.; Vargas, P.; Jimenez, A.J.; Lautenschlaeger, F.; Voituriez, R.; Lennon-Dumenil, A.-M.; Manel, N.; et al. ESCRT III repairs nuclear envelope ruptures during cell migration to limit DNA damage and cell death. *Science* **2016**, *352*, 359–362. [[CrossRef](#)]
16. Chen, N.Y.; Kim, P.H.; Fong, L.G.; Young, S.G. Nuclear membrane ruptures, cell death, and tissue damage in the setting of nuclear lamin deficiencies. *Nucleus* **2020**, *11*, 237–249. [[CrossRef](#)] [[PubMed](#)]
17. Dahl, K.N.; Ribeiro, A.J.S.; Lammerding, J. Nuclear Shape, mechanics, and mechanotransduction. *Circ. Res.* **2008**, *102*, 1307–1318. [[CrossRef](#)]
18. Janota, C.S.; Calero-Cuenca, F.J.; Gomes, E.R. The role of the cell nucleus in mechanotransduction. *Curr. Opin. Cell Biol.* **2020**, *63*, 204–211. [[CrossRef](#)]
19. Enyedi, B.; Niethammer, P. Nuclear membrane stretch and its role in mechanotransduction. *Nucleus* **2017**, *8*, 156–161. [[CrossRef](#)] [[PubMed](#)]
20. Stephens, A.D.; Banigan, E.J.; Adam, S.A.; Goldman, R.D.; Marko, J.F. Chromatin and lamin A determine two different mechanical response regimes of the cell nucleus. *Mol. Biol. Cell* **2017**, *28*, 1984–1996. [[CrossRef](#)]
21. Stephens, A.D.; Banigan, E.J.; Marko, J.F. Separate roles for chromatin and lamins in nuclear mechanics. *Nucleus* **2018**, *9*, 119–124. [[CrossRef](#)]
22. Nava, M.M.; Miroshnikova, Y.A.; Biggs, L.C.; Whitefield, D.B.; Metge, F.; Boucas, J.; Vihinen, H.; Jokitalo, E.; Li, X.; García Arcos, J.M.; et al. Heterochromatin-Driven nuclear softening protects the genome against mechanical stress-induced damage. *Cell* **2020**, *181*, 800–817.e22. [[CrossRef](#)] [[PubMed](#)]
23. Stephens, A.D.; Banigan, E.J.; Marko, J.F. Chromatin’s physical properties shape the nucleus and its functions. *Curr. Opin. Cell Biol.* **2019**, *58*, 76–84. [[CrossRef](#)]
24. Flück, M.; Hoppeler, H. Molecular basis of skeletal muscle plasticity—From gene to form and function. *Rev. Physiol. Biochem. Pharmacol.* **2003**, *146*, 159–216. [[PubMed](#)]
25. Martino, F.; Perestrelo, A.R.; Vinarský, V.; Pagliari, S.; Forte, G. Cellular mechanotransduction: From tension to function. *Front. Physiol.* **2018**, *9*, 824. [[CrossRef](#)]
26. Essawy, N.; Samson, C.; Petitalot, A.; Moog, S.; Bigot, A.; Herrada, I.; Marcelot, A.; Arteni, A.-A.; Coirault, C.; Zinn-Justin, S. An emerin LEM-domain mutation Impairs cell response to mechanical stress. *Cells* **2019**, *8*, 570. [[CrossRef](#)]
27. Roman, W.; Martins, J.P.; Carvalho, F.A.; Voituriez, R.; Abella, J.V.G.; Santos, N.C.; Cadot, B.; Way, M.; Gomes, E.R. Myofibril contraction and crosslinking drive nuclear movement to the periphery of skeletal muscle. *Nat. Cell Biol.* **2017**, *19*, 1189–1201. [[CrossRef](#)]
28. Fischer, M.; Rikeit, P.; Knaus, P.; Coirault, C. YAP-mediated mechanotransduction in skeletal muscle. *Front. Physiol.* **2016**, *7*. [[CrossRef](#)]
29. Owens, D.J.; Fischer, M.; Jabre, S.; Moog, S.; Mamchaoui, K.; Butler-Browne, G.; Coirault, C. Lamin Mutations cause increased YAP Nuclear entry in muscle stem cells. *Cells* **2020**, *9*, 816. [[CrossRef](#)]
30. Jorgenson, K.W.; Phillips, S.M.; Hornberger, T.A. Identifying the Structural adaptations that drive the mechanical load-induced growth of skeletal muscle: A Scoping review. *Cells* **2020**, *9*, 1658. [[CrossRef](#)]
31. Owens, D.J.; Messeant, J.; Moog, S.; Viggars, M.; Ferry, A.; Mamchaoui, K.; Lacene, E.; Romero, N.; Brull, A.; Bonne, G.; et al. Lamin-Related congenital muscular dystrophy alters mechanical signaling and skeletal muscle growth. *Int. J. Mol. Sci.* **2020**, *22*, 306. [[CrossRef](#)]
32. D’Alessandro, M.; Hnia, K.; Gache, V.; Koch, C.; Gavriilidis, C.; Rodriguez, D.; Nicot, A.-S.; Romero, N.B.; Schwab, Y.; Gomes, E.; et al. Amphiphysin 2 Orchestrates nucleus positioning and shape by linking the nuclear envelope to the actin and microtubule cytoskeleton. *Dev. Cell* **2015**, *35*, 186–198. [[CrossRef](#)]

33. Kim, J.-K.; Louhghalam, A.; Lee, G.; Schafer, B.W.; Wirtz, D.; Kim, D.-H. Nuclear lamin A/C harnesses the perinuclear apical actin cables to protect nuclear morphology. *Nat. Commun.* **2017**, *8*, 2123. [[CrossRef](#)]
34. Heo, S.-J.; Driscoll, T.P.; Thorpe, S.D.; Nerurkar, N.L.; Baker, B.M.; Yang, M.T.; Chen, C.S.; Lee, D.A.; Mauck, R.L. Differentiation alters stem cell nuclear architecture, mechanics, and mechano-sensitivity. *eLife* **2016**, *5*, e18207. [[CrossRef](#)]
35. Onuh, J.O.; Qiu, H. Serum response factor-cofactor interactions and their implications in disease. *FEBS J.* **2020**. [[CrossRef](#)] [[PubMed](#)]
36. Watt, K.I.; Goodman, C.A.; Hornberger, T.A.; Gregorevic, P. The Hippo signaling pathway in the regulation of skeletal muscle mass and function. *Exerc. Sport Sci. Rev.* **2018**, *46*, 92–96. [[CrossRef](#)] [[PubMed](#)]
37. Gnimassou, O.; Francaux, M.; Deldicque, L. Hippo pathway and skeletal muscle mass regulation in mammals: A controversial relationship. *Front. Physiol.* **2017**, *8*, 190. [[CrossRef](#)] [[PubMed](#)]
38. Gabriel, B.M.; Hamilton, D.L.; Tremblay, A.M.; Wackerhage, H. The Hippo signal transduction network for exercise physiologists. *J. Appl. Physiol.* **2016**, *120*, 1105–1117. [[CrossRef](#)] [[PubMed](#)]
39. Maniotis, A.J.; Chen, C.S.; Ingber, D.E. Demonstration of mechanical connections between integrins, cytoskeletal filaments, and nucleoplasm that stabilize nuclear structure. *Proc. Natl. Acad. Sci. USA* **1997**, *94*, 849–854. [[CrossRef](#)]
40. Wang, N.; Tytell, J.D.; Ingber, D.E. Mechanotransduction at a distance: Mechanically coupling the extracellular matrix with the nucleus. *Nat. Rev. Mol. Cell Biol.* **2009**, *10*, 75–82. [[CrossRef](#)]
41. Zhang, J.; Alisafaei, F.; Nikolić, M.; Nou, X.A.; Kim, H.; Shenoy, V.B.; Scarcelli, G. Nuclear mechanics within intact cells Is regulated by cytoskeletal network and internal nanostructures. *Small* **2020**, *16*, 1907688. [[CrossRef](#)]
42. Ramdas, N.M.; Shivashankar, G.V. Cytoskeletal Control of nuclear morphology and chromatin organization. *J. Mol. Biol.* **2015**, *427*, 695–706. [[CrossRef](#)]
43. Haque, F.; Mazzeo, D.; Patel, J.T.; Smallwood, D.T.; Ellis, J.A.; Shanahan, C.M.; Shackleton, S. Mammalian SUN protein interaction networks at the inner nuclear membrane and their role in laminopathy disease processes. *J. Biol. Chem.* **2010**, *285*, 3487–3498. [[CrossRef](#)] [[PubMed](#)]
44. Crisp, M.; Burke, B. The nuclear envelope as an integrator of nuclear and cytoplasmic architecture. *FEBS Lett.* **2008**, *582*, 2023–2032. [[CrossRef](#)] [[PubMed](#)]
45. Crisp, M.; Liu, Q.; Roux, K.; Rattner, J.B.; Shanahan, C.; Burke, B.; Stahl, P.D.; Hodzic, D. Coupling of the nucleus and cytoplasm: Role of the LINC complex. *J. Cell Biol.* **2006**, *172*, 41–53. [[CrossRef](#)]
46. Ingber, D.E. Cellular mechanotransduction: Putting all the pieces together again. *FASEB J.* **2006**, *20*, 811–827. [[CrossRef](#)] [[PubMed](#)]
47. Khatau, S.B.; Hale, C.M.; Stewart-Hutchinson, P.J.; Patel, M.S.; Stewart, C.L.; Searson, P.C.; Hodzic, D.; Wirtz, D. A perinuclear actin cap regulates nuclear shape. *Proc. Natl. Acad. Sci. USA* **2009**, *106*, 19017–19022. [[CrossRef](#)]
48. Luxton, G.W.G.; Gomes, E.R.; Folker, E.S.; Vintinner, E.; Gundersen, G.G. Linear arrays of nuclear envelope proteins harness retrograde actin flow for nuclear movement. *Science* **2010**, *329*, 956–959. [[CrossRef](#)]
49. Kim, D.-H.; Chambliss, A.B.; Wirtz, D. The multi-faceted role of the actin cap in cellular mechanosensation and mechanotransduction. *Soft Matter* **2013**, *9*, 5516. [[CrossRef](#)] [[PubMed](#)]
50. Chambliss, A.B.; Khatau, S.B.; Erdenberger, N.; Robinson, D.K.; Hodzic, D.; Longmore, G.D.; Wirtz, D. The LINC-anchored actin cap connects the extracellular milieu to the nucleus for ultrafast mechanotransduction. *Sci. Rep.* **2013**, *3*, 1087. [[CrossRef](#)] [[PubMed](#)]
51. Neelam, S.; Chancellor, T.J.; Li, Y.; Nickerson, J.A.; Roux, K.J.; Dickinson, R.B.; Lele, T.P. Direct force probe reveals the mechanics of nuclear homeostasis in the mammalian cell. *Proc. Natl. Acad. Sci. USA* **2015**, *112*, 5720–5725. [[CrossRef](#)]
52. Shiu, J.-Y.; Aires, L.; Lin, Z.; Vogel, V. Nanopillar force measurements reveal actin-cap-mediated YAP mechanotransduction. *Nat. Cell Biol.* **2018**, *20*, 262–271. [[CrossRef](#)]
53. Khatau, S.B.; Kusuma, S.; Hanjaya-Putra, D.; Mali, P.; Cheng, L.; Lee, J.S.H.; Gerecht, S.; Wirtz, D. The differential formation of the LINC-Mediated perinuclear actin cap in pluripotent and somatic cells. *PLoS ONE* **2012**, *7*, e36689. [[CrossRef](#)] [[PubMed](#)]
54. Cadot, B.; Gache, V.; Gomes, E.R. Moving and positioning the nucleus in skeletal muscle—One step at a time. *Nucleus* **2015**, *6*, 373–381. [[CrossRef](#)]
55. Falcone, S.; Roman, W.; Hnia, K.; Gache, V.; Didier, N.; Lainé, J.; Auradé, F.; Marty, I.; Nishino, I.; Charlet-Berguerand, N.; et al. N-WASP is required for Amphiphysin-2/BIN 1-dependent nuclear positioning and triad organization in skeletal muscle and is involved in the pathophysiology of centronuclear myopathy. *EMBO Mol. Med.* **2014**, *6*, 1455–1475. [[CrossRef](#)]
56. Lloyd, C.M.; Berendse, M.; Lloyd, D.G.; Schevzov, G.; Grounds, M.D. A novel role for non-muscle γ -actin in skeletal muscle sarcomere assembly. *Exp. Cell Res.* **2004**, *297*, 82–96. [[CrossRef](#)] [[PubMed](#)]
57. Sanger, J.W.; Kang, S.; Siebrands, C.C.; Freeman, N.; Du, A.; Wang, J.; Stout, A.L.; Sanger, J.M. How to build a myofibril. *J. Muscle Res. Cell Motil.* **2006**, *26*, 343–354. [[CrossRef](#)]
58. Hotulainen, P.; Lappalainen, P. Stress fibers are generated by two distinct actin assembly mechanisms in motile cells. *J. Cell Biol.* **2006**, *173*, 383–394. [[CrossRef](#)]
59. Bains, W.; Ponte, P.; Blau, H.; Kedes, L. Cardiac actin is the major actin gene product in skeletal muscle cell differentiation in vitro. *Mol. Cell. Biol.* **1984**, *4*, 1449–1453. [[CrossRef](#)]
60. Lin, J.J.; Lin, J.L. Assembly of different isoforms of actin and tropomyosin into the skeletal tropomyosin-enriched microfilaments during differentiation of muscle cells in vitro. *J. Cell Biol.* **1986**, *103*, 2173–2183. [[CrossRef](#)]

61. Otey, C.A.; Kalnoski, M.H.; Bulinski, J.C. Immunolocalization of muscle and nonmuscle isoforms of actin in myogenic cells and adult skeletal muscle. *Cell Motil. Cytoskelet.* **1988**, *9*, 337–348. [[CrossRef](#)]
62. Craig, S.W.; Pardo, J.V. Gamma actin, spectrin, and intermediate filament proteins colocalize with vinculin at costameres, myofibril-to-sarcolemma attachment sites. *Cell Motil.* **1983**, *3*, 449–462. [[CrossRef](#)]
63. Rybakova, I.N.; Patel, J.R.; Ervasti, J.M. The Dystrophin complex forms a mechanically strong link between the sarcolemma and costameric actin. *J. Cell Biol.* **2000**, *150*, 1209–1214. [[CrossRef](#)]
64. Ervasti, J.M. Costameres: The Achilles' heel of Herculean muscle. *J. Biol. Chem.* **2003**, *278*, 13591–13594. [[CrossRef](#)] [[PubMed](#)]
65. Pegoraro, A.F.; Janmey, P.; Weitz, D.A. Mechanical properties of the cytoskeleton and cells. *Cold Spring Harb. Perspect. Biol.* **2017**, *9*, a022038. [[CrossRef](#)] [[PubMed](#)]
66. Musa, H.; Orton, C.; Morrison, E.E.; Peckham, M. Microtubule assembly in cultured myoblasts and myotubes following nocodazole induced microtubule depolymerisation. *J. Muscle Res. Cell Motil.* **2003**, *24*, 301–308. [[CrossRef](#)]
67. Becker, R.; Leone, M.; Engel, F. Microtubule Organization in striated muscle cells. *Cells* **2020**, *9*, 1395. [[CrossRef](#)]
68. Chang, W.; Worman, H.J.; Gundersen, G.G. Accessorizing and anchoring the LINC complex for multifunctionality. *J. Cell Biol.* **2015**, *208*, 11–22. [[CrossRef](#)] [[PubMed](#)]
69. Webster, M.; Witkin, K.L.; Cohen-Fix, O. Sizing up the nucleus: Nuclear shape, size and nuclear-envelope assembly. *J. Cell Sci.* **2009**, *122*, 1477–1486. [[CrossRef](#)]
70. Starr, D.A. Muscle development: Nucleating Microtubules at the nuclear envelope. *Curr. Biol.* **2017**, *27*, R1071–R1073. [[CrossRef](#)]
71. Srsen, V.; Fant, X.; Heald, R.; Rabouille, C.; Merdes, A. Centrosome proteins form an insoluble perinuclear matrix during muscle cell differentiation. *BMC Cell Biol.* **2009**, *10*, 28. [[CrossRef](#)]
72. Warren, R.H. Microtubular organization in elongating myogenic cells. *J. Cell Biol.* **1974**, *63*, 550–566. [[CrossRef](#)] [[PubMed](#)]
73. Pizon, V.; Gerbal, F.; Diaz, C.C.; Karsenti, E. Microtubule-dependent transport and organization of sarcomeric myosin during skeletal muscle differentiation. *EMBO J.* **2005**, *24*, 3781–3792. [[CrossRef](#)] [[PubMed](#)]
74. Wang, S.; Reuveny, A.; Volk, T. Nesprin provides elastic properties to muscle nuclei by cooperating with spectraplakins and EB1. *J. Cell Biol.* **2015**, *209*, 529–538. [[CrossRef](#)] [[PubMed](#)]
75. Mian, I.; Pierre-Louis, W.S.; Dole, N.; Gilberti, R.M.; Dodge-Kafka, K.; Tirnauer, J.S. LKB1 Destabilizes microtubules in myoblasts and contributes to myoblast differentiation. *PLoS ONE* **2012**, *7*, e31583. [[CrossRef](#)]
76. Gundersen, G.G.; Khawaja, S.; Bulinski, J.C. Generation of a stable, posttranslationally modified microtubule array is an early event in myogenic differentiation. *J. Cell Biol.* **1989**, *109*, 2275–2288. [[CrossRef](#)]
77. Gimpel, P.; Lee, Y.L.; Sobota, R.M.; Calvi, A.; Koullourou, V.; Patel, R.; Mamchaoui, K.; Nédélec, F.; Shackleton, S.; Schmoranz, J.; et al. Nesprin-1 α -dependent microtubule nucleation from the nuclear envelope via Akap450 is necessary for nuclear positioning in muscle cells. *Curr. Biol.* **2017**, *27*, 2999–3009.e9. [[CrossRef](#)]
78. Block, J.; Schroeder, V.; Pawelczyk, P.; Willenbacher, N.; Köster, S. Physical properties of cytoplasmic intermediate filaments. *Biochimica et Biophysica Acta (BBA) Mol. Cell Res.* **2015**, *1853*, 3053–3064. [[CrossRef](#)]
79. Fudge, D.S.; Gardner, K.H.; Forsyth, V.T.; Riekel, C.; Gosline, J.M. The mechanical properties of hydrated intermediate filaments: Insights from hagfish slime threads. *Biophys. J.* **2003**, *85*, 2015–2027. [[CrossRef](#)]
80. Kreplak, L.; Bär, H.; Leterrier, J.F.; Herrmann, H.; Aebi, U. Exploring the mechanical behavior of single intermediate filaments. *J. Mol. Biol.* **2005**, *354*, 569–577. [[CrossRef](#)]
81. Wagner, O.I.; Rammensee, S.; Korde, N.; Wen, Q.; Leterrier, J.-F.; Janmey, P.A. Softness, strength and self-repair in intermediate filament networks. *Exp. Cell Res.* **2007**, *313*, 2228–2235. [[CrossRef](#)]
82. Kim, S.; Coulombe, P.A. Intermediate filament scaffolds fulfill mechanical, organizational, and signaling functions in the cytoplasm. *Genes Dev.* **2007**, *21*, 1581–1597. [[CrossRef](#)]
83. Block, J.; Witt, H.; Candelli, A.; Peterman, E.J.G.; Wuite, G.J.L.; Janshoff, A.; Köster, S. Nonlinear loading-rate-dependent force response of individual vimentin intermediate filaments to applied strain. *Phys. Rev. Lett.* **2017**, *118*, 048101. [[CrossRef](#)]
84. Lorenz, C.; Forsting, J.; Schepers, A.V.; Kraxner, J.; Bauch, S.; Witt, H.; Klumpp, S.; Köster, S. Lateral Subunit coupling determines intermediate filament mechanics. *Phys. Rev. Lett.* **2019**, *123*, 188102. [[CrossRef](#)] [[PubMed](#)]
85. Smoler, M.; Coceano, G.; Testa, I.; Bruno, L.; Levi, V. Apparent stiffness of vimentin intermediate filaments in living cells and its relation with other cytoskeletal polymers. *Biochimica et Biophysica Acta (BBA) Mol. Cell Res.* **2020**, *1867*, 118726. [[CrossRef](#)]
86. Lammerding, J.; Fong, L.G.; Ji, J.Y.; Reue, K.; Stewart, C.L.; Young, S.G.; Lee, R.T. Lamins A and C but Not Lamin B1 Regulate Nuclear Mechanics. *J. Biol. Chem.* **2006**, *281*, 25768–25780. [[CrossRef](#)] [[PubMed](#)]
87. Patteson, A.E.; Vahabikashi, A.; Pogoda, K.; Adam, S.A.; Mandal, K.; Kittisopikul, M.; Sivagurunathan, S.; Goldman, A.; Goldman, R.D.; Janmey, P.A. Vimentin protects cells against nuclear rupture and DNA damage during migration. *J. Cell Biol.* **2019**, *218*, 4079–4092. [[CrossRef](#)]
88. Hu, J.; Li, Y.; Hao, Y.; Zheng, T.; Gupta, S.K.; Parada, G.A.; Wu, H.; Lin, S.; Wang, S.; Zhao, X.; et al. High stretchability, strength, and toughness of living cells enabled by hyperelastic vimentin intermediate filaments. *Proc. Natl. Acad. Sci. USA* **2019**, *116*, 17175–17180. [[CrossRef](#)] [[PubMed](#)]
89. Kreplak, L.; Herrmann, H.; Aebi, U. Tensile properties of single desmin intermediate filaments. *Biophys. J.* **2008**, *94*, 2790–2799. [[CrossRef](#)]
90. Banwell, B.L. Intermediate filament-related myopathies. *Pediatric Neurol.* **2001**, *24*, 257–263. [[CrossRef](#)]
91. Paulin, D.; Huet, A.; Khanamirian, L.; Xue, Z. Desminopathies in muscle disease. *J. Pathol.* **2004**, *204*, 418–427. [[CrossRef](#)]

92. Paulin, D.; Hovhannisyan, Y.; Kasakyan, S.; Agbulut, O.; Li, Z.; Xue, Z. Synemin-related skeletal and cardiac myopathies: An overview of pathogenic variants. *Am. J. Physiol. Cell Physiol.* **2020**, *318*, C709–C718. [[CrossRef](#)] [[PubMed](#)]
93. Capetanaki, Y.; Bloch, R.J.; Kouloumenta, A.; Mavroidis, M.; Psarras, S. Muscle intermediate filaments and their links to membranes and membranous organelles. *Exp. Cell Res.* **2007**, *313*, 2063–2076. [[CrossRef](#)] [[PubMed](#)]
94. Sejersen, T.; Lendahl, U. Transient expression of the intermediate filament nestin during skeletal muscle development. *J. Cell Sci.* **1993**, *106*, 1291–1300.
95. Lazarides, E.; Hubbard, B.D. Immunological characterization of the subunit of the 100 A filaments from muscle cells. *Proc. Natl. Acad. Sci. USA* **1976**, *73*, 4344–4348. [[CrossRef](#)] [[PubMed](#)]
96. Mermelstein, C.S.; Andrade, L.R.; Portilho, D.M.; Costa, M.L. Desmin filaments are stably associated with the outer nuclear surface in chick myoblasts. *Cell Tissue Res.* **2006**, *323*, 351–357. [[CrossRef](#)] [[PubMed](#)]
97. Wilhelmsen, K.; Litjens, S.H.; Kuikman, I.; Tshimbalanga, N.; Janssen, H.; van den Bout, I.; Raymond, K.; Sonnenberg, A. Nesprin-3, a novel outer nuclear membrane protein, associates with the cytoskeletal linker protein plectin. *J. Cell Biol.* **2005**, *171*, 799–810. [[CrossRef](#)]
98. Lazarides, E. Intermediate filaments as mechanical integrators of cellular space. *Nature* **1980**, *283*, 249–256. [[CrossRef](#)]
99. Capetanaki, Y. Desmin cytoskeleton A Potential regulator of muscle mitochondrial behavior and function. *Trends Cardiovasc. Med.* **2002**, *12*, 339–348. [[CrossRef](#)]
100. Reipert, S. Association of mitochondria with plectin and desmin intermediate filaments in striated muscle. *Exp. Cell Res.* **1999**, *252*, 479–491. [[CrossRef](#)] [[PubMed](#)]
101. Winter, D.L.; Paulin, D.; Mericskay, M.; Li, Z. Posttranslational modifications of desmin and their implication in biological processes and pathologies. *Histochem. Cell Biol.* **2014**, *141*, 1–16. [[CrossRef](#)]
102. Snider, N.T.; Omary, M.B. Post-translational modifications of intermediate filament proteins: Mechanisms and functions. *Nat. Rev. Mol. Cell Biol.* **2014**, *15*, 163–177. [[CrossRef](#)]
103. Gao, Q.Q.; McNally, E.M. The Dystrophin Complex: Structure, Function, and Implications for Therapy. In *Comprehensive Physiology*; Terjung, R., Ed.; John Wiley & Sons, Inc.: Hoboken, NJ, USA, 2015; pp. 1223–1239.
104. Boudriau, S.; Vincent, M.; Côté, C.H.; Rogers, P.A. Cytoskeletal structure of skeletal muscle: Identification of an intricate exosarcomeric microtubule lattice in slow- and fast-twitch muscle fibers. *J. Histochem. Cytochem.* **1993**, *41*, 1013–1021. [[CrossRef](#)]
105. Wang, K.; Ramirez-Mitchell, R. A network of transverse and longitudinal intermediate filaments is associated with sarcomeres of adult vertebrate skeletal muscle. *J. Cell Biol.* **1983**, *96*, 562–570. [[CrossRef](#)]
106. Li, Z.; Colucci-Guyon, E.; Pinçon-Raymond, M.; Mericskay, M.; Pournin, S.; Paulin, D.; Babinet, C. Cardiovascular lesions and Skeletal myopathy in mice lacking desmin. *Dev. Biol.* **1996**, *175*, 362–366. [[CrossRef](#)]
107. Price, M.G. Molecular analysis of intermediate filament cytoskeleton—A putative load-bearing structure. *Am. J. Physiol.* **1984**, *246*, H566–H572. [[CrossRef](#)] [[PubMed](#)]
108. Galou, M.; Gao, J.; Humbert, J.; Mericskay, M.; Li, Z.; Paulin, D.; Vicart, P. The importance of intermediate filaments in the adaptation of tissues to mechanical stress: Evidence from gene knockout studies. *Biol. Cell* **1997**, *89*, 85–97. [[CrossRef](#)]
109. Tolstonog, G.V.; Sabasch, M.; Traub, P. Cytoplasmic Intermediate filaments are stably associated with nuclear matrices and potentially modulate their DNA-binding function. *DNA Cell Biol.* **2002**, *21*, 213–239. [[CrossRef](#)] [[PubMed](#)]
110. Boriak, A.M.; Capetanaki, Y.; Hwang, W.; Officer, T.; Badshah, M.; Rodarte, J.; Tidball, J.G. Desmin integrates the three-dimensional mechanical properties of muscles. *Am. J. Physiol. Cell Physiol.* **2001**, *280*, C46–C52. [[CrossRef](#)] [[PubMed](#)]
111. Heffler, J.; Shah, P.P.; Robison, P.; Phyto, S.; Veliz, K.; Uchida, K.; Bogush, A.; Rhoades, J.; Jain, R.; Prosser, B.L. A Balance between intermediate filaments and microtubules maintains nuclear architecture in the cardiomyocyte. *Circ. Res.* **2020**, *126*, e10–e26. [[CrossRef](#)] [[PubMed](#)]
112. Langer, H.T.; Mossakowski, A.A.; Willis, B.J.; Grimsrud, K.N.; Wood, J.A.; Lloyd, K.C.K.; Zbinden-Foncea, H.; Baar, K. Generation of desminopathy in rats using CRISPR-Cas9. *J. Cachexiasarcopenia Muscle* **2020**. [[CrossRef](#)]
113. Starr, D.A.; Fridolfsson, H.N. Interactions Between nuclei and the cytoskeleton are mediated by SUN-KASH Nuclear-envelope bridges. *Annu. Rev. Cell Dev. Biol.* **2010**, *26*, 421–444. [[CrossRef](#)]
114. Lombardi, M.L.; Lammerding, J. Keeping the LINC: The importance of nucleocytoplasmic coupling in intracellular force transmission and cellular function. *Biochem. Soc. Trans.* **2011**, *39*, 1729–1734. [[CrossRef](#)] [[PubMed](#)]
115. Torbati, M.; Lele, T.P.; Agrawal, A. An unresolved LINC in the nuclear envelope. *Cell. Mol. Bioeng.* **2016**, *9*, 252–257. [[CrossRef](#)] [[PubMed](#)]
116. Zhang, Q.; Skepper, J.N.; Yang, F.; Davies, J.D.; Hegyi, L.; Roberts, R.G.; Weissberg, P.L.; Ellis, J.A.; Shanahan, C.M. Nesprins: A novel family of spectrin-repeat-containing proteins that localize to the nuclear membrane in multiple tissues. *J. Cell Sci.* **2001**, *114*, 4485–4498. [[PubMed](#)]
117. Roux, K.J.; Crisp, M.L.; Liu, Q.; Kim, D.; Kozlov, S.; Stewart, C.L.; Burke, B. Nesprin 4 is an outer nuclear membrane protein that can induce kinesin-mediated cell polarization. *Proc. Natl. Acad. Sci. USA* **2009**, *106*, 2194–2199. [[CrossRef](#)] [[PubMed](#)]
118. Randles, K.N.; Lam, L.T.; Sewry, C.A.; Puckelwartz, M.; Furling, D.; Wehnert, M.; McNally, E.M.; Morris, G.E. Nesprins, but not sun proteins, switch isoforms at the nuclear envelope during muscle development. *Dev. Dyn.* **2010**, *239*, 998–1009. [[CrossRef](#)]
119. Holt, I.; Fuller, H.R.; Lam, L.T.; Sewry, C.A.; Shirran, S.L.; Zhang, Q.; Shanahan, C.M.; Morris, G.E. Nesprin-1-alpha2 associates with kinesin at myotube outer nuclear membranes, but is restricted to neuromuscular junction nuclei in adult muscle. *Sci. Rep.* **2019**, *9*, 14202. [[CrossRef](#)]

120. Wilson, M.H.; Holzbaur, E.L.F. Nesprins anchor kinesin-1 motors to the nucleus to drive nuclear distribution in muscle cells. *Development* **2015**, *142*, 218–228. [[CrossRef](#)]
121. Chapman, M.A.; Zhang, J.; Banerjee, I.; Guo, L.T.; Zhang, Z.; Shelton, G.D.; Ouyang, K.; Lieber, R.L.; Chen, J. Disruption of both nesprin 1 and desmin results in nuclear anchorage defects and fibrosis in skeletal muscle. *Hum. Mol. Genet.* **2014**, *23*, 5879–5892. [[CrossRef](#)]
122. Zhang, Q. Nesprin-2 is a multi-isomeric protein that binds lamin and emerin at the nuclear envelope and forms a subcellular network in skeletal muscle. *J. Cell Sci.* **2005**, *118*, 673–687. [[CrossRef](#)]
123. Tapley, E.C.; Starr, D.A. Connecting the nucleus to the cytoskeleton by SUN–KASH bridges across the nuclear envelope. *Curr. Opin. Cell Biol.* **2013**, *25*, 57–62. [[CrossRef](#)]
124. Rajgor, D.; Mellad, J.A.; Autore, F.; Zhang, Q.; Shanahan, C.M. Multiple novel nesprin-1 and nesprin-2 Variants act as versatile tissue-specific intracellular scaffolds. *PLoS ONE* **2012**, *7*, e40098. [[CrossRef](#)]
125. Puckelwartz, M.J.; Kessler, E.; Zhang, Y.; Hodzic, D.; Randles, K.N.; Morris, G.; Earley, J.U.; Hadhazy, M.; Holaska, J.M.; Mewborn, S.K.; et al. Disruption of nesprin-1 produces an Emery Dreifuss muscular dystrophy-like phenotype in mice. *Hum. Mol. Genet.* **2009**, *18*, 607–620. [[CrossRef](#)]
126. Zhang, X.; Xu, R.; Zhu, B.; Yang, X.; Ding, X.; Duan, S.; Xu, T.; Zhuang, Y.; Han, M. Syne-1 and Syne-2 play crucial roles in myonuclear anchorage and motor neuron innervation. *Development* **2007**, *134*, 901–908. [[CrossRef](#)]
127. Zhang, J.; Felder, A.; Liu, Y.; Guo, L.T.; Lange, S.; Dalton, N.D.; Gu, Y.; Peterson, K.L.; Mizisin, A.P.; Shelton, G.D.; et al. Nesprin 1 is critical for nuclear positioning and anchorage. *Hum. Mol. Genet.* **2010**, *19*, 329–341. [[CrossRef](#)]
128. Duong, N.T.; Morris, G.E.; Lam, L.T.; Zhang, Q.; Sewry, C.A.; Shanahan, C.M.; Holt, I. Nesprins: Tissue-specific expression of epsilon and other short isoforms. *PLoS ONE* **2014**, *9*, e94380. [[CrossRef](#)]
129. Mislow, J.M.K.; Holaska, J.M.; Kim, M.S.; Lee, K.K.; Segura-Totten, M.; Wilson, K.L.; McNally, E.M. Nesprin-1 α self-associates and binds directly to emerin and lamin A in vitro. *FEBS Lett.* **2002**, *525*, 135–140. [[CrossRef](#)]
130. Wheeler, M.A.; Davies, J.D.; Zhang, Q.; Emerson, L.J.; Hunt, J.; Shanahan, C.M.; Ellis, J.A. Distinct functional domains in nesprin-1 α and nesprin-2 β bind directly to emerin and both interactions are disrupted in X-linked Emery–Dreifuss muscular dystrophy. *Exp. Cell Res.* **2007**, *313*, 2845–2857. [[CrossRef](#)]
131. Holt, I.; Duong, N.T.; Zhang, Q.; Lam, L.T.; Sewry, C.A.; Mamchaoui, K.; Shanahan, C.M.; Morris, G.E. Specific localization of nesprin-1- α 2, the short isoform of nesprin-1 with a KASH domain, in developing, fetal and regenerating muscle, using a new monoclonal antibody. *BMC Cell Biol.* **2016**, *17*, 26. [[CrossRef](#)]
132. Roman, W.; Gomes, E.R. Nuclear positioning in skeletal muscle. *Semin. Cell Dev. Biol.* **2018**, *82*, 51–56. [[CrossRef](#)] [[PubMed](#)]
133. Zhou, C.; Rao, L.; Shanahan, C.M.; Zhang, Q. Nesprin-1/2: Roles in nuclear envelope organisation, myogenesis and muscle disease. *Biochem. Soc. Trans.* **2018**, *46*, 311–320. [[CrossRef](#)] [[PubMed](#)]
134. Liao, L.; Qu, R.; Ouang, J.; Dai, J. A glance at the nuclear envelope spectrin repeat protein 3. *Biomed Res. Int.* **2019**, *2019*, 1651805. [[CrossRef](#)] [[PubMed](#)]
135. Ketema, M.; Wilhelmsen, K.; Kuikman, I.; Janssen, H.; Hodzic, D.; Sonnenberg, A. Requirements for the localization of nesprin-3 at the nuclear envelope and its interaction with plectin. *J. Cell Sci.* **2007**, *120*, 3384–3394. [[CrossRef](#)]
136. Wiche, G. Role of plectin in cytoskeleton organization and dynamics. *J. Cell Sci.* **1998**, *111*, 2477–2486.
137. Staszewska, I.; Fischer, I.; Wiche, G. Plectin isoform 1-dependent nuclear docking of desmin networks affects myonuclear architecture and expression of mechanotransducers. *Hum. Mol. Genet.* **2015**, *24*, 7373–7389. [[CrossRef](#)]
138. Folker, E.S.; Östlund, C.; Luxton, G.W.G.; Worman, H.J.; Gundersen, G.G. Lamin A variants that cause striated muscle disease are defective in anchoring transmembrane actin-associated nuclear lines for nuclear movement. *Proc. Natl. Acad. Sci. USA* **2011**, *108*, 131–136. [[CrossRef](#)]
139. Ho, C.Y.; Lammerding, J. Lamins at a glance. *J. Cell Sci.* **2012**, *125*, 2087–2093. [[CrossRef](#)]
140. Hieda, M. Signal Transduction across the Nuclear envelope: Role of the LINC complex in bidirectional signaling. *Cells* **2019**, *8*, 124. [[CrossRef](#)]
141. Burke, B.; Roux, K.J. Nuclei Take a position: Managing nuclear location. *Dev. Cell* **2009**, *17*, 587–597. [[CrossRef](#)]
142. Fridolfsson, H.N.; Ly, N.; Meyerzon, M.; Starr, D.A. UNC-83 coordinates kinesin-1 and dynein activities at the nuclear envelope during nuclear migration. *Dev. Biol.* **2010**, *338*, 237–250. [[CrossRef](#)]
143. Jain, N.; Iyer, K.V.; Kumar, A.; Shivashankar, G.V. Cell geometric constraints induce modular gene-expression patterns via redistribution of HDAC3 regulated by actomyosin contractility. *Proc. Natl. Acad. Sci. USA* **2013**, *110*, 11349–11354. [[CrossRef](#)]
144. Lei, K.; Zhang, X.; Ding, X.; Guo, X.; Chen, M.; Zhu, B.; Xu, T.; Zhuang, Y.; Xu, R.; Han, M. SUN1 and SUN2 play critical but partially redundant roles in anchoring nuclei in skeletal muscle cells in mice. *Proc. Natl. Acad. Sci. USA* **2009**, *106*, 10207–10212. [[CrossRef](#)]
145. Wu, Y.K.; Umeshima, H.; Kurisu, J.; Kengaku, M. Nesprins and opposing microtubule motors generate a point force that drives directional nuclear motion in migrating neurons. *Development* **2018**, *145*, dev158782. [[CrossRef](#)] [[PubMed](#)]
146. Kengaku, M. Cytoskeletal control of nuclear migration in neurons and non-neuronal cells. *Proc. Jpn. Acad. Ser. B* **2018**, *94*, 337–349. [[CrossRef](#)]
147. Zhang, Q.; Bethmann, C.; Worth, N.F.; Davies, J.D.; Wasner, C.; Feuer, A.; Ragnauth, C.D.; Yi, Q.; Mellad, J.A.; Warren, D.T.; et al. Nesprin-1 and -2 are involved in the pathogenesis of Emery–Dreifuss muscular dystrophy and are critical for nuclear envelope integrity. *Hum. Mol. Genet.* **2007**, *16*, 2816–2833. [[CrossRef](#)] [[PubMed](#)]

148. Stroud, M.J.; Feng, W.; Zhang, J.; Veevers, J.; Fang, X.; Gerace, L.; Chen, J. Nesprin 1 α 2 is essential for mouse postnatal viability and nuclear positioning in skeletal muscle. *J. Cell Biol.* **2017**, *216*, 1915–1924. [[CrossRef](#)] [[PubMed](#)]
149. Zhou, C.; Li, C.; Zhou, B.; Sun, H.; Koullourou, V.; Holt, I.; Puckelwartz, M.J.; Warren, D.T.; Hayward, R.; Lin, Z.; et al. Novel nesprin-1 mutations associated with dilated cardiomyopathy cause nuclear envelope disruption and defects in myogenesis. *Hum. Mol. Genet.* **2017**, *26*, 2258–2276. [[CrossRef](#)]
150. Schwartz, C.; Fischer, M.; Mamchaoui, K.; Bigot, A.; Lok, T.; Verdier, C.; Duperray, A.; Michel, R.; Holt, I.; Voit, T.; et al. Lamins and nesprin-1 mediate inside-out mechanical coupling in muscle cell precursors through FHOD1. *Sci. Rep.* **2017**, *7*, 1253. [[CrossRef](#)] [[PubMed](#)]
151. Jahed, Z.; Mofrad, M.R. The nucleus feels the force, LINCed in or not! *Curr. Opin. Cell Biol.* **2019**, *58*, 114–119. [[CrossRef](#)]
152. Li, Y.; Lovett, D.; Zhang, Q.; Neelam, S.; Kuchibhotla, R.A.; Zhu, R.; Gundersen, G.G.; Lele, T.P.; Dickinson, R.B. Moving Cell boundaries drive nuclear shaping during cell spreading. *Biophys. J.* **2015**, *109*, 670–686. [[CrossRef](#)] [[PubMed](#)]
153. Szczesny, S.E.; Mauck, R.L. The Nuclear option: Evidence Implicating the cell nucleus in mechanotransduction. *J. Biomech. Eng.* **2017**, *139*, 021006. [[CrossRef](#)] [[PubMed](#)]
154. Aebi, U.; Cohn, J.; Buhle, L.; Gerace, L. The nuclear lamina is a meshwork of intermediate-type filaments. *Nature* **1986**, *323*, 560–564. [[CrossRef](#)]
155. Turgay, Y.; Eibauer, M.; Goldman, A.E.; Shimi, T.; Khayat, M.; Ben-Harush, K.; Dubrovsky-Gaup, A.; Sapra, K.T.; Goldman, R.D.; Medalia, O. The molecular architecture of lamins in somatic cells. *Nature* **2017**, *543*, 261–264. [[CrossRef](#)] [[PubMed](#)]
156. Burke, B.; Stewart, C.L. The nuclear lamins: Flexibility in function. *Nat. Rev. Mol. Cell Biol.* **2013**, *14*, 13–24. [[CrossRef](#)]
157. Simon, D.N.; Wilson, K.L. The nucleoskeleton as a genome-associated dynamic ‘network of networks’. *Nat. Rev. Mol. Cell Biol.* **2011**, *12*, 695–708. [[CrossRef](#)]
158. Korfali, N.; Wilkie, G.S.; Swanson, S.K.; Srsen, V.; de las Heras, J.; Batrakou, D.G.; Malik, P.; Zuleger, N.; Kerr, A.R.W.; Florens, L.; et al. The nuclear envelope proteome differs notably between tissues. *Nucleus* **2012**, *3*, 552–564. [[CrossRef](#)]
159. Hieda, M. Implications for diverse functions of the LINC Complexes based on the structure. *Cells* **2017**, *6*, 3. [[CrossRef](#)]
160. Kalinowski, A.; Qin, Z.; Coffey, K.; Kodali, R.; Buehler, M.J.; Lösche, M.; Dahl, K.N. Calcium causes a Conformational change in lamin A Tail domain that promotes farnesyl-mediated membrane association. *Biophys. J.* **2013**, *104*, 2246–2253. [[CrossRef](#)]
161. Osmanagic-Myers, S.; Dechat, T.; Foisner, R. Lamins at the crossroads of mechanosignaling. *Genes Dev.* **2015**, *29*, 225–237. [[CrossRef](#)] [[PubMed](#)]
162. Bianchi, A.; Manti, P.G.; Lucini, F.; Lanzuolo, C. Mechanotransduction, nuclear architecture and epigenetics in Emery Dreifuss Muscular dystrophy: Tous pour un, un pour tous. *Nucleus* **2018**, *9*, 321–335. [[CrossRef](#)] [[PubMed](#)]
163. Coffinier, C.; Jung, H.J.; Nobumori, C.; Chang, S.; Tu, Y.; Barnes, R.H., 2nd; Yoshinaga, Y.; de Jong, P.J.; Vergnes, L.; Reue, K.; et al. Deficiencies in lamin B1 and lamin B2 cause neurodevelopmental defects and distinct nuclear shape abnormalities in neurons. *Mol. Biol. Cell* **2011**, *22*, 4683–4693. [[CrossRef](#)] [[PubMed](#)]
164. Dahl, K.N. The nuclear envelope lamina network has elasticity and a compressibility limit suggestive of a molecular shock absorber. *J. Cell Sci.* **2004**, *117*, 4779–4786. [[CrossRef](#)]
165. Shimi, T.; Kittisopikul, M.; Tran, J.; Goldman, A.E.; Adam, S.A.; Zheng, Y.; Jaqaman, K.; Goldman, R.D. Structural organization of nuclear lamins A, C, B1, and B2 revealed by superresolution microscopy. *Mol. Biol. Cell* **2015**, *26*, 4075–4086. [[CrossRef](#)] [[PubMed](#)]
166. Swift, J.; Ivanovska, I.L.; Buxboim, A.; Harada, T.; Dingal, P.C.D.P.; Pinter, J.; Pajeroski, J.D.; Spinler, K.R.; Shin, J.-W.; Tewari, M.; et al. Nuclear lamin-A Scales with tissue stiffness and enhances matrix-directed differentiation. *Science* **2013**, *341*, 1240104. [[CrossRef](#)] [[PubMed](#)]
167. Buxboim, A.; Irianto, J.; Swift, J.; Athirasala, A.; Shin, J.-W.; Rehfeldt, F.; Discher, D.E. Coordinated increase of nuclear tension and lamin-A with matrix stiffness outcompetes lamin-B receptor that favors soft tissue phenotypes. *Mol. Biol. Cell* **2017**, *28*, 3333–3348. [[CrossRef](#)]
168. Guilly, C.; Burrridge, K. Nuclear mechanotransduction: Forcing the nucleus to respond. *Nucleus* **2015**, *6*, 19–22. [[CrossRef](#)]
169. Guilly, C.; Osborne, L.D.; Van Landeghem, L.; Sharek, L.; Superfine, R.; Garcia-Mata, R.; Burrridge, K. Isolated nuclei adapt to force and reveal a mechanotransduction pathway in the nucleus. *Nat. Cell Biol.* **2014**, *16*, 376–381. [[CrossRef](#)]
170. Bera, M.; Kotamarthi, H.C.; Dutta, S.; Ray, A.; Ghosh, S.; Bhattacharyya, D.; Ainaravapu, S.R.K.; Sengupta, K. Characterization of Unfolding mechanism of human lamin A Ig Fold by single-molecule force spectroscopy—Implications in EDMD. *Biochemistry* **2014**, *53*, 7247–7258. [[CrossRef](#)]
171. Buxboim, A.; Swift, J.; Irianto, J.; Spinler, K.R.; Dingal, P.C.D.P.; Athirasala, A.; Kao, Y.-R.C.; Cho, S.; Harada, T.; Shin, J.-W.; et al. Matrix Elasticity regulates lamin-A,C Phosphorylation and turnover with feedback to actomyosin. *Curr. Biol.* **2014**, *24*, 1909–1917. [[CrossRef](#)]
172. Xia, Y.; Pfeifer, C.R.; Cho, S.; Discher, D.E.; Irianto, J. Nuclear mechanosensing. *Emerg. Top. Life Sci.* **2018**, *2*, 713–725.
173. Makarov, A.A.; Zou, J.; Houston, D.R.; Spanos, C.; Solovyova, A.S.; Cardenal-Peralta, C.; Rappsilber, J.; Schirmer, E.C. Lamin A molecular compression and sliding as mechanisms behind nucleoskeleton elasticity. *Nat. Commun.* **2019**, *10*, 3056. [[CrossRef](#)] [[PubMed](#)]
174. Pajeroski, J.D.; Dahl, K.N.; Zhong, F.L.; Sammak, P.J.; Discher, D.E. Physical plasticity of the nucleus in stem cell differentiation. *Proc. Natl. Acad. Sci. USA* **2007**, *104*, 15619–15624. [[CrossRef](#)] [[PubMed](#)]

175. Guelen, L.; Pagie, L.; Brasset, E.; Meuleman, W.; Faza, M.B.; Talhout, W.; Eussen, B.H.; de Klein, A.; Wessels, L.; de Laat, W.; et al. Domain organization of human chromosomes revealed by mapping of nuclear lamina interactions. *Nature* **2008**, *453*, 948–951. [[CrossRef](#)] [[PubMed](#)]
176. Miroshnikova, Y.A.; Nava, M.M.; Wickström, S.A. Emerging roles of mechanical forces in chromatin regulation. *J. Cell Sci.* **2017**, *130*, 2243–2250. [[CrossRef](#)]
177. Le, H.Q.; Ghatak, S.; Yeung, C.-Y.C.; Tellkamp, F.; Günschmann, C.; Dieterich, C.; Yeroslaviz, A.; Habermann, B.; Pombo, A.; Niessen, C.M.; et al. Mechanical regulation of transcription controls Polycomb-mediated gene silencing during lineage commitment. *Nat. Cell Biol.* **2016**, *18*, 864–875. [[CrossRef](#)]
178. Robson, M.I.; de las Heras, J.I.; Czapiewski, R.; Lê Thành, P.; Booth, D.G.; Kelly, D.A.; Webb, S.; Kerr, A.R.W.; Schirmer, E.C. Tissue-specific Gene repositioning by muscle nuclear membrane proteins enhances repression of critical developmental genes during myogenesis. *Mol. Cell* **2016**, *62*, 834–847. [[CrossRef](#)]
179. Donnalaja, F.; Carnevali, F.; Jacchetti, E.; Raimondi, M.T. Lamin A/C Mechanotransduction in laminopathies. *Cells* **2020**, *9*, 1306. [[CrossRef](#)]
180. Gruenbaum, Y.; Foisner, R. Lamins: Nuclear Intermediate filament proteins with fundamental functions in nuclear mechanics and genome regulation. *Annu. Rev. Biochem.* **2015**, *84*, 131–164. [[CrossRef](#)]
181. Janin, A.; Gache, V. Nesprins and Lamins in health and diseases of cardiac and skeletal muscles. *Front. Physiol.* **2018**, *9*, 1277. [[CrossRef](#)]
182. Brull, A.; Morales Rodriguez, B.; Bonne, G.; Muchir, A.; Bertrand, A.T. The Pathogenesis and therapies of striated muscle laminopathies. *Front. Physiol.* **2018**, *9*, 1533. [[CrossRef](#)]
183. Quijano-Roy, S.; Mbielleu, B.; Bönnemann, C.G.; Jeannot, P.-Y.; Colomer, J.; Clarke, N.F.; Cuisset, J.-M.; Roper, H.; De Meirleir, L.; D’Amico, A.; et al. De novo LMNA mutations cause a new form of congenital muscular dystrophy. *Ann. Neurol.* **2008**, *64*, 177–186. [[CrossRef](#)] [[PubMed](#)]
184. Lammerding, J.; Schulze, P.C.; Takahashi, T.; Kozlov, S.; Sullivan, T.; Kamm, R.D.; Stewart, C.L.; Lee, R.T. Lamin A/C deficiency causes defective nuclear mechanics and mechanotransduction. *J. Clin. Investig.* **2004**, *113*, 370–378. [[CrossRef](#)] [[PubMed](#)]
185. Lammerding, J.; Hsiao, J.; Schulze, P.C.; Kozlov, S.; Stewart, C.L.; Lee, R.T. Abnormal nuclear shape and impaired mechanotransduction in emerin-deficient cells. *J. Cell Biol.* **2005**, *170*, 781–791. [[CrossRef](#)] [[PubMed](#)]
186. Hale, C.M.; Shrestha, A.L.; Khatau, S.B.; Stewart-Hutchinson, P.J.; Hernandez, L.; Stewart, C.L.; Hodzic, D.; Wirtz, D. Dysfunctional connections between the nucleus and the actin and microtubule networks in laminopathic models. *Biophys. J.* **2008**, *95*, 5462–5475. [[CrossRef](#)]
187. Zhang, Q.; Tamashunas, A.C.; Agrawal, A.; Torbati, M.; Katiyar, A.; Dickinson, R.B.; Lammerding, J.; Lele, T.P. Local, transient tensile stress on the nuclear membrane causes membrane rupture. *Mol. Biol. Cell* **2019**, *30*, 899–906. [[CrossRef](#)]
188. Earle, A.J.; Kirby, T.J.; Fedorchak, G.R.; Isermann, P.; Patel, J.; Iruvanti, S.; Moore, S.A.; Bonne, G.; Wallrath, L.L.; Lammerding, J. Mutant lamins cause nuclear envelope rupture and DNA damage in skeletal muscle cells. *Nat. Mater.* **2020**, *19*, 464–473. [[CrossRef](#)]
189. Solovei, I.; Wang, A.S.; Thanisch, K.; Schmidt, C.S.; Krebs, S.; Zwerger, M.; Cohen, T.V.; Devys, D.; Foisner, R.; Peichl, L.; et al. LBR and Lamin A/C sequentially tether peripheral heterochromatin and inversely regulate differentiation. *Cell* **2013**, *152*, 584–598. [[CrossRef](#)]
190. Mattout, A.; Pike, B.L.; Towbin, B.D.; Bank, E.M.; Gonzalez-Sandoval, A.; Stadler, M.B.; Meister, P.; Gruenbaum, Y.; Gasser, S.M. An EDMD mutation in *C. elegans* Lamin blocks muscle-specific gene relocation and compromises muscle integrity. *Curr. Biol.* **2011**, *21*, 1603–1614. [[CrossRef](#)]
191. Emerson, L.J.; Holt, M.R.; Wheeler, M.A.; Wehnert, M.; Parsons, M.; Ellis, J.A. Defects in cell spreading and ERK1/2 activation in fibroblasts with lamin A/C mutations. *Biochimica et Biophysica Acta (BBA) Mol. Basis Dis.* **2009**, *1792*, 810–821. [[CrossRef](#)]
192. Bertrand, A.T.; Ziaei, S.; Ehret, C.; Duchemin, H.; Mamchaoui, K.; Bigot, A.; Mayer, M.; Quijano-Roy, S.; Desguerre, I.; Lainé, J.; et al. Cellular microenvironments reveal defective mechanosensing responses and elevated YAP signaling in LMNA-mutated muscle precursors. *J. Cell Sci.* **2014**, *127*, 2873–2884. [[CrossRef](#)]
193. Furusawa, T.; Rochman, M.; Taher, L.; Dimitriadis, E.K.; Nagashima, K.; Anderson, S.; Bustin, M. Chromatin decompaction by the nucleosomal binding protein HMGN5 impairs nuclear sturdiness. *Nat. Commun.* **2015**, *6*, 6138. [[CrossRef](#)] [[PubMed](#)]
194. Krause, M.; Te Riet, J.; Wolf, K. Probing the compressibility of tumor cell nuclei by combined atomic force-confocal microscopy. *Phys. Biol.* **2013**, *10*, 065002. [[CrossRef](#)]
195. Lherbette, M.; Dos Santos, Á.; Hari-Gupta, Y.; Fili, N.; Toseland, C.P.; Schaap, I.A.T. Atomic force microscopy micro-rheology reveals large structural inhomogeneities in single cell-nuclei. *Sci. Rep.* **2017**, *7*, 8116. [[CrossRef](#)] [[PubMed](#)]
196. Schäpe, J.; Prausse, S.; Radmacher, M.; Stick, R. Influence of lamin A on the mechanical properties of amphibian oocyte nuclei measured by atomic force microscopy. *Biophys. J.* **2009**, *96*, 4319–4325. [[CrossRef](#)] [[PubMed](#)]
197. Hubner, M.R.; Spector, D.L. Chromatin dynamics. *Annu. Rev. Biophys.* **2010**, *39*, 471–489. [[CrossRef](#)]
198. Sexton, T.; Schober, H.; Fraser, P.; Gasser, S.M. Gene regulation through nuclear organization. *Nat. Struct. Mol. Biol.* **2007**, *14*, 1049–1055. [[CrossRef](#)]
199. Jost, K.L.; Rottach, A.; Mildner, M.; Bertulat, B.; Becker, A.; Wolf, P.; Sandoval, J.; Petazzi, P.; Huertas, D.; Esteller, M.; et al. Generation and characterization of rat and mouse monoclonal antibodies specific for MeCP2 and their use in X-inactivation studies. *PLoS ONE* **2011**, *6*, e26499. [[CrossRef](#)]

200. Peric-Hupkes, D.; van Steensel, B. Role of the Nuclear lamina in genome organization and gene expression. *Cold Spring Harb. Symp. Quant. Biol.* **2010**, *75*, 517–524. [[CrossRef](#)]
201. Schubeler, D.; Francastel, C.; Cimbora, D.M.; Reik, A.; Martin, D.I.; Groudine, M. Nuclear localization and histone acetylation: A pathway for chromatin opening and transcriptional activation of the human beta-globin locus. *Genes Dev.* **2000**, *14*, 940–950. [[PubMed](#)]
202. Thomas, C.H.; Collier, J.H.; Sfeir, C.S.; Healy, K.E. Engineering gene expression and protein synthesis by modulation of nuclear shape. *Proc. Natl. Acad. Sci. USA* **2002**, *99*, 1972–1977. [[CrossRef](#)]
203. Heo, S.J.; Nerurkar, N.L.; Baker, B.M.; Shin, J.W.; Elliott, D.M.; Mauck, R.L. Fiber stretch and reorientation modulates mesenchymal stem cell morphology and fibrous gene expression on oriented nanofibrous microenvironments. *Ann. Biomed. Eng.* **2011**, *39*, 2780–2790. [[CrossRef](#)]
204. Driscoll, T.P.; Cosgrove, B.D.; Heo, S.J.; Shurden, Z.E.; Mauck, R.L. Cytoskeletal to Nuclear strain transfer regulates YAP Signaling in mesenchymal stem cells. *Biophys. J.* **2015**, *108*, 2783–2793. [[CrossRef](#)]
205. Banerjee, I.; Zhang, J.; Moore-Morris, T.; Pfeiffer, E.; Buchholz, K.S.; Liu, A.; Ouyang, K.; Stroud, M.J.; Gerace, L.; Evans, S.M.; et al. Targeted ablation of nesprin 1 and nesprin 2 from murine myocardium results in cardiomyopathy, altered nuclear morphology and inhibition of the biomechanical gene response. *PLoS Genet.* **2014**, *10*, e1004114. [[CrossRef](#)]
206. Martins, R.P.; Finan, J.D.; Guilak, F.; Lee, D.A. Mechanical regulation of nuclear structure and function. *Annu. Rev. Biomed. Eng.* **2012**, *14*, 431–455. [[CrossRef](#)]
207. Jakkaraju, S.; Zhe, X.; Pan, D.; Choudhury, R.; Schuger, L. TIPs are tension-responsive proteins involved in myogenic versus adipogenic differentiation. *Dev. Cell* **2005**, *9*, 39–49. [[CrossRef](#)] [[PubMed](#)]
208. Tajik, A.; Zhang, Y.; Wei, F.; Sun, J.; Jia, Q.; Zhou, W.; Singh, R.; Khanna, N.; Belmont, A.S.; Wang, N. Transcription upregulation via force-induced direct stretching of chromatin. *Nat. Mater.* **2016**, *15*, 1287–1296. [[CrossRef](#)]
209. Folker, E.S.; Baylies, M.K. Nuclear positioning in muscle development and disease. *Front. Physiol.* **2013**, *4*. [[CrossRef](#)] [[PubMed](#)]
210. Metzger, T.; Gache, V.; Xu, M.; Cadot, B.; Folker, E.S.; Richardson, B.E.; Gomes, E.R.; Baylies, M.K. MAP and kinesin-dependent nuclear positioning is required for skeletal muscle function. *Nature* **2012**, *484*, 120–124. [[CrossRef](#)] [[PubMed](#)]
211. Azevedo, M.; Baylies, M.K. Getting into position: Nuclear Movement in muscle cells. *Trends Cell Biol.* **2020**, *30*, 303–316. [[CrossRef](#)]
212. Romero, N.B. Centronuclear myopathies: A widening concept. *Neuromuscul. Disord.* **2010**, *20*, 223–228. [[CrossRef](#)] [[PubMed](#)]

Article

Lamin Mutations Cause Increased YAP Nuclear Entry in Muscle Stem Cells

Daniel J. Owens ^{1,2} , Martina Fischer ¹, Saline Jabre ¹, Sophie Moog ³, Kamel Mamchaoui ⁴, Gillian Butler-Browne ¹ and Catherine Coirault ^{1,*} 

¹ INSERM UMRS_974, Centre for Research in Myology, Sorbonne Université, 75013 Paris, France; D.J.Owens@ljmu.ac.uk (D.J.O.); mfischer.p@googlemail.com (M.F.); saline.j.jabr@net.usek.edu.lb (S.J.); gillian.butler-browne@upmc.fr (G.B.-B.)

² Research Institute for Sport and Exercise Science, Liverpool John Moores University, Liverpool L3 3AF, UK

³ Inovarion, 75013 Paris, France; sophie.moog@inovarion.com

⁴ Association Institut de Myology, 75013 Paris, France; kamel.mamchaoui@upmc.fr

* Correspondence: catherine.coirault@inserm.fr; Tel.: +33-142-16-57-08

Received: 26 February 2020; Accepted: 24 March 2020; Published: 27 March 2020



Abstract: Mutations in the *LMNA* gene, encoding the nuclear envelope A-type lamins, are responsible for muscular dystrophies, the most severe form being the *LMNA*-related congenital muscular dystrophy (L-CMD), with severe defects in myonucleus integrity. We previously reported that L-CMD mutations compromise the ability of muscle stem cells to modulate the yes-associated protein (YAP), a pivotal factor in mechanotransduction and myogenesis. Here, we investigated the intrinsic mechanisms by which lamins influence YAP subcellular distribution, by analyzing different conditions affecting the balance between nuclear import and export of YAP. In contrast to wild type (WT) cells, *LMNA*^{DK32} mutations failed to exclude YAP from the nucleus and to inactivate its transcriptional activity at high cell density, despite activation of the Hippo pathway. Inhibiting nuclear pore import abolished YAP nuclear accumulation in confluent mutant cells, thus showing persistent nuclear import of YAP at cell confluence. YAP deregulation was also present in congenital myopathy related to nesprin-1^{KASH1} mutation, but not in cells expressing the *LMNA*^{H222P} mutation, the adult form of lamin-related muscle dystrophy with reduced nuclear deformability. In conclusion, our data showed that L-CMD mutations increased YAP nuclear localization via an increased nuclear import and implicated YAP as a pathogenic contributor in muscle dystrophies caused by nuclear envelope defects.

Keywords: lamins; congenital myopathy; nucleo-cytoskeletal translocation; nuclear envelope

1. Introduction

The nuclear lamins A/C are type V intermediate filament proteins encoded by the *LMNA* gene. Lamins form complexes with other proteins of the nuclear membrane to influence mechanical cues and signaling pathways crucial for cellular proliferation and differentiation [1]. Mutations in the *LMNA* gene cause laminopathies, a highly heterogeneous group of disorders, including muscular dystrophies and cardiomyopathies [2,3]. The disease mechanisms underlying *LMNA*-related muscular dystrophy remains somewhat elusive.

There is clear evidence that A-type lamins and nuclear envelope proteins play a critical role in responding to mechanical cues from the extracellular matrix by adjusting the cytoskeleton and nuclear stiffness with the stiffness of the tissue microenvironments [4,5]. Structural changes in lamin A/C can also affect several signaling pathways, by altering either direct or indirect interactions of signaling molecules with A-type lamins [6,7]. Lamins A/C have already been shown to regulate the nuclear translocation and downstream signaling of the mechanosensitive transcription factor megakaryoblastic

leukemia 1 (MKL1), a myocardin family member pivotal in cardiac development and function [8]. In muscle stem cells (MuSCs) from patients carrying A-type lamin mutations, we recently reported an impaired ability to sense matrix stiffness [9] and to withstand mechanical stretching of the extracellular matrix, causing aberrant regulation of the yes-associated protein (YAP) [10].

YAP is a transcriptional co-regulator that is modulated by diverse biomechanical signals and transduces them into cell-specific transcriptional responses, regulating cell proliferation and survival, organ growth, stem-cell renewal, and cell differentiation [11]. A major mechanism of YAP regulation occurs at the level of its subcellular localization, as YAP nuclear accumulation promotes target gene transcription and cell proliferation (reviewed in [11,12]). After phosphorylation by LATS1/2 kinase, YAP binds to 14–3–3 proteins, leading to its cytoplasmic retention and degradation (reviewed in [11,12]), and favoring skeletal muscle differentiation [12].

A-type lamins influence the localization and transcriptional activity of YAP [10]. It has been shown that lamin-A overexpression decreases both total YAP levels and nuclear localization in mesenchymal stem cells [5]. In contrast, increased YAP nuclear localization and activity in combination with reduced lamin levels is observed in cancers of many organ types (reviewed in [13]), as well as in *LMNA* mutant MuSCs cultured on soft matrices [10]. However, it remains unclear as to how mutant lamins cause defects in the YAP signaling pathway. Abnormal nuclear shape is observed in diseases where the A-type lamins are altered, including cancer [14,15] and laminopathies [16]. Altered nuclear morphology can in turn increase the rate of YAP import [17,18], by opening up nuclear pores [17]. One can hypothesize that A-type lamin mutations, responsible for severe skeletal muscle laminopathies, will cause an increase YAP nuclear localization because of an increased nuclear import.

To test this hypothesis, we investigated YAP subcellular distribution/activity in MuSCs with A-type lamin mutations responsible for severe congenital muscle dystrophy (L-CMD) in different conditions affecting the balance between nuclear import and export of YAP. Our study provides evidence that A-type lamin mutations impair YAP regulation by increasing the nuclear import of YAP. Intriguingly, we also found YAP nuclear accumulation in cells with nesprin-1 mutation responsible for a congenital myopathy and associated with defects in nuclear morphology [9,19], but not in cells carrying the *LMNA*^{H222P} mutation responsible for a less severe form of the disease and much milder nuclear envelope structural defects. These findings support a causative role of nuclear envelope defects in abnormal YAP signaling and implicated YAP as a pathogenic contributor in the severity of muscle dystrophies caused by nuclear envelope mutations. Overall, our study gains insight into broader questions of how lamins and nuclear shape impact cellular function.

2. Materials and Methods

2.1. Human Cells and Cell Culture

We obtained muscle biopsies from the Bank of Tissues for Research (Myobank, a partner in the EU network EuroBioBank) in accordance with European recommendations and French legislation. All patients provided written informed consent and experimental protocols were approved by our institution (INSERM) (approval number AC-2013-1868, 28 May 2014 and AC-2019-3502, 2 Dec 2019). Experiments were performed using immortalized L-CMD human myoblasts carrying a heterozygous *LMNA*_{Ac.94_96delAAG}, p.Lys32del (referred to as Δ K32), *LMNA* p.Arg249Trp (referred to as R249W), or *LMNA* p.Leu380Ser (referred to as L380S) mutation. Immortalized human myoblasts carrying SYNE-1 homozygous c.23560 G<T, p.E7854X leading to a stop codon in exon 133 and deletion of the carboxy-terminal KASH domain (referred to as nesprin-1 ^{Δ KASK}) were also analyzed, given that this mutation alters the nuclear shape of MuSCs [9,20]. Immortalized myoblasts, obtained from two healthy control subjects without muscular disorders, were used as controls (hereafter referred to wild-type, WT).

We also analyzed myogenic cells derived from fibroblasts obtained from a patient with classical form of EDMD and carrying the *LMNA* p.H222P mutation (*LMNA*^{H222P}), and from a control

patient [21]. Fibroblasts were obtained from skin biopsies and immortalized as previously described [22]. Doxycycline-inducible Myod1 lentivirus was used to induce myogenic conversion [23].

Following muscular biopsy, MuSCs were immortalized and cultured in growth medium consisting of 1 vol 199 Medium /4 vol DMEM (Life Technologies, Carlsbad, CA, USA) supplemented with 20% fetal calf serum (Life Technologies), 5 ng/mL hEGF (Life Technologies), 0.5 ng/mL β FGF, 0.1 mg/mL Dexamethasone (Sigma-Aldrich, St. Louis, MO, USA), 50 μ g/mL fetuin (Life Technologies), 5 μ g/mL insulin (Life Technologies), and 50 mg/mL Gentamycin (Gibco™, Life Technologies, Carlsbad, CA, USA). MyoD-transfected fibroblasts were cultured in a proliferation medium consisting of DMEM, supplemented with 10% fetal bovine serum (Life Technologies) and 0.1% gentamycin (Invitrogen, Carlsbad, CA, USA).

All cells were cultured on classic glass or plastic substrates. In addition, micro patterned glass slides with round islands of 700 μ m² (4D Cell, Montreuil, France) were coated with fibronectin and cells were seeded in a 200 μ L drop at the center of the dish. After attachment, the wells containing the micro patterned slides were filled with proliferative medium for 24 h.

2.2. Drug Treatments

Importazole, a drug that blocks importin- β -dependent nuclear import [24], Leptomycin B, a drug that blocks CRM1-dependent nuclear export [25] or Dasatinib, Src-family kinase inhibitor drugs were diluted to final concentration of 40 μ M, 100 nM, or 100 nM, respectively, for 24, 24, or 1 h. Latrunculin-A (Lat A, Sigma-Aldrich) or Cytochalasin D (Sigma-Aldrich) were diluted to final concentration of 2.0 and 1 μ M, respectively, for 20 or 30 min. Vehicle control experiments using appropriate doses and time of dimethylsulfoxide (DMSO) were used to assess the effects of specific drugs.

2.3. Luciferase Reporter Assays

MuSCs were transfected with Lipofectamine® 2000 (Invitrogen) reagents in growth media without antibiotics according to manufacturer's instructions. TBS (Tead binding sequence: 14 times GGAATG)-Firefly Luciferase reporter constructs were used at a 1:5 ratio to the co-reporter vector for the weak constitutive expression of wild-type Renilla luciferase (pRL-TK, Promega GmbH, Mannheim, Germany). Transfected cells were seeded onto 24-, 48-, or 96-well plates and recovered overnight in growth medium. For the luciferase assay, cells were cultivated for 24 h after transfection under the stated conditions. The cells were lysed with passive lysis buffer (PJK GmbH, Kleinblittersdorf, Germany) and activity of the reporter was quantified by addition of firefly Luciferase substrate Beetle Juice (PJK GmbH). The activity of Renilla luciferase was quantified by addition of Renilla Juice (PJK GmbH) and measuring luciferase activity with Mithras LB940 Luminometer (Wildbad, Germany). Three separate experiments were performed per condition.

2.4. Immunocytochemistry and Image Analysis

MuSCs were fixed for 5 min with 4% formaldehyde, permeabilized with 0.1% Triton X100, and blocked with 10% bovine serum albumin (BSA) diluted in PBS. Cells were stained with Phalloidin-Alexa 568 to label F-actin (Interchim, Montluçon, France). The following primary antibodies were used for immunostaining: anti-Yes-associated protein (YAP)/transcriptional coactivator with PDZ-binding motif (TAZ) (Santa-Cruz, Dallas, TX, USA, sc-10119s), anti-phosphorylated Ser127 YAP (p^{S127}-YAP) (Cell Signaling, Danvers, MA, USA, cs-4911), and anti-phosphorylated Tyr357-YAP (p^{Y357}-YAP) (Abcam, Paris, France, ab62751). Secondary antibodies (Life Technologies, Saint-Aubin, France; 1/500) were Alexa Fluor 488 donkey anti-mouse IgG or Alexa Fluor 488 donkey anti-rabbit IgG. Nuclei were stained with Hoechst (ThermoFischer, Carlsbad, CA, USA) and Mowiol was used as mounting medium. Confocal images were taken with an Olympus FV 1200 (Olympus, Hamilton, Bermuda) and a laser-scanning microscopy Nikon Ti2 coupled to a Yokogawa CSU-W1 head (Nikon, Tokyo, Japan).

All image analyses were performed using Fiji software (NIH Image, version 1.51). For immunostained cells, Z-stacks of images were acquired for each channel, and the middle confocal

slice was chosen from the images of the nucleus detected in the Hoechst channel. On the corresponding slice in the YAP channel, the average fluorescence intensity in the nucleus and just outside the nucleus (cytoplasm) was measured to determine the nuclear/cytoplasmic ratio.

2.5. SDS-PAGE and Protein Analysis

Cells were lysed in total protein extraction buffer (50 mM Tris-HCl, pH 7.5, 2% SDS, 250 mM sucrose, 75 mM urea, 1 mM DTT) with added protease inhibitors (25 µg/mL Aprotinin, 10 µg/mL Leupeptin, 1 mM 4-[2-aminoethyl]-benzene sulfonylfluoride hydrochloride, and 2 mM Na₃VO₄) or directly in 2× Laemmli buffer. Protein lysates were separated by SDS-PAGE and transferred on PVDF or nitrocellulose membranes. After blocking with bovine serum albumin, membranes were incubated with anti-YAP (Santa-Cruz, CA, USA, sc-10119), anti-p^{S127}-YAP (Cell Signaling, Danvers, MA, USA, cs-4911), and anti-p^{Y357}-YAP (Abcam, Paris, France, ab62751) or anti-GAPDH (Cell Signaling, cs-2118). Goat anti-mouse, goat anti-rat, or donkey anti-goat HRP conjugates were used for HRP-based detection. Detection of adsorbed HRP-coupled secondary antibodies was performed by ECL reaction with Immobilon Western Chemiluminescent HRP Substrate (Millipore, Billerica, MA, USA). HRP signals were detected using a CCD-based detection system (Vilber Lourmat, Marne-La-Vallée, France) or a G-box system with GeneSnap software (Ozyme, Saint-Quentin, France). Membranes subjected to a second round of immunoblotting were stripped with stripping buffer (62.5 mM Tris-HCl pH 6.8, 2% sodium dodecyl sulfate (SDS), 100 mM β-mercaptoethanol) and incubated at 55 °C for 30 min with mild shaking before excessive washing with deionized water and re-blocking. Quantification was performed using ImageJ (NIH Image).

2.6. Quantification of Gene Expression

The mRNA was isolated from cell lysates using the RNeasy mini kit (Qiagen, Hilden, Germany) with the Proteinase K step, according to the manufacturer instructions. The complementary DNA (cDNA) was transcribed by SuperscriptIII (ThermoFischer, Carlsbad, CA, USA). Gene expression was quantified by using PerfeCTa-SYBR[®]Green SuperMix (Quanta, Biosciences, Gaithersburg, MD, USA) with the help of LightCycler 480 II (Roche Diagnostics GmbH, Mannheim, Germany). The primers were designed by Primer-BLAST (NCBI) and synthesized by Eurogentec (Liège, Belgium). Expression of all target genes was normalized to the expression of the reference gene RPLP0. Primer sequences are listed in Table 1.

Table 1. Primer sequences.

Gene name	Abbreviation	Forward/Reverse	Sequence
Human Yes-associated protein 1	hYAP1	fw rev	GCTACAGTGTCCCTCGAACC CCGGTGCAATGTCTCCTTA
Human Connective tissue growth factor	h-CTGF	fw rev	ACCGACTGGAAGACACGTTTG CCAGGTCAGCTTCGCAAGG
Human Connective tissue growth factor	h-RPLP0	fw rev	CTCCAAGCAGATGCAGCAGA ATAGCCTTGCGCATCATGGT
Human Glyceraldehyde 3-phosphate dehydrogenase	h-GAPDH	fw rev	TGC-CAT-GTA-GAC-CCC-TTG-AA TGG-TTG-AGC-ACA-GGG-TAG-TT
Human Myosin light chain 9	h-Myl9	fw rev	CGA-ATA-CCT-GGA-GGG-CAT-GAT AAA-CCT-GAG-GCT-TCC-TCG-TC

2.7. Statistical Analysis

Graphpad Prism (Graphpad Software, La Jolla, CA, USA) was used to calculate and plot mean and standard error of the mean (SEM). Statistical significances were assessed by ANOVA followed by Bonferroni or two-tailed unpaired *t*-tests. Differences between conditions were considered significant at *p* < 0.05. Figures were plotted with Graphpad Prism.

3. Results

3.1. Impaired Yes-Associated Protein (YAP) Nuclear Exclusion in Confluent LMNA Mutant Muscle Stem Cells (MuSCs)

Wild-type (WT) MuSCs were plated either at low (10,000 cells/cm²) or high (40,000 cells/cm²) density and stained for YAP localization (Figure 1A,B). At low density, YAP was predominantly localized to the nucleus (Figure 1A,B). However, at high density conditions, WT cells showed predominantly cytoplasmic YAP, confirming previous reports for other cell types [26–28]. Similar YAP localization was observed in cells with the *LMNA*^{H222P} mutation (Figure S1A,B) As expected, inhibition of CRM1-dependent nuclear export using Leptomycin B maintained preferential YAP nuclear distribution in confluent WT cells (Figure S2A).

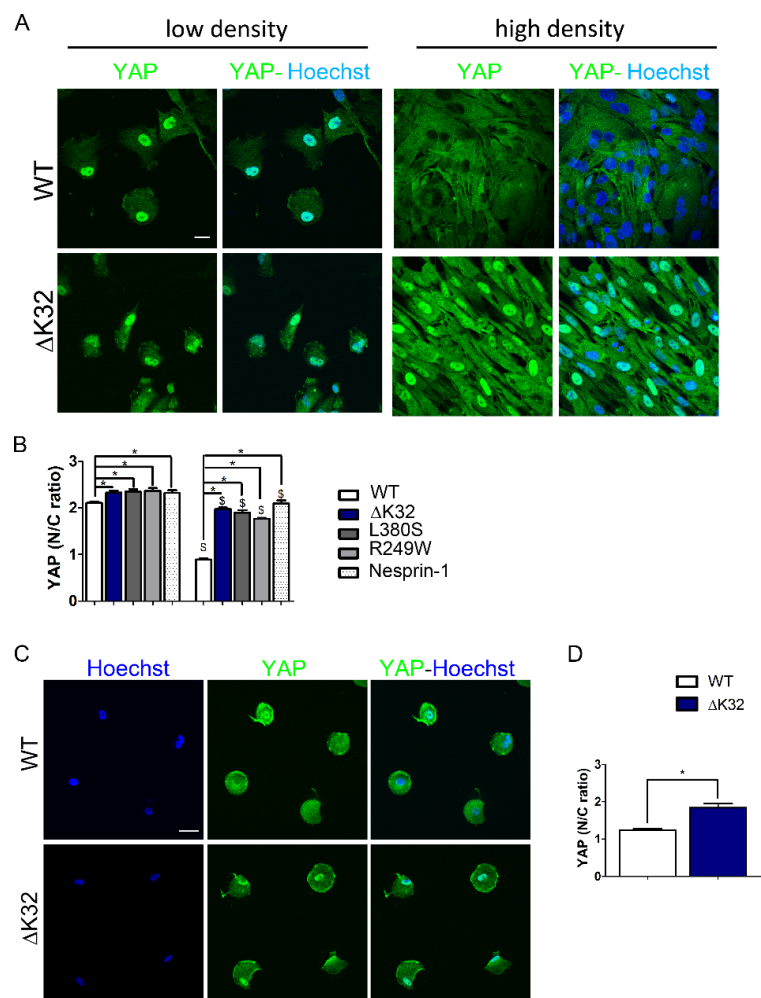


Figure 1. Modulation of yes-associated protein (YAP) localization in wild-type (WT) and mutant muscle stem cells (MuSCs). (A) Confocal images of YAP (green) in WT and *LMNA*^{ΔK32} mutant MuSCs cultured in low and high density conditions. Nuclei are stained with Hoechst (blue). Scale bar: 20 μm. (B) Quantification of YAP nucleo-cytoplasmic (N/C) ratio in WT, *LMNA*^{ΔK32}, *LMNA*^{L380S}, *LMNA*^{R249W}, and nesprin-1^{KASK} mutant MuSCs. Pooled values of WT (WT1 and WT2) are presented. Values are expressed as mean ± SEM, *n* = 200 cells for each cell line. * *p* < 0.05 vs WT; \$ < 0.05 vs. corresponding sparse condition. (C) Micro-patterning modulation of YAP. Confocal images of YAP (green) in WT and *LMNA*^{ΔK32} cells cultured on small ECM substrate that limits cell spreading. Nuclei are stained with Hoechst (blue). Scale bar: 30 μm. (D) Quantification of YAP nucleo-cytoplasmic (N/C) ratio on small ECM substrates. Values are expressed as mean ± SEM, *n* ≥ 62 cells for each cell line. * *p* < 0.05 vs. WT.

Interestingly, *LMNA* mutant cells plated at high density showed impaired density-dependent YAP subcellular localization and failed to exclude YAP from the nucleus (Figure 1A,B and Figure S2B).

Lamin A/C's are linked to the outer nuclear membrane protein nesprin-1 via SUN proteins in the lumen of the nuclear membrane. Nesprin-1^{KASK} mutation causes congenital myopathy and is also known to affect the nuclear shape [9,19]. Interestingly, nesprin-1^{KASK} cells displayed preferential nuclear YAP at high cell density (Figure 1B). Together, these findings revealed a striking correlation between the YAP mislocalization observed in vitro and the severity of the diseases.

Apart from cell–cell contacts, mechanical environments characterized by cell morphology and actin contractility regulate YAP nuclear localization [28]. Small cell surface adhesion is a known determinant for YAP nuclear exclusion [28]. Accordingly, WT cells on round micro-patterned surfaces of 700 μm^2 displayed low nuclear staining of YAP (Figure 1C,D). In contrast, YAP was preferentially nuclear in *LMNA* ^{ΔK32} cells cultured on small ECM substrates (Figure 1C,D). However, at low density, treatment with LatA induced YAP exclusion from the nucleus both in *LMNA* ^{ΔK32} mutant and WT cells (Figure S2C), thus supporting a dominant regulation of YAP localization by actin polymerization.

3.2. Phosphorylated Ser127-YAP Accumulates in the Nucleus of *LMNA* Mutated Muscle Stem Cells (MuSCs)

YAP phosphorylation on Ser 127 residue by LATS1/2 allows interaction with 14–3–3 protein and thereby nuclear exclusion of YAP [29]. We thus asked whether persistent nuclear localization in *LMNA* ^{ΔK32} could be mediated by impaired LATS1/2 activity.

We found that under high density conditions *LMNA* ^{ΔK32} cells accumulated p^{S127}-YAP in the nucleus, in contrast to WT cells (Figure 2A,B). Interestingly, cell treatment with cytochalasin D a drug known to activate the Hippo pathway, increased the intensity of p^{S127}YAP staining (Figure S3), thus supporting the specificity of the p^{S127}-YAP staining.

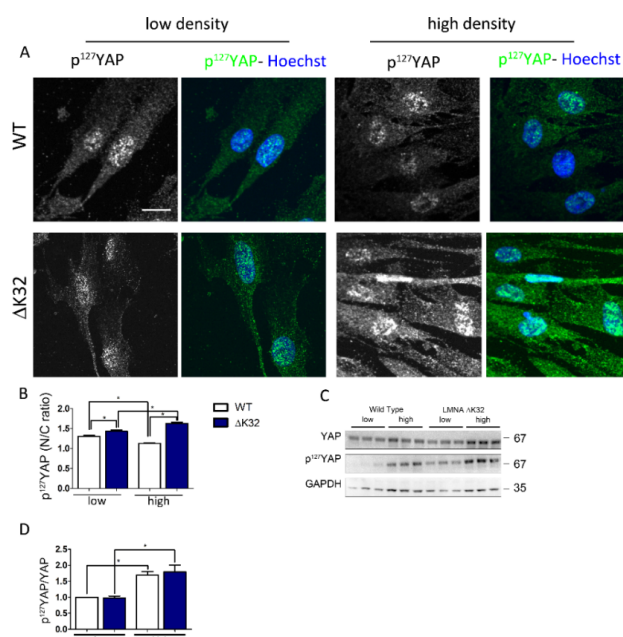


Figure 2. p^{S127}-YAP accumulates in the nucleus of *LMNA* ^{ΔK32} MuSCs. (A) Confocal images of p^{S127}-YAP (green), in WT and *LMNA* ^{ΔK32} mutant MuSCs cultured at low and high density conditions. Nuclei are stained with Hoechst (blue). Scale bar: 20 μm . (B) Quantification of p^{S127}-YAP nucleo-cytoplasmic (N/C) ratio. Values are expressed as mean \pm SEM, $n = 150$ cells for each cell line. * $p < 0.005$ compared with WT. (C) Representative Western-blot of YAP, p^{S127}-YAP, and GAPDH in WT and *LMNA* ^{ΔK32} MuSCs plated at low and high cell density. (D) Quantification of p^{S127}-YAP/YAP protein levels in low and high density conditions, expressed in arbitrary units (a.u.). GAPDH was used as a loading control. Pooled values of WT (WT1 and WT2) are presented. Values are mean \pm SEM, $n \geq 4$ per conditions. * $p < 0.005$ compared with WT.

At low density, the amount of p^{S127}-YAP did not differ between WT and *LMNA*^{ΔK32}, and the level of p^{S127}-YAP and the p^{S127}-YAP/YAP ratio significantly increase with cell density in both cell lines (Figure 1C,D). This is in line with data reporting a cell density-dependent activation of the Hippo pathway [26].

3.3. Src-Dependent Tyr Phosphorylation of YAP is Activated in *LMNA*^{ΔK32} MuSCs

Aside from p^{S127}-YAP, tyrosine phosphorylation of YAP by Src-kinase family modulates the transcriptional activity of YAP and indirectly its localization [30]. In both WT and *LMNA*^{ΔK32} cells, p^{Y357}-YAP was predominantly localized to the nucleus in low density conditions (Figure 3A,B).

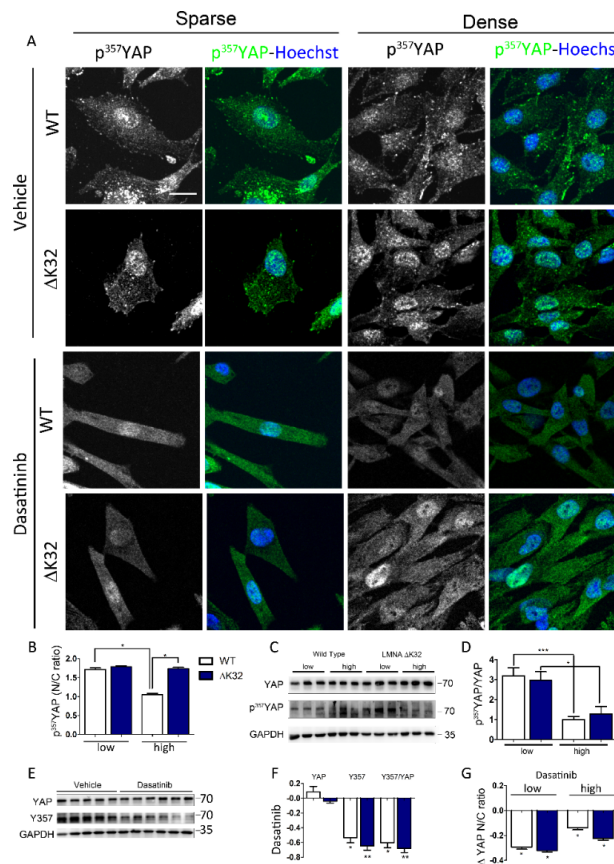


Figure 3. Y357 phosphorylation of YAP in WT and *LMNA* mutated MuSCs. (A) Confocal images of p^{Y357}-YAP (green) in WT and *LMNA*^{ΔK32} mutant MuSCs cultured in low and high density conditions, at baseline and after treatment with Dasatinib. Nuclei are stained with Hoechst (blue). Scale bar: 20 μm. (B) Quantification of p^{Y357}-YAP nucleo-cytoplasmic (N/C) ratio. Values are expressed as mean ± SEM, *n* = 150 cells for each cell line. (C) Representative Western-blot of YAP, p^{Y357}-YAP, and GAPDH in WT and *LMNA*^{ΔK32} MuSCs plated at low and high cell density. (D) Quantification of p^{Y357}-YAP/YAP protein levels in low and high density conditions, expressed in arbitrary units (a.u.). GAPDH was used as a loading control. Pooled values of WT (WT1 and WT2) are presented. Values are mean ± SEM, *n* ≥ 4 per conditions. * *p* < 0.005, ** *p* < 0.01, *** *p* < 0.001 compared with WT. (E) Representative Western-blot of YAP, p^{Y357}-YAP, and GAPDH in WT and *LMNA*^{ΔK32} MuSCs treated with vehicle or Dasatinib. (F) Quantification of YAP, p^{Y357}-YAP, and p^{Y357}-YAP/YAP protein levels after treatment with Dasatinib. Values are expressed as percent change of values obtained without treatment. GAPDH was used as a loading control. Pooled values of WT (WT1 and WT2) are presented. Values are mean ± SEM, *n* ≥ 4 per conditions. * *p* < 0.005, ** *p* < 0.01, compared with WT. (G) Quantification of p^{Y357}-YAP nucleo-cytoplasmic (N/C) ratio after Dasatinib treatment expressed as a fraction of control value obtained in sparse or dense conditions before Dasatin treatment. Values are expressed as mean ± SEM, *n* ≥ 110 cells for each cell line.

The nucleo-cytoplasmic ratio of p^{Y357}-YAP significantly decreased at high densities in WT but not in *LMNA*^{ΔK32} mutant cells (Figure 3A,B). However, at the protein level, the p^{Y357}-YAP/YAP ratio did not differ between cell lines and decreased with cell density in both cell lines (Figure 3C,D). Dasatinib, an Abl and Src-family kinase inhibitor, significantly reduced the amount of p^{Y357}-YAP phosphorylation and the p^{Y357}-YAP/YAP ratio (Figure 3F,G) as well as the nucleo-cytoplasmic ratio of p^{Y357}-YAP (Figure 3A,H).

3.4. Blockade of Nuclear Import Inhibits Nuclear Accumulation of YAP in Confluent *LMNA*^{ΔK32} MuSCs

It is clearly established that YAP localization depends on its dynamic shuttling between the cytoplasm and the nucleus, and is maintained at a steady state by a balance between nuclear export and import rates. To exclude the possibility of nonspecific permeabilization of the nuclear envelope due to the lamin mutation, and generally to determine the exact pathway of nuclear import of YAP, we used importazole, an importin β-specific inhibitor [24]. In low density cultures, importazole inhibited YAP nuclear localization in both WT and *LMNA*^{ΔK32} cells, with no significant difference in YAP nucleo-cytoplasmic ratio between cell lines (Figure 4; each $p < 0.001$). In high density cultures, importazole significantly reduced nuclear localization of YAP in *LMNA*^{ΔK32} cells (Figure 4A,B, each $p < 0.001$), but not in WT cells, thus attesting to a persistent nuclear import of YAP in high density *LMNA*^{ΔK32} cell cultures.

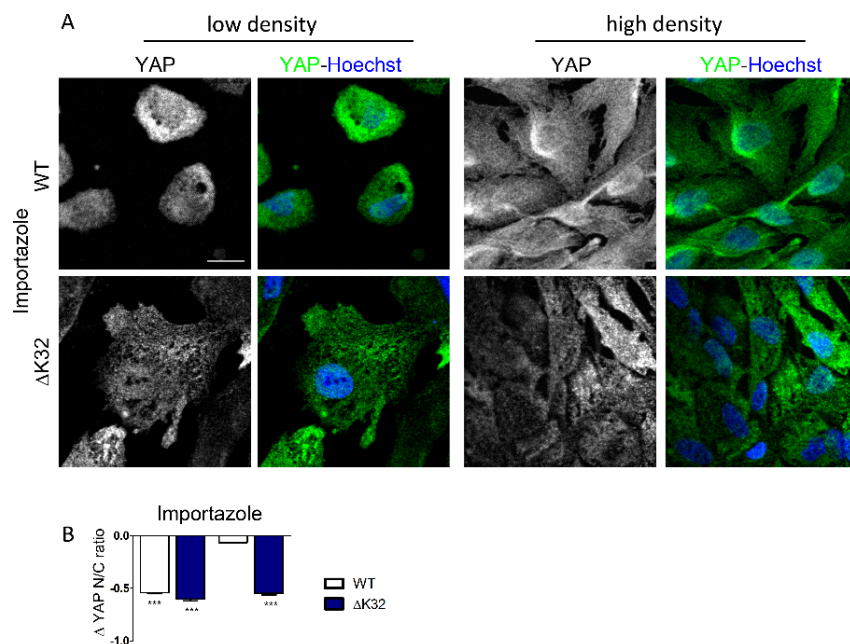


Figure 4. Importazole inhibits nuclear localization of YAP in WT and mutant MuSCs. (A) Confocal images of YAP (green) in WT and *LMNA*^{ΔK32} mutant MuSCs cultured in low and high density conditions. Nuclei are stained with Hoechst (blue). Scale bar: 20 μm. (B) Quantification of YAP nucleo-cytoplasmic (N/C) ratio after importazole treatment. Values are expressed as mean ± SEM, as a fraction of value obtained before importazole treatment, $n \geq 60$ cell in each cell line.

3.5. Functional Consequences of YAP Nuclear Accumulation in High Density *LMNA*^{ΔK32} MuSCs

To characterize the consequences of altered YAP translocation, we assessed expression of select YAP target genes and TEAD-dependent transcriptional activity using a luciferase reporter. Confluent *LMNA*^{ΔK32} cells had an increased expression of YAP and YAP target genes *CTGF* and *MYL9* (Figure 5A). Moreover, *LMNA*^{ΔK32} cells show increased TEAD-dependent luciferase reporter activity when compared to WT cells (Figure 5B), thus confirming elevated YAP transcriptional

activity. Taken together, these data indicate that the *LMNA*^{ΔK32} mutation affects YAP localization and density-dependent inactivation of YAP.

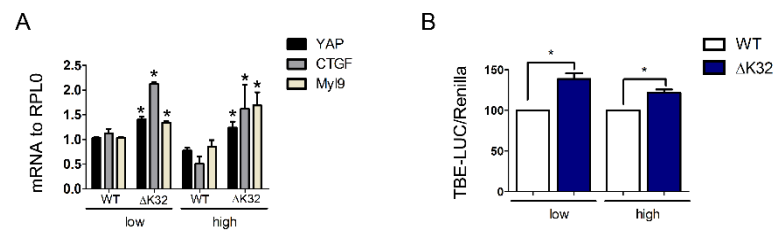


Figure 5. Transcriptional activity of YAP. **(A)** Histogram represents mRNA transcripts of *YAP*, *CTGF*, and *Myl9* normalized to *RPLP0* and expressed as fold-changes. Values are \pm SEM, $n = 3$ separate experiments. * $p < 0.05$ compared with WT. **(B)** Quantification of *YAP* activity using the TBE-Luciferase (LUC)/Renilla reporter. Values are \pm SEM, $n = 3$ separate experiments. * $p < 0.05$ compared with WT cells.

4. Discussion

In this study, we showed that A-type lamin mutations which are responsible for congenital muscle disorders impacted the yes-associated protein (YAP) signaling pathway by increasing the nuclear import of YAP through the nuclear pore complexes. More importantly, YAP was transcriptionally active despite activation of the Hippo pathway, and thus may contribute to the impaired muscle differentiation in congenital muscle dystrophies. In addition, our data revealed a striking correlation between YAP deregulation, nuclear envelope defects, and disease severity, thus supporting a critical role of nuclear morphology in regulating YAP nuclear import.

4.1. Canonical Regulation of YAP Nucleo-Cytoplasmic Localization Via the Hippo Pathway

In skeletal muscle, YAP/transcriptional coactivator with PDZ-binding motif (TAZ) are powerful co-transcription factors which regulate muscle cell proliferation and differentiation [31,32] and play critical roles in controlling muscle growth [32,33]. The nuclear presence and the transcriptional activity of YAP/TAZ can be modulated by mechanical cues, such as substrate stiffness, cell spreading, and stretching (review in [34]) as well as by non-mechanical cues [26,35]. In previous work [10], we have shown that mutations in the *LMNA* gene associated to congenital muscle dystrophy cause a loss of environmental mechanosensing with elevated YAP signaling despite the soft environment, thus suggesting that A-type lamins modulate the mechanical regulation of YAP. Consistent with an abnormal mechanical regulation of YAP, we found that reducing cell spreading was ineffective to induce cytoplasmic relocalization of YAP in *LMNA*^{ΔK32} mutant cells (Figure 1C,D). In addition, here we also showed that cell–cell contact failed to inhibit YAP nuclear localization and activity in *LMNA* mutant cells from *LMNA*-related congenital muscular dystrophy (L-CMD), contrary to what was observed in our wild-type (WT) (Figure 1A,B) and *LMNA*^{H222P} (Figure S1) cells and in other non-cancer cells [26–28]. Taken as a whole, these data showed that defective nucleo-cytoplasmic shuttling of YAP was a hallmark of the most severe muscle dystrophies related to nuclear envelope mutations. Moreover, abnormal YAP regulation in *LMNA* mutant cells from L-CMD involved both mechanical and non-mechanical regulations of YAP nucleo-cytoplasmic shuttling. While our study mainly focused on YAP, whether mutations in nuclear envelope proteins also affect the nucleo-cytoplasmic shuttling of TAZ remain to be precisely determined.

The mechanisms by which cell density modulates YAP activation and nucleo/cytoskeletal shuttling have been extensively studied during the last decade [11,36,37]. The Hippo signaling pathway critically regulates cell–cell contact-mediated YAP cytoplasmic translocation [38–40]. In cells grown at low density, YAP is primarily localized to the nucleus where it promotes target gene transcription and proliferation. When cells reach a critical density, YAP translocates to the cytoplasm [26–28], thus underlying the classical paradigm of the contact inhibition of proliferation [26]. The Hippo

signaling pathway functions as a highly conserved canonical upstream regulator of YAP activity and localization [41]. At the core of the Hippo pathway, LAT1/2 mediates serine phosphorylation on several serine residues, including serine 127, thus mediating YAP nuclear export and subsequent cytoplasmic association with 14-3-3 proteins [40,42–44]. In confluent cultures, loss of Ser127 phosphorylation and LATS1/2 activity with persistent nuclear localization of YAP is a hallmark of cancer cells [30]. In contrast, the high density cultures of *LMNA* mutated cells exhibited high protein levels of p^{S127}-YAP and persistent nuclear localization of p^{S127}-YAP (Figure 2), thus indicating activation of the Hippo pathway signaling. This nuclear accumulation of YAP and p^{S127}-YAP in *LMNA*^{ΔK32} cells suggests that YAP nuclear export is insufficient to counterbalance YAP nuclear entry. Accordingly, it is known that the presence of p^{S122}-YAP is a prerequisite, but is not sufficient for nuclear exclusion of YAP [45,46]. Although the role of exportin1 in YAP nuclear export has been clearly identified [29,47,48], however, regulation of YAP nuclear export remains largely unknown.

Regulation of YAP localization is also modulated by other kinases, including NLK [35] and Src-family kinases [47,49]. Whereas YAP phosphorylation on Ser residues are well-known negative regulators of YAP stability, Src-mediated phosphorylation of tyrosine 357 has been correlated with nuclear localization and increased YAP transcriptional activity [18,47,49]. Higher p^{Y357}-YAP levels in *LMNA*^{ΔK32} cells may thus contribute to the nuclear retention by promoting binding between YAP and TEAD transcription factors. Whether increased nuclear p^{Y357}-YAP at both low and high cell densities could explain the increased transcriptional activity of YAP observed in *LMNA*^{ΔK32} cells (Figure 5) remains to be determined.

4.2. Nuclear Import of YAP in *LMNA*^{ΔK32} Mutant Cells

YAP nuclear import is mediated by active translocation involving importins through nuclear pores [50]. To interfere with active nuclear import, we used importazole, a drug known to inhibit importin-dependent nuclear translocation [24] and YAP nuclear localization [18]. In low density conditions, blocking nuclear entry considerably reduced nuclear localization of YAP in both WT and *LMNA* mutant cells (Figure 4). Thus, in low density conditions, YAP nuclear entry was mediated by an importin-dependent nuclear import in both WT and *LMNA*^{ΔK32} mutated MuSCs. Passive diffusion across the damaged nuclear envelope [51,52], if any, was not a main contributor of YAP nuclear import in *LMNA*^{ΔK32} mutant MuSCs. Moreover, importazole inhibited YAP nuclear localization in high density *LMNA*^{ΔK32} but not in WT cells. Therefore, in WT cells, at high cell density active nuclear import of YAP was inhibited and no further inhibition was observed after treatment with importazole. In contrast, active nuclear import of YAP persisted in *LMNA*^{ΔK32} cells, a finding consistent with a dominant active nuclear import of YAP at cell confluence (Figure S4). MuSCs carrying a mutation in the gene encoding the nuclear envelope protein nesprin1, also failed to regulate YAP localization, thus suggesting a nuclear envelope-related dysfunction.

Nuclear deformability is specific to *LMNA* and nesprin mutations rather than to muscular dystrophy and specifically affected the most severe forms of muscle disorders related to nuclear envelope defects [16,52]. Recent studies have reported that force-induced nuclear deformations increase YAP nuclear translocation through the nuclear pore complex [17,18]. It is thus conceivable that nuclear deformations per se drive nuclear translocation of YAP in *LMNA* and nesprin-1^{ΔKASH} mutant MuSCs (Figure S4), regardless of how nuclear deformation can be caused [53].

4.3. Functional Consequence of YAP Deregulation in Myogenesis

Nuclear localization of the transcriptional co-activator YAP and activation of the TEAD family transcription factors are required to promote proliferation but prevent differentiation of human stem cells [54,55]. In myogenic cell precursors cultured in vitro, high YAP expression and activity promotes proliferation of myogenic cell precursors whilst preventing their differentiation [31]. Therefore, one can speculate that persistent activation of YAP in *LMNA* mutant MuSCs has additive negative effects on

skeletal muscle differentiation. Further studies are needed to precisely determine their contribution in the physiopathology of lamin-related muscle dystrophy.

Supplementary Materials: The following are available online at <http://www.mdpi.com/2073-4409/9/4/816/s1>, Figure S1: (A) Confocal images of YAP (green) in confluent WT and *LMNA*^{H222P} myogenic cells cultured in low and high density conditions. Nuclei are stained with Hoechst (blue). Scale bar: 50 μ m. (B) Quantification of YAP nucleo-cytoplasmic (N/C) ratio. Values are expressed as mean \pm SEM, $n \geq 50$ cells for each cell line, Figure S2: (A) Confocal images of YAP (green) and nuclei (blue) in confluent WT MuSCs treated with Leptomycin B (LB). Scale bar = 20 μ m; (B) Confocal images of YAP (green) and nuclei (blue) in WT and *LMNA* ^{Δ K32} mutant MuSCs cultured in low and high density conditions. Nuclei are stained with Hoechst (blue). Scale bar: 20 μ m. (C) Confocal images of YAP (green) and nuclei (blue) in confluent WT MuSCs treated with latrunculin A (LatA). Scale bar = 20 μ m; (D) Quantification of YAP nucleo-cytoplasmic (N/C) ratio after Lat A treatment expressed as a fraction of control value obtained in sparse conditions. Values are expressed as mean \pm SEM, $n \geq 60$ cells for each cell line, *** $p < 0.001$ versus value obtained before LatA treatment, Figure S3: Confocal images of p¹²⁷-YAP (green) and nuclei (blue) in WT MuSCs treated with vehicle (DMSO) or Cytochalasin D (cyto D). Scale bar = 50 μ m, Figure S4: Proposed model of the mechanisms by which lamins influence YAP subcellular distribution at high cell density. (A) In WT MuSCs plated at high cell density, the Hippo pathway is activated, and p¹²⁷-YAP was excluded from the nucleus. YAP nuclear entry was lower than YAP nuclear export. (B) In L-CMD and nesprin-1^{DKASH} mutations, YAP nuclear export is insufficient to counterbalance YAP nuclear entry despite activation of the Hippo pathway. This results in persistent nuclear localization of p⁵¹²⁷-YAP nuclear import. Potential mechanisms imply increased nuclear deformability and/or dysfunctional LINC complex.

Author Contributions: Conceptualization, C.C.; methodology, C.C., M.F. and D.J.O.; validation, C.C.; formal analysis, C.C., D.J.O., and M.F.; investigation, C.C., M.F., S.M., S.J.; resources, K.M.; writing—original draft preparation, C.C.; writing—review and editing, M.F., D.O., G.B.-B.; supervision, C.C.; project administration, C.C.; funding acquisition, C.C. All authors have read and agree to the published version of the manuscript.

Funding: This research was funded by ANR Sorbonne-University grant (ANR-11-IDEX-0004-02).

Acknowledgments: We thank the IRIS-platform (Sorbonne University) for imaging facility. We also thank Petra Knaus for providing constructs for the luciferase reporter assays.

Conflicts of Interest: The authors declare no conflict of interest. The funders had no role in the design of the study; in the collection, analyses, or interpretation of data; in the writing of the manuscript, or in the decision to publish the results.

References

- Osmanagic-Myers, S.; Dechat, T.; Foisner, R. Lamins at the crossroads of mechanosignaling. *Genes Dev.* **2015**, *29*, 225–237. [[CrossRef](#)] [[PubMed](#)]
- Worman, H.J.; Bonne, G. “Laminopathies”: A wide spectrum of human diseases. *Exp. Cell Res.* **2007**, *313*, 2121–2133. [[CrossRef](#)] [[PubMed](#)]
- Bertrand, A.T.; Chikhaoui, K.; Yaou, R.B.; Bonne, G. Clinical and genetic heterogeneity in laminopathies. *Biochem. Soc. Trans.* **2011**, *39*, 1687–1692. [[CrossRef](#)] [[PubMed](#)]
- Guilluy, C.; Osborne, L.D.; Van Landeghem, L.; Sharek, L.; Superfine, R.; Garcia-Mata, R.; Burrridge, K. Isolated nuclei adapt to force and reveal a mechanotransduction pathway in the nucleus. *Nat. Cell Biol.* **2014**, *16*, 376–381. [[CrossRef](#)] [[PubMed](#)]
- Swift, J.; Ivanovska, I.L.; Buxboim, A.; Harada, T.; Dingal, P.C.; Pinter, J.; Pajerowski, J.D.; Spinler, K.R.; Shin, J.W.; Tewari, M.; et al. Nuclear lamin-A scales with tissue stiffness and enhances matrix-directed differentiation. *Science* **2013**, *341*, 1240104. [[CrossRef](#)]
- Vaughan, A.; Alvarez-Reyes, M.; Bridger, J.M.; Broers, J.L.; Ramaekers, F.C.; Wehnert, M.; Morris, G.E.; Whitfield, W.G.F.; Hutchison, C.J. Both emerin and lamin C depend on lamin A for localization at the nuclear envelope. *J. Cell Sci.* **2001**, *114*, 2577–2590.
- Markiewicz, E.; Tilgner, K.; Barker, N.; van de Wetering, M.; Clevers, H.; Dorobek, M.; Hausmanowa-Petrusewicz, I.; Ramaekers, F.C.; Broers, J.L.; Blankesteyn, W.M.; et al. The inner nuclear membrane protein emerin regulates beta-catenin activity by restricting its accumulation in the nucleus. *EMBO J.* **2006**, *25*, 3275–3285. [[CrossRef](#)]
- Ho, C.Y.; Jaalouk, D.E.; Vartiainen, M.K.; Lammerding, J. Lamin A/C and emerin regulate MKL1-SRF activity by modulating actin dynamics. *Nature* **2013**, *497*, 507–511. [[CrossRef](#)]

9. Schwartz, C.; Fischer, M.; Mamchaoui, K.; Bigot, A.; Lok, T.; Verdier, C.; Duperray, A.; Michel, R.; Holt, I.; Voit, T.; et al. Lamins and nesprin-1 mediate inside-out mechanical coupling in muscle cell precursors through FHOD1. *Sci. Rep.* **2017**, *7*, 1253. [[CrossRef](#)]
10. Bertrand, A.T.; Ziaei, S.; Ehret, C.; Duchemin, H.; Mamchaoui, K.; Bigot, A.; Mayer, M.; Quijano-Roy, S.; Desguerre, I.; Laine, J.; et al. Cellular microenvironments reveal defective mechanosensing responses and elevated YAP signaling in LMNA-mutated muscle precursors. *J. Cell Sci.* **2014**, *127*, 2873–2884. [[CrossRef](#)]
11. Panciera, T.; Azzolin, L.; Cordenonsi, M.; Piccolo, S. Mechanobiology of YAP and TAZ in physiology and disease. *Nat. Rev. Mol. Cell Biol.* **2017**, *18*, 758–770. [[CrossRef](#)] [[PubMed](#)]
12. Fischer, M.; Rikeit, P.; Knaus, P.; Coirault, C. YAP-Mediated Mechanotransduction in Skeletal Muscle. *Front. Physiol.* **2016**, *7*, 41. [[CrossRef](#)] [[PubMed](#)]
13. Irianto, J.; Pfeifer, C.R.; Ivanovska, I.L.; Swift, J.; Discher, D.E. Nuclear lamins in cancer. *Cell. Mol. Bioeng.* **2016**, *9*, 258–267. [[CrossRef](#)]
14. Chow, K.H.; Factor, R.E.; Ullman, K.S. The nuclear envelope environment and its cancer connections. *Nat. Rev. Cancer* **2012**, *12*, 196–209. [[CrossRef](#)] [[PubMed](#)]
15. Zink, D.; Fischer, A.H.; Nickerson, J.A. Nuclear structure in cancer cells. *Nat. Rev. Cancer* **2004**, *4*, 677–687. [[CrossRef](#)] [[PubMed](#)]
16. Dahl, K.N.; Ribeiro, A.J.; Lammerding, J. Nuclear shape, mechanics, and mechanotransduction. *Circ. Res.* **2008**, *102*, 1307–1318. [[CrossRef](#)] [[PubMed](#)]
17. Elosegui-Artola, A.; Trepast, X.; Roca-Cusachs, P. Control of Mechanotransduction by Molecular Clutch Dynamics. *Trends Cell Biol.* **2018**, *28*, 356–367. [[CrossRef](#)]
18. Aureille, J.; Buffiere-Ribot, V.; Harvey, B.E.; Boyault, C.; Pernet, L.; Andersen, T.; Bacola, G.; Balland, M.; Fraboulet, S.; Van Landeghem, L.; et al. Nuclear envelope deformation controls cell cycle progression in response to mechanical force. *EMBO Rep.* **2019**, *20*, e48084. [[CrossRef](#)]
19. Zhou, C.; Rao, L.; Shanahan, C.M.; Zhang, Q. Nesprin-1/2: Roles in nuclear envelope organisation, myogenesis and muscle disease. *Biochem. Soc. Trans.* **2018**, *46*, 311–320. [[CrossRef](#)]
20. Puckelwartz, M.J.; Kessler, E.J.; Kim, G.; Dewitt, M.M.; Zhang, Y.; Earley, J.U.; Depreux, F.F.; Holaska, J.; Mewborn, S.K.; Pytel, P.; et al. Nesprin-1 mutations in human and murine cardiomyopathy. *J. Mol. Cell. Cardiol.* **2010**, *48*, 600–608. [[CrossRef](#)]
21. Perovanovic, J.; Dell’Orso, S.; Gnoch, V.F.; Jaiswal, J.K.; Sartorelli, V.; Vigouroux, C.; Mamchaoui, K.; Mouly, V.; Bonne, G.; Hoffman, E.P. Laminopathies disrupt epigenomic developmental programs and cell fate. *Sci. Transl. Med.* **2016**, *8*, 335ra358. [[CrossRef](#)] [[PubMed](#)]
22. Aure, K.; Mamchaoui, K.; Frachon, P.; Butler-Browne, G.S.; Lombes, A.; Mouly, V. Impact on oxidative phosphorylation of immortalization with the telomerase gene. *Neuromuscul. Disord.* **2007**, *17*, 368–375. [[CrossRef](#)] [[PubMed](#)]
23. Chaouch, S.; Mouly, V.; Goyenvall, A.; Vulin, A.; Mamchaoui, K.; Negroni, E.; Di Santo, J.; Butler-Browne, G.; Torrente, Y.; Garcia, L.; et al. Immortalized skin fibroblasts expressing conditional MyoD as a renewable and reliable source of converted human muscle cells to assess therapeutic strategies for muscular dystrophies: Validation of an exon-skipping approach to restore dystrophin in Duchenne muscular dystrophy cells. *Hum. Gene Ther.* **2009**, *20*, 784–790. [[PubMed](#)]
24. Soderholm, J.F.; Bird, S.L.; Kalab, P.; Sampathkumar, Y.; Hasegawa, K.; Uehara-Bingen, M.; Weis, K.; Heald, R. Importazole, a small molecule inhibitor of the transport receptor importin-beta. *ACS Chem. Biol.* **2011**, *6*, 700–708. [[CrossRef](#)] [[PubMed](#)]
25. Kudo, N.; Wolff, B.; Sekimoto, T.; Schreiner, E.P.; Yoneda, Y.; Yanagida, M.; Horinouchi, S.; Yoshida, M. Leptomycin B inhibition of signal-mediated nuclear export by direct binding to CRM1. *Exp. Cell Res.* **1998**, *242*, 540–547. [[CrossRef](#)]
26. Kim, N.G.; Koh, E.; Chen, X.; Gumbiner, B.M. E-cadherin mediates contact inhibition of proliferation through Hippo signaling-pathway components. *Proc. Natl. Acad. Sci. USA* **2011**, *108*, 11930–11935. [[CrossRef](#)]
27. Zhao, B.; Wei, X.; Li, W.; Udan, R.S.; Yang, Q.; Kim, J.; Xie, J.; Ikenoue, T.; Yu, J.; Li, L.; et al. Inactivation of YAP oncoprotein by the Hippo pathway is involved in cell contact inhibition and tissue growth control. *Genes Dev.* **2007**, *21*, 2747–2761. [[CrossRef](#)]
28. Aragona, M.; Panciera, T.; Manfrin, A.; Giulitti, S.; Michielin, F.; Elvassore, N.; Dupont, S.; Piccolo, S. A mechanical checkpoint controls multicellular growth through YAP/TAZ regulation by actin-processing factors. *Cell* **2013**, *154*, 1047–1059. [[CrossRef](#)]

29. Dupont, S.; Morsut, L.; Aragona, M.; Enzo, E.; Giulitti, S.; Cordenonsi, M.; Zanconato, F.; Le Digabel, J.; Forcato, M.; Bicciato, S.; et al. Role of YAP/TAZ in mechanotransduction. *Nature* **2011**, *474*, 179–183. [[CrossRef](#)]
30. Calvo, F.; Ege, N.; Grande-Garcia, A.; Hooper, S.; Jenkins, R.P.; Chaudhry, S.I.; Harrington, K.; Williamson, P.; Moendary, E.; Charras, G.; et al. Mechanotransduction and YAP-dependent matrix remodelling is required for the generation and maintenance of cancer-associated fibroblasts. *Nat. Cell Biol.* **2013**, *15*, 637–646. [[CrossRef](#)]
31. Judson, R.N.; Tremblay, A.M.; Knopp, P.; White, R.B.; Urcia, R.; De Bari, C.; Zammit, P.S.; Camargo, F.D.; Wackerhage, H. The Hippo pathway member Yap plays a key role in influencing fate decisions in muscle satellite cells. *J. Cell Sci.* **2012**, *125*, 6009–6019. [[CrossRef](#)] [[PubMed](#)]
32. Wackerhage, H.; Del Re, D.P.; Judson, R.N.; Sudol, M.; Sadoshima, J. The Hippo signal transduction network in skeletal and cardiac muscle. *Sci. Signal* **2014**, *7*, re4. [[CrossRef](#)] [[PubMed](#)]
33. Goodman, C.A.; Dietz, J.M.; Jacobs, B.L.; McNally, R.M.; You, J.S.; Hornberger, T.A. Yes-Associated Protein is up-regulated by mechanical overload and is sufficient to induce skeletal muscle hypertrophy. *FEBS Lett.* **2015**, *589*, 1491–1497. [[CrossRef](#)] [[PubMed](#)]
34. Dupont, S. Role of YAP/TAZ in cell-matrix adhesion-mediated signalling and mechanotransduction. *Exp. Cell Res.* **2016**, *343*, 42–53. [[CrossRef](#)] [[PubMed](#)]
35. Moon, S.; Kim, W.; Kim, S.; Kim, Y.; Song, Y.; Bilousov, O.; Kim, J.; Lee, T.; Cha, B.; Kim, M.; et al. Phosphorylation by NLK inhibits YAP-14-3-3-interactions and induces its nuclear localization. *EMBO Rep.* **2017**, *18*, 61–71. [[CrossRef](#)]
36. Zanconato, F.; Cordenonsi, M.; Piccolo, S. YAP/TAZ at the Roots of Cancer. *Cancer Cell* **2016**, *29*, 783–803. [[CrossRef](#)]
37. Yu, F.X.; Zhao, B.; Guan, K.L. Hippo Pathway in Organ Size Control, Tissue Homeostasis, and Cancer. *Cell* **2015**, *163*, 811–828. [[CrossRef](#)]
38. Oh, H.; Irvine, K.D. In vivo regulation of Yorkie phosphorylation and localization. *Development* **2008**, *135*, 1081–1088. [[CrossRef](#)]
39. Zhao, B.; Lei, Q.Y.; Guan, K.L. The Hippo-YAP pathway: New connections between regulation of organ size and cancer. *Curr. Opin. Cell Biol.* **2008**, *20*, 638–646. [[CrossRef](#)]
40. Chan, E.H.; Nousiainen, M.; Chalamalasetty, R.B.; Schafer, A.; Nigg, E.A.; Sillje, H.H. The Ste20-like kinase Mst2 activates the human large tumor suppressor kinase Lats1. *Oncogene* **2005**, *24*, 2076–2086. [[CrossRef](#)]
41. Mo, J.S.; Park, H.W.; Guan, K.L. The Hippo signaling pathway in stem cell biology and cancer. *EMBO Rep.* **2014**, *15*, 642–656. [[CrossRef](#)] [[PubMed](#)]
42. Hao, Y.; Chun, A.; Cheung, K.; Rashidi, B.; Yang, X. Tumor suppressor LATS1 is a negative regulator of oncogene YAP. *J. Biol. Chem.* **2008**, *283*, 5496–5509. [[CrossRef](#)] [[PubMed](#)]
43. Lei, Q.Y.; Zhang, H.; Zhao, B.; Zha, Z.Y.; Bai, F.; Pei, X.H.; Zhao, S.; Xiong, Y.; Guan, K.L. TAZ promotes cell proliferation and epithelial-mesenchymal transition and is inhibited by the hippo pathway. *Mol. Cell. Biol.* **2008**, *28*, 2426–2436. [[CrossRef](#)] [[PubMed](#)]
44. Oka, T.; Mazack, V.; Sudol, M. Mst2 and Lats kinases regulate apoptotic function of Yes kinase-associated protein (YAP). *J. Biol. Chem.* **2008**, *283*, 27534–27546. [[CrossRef](#)] [[PubMed](#)]
45. Wada, K.; Itoga, K.; Okano, T.; Yonemura, S.; Sasaki, H. Hippo pathway regulation by cell morphology and stress fibers. *Development* **2011**, *138*, 3907–3914. [[CrossRef](#)]
46. Das, A.; Fischer, R.S.; Pan, D.; Waterman, C.M. YAP Nuclear Localization in the Absence of Cell-Cell Contact Is Mediated by a Filamentous Actin-dependent, Myosin II- and Phospho-YAP-independent Pathway during Extracellular Matrix Mechanosensing. *J. Biol. Chem.* **2016**, *291*, 6096–6110. [[CrossRef](#)]
47. Ege, N.; Dowbaj, A.M.; Jiang, M.; Howell, M.; Hooper, S.; Foster, C.; Jenkins, R.P.; Sahai, E. Quantitative Analysis Reveals that Actin and Src-Family Kinases Regulate Nuclear YAP1 and Its Export. *Cell Syst.* **2018**, *6*, 692.e13–708.e13. [[CrossRef](#)]
48. Kofler, M.; Speight, P.; Little, D.; Di Ciano-Oliveira, C.; Szaszi, K.; Kapus, A. Mediated nuclear import and export of TAZ and the underlying molecular requirements. *Nat. Commun.* **2018**, *9*, 4966. [[CrossRef](#)]
49. Levy, D.; Adamovich, Y.; Reuven, N.; Shaul, Y. Yap1 phosphorylation by c-Abl is a critical step in selective activation of proapoptotic genes in response to DNA damage. *Mol. Cell* **2008**, *29*, 350–361. [[CrossRef](#)]

50. Wang, S.; Li, H.; Wang, G.; Zhang, T.; Fu, B.; Ma, M.; Quan, Z.; Chen, G. Yes-associated protein (YAP) expression is involved in epithelial-mesenchymal transition in hepatocellular carcinoma. *Clin. Transl. Oncol.* **2016**, *18*, 172–177. [[CrossRef](#)]
51. Zwerger, M.; Jaalouk, D.E.; Lombardi, M.L.; Isermann, P.; Mauermann, M.; Dialynas, G.; Herrmann, H.; Wallrath, L.L.; Lammerding, J. Myopathic lamin mutations impair nuclear stability in cells and tissue and disrupt nucleo-cytoskeletal coupling. *Hum. Mol. Genet.* **2013**, *22*, 2335–2349. [[CrossRef](#)] [[PubMed](#)]
52. Earle, A.J.; Kirby, T.J.; Fedorchak, G.R.; Isermann, P.; Patel, J.; Iruvanti, S.; Moore, S.A.; Bonne, G.; Wallrath, L.L.; Lammerding, J. Mutant lamins cause nuclear envelope rupture and DNA damage in skeletal muscle cells. *Nat. Mater.* **2019**. [[CrossRef](#)] [[PubMed](#)]
53. Jahed, Z.; Mofrad, M.R. The nucleus feels the force, LINCed in or not! *Curr. Opin. Cell Biol.* **2019**, *58*, 114–119. [[CrossRef](#)]
54. Ohgushi, M.; Minaguchi, M.; Sasai, Y. Rho-Signaling-Directed YAP/TAZ Activity Underlies the Long-Term Survival and Expansion of Human Embryonic Stem Cells. *Cell Stem Cell* **2015**, *17*, 448–461. [[CrossRef](#)]
55. Musah, S.; Wrighton, P.J.; Zaltsman, Y.; Zhong, X.; Zorn, S.; Parlato, M.B.; Hsiao, C.; Palecek, S.P.; Chang, Q.; Murphy, W.L.; et al. Substratum-induced differentiation of human pluripotent stem cells reveals the coactivator YAP is a potent regulator of neuronal specification. *Proc. Natl. Acad. Sci. USA* **2014**, *111*, 13805–13810. [[CrossRef](#)]



© 2020 by the authors. Licensee MDPI, Basel, Switzerland. This article is an open access article distributed under the terms and conditions of the Creative Commons Attribution (CC BY) license (<http://creativecommons.org/licenses/by/4.0/>).